

Adsorption mechanism of MV6B on PAL/Fe₃O₄ composite adsorbent

Source: Rodil MSP, Sacdalan CD, Robero RR, Salinas MEL, Santander TN. Phenolated alkali lignin/magnetite composite as an adsorbent for methyl violet 6B in wastewater. Page 257-269.



AIMS AND SCOPE

The Environment and Natural Resources Journal is a peer-reviewed journal, which provides insight scientific knowledge into the diverse dimensions of integrated environmental and natural resource management. The journal aims to provide a platform for exchange and distribution of the knowledge and cutting-edge research in the fields of environmental science and natural resource management to academicians, scientists and researchers. The journal accepts a varied array of manuscripts on all aspects of environmental science and natural resource management. The journal scope covers the integration of multidisciplinary sciences for prevention, control, treatment, environmental clean-up and restoration. The study of the existing or emerging problems of environment and natural resources in the region of Southeast Asia and the creation of novel knowledge and/or recommendations of mitigation measures for sustainable development policies are emphasized.

The subject areas are diverse, but specific topics of interest include:

- Biodiversity
- Climate change
- Detection and monitoring of polluted sources e.g., industry, mining
- Disaster e.g., forest fire, flooding, earthquake, tsunami, or tidal wave
- Ecological/Environmental modelling
- Emerging contaminants/hazardous wastes investigation and remediation
- Environmental dynamics e.g., coastal erosion, sea level rise
- Environmental assessment tools, policy and management e.g., GIS, remote sensing, Environmental Management System (EMS)
- Environmental pollution and other novel solutions to pollution
- Remediation technology of contaminated environments
- Transboundary pollution
- Waste and wastewater treatments and disposal technology

Schedule

Environment and Natural Resources Journal (EnNRJ) is published 6 issues per year in January-February, March-April, May-June, July-August, September-October, and November-December.

Publication Fees

There is no cost of the article-processing and publication.

Ethics in publishing

EnNRJ follows closely a set of guidelines and recommendations published by Committee on Publication Ethics (COPE).

EXECUTIVE CONSULTANT TO EDITOR

Associate Professor Dr. Kitikorn Charmondusit

(Mahidol University, Thailand)

Associate Professor Dr. Benjaphorn Prapagdee

(Mahidol University, Thailand)

EDITOR

Associate Professor Dr. Noppol Arunrat

(Mahidol University, Thailand)

ASSOCIATE EDITOR

Assistant Professor Dr. Piangjai Peerakiatkhajohn

(Mahidol University, Thailand)

Dr. Thomas Neal Stewart

(Mahidol University, Thailand)

EDITORIAL BOARD

Professor Dr. Anthony SF Chiu

(De La Salle University, Philippines)

Professor Dr. Chongrak Polprasert

(Thammasat University, Thailand)

Professor Dr. Gerhard Wiegler

(Brandenburgische Technische Universität Cottbus, Germany)

Professor Dr. Hermann Knoflacher

(University of Technology Vienna, Austria)

Professor Dr. Hideki Nakayama

(Nagasaki University)

Professor Dr. Jurgen P. Kropp

(University of Potsdam, Germany)

Professor Dr. Manish Mehta

(Wadia Institute of Himalayan Geology, India)

Professor Dr. Mark G. Robson

(Rutgers University, USA)

Professor Dr. Mohamed Fassy Yassin

(University of Kuwait, Kuwait)

Professor Dr. Nipon Tangtham

(Kasetsart University, Thailand)

Professor Dr. Pranom Chantaranonthai

(Khon Kaen University, Thailand)

Professor Dr. Shuzo Tanaka

(Meisei University, Japan)

Professor Dr. Sompon Wanwimolruk
(Mahidol University, Thailand)
Professor Dr. Takehiko Kenzaka
(Osaka Ohtani University, Japan)
Professor Dr. Tamao Kasahara
(Kyushu University, Japan)
Professor Dr. Warren Y. Brockelman
(Mahidol University, Thailand)
Professor Dr. Yeong Hee Ahn
(Dong-A University, South Korea)
Associate Professor Dr. Kathleen R Johnson
(Department of Earth System Science, USA)
Associate Professor Dr. Marzuki Ismail
(University Malaysia Terengganu, Malaysia)
Associate Professor Dr. Sate Sampattagul
(Chiang Mai University, Thailand)
Associate Professor Dr. Uwe Strotmann
(University of Applied Sciences, Germany)
Assistant Professor Dr. Devi N. Choesin
(Institut Teknologi Bandung, Indonesia)
Assistant Professor Dr. Said Munir
(Umm Al-Qura University, Saudi Arabia)
Dr. Norberto Asensio
(University of Basque Country, Spain)

ASSISTANT TO EDITOR

Dr. Jakkapon Phanthuwongpakdee
Dr. Praewa Wongburi
Dr. Thunyapat Sattraburut

JOURNAL MANAGER

Isaree Apinya

JOURNAL EDITORIAL OFFICER

Nattakarn Ratchakun
Parynya Chowwiwattanaporn

Editorial Office Address

Research and Academic Services Department,
Faculty of Environment and Resource Studies, Mahidol University
999, Phutthamonthon Sai 4 Road, Salaya, Phutthamonthon, Nakhon Pathom, Thailand, 73170
Phone +662 441 5000 ext. 2108 Fax. +662 441 9509-10
Website: <https://ph02.tci-thaijo.org/index.php/ennrj/index>
E-mail: ennrjournal@gmail.com

CONTENT

- Factors in Community Adaptation for Climate Change Mitigation in Thailand** 197
Tipmol Traiyut, Patranit Srijuntrapun, and Wee Rawang
- Seagrass Community Structure and Ecosystem Carbon Stocks Along the Shoreline of Semujur Island, Bangka Belitung Province, Indonesia** 210
Aldina Himmarila Muliawati and Devi N. Choesin
- Characteristics of Fine Particulate Matter (PM_{2.5}) Chemical Composition in the North Jakarta Industrial Area** 222
Zeni Anggraini, Muhayatun Santoso, and Asep Sofyan
- Exergy Analysis of Waste-to-Energy Technologies for Municipal Solid Waste Management** 232
Nuhu Caleb Amulah, Mohammed Ben Oumarou, and Abba Bashir Muhammad
- Willingness to Pay Estimation for the Restoration of Water Quality of a Eutrophic Lake** 244
Mc Jervis Soltura Villaruel
- Phenolated Alkali Lignin/Magnetite Composite as an Adsorbent for Methyl Violet 6B in Wastewater** 257
Mary Sheenayn P. Rodil, Corazon D. Sacdalan, Rissabell R. Robero, Maria Evytha L. Salinas, and Trixie N. Santander
- Demography, Structure, and Composition of a Low-Disturbance Forest in Luzon, Philippines** 270
Jeri E. Latorre, John Michael M. Galindon, Nestor A. Bartolome Jr., Melizar V. Duya, and Lillian Jennifer V. Rodriguez
- Formulation of Novel Microbial Consortia for Rapid Composting of Biodegradable Municipal Solid Waste: An Approach in the Circular Economy** 283
P. A. K. C. Wijerathna, K. P. P. Udayagee, F. S. Idroos, and Pathmalal M. Manage

Factors in Community Adaptation for Climate Change Mitigation in Thailand

Tipmol Traiyut*, Patranit Srijuntrapun, and Wee Rawang

Environmental Education Program, Department of Education, Faculty of Social Sciences and Humanities, Mahidol University, Nakhon Pathom 73170, Thailand

ARTICLE INFO

Received: 10 Oct 2023
Received in revised: 9 Feb 2024
Accepted: 19 Feb 2024
Published online: 8 May 2024
DOI: 10.32526/ennrj/22/20230282

Keywords:

Common factor/ Community adaptation/ Climate change adaptation/ Reduce vulnerability/ Build resilience

* Corresponding author:

E-mail: tipmol@gmail.com

ABSTRACT

This study reflects the experiences of communities who have adapted to climate change in three different geological locations in the country of Thailand: by the riverside, coast, and in the mountains. The communities presented the lessons learned and identified key adaptation factors. The study used in-depth interviews and focus group discussions, with results showing that the community's learning and adaptation to climate change were at a high level. The results broaden understanding of climate change in these locations and provide information for resource management approaches. Among the seven factors, five factors illustrated that they were highly adapted, including: (1) applying knowledge about nature, ecosystems, and traditional wisdom; (2) management that allowed the use of adaptations; (3) a shared vision of success; (4) collaboration; and (5) having a variety of options and approaches. Two factors that illustrated that the community was only moderately adapted included: (1) learning about violent events and disasters; and (2) following government guidelines. It was found that a lack of information about the ecosystems and environmental resources they required for large-scale infrastructure construction caused issues. This is a problem, and the government must consult with local communities when setting long-term plans and assessing needs, because communities have diverse livelihoods and depend on natural resources. Hence, future studies should include climate change awareness and understanding of what is required by adding community needs linked to climate change adaptation into state development plans as well as utilizing the wisdom and traditional knowledge involving ecology held by these communities into sustainability plans.

1. INTRODUCTION

Humans can negatively affect the environment (Rambaree et al., 2019), with population change, development, and urbanization blamed by many for climate change. The Inter-Governmental Panel on Climate Change (IPCC, 2014) reported that since the year 2000 climate change has caused more climate-related changes, with extremes such as increased rainfall and drought becoming more common. These events lead to problems such as coastal erosion, which are consequence of climate change causing rising sea levels. The 2021 global climate risk index ranked Thailand ninth for risk (Eckstein et al., 2021), and

“climate change 2022: Impacts, adaptation, and vulnerability” described possible consequences up to 2100, stating that approximately 3.3 to 3.6 billion people live in locations that are highly vulnerable to climate change (IPCC, 2023). Climate change affects agriculture, health, and tourism, so it should be considered in policy formulation (Reynolds and Ortiz, 2010), yet a study by Mastrandrea et al. (2010) indicated that government policies does not reflect the needs of communities.

Globally, attention has been drawn to vulnerable communities affected by climate change. Vogel et al. (2020) showed that local communities are those most

severely affected by climate change. Therefore, climate resilience must be built-in to reduce the impacts of climate change on these locations. Currently, most research and development focuses on collaborative development issues but decision support tools must be developed, the integration of databases including fundamental vulnerabilities in health, socio-economic factors, infrastructure, and the local environment (Tee Lewis et al., 2023). The American Agency for International Development (USAID) (2022) states that Southeast Asia faces challenges because it is the region most vulnerable to climate change.

Thailand suffers from extreme weather that causes issues leading to coastal erosion, and increased salinity in fresh water supplies (Smith et al., 2021). Disasters have become more frequent and severe over the past decade (IPCC, 2023), with the 2011 flooding the most devastating natural disaster in seventy years, causing billions of dollars of damage to the Thai economy. The National Economic and Social Development Plan (NESDP) (2023-2027) formulated development goals to counteract the issues (NESDP, 2021), with human settlements the primary focus in the Thai Climate Change Master Plan (MNRE, 2015). The plan aims to support vulnerable communities, helping them adapt to climate change and to learn from their collective experiences (Anh Tran, 2020). Agriculture remains critically important to Thailand, but if vulnerable communities had a model framework for analyzing experiences collectively, they could adapt by accessing knowledge related to culture, ethnicity, values, motivations, norms, beliefs, and behaviors, both social and environmental (Steg, 2016; Mohr Carney et al., 2022). Thailand's communities would generate knowledge by learning and brainstorming in order to solve problems in practice (Coppock et al., 2022). Brown et al. (2020) define community resilience as the existence, development, and participation of community resources in an environment of uncertainty and unpredictability. United States Environmental Protection Agency (U.S. EPA.) (2015) states that communities need critical knowledge to adapt and reduce the impacts of climate change. Therefore, the knowledge used for mitigation may vary from area to area.

The research objectives are as follows: (1) to identify common factors and levels in community learning that could be used to adapt and mitigate the effects of climate change; (2) to study learning and experience in managing community resources; and (3) to synthesize models of community adaptation to assist

adaptation to climate change. Guideline for climate change mitigation, adaptation, and resilience, which can be applied to other communities will be formed.

2. METHODOLOGY

2.1 Study area

This study aimed to identify common factors in community adaptation to climate change using a mixed-methods approach (Ishtiaq, 2019). The study areas selected were surveyed using purposive sampling based on the behaviour demonstrated in human settlements, as communities in high risk locations are more likely to be affected (Aboda et al., 2023). The communities were selected from the areas shown in Figure 1 (a), (b), and (c).

2.2 Participants and data collection

The study was separated into three phases. The first identified common factors and levels of community learning used to adapt and mitigate the effects of climate change. Structured interviews (Rashidi et al., 2014) surveyed a total of 3,700 households, and results were calculated using Yamane (1973) with a 95% confidence level, and a p-value of 0.5 was assumed.

$$\text{Formula} \quad n = \frac{N}{1+Ne^2} \quad (1)$$

Where; n=the sample size; N=the population size; e=the acceptable sample error.

$$\begin{aligned} \text{Substituting the formula} \quad n &= \frac{3,700}{1+(3,700)(0.05)^2} \\ &= 361 \end{aligned}$$

The second phase studied the learning and experiences used when managing community resources. The first in this two-step process was to undertake in-depth interviews to gain insights and rich experiences from different target groups. The sampling method used the snowball sampling technique, and the data collection used was that of standardized or structured interviews to collect information from key informants. The sample size was small with small group discussions five participants per area, totalling fifteen participants. Data collection from community leaders and experienced community members who understood the local context and had lived in the area for at least ten years, such as monks, local politicians, and volunteers. The data collection was hand-written and audio-recorded, taking approximately two hours per individual over three months.

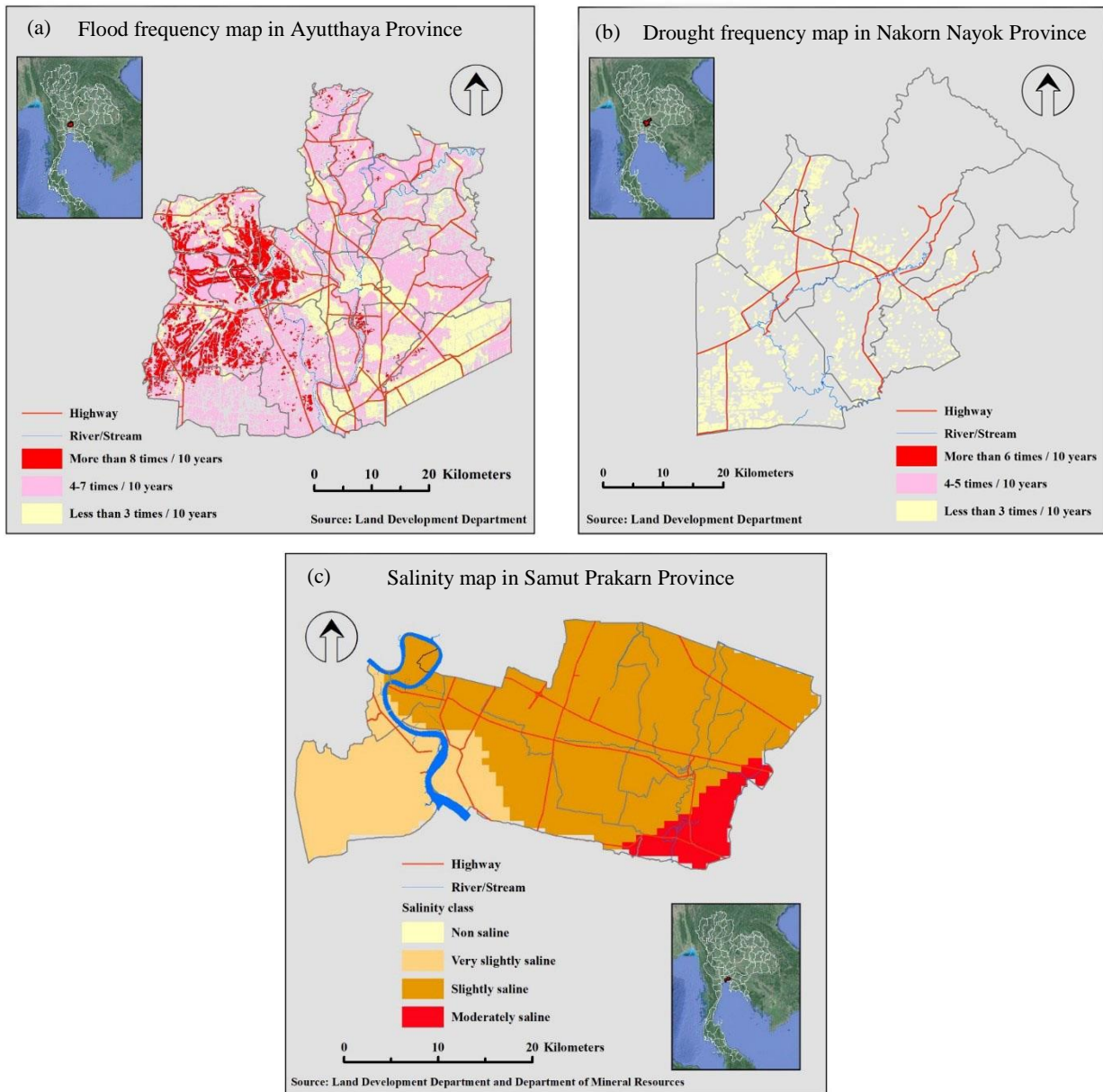


Figure 1. (a) Hua Wiang Sub-District, Sena District, Ayutthaya as riverside communities; (b) Pa Kha Sub-District, Ban Na District, Nakhon Nayok, as the mountainous communities; and (c) Bang Nam Phueng Sub-District, Phra Pra Daeng District, Samut Prakan as the coastal communities

The second stage used small group discussions or focus groups (Krueger et al., 2001). The sampling method uses the purposive sampling method technique to obtain diverse perspectives and group conclusions. The sample size used in the small group discussions was six participants per area, totalling eighteen participants. These discussions were a process of both learning about the experiences of different vulnerable groups in locations affected by climate change. The data collection by observation was hand-written as well as audio-recorded, and took three hours per group over a period of two months.

The third step involved synthesizing community adaptation models with climate change in

local geographic areas. Both quantitative and qualitative studies were used to design innovative environmental resources by synthesizing community adaptation models.

2.3 Data analysis

Quantitative data analysis was obtained from the questionnaire to study the situations, people, and experiences in communities affected. Three hundred and sixty-one quantitative datasets from households were obtained from the questionnaires.

Qualitative data analysis, including content analysis, consists of data, opinions, situations, experiences, and community adaptations to climate

change. The process was: (1) analysis of recording transcriptions and handwritten documents for a preliminary conclusion; (2) coding, data analytical, and interpretation; (3) content analysis based on the framework of community adaptation; (4) analysis of the collected data using MS Office (Word and Excel); and (5) analysis of the results to achieve the objectives of the study. The content analysis followed the requirements of human research ethics and a variety of participants were selected to address the limitations in the research tool (Carter et al., 2021).

2.4 Research statistics

Quantitative data analysis was obtained from the questionnaire and analyzed using statistical software packages. Data processing discovered the mean (mean score), standard deviation (SD), and weighted mean score (WMS), in order to explain the levels of learning and analyze the capacity for adaptation in communities to cope the rating scale, based on the Likert (1967) method, has interpretation criteria to determine the average grade level, defined as the range of scores, and the range was divided for each grade using the interval scale as a data scale to determine both the direction and size of the data differences.

$$\begin{aligned}
 \text{Range} &= \frac{\text{max score} - \text{min score}}{\text{frequency}} & (2) \\
 &= \frac{5 - 1}{5} \\
 &= 0.80
 \end{aligned}$$

In the case of levels 1-5, the mean score was level: The means were interpreted as follows: The lowest level was in the point range of 1.00-1.80, low level: 1.81-2.60, moderate level: 2.61-3.40, high level: 3.41-4.20, and the highest level: 4.21-5.00 as shown in (Table 1).

Table 1. The criteria for the distribution of the scores

Likert-scale description	Likert-scale	Likert scale interval
Lowest level	1	1.00-1.80
Low level	2	1.81-2.60
Moderate	3	2.61-3.40
High level	4	3.41-4.20
The highest level	5	4.21-5.00

3. RESULTS AND DISCUSSION

Factors in community adaptation to mitigate climate change in Thailand are presented in this section, including the results of the study and a discussion on the separate elements, according to the objective of the study. The phenomenology and theoretical framework of Howard’s (2013) were applied to help gain perspectives on experiential learning, adaptation, community organizing, and resilience for climate change mitigation, with the results as follows:

3.1 Common factors and levels of community learning used to adapt and mitigate the effects of climate change

The results in (Table 2) show that informants were learning about and adapting to climate change to a high level (\bar{x} =3.41) However, there are two factors in which learning is moderate: (1) learning about violent events and disasters or understanding risks; Communities should accelerate awareness building (van Valkengoed et al., 2022; Abid et al., 2019); and (2) government support or policy approaches that require a participatory process, where the government should support projects that help communities reduce the impacts (Nydrioti et al., 2023).

Table 2. Common factors for learning about and adapting to climate change (361 households)

Learning elements and community adaptation	\bar{x}	S.D.	Learning level
1. Learning about violent events and disasters	3.05	0.971	moderate
2. Applying knowledge about the nature, ecosystems, and traditional wisdom relating to adaptation	3.56	0.941	high
3. The management needed to achieve adaptability	3.41	1.220	high
4. A shared vision success in adaptation	3.44	1.070	high
5. Collaboration	3.54	0.992	high
6. Adaptation options	3.53	0.971	high
7. Supporting guidelines or policy guidelines from the government	3.36	1.061	moderate
Total average	3.41	1.032	high

3.2 Learning and experiences in community resource management

To study the learning and experiences in community resource management, presenting the results and discussing the effects of phenomena, experiences, and learning used in adaptation, which will vary depending on the three different areas studied.

According to the study, “understanding of risk” is a factor in all three locations studied. In the riverside community, people understand that flooding is normal, as it occurs most years, as shown in (Figure 2), with heavy flooding every four years. The tillering of bamboo tops, or ant migration are indicators of flooding, signaling that the community must prepare to mitigate the impact. Steps such as preparing boats

are taken, and the community has a good understanding of risk and reduce its vulnerability. Where the community are accepting of recurring flooding, there is a change from negative to positive attitude, with boat races organized during floods. Adapting from crisis situations to opportunities is a coping mechanism, with flooding bringing fish, which are caught, dried, and sold to generate income for households, and also reduce the loss of income caused by the floods. In the mountain community, the people understand the signs and impacts of drought, so they have reduced the impact of climate change through integrated farming, which reduces water consumption. Finally, the coastal community has learned knowledge about ecology, making it possible to understand that the soil and water in the area accumulate salinity.




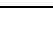



Figure 2. Flooded Hua Wiang District in 2022

Carmen et al. (2022) proposes that the use of social capital can promote adaptation and assist in proactive recovery, while Hosen et al. (2020) discusses the use of conventional ecological knowledge and observations of landscapes, plants, and soil (Table 3). Shahid et al. (2018) discusses salt degradation of soil, as soil salinity undermines the resource base and reduces soil quality, negatively impacting agricultural productivity and sustainability. The impact of these conditions can be mitigated

against by developing soil use and management policies. However, it is important that communities can organize and manage themselves, so stimulating awareness in the community is necessary for them to participate in adaptation. This is in line with Abid et al. (2019), who reflect on the steps of adaptation, beginning with perception, intention, and adaptability. There are also other factors such as education, experience, cooperation, access to weather forecasts.

Table 3. Learning about violent events and disasters

	Statement of fact	Reference
	Understanding about the landscape, plants, and soil	Hosen et al. (2020)
	Understand and awareness in flood disaster management	Frank Jerome (2021)
	Farmers who are knowledgeable about mixed farming can better adapt to it	Abunyewah et al. (2023)
	Threatened biodiversity, local economy, and society	Romero Manrique et al. (2018)
	Affected by the salinity of the soil and water	Shahid et al. (2018)

“Local wisdom” is knowledge that comes from experience in working with local resources and ecosystems. In the riverside community, the experience of living through repeated floods led to knowledge being gained that *Elaeocarpus hygrophilus* Kurz are the only fruit trees that can survive in extreme flood situations. Mountain communities know to reduce the evaporation of groundwater by providing shade with banana trees, thereby allowing their vegetables to obtain water naturally, so farmers do not need to water their vegetables as much. In coastal communities, most of the soil has high levels of salinity, so wisdom advises locals to improve the soil or import the soil from outside and using it in elevated pots to generate income (Figure 3). Collectively, the reviews of conventional wisdom to discover species of plants that have good growth properties in saline

conditions, such as coconut palms, betel nut trees, and mango are encouraged (Figure 4).

Local wisdom is a common and simple approach used by communities when faced with problems. Dhungana et al. (2023) states that knowledge from past experiences can help communities gain acceptance because those experiences relate to the lifestyle of the community (Table 4). In addition, communities use local wisdom to assess the situation (Kansuntisukmongkol, 2017), such as when predicting the expected flooding or drought levels each year. Mountain communities aim at sustainability in food production systems, in line with Singh and Singh (2017), who state that recognizes that conventional wisdom in farming has been around for a long time and is a wise approach when adaptation is needed because of a changing climate to produce sustainable levels of food.






Figure 3. Planting ornamental plants in pots to solve soil and salinity issues



Figure 4. Original garden or raised grove garden trees in the ground

Table 4. Applying knowledge about the nature, ecosystems, and traditional wisdom relating to adaptation

	Statement of fact	Reference
	Integrating traditional knowledge into strategic	Kansuntisukmongkol (2017)
	Knowledge from past experiences can help with acceptance	Dhungana et al. (2023)
	Traditional agriculture in the context of sustainable food is a climate-smart approach	Singh and Singh (2017)
	Traditional ecological knowledge in coastal communities	Leonard (2021)

Communities need to create local management systems to adapt systematically as the increased levels of climate change cause seasonal shifts. The rainy season is arriving earlier than usual more often, and floods are occurring at an increasing rate. Therefore, the riverside community needs to plan the crops planted in advance, shifting the seeding time to earlier than before and encouraging new seedling sowing times to be faster than ever before.




In the communities studied, they have managed this themselves by creating local management systems that have developed a water management

system that uses a systematic manner to allow water flow paths to be linked with household water systems ([Figure 5](#)). The mountain community uses local management systems to assess the situation, plan, and supervise water management systematically, in line with a study by [Ghorbani et al. \(2021\)](#) that discussed that local management systems can occur spontaneously, and help enhance resilience from drought ([Table 5](#)). [Adger et al. \(2009\)](#) recommends integrating climate change risks into lifestyles, where knowledge, skills and practices change attitudes or behaviors in each society.



Figure 5. Household water management by storing water in shallow wells

Table 5. The management needed to achieve adaptability

	Statement of fact	Reference
	Importance of participatory, planning, and ecosystem-based adaptation	Reid (2016)
	Water management, store aqueducts' water inside the pool, reservoirs, and natural dams	Ghorbani et al. (2021)
	Low-cost agriculture by producing organic fertilizer instead of chemical fertilizers	Heisse and Morimoto (2023)
	Study on the planting of salt-tolerant plants	Rivero et al. (2022)

Community practice is an informal coherence, with households in mountain communities reducing their dependence on water for agricultural use during the dry season, and restoring household wells to increase the amount available. Coastal communities have created floating markets, and riverside community building a common consensus on using public spaces to provide assistance to the vulnerable households affected by flooding. By sharing private




land and creating evacuation sites for the victims, the community can quickly return to normalcy. Focus on building partnerships and building resilience to adaptation.

“Shared public spaces” is a concrete form of riverside community practice, where farmers have adopted adaptation practices to reduce their impacts ([Khanal et al., 2019](#)). Public spaces are connected to passable roads to enable connection to public

transportation, which reduces journey times dramatically. Space also allows use for other purposes, such as setting up tents for victims, and the creation of public restrooms. The project was successful as it enhanced the livelihoods and security of the community.

There are tangible results from the project, including the reduction in dependence from external agencies as communities worked together to create common goals to achieve justice and equality. Those who participated felt a more meaningful connection to the community (Ardoin et al., 2023) (Table 6).

Table 6. A shared vision success in adaptation





Statement of fact	Reference
 Connection between civic engagement and environment education in area	Ardoin et al. (2023)
 Water management link to small farmers	Chandra et al. (2023)
 Stakeholder engagement in floating market	Kulsum et al. (2020)

Community collaboration in the three locations has different patterns, depending on the problems and situations affected by climate change. Community collaboration focuses on integration and networking, and in the riverside community, collaboration between communities and government agencies through communication channels, mainly LINE groups, was used to closely monitor water levels. In the mountain community, fruit growers shared knowledge between community leaders, volunteers, and farmers, providing advice on high-quality cultivation techniques amid climate change. In the coastal community, collaboration between different agencies helped communities adapt.

A study by Vogel et al. (2020) indicated that community levels are most severely affected by climate change, so, it is imperative to bring collaboration into local adaptation policies and planning. Carmen et al. (2022) stated that climate

change challenges are complex issues that require partnerships to be built to encourage a proactive recovery. The coastal community created a collaborative network that coordinates joint action. Such cooperation is a social strategy to reduce risk, which can occur in the form of product networks, knowledge, cooperatives, enterprises, and occupational groups, in line with the work of (Kansuntisukmongkol, 2017). Communities collaborate with networks and agencies at (1) group level, “Bang Num Phueng Sufficiency Economy Group”, (2) local level, there are six sub-districts “Khung BangKachao Network” (Rambaree et al., 2019) (Table 7), and (3) at the national level “OUR Khung BangKachao” in which thirty-four organizations in the private and public sectors collaborate. Holme and Rocha (2023) reflect that networking can help address the complexity of climate change.

Table 7. Community collaboration

Statement of fact	Reference
 Awareness network and participatory manner with government agencies	Orathai et al. (2019)
 Supporting innovative agricultural practices	Ensor et al. (2019)
 The loosely organized group “Bang KaChao Group”	Case and Zeglen (2018)
 Development work between the local municipal and community	Rambaree et al. (2019)

Adaptation options are created after climate change is recognized, understood, and accepted. The three communities had separate coping mechanisms, with the riverside community formulating a disaster response plan, whereas the coastal community looked towards income generation. Opportunities related to community tourism, such as bicycle rental, boat rental, cafes, home stays, food sales, and Thai massage were common. In the mountain community, the people had

adapted by connecting a variety of adaptation options, such as switching from a monoculture to an integrated farming method to reduce the risks of drought (Figure 6), which resulted in a diversified income for the community. Previously, there was one annual income from selling rice, but now there was added value from agricultural products.

In addition, resources were being maximized for benefit (Feleke et al., 2016) (Table 8), including

the processing of santol, as the skin is damaged by off-season rains. [Nonvide \(2023\)](#) reflects that if farmers have land security, they should make strategic choices to adapt to climate change. As such, farmers have changed their focus from mass production to high-quality products, including high-quality organic fruits

([Yakah, 2016](#)). Adaptation has resulted in a better quality of life for people in the community, both economically and socially, and they are more motivated to protect themselves rather than be afraid of the higher risks ([Bagambilana and Rugumamu, 2023](#)).



Figure 6. Integrated vegetable and fruit planting to diversify the risks of climate change

Table 8. Adaptation options

	Statement of fact	Reference
	Changing the sowing time to be faster	Nonvide (2023)
	Agriculture and ecology influence adaptation	Feleke et al. (2016)
	Water system interconnections by community	Maliva (2021)
	Diversity of income, market development, and prompt households to diversity activities	Jalal et al. (2021)

Government support can result in two resolutions: (1) it can support efficient adaptation; and (2) it can resist the community led adaptations. The three locations received support that led to both resolutions. The mountain community, which received support from the government, shifted how it worked with communities to be proactive, reducing dependence on the climate in the economic dimension and improved human empowerment.

The coastal community benefitted from the construction of large public dams, but they proved to be a barrier to the community’s adaptation as the community had not adapted successfully to the circulation of water being halted by the dams. Salt water accumulated in the area, resulting in salinity in the soil and water. Before the dams, the tide removed salinity from the soil. According to [Mei et al. \(2016\)](#), government policy of building large structures hoped to control downstream flooding. [Lempérière \(2017\)](#) and [Kundzewicz et al. \(2018\)](#) discussed when investigated how dam construction regulated the flow





of water ([Table 9](#)). The state has facilitated the construction of dams for the right reasons, but it has caused difficulties for the communities. Therefore, it can be seen that flood prevention policies with dam construction is not successful for all areas, and that dam construction needs to be accompanied by assistance with adaptation ([Jayadas and Ambujam, 2023](#)).

This contrasts with riverside communities, which are good examples of stakeholder participatory work. Government and communities have worked together to recognize floods and reduce their impacts. For these communities, the government support has been a force for good, with governor-led community consultation on the accumulated release of water from the north and the rainfall in the area helpful. Both parties agreed to determine when water would be released into the fields, resulting in the decision to release it on September 15th every year. The government support has led to action for community adaptation, with [Kansuntisukmongkol \(2017\)](#)

documenting planting adaptation by advanced planning in areas with shifting seasons. Efficient plans also reduce the costs for government budgets, and increase revenues for the communities, as if the rice is not harvested in time, the government is required to

pay compensation based on the value of the damage. In addition, the state has to spend money on rehabilitation for farmers after another disaster (Young et al., 2019).

Table 9. Supporting guidelines or policy guidelines from the government

Statement of fact	Reference
 Adaptation policy of the flooding situation by the governor and community	Young et al. (2019)
 Stakeholder perception, awareness, and involvement	Nydrioti et al. (2023)
 Integrated water management, and implement a drought policy that would be proactive	Marengo et al. (2022)
 The construction of a dam to block salt water	Lempérière (2017)

3.3 Community adaptation patterns to cope with climate change

Community adaptation patterns to cope with climate change by creating environmental education models based on community adaptation to climate

change. Howard’s (2013) theoretical and model framework of phenomenon theory was applied in this study, which focuses on situations from the perspectives of experience and adaptation, as shown in Figure 7.

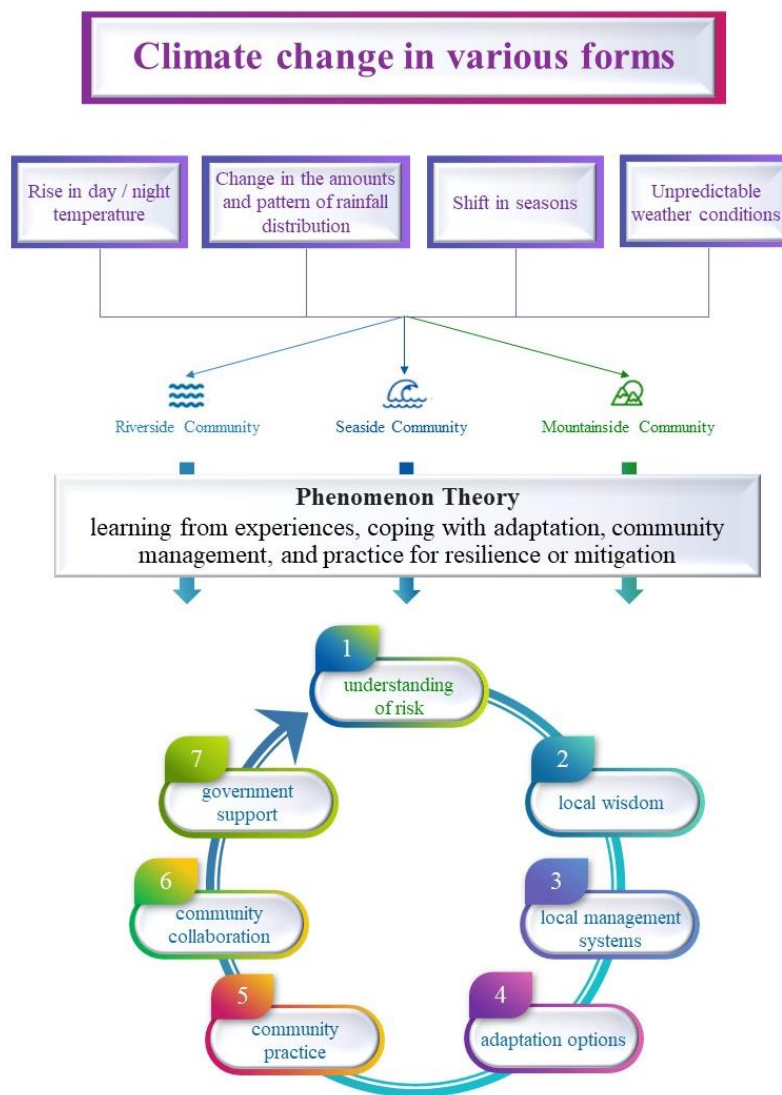


Figure 7. A framework of community adaptation for climate change

4. CONCLUSIONS

Common factors in community adaptation to mitigate the impacts of climate change consist of seven factors: (1) understanding of risk; (2) local wisdom; (3) local management systems; (4) adaptation options; (5) community practice; (6) community collaboration; and (7) government support. Overall, communities have learned to adapt to climate change at a high level. From the study of experience and learning to manage community resources, it was found that strong communities are characterized by self-management and community, relying on the resource base and environment before outside assistance. However, when provided, they are, accepting, open-minded, and have a positive attitude, which helps to reduce the impact of climate change. In addition, economic, social, and natural resources and environmental factors differ each area. Researchers have developed an environmental education model for community adaptation to climate change, an innovative integrated environmental education that can be used as a guideline to develop people in the community to raise environmental awareness in other community areas. However, future research is recommended, and they should select study locations that cover all regions, and a comparative study should be conducted.

ACKNOWLEDGEMENTS

Many thanks are due to the Human Research Ethics Committee of Mahidol University, Thailand (Certificate of Approval Number 2017/134.2706) for their approval. Finally, we thank all the community residents and community organisations for their support and enthusiasm for this study.

REFERENCES

- Abid M, Scheffran J, Schneider UA, Elahi E. Farmer perceptions of climate change, observed trends and adaptation of agriculture in Pakistan. *Environmental Management* 2019;63(1):110-23.
- Aboda C, Vedeld PO, Byakagaba P, Lein H, Nakakaawa CA. Household capacity to adapt to resettlement due to land acquisition for the oil refinery development project in Uganda. *Environment, Development and Sustainability* 2023;25(11):13125-47.
- Abunywah M, Erdiaw-Kwasie MO, Acheampong AO, Arhin P, Okyere SA, Zanders K, et al. Understanding climate change adaptation in Ghana: The role of climate change anxiety, experience, and knowledge. *Environmental Science and Policy* 2023;150:Article No. 103594.
- Adger WN, Lorenzoni I, O'Brien KL. Adaptation now. In: Lorenzoni I, O'Brien KL, Adger WN, editors. *Adapting to Climate Change: Thresholds, Values, Governance*. Cambridge: Cambridge University Press; 2009. p. 1-22.
- Anh Tran T. Learning as an everyday adaptation practice in the rural Vietnamese Mekong Delta. *Climate and Development* 2020;12(7):610-3.
- Ardoin NM, Bowers AW, Gaillard E. A systematic mixed studies review of civic engagement outcomes in environmental education. *Environmental Education Research* 2023;29(1):1-26.
- Bagambilana FR, Rugumamu WM. Determinants of farmers' adaptation intent and adoption of adaptation strategies to climate change and variability in Mwanza District, Tanzania. *Environmental Management* 2023;72(4):785-804.
- Brown C, Boltz F, Freeman S, Tront J, Rodriguez D. Resilience by design: A deep uncertainty approach for water systems in a changing world. *Water Security* 2020;9:Article No. 100051.
- Carmen E, Fazey I, Ross H, Bedinger M, Smith FM, Prager K, et al. Building community resilience in a context of climate change: The role of social capital. *Ambio* 2022;51:1371-87.
- Carter SM, Shih P, Williams J, Degeling C, Mooney-Somers J. Conducting qualitative research online: Challenges and solutions. *The Patient-Patient-Centered Outcomes Research* 2021;(14):711-8.
- Case RA, Zeglen L. Exploring the ebbs and flows of community engagement: The pyramid of engagement and water activism in two Canadian communities. *Journal of Community Practice* 2018;26(2):184-203.
- Chandra A, Heeren DM, Odhiambo L, Brozović N. Water-energy-food linkages in community smallholder irrigation schemes: Center pivot irrigation in Rwanda. *Agricultural Water Management* 2023;289:Article No. 108506.
- Coppock DL, Pandey N, Tulachan S, Duwal D, Dhungana M, Dulal BP, et al. Non-formal education promotes innovation and climate change preparedness among isolated Nepalese farmers. *Climate and Development* 2022;14(4):297-310.
- Dhungana G, Pal I, Ghimire R, Dhungana RK, Tuladhar N. Foundation of indigenous knowledge theory for disaster risk reduction. In: Pal I, Shaw R, editors. *Multi-Hazard Vulnerability and Resilience Building*. Elsevier; 2023. p. 347-61.
- Eckstein D, Künzel V, Schäfer L, Wings M. *Global Climate Risk Index 2021: Who suffers most from extreme weather events? Weather-related loss events in 2019 and 2000 to 2019*. Bonn: Germanwatch e.V; 2021.
- Ensor JE, Wennström P, Bhattarai A, Nightingale AJ, Eriksen S, Sillmann J. Asking the right questions in adaptation research and practice: Seeing beyond climate impacts in rural Nepal. *Environmental Science and Policy* 2019;94:227-36.
- United States Environmental Protection Agency (U.S. EPA). Report on the 2015 U.S. Environmental Protection Agency (EPA) International Decontamination Research and Development Conference. EPA/600/R-15/283. Washington DC: U.S. Environmental Protection Agency; 2015.
- Feleke FB, Berhe M, Gebru G, Hoag D. Determinants of adaptation choices to climate change by sheep and goat farmers in Northern Ethiopia: The case of Southern and Central Tigray, Ethiopia. *Springerplus* 2016;5(1):Article No. 1692.
- Frank Jerome G. Flood disaster hazards; Causes, impacts and management: A state-of-the-art review. In: Ehsan Noroozinejad F, editor. *Natural Hazards*. Rijeka: IntechOpen; 2021. p. 1-18.
- Ghorbani M, Eskandari-Damaneh H, Cotton M, Ghoochani OM, Borji M. Harnessing indigenous knowledge for climate

- change-resilient water management-lessons from an ethnographic case study in Iran. *Climate and Development* 2021;13(9):766-79.
- Hesse C, Morimoto R. Climate vulnerability and fertilizer use-panel evidence from Tanzanian maize farmers. *Climate and Development* 2023. DOI: 10.1080/17565529.2023.2206373.
- Holme P, Rocha JC. Networks of climate change: Connecting causes and consequences. *Applied Network Science* 2023;8:Article No. 10.
- Hosen N, Nakamura H, Hamzah A. Adaptation to climate change: Does traditional ecological knowledge hold the key? *Sustainability* 2020;12(2):Article No. 676.
- Howard P. "Everywhere you go always take the weather with you": Phenomenology and the pedagogy of climate change education. *Phenomenology and Practice* 2013;7(2):3-18.
- Intergovernmental Panel on Climate Change (IPCC). *Climate Change 2014-Impacts, Adaptation and Vulnerability: Working Group II Contribution to the Fifth Assessment Report of the Intergovernmental Panel on Climate Change*. Cambridge: Cambridge University Press; 2014.
- Intergovernmental Panel on Climate Change (IPCC). *Climate Change 2022-Impacts, Adaptation and Vulnerability: Working Group II Contribution to the Sixth Assessment Report of the Intergovernmental Panel on Climate Change*. Cambridge: Cambridge University Press; 2023.
- Ishtiaq M. Book review Creswell, J. W. 2014. *Research design: Qualitative, quantitative and mixed methods approaches*. (4th ed.), Thousand Oaks CA: Sage. *English Language Teaching* 2019;12(5):40-1.
- Jalal MJE, Khan MA, Hossain ME, Yedla S, Alam GMM. Does climate change stimulate household vulnerability and income diversity? Evidence from southern coastal region of Bangladesh. *Heliyon* 2021;7(9):Article No. 07990.
- Jayadas A, Ambujam NK. A quantitative assessment of vulnerability of farming communities to extreme precipitation events in Lower Vellar River sub-basin, India. *Environment, Development and Sustainability* 2023;25(11):13541-63.
- Khanal U, Wilson C, Hoang V-N, Lee B. Impact of community-based organizations on climate change adaptation in agriculture: Empirical evidence from Nepal. *Environment, Development and Sustainability* 2019;21(2):621-35.
- Krueger R, Casey MA. Designing and conducting focus group interviews. In: Krueger R, Casey MA, Donner J, Kirsch S, Maack J, editors. *Social Analysis: Select Tools and Techniques*. Washington, DC: The World Bank; 2001. p. 4-23.
- Kulsum U, Timmermans J, Khan MSA, Thissen W. A conceptual model-based approach to explore community livelihood adaptation under uncertainty for adaptive delta management. *International Journal of Sustainable Development and World Ecology* 2020;27(7):583-95.
- Kansantisukmongkol K. Philosophy of sufficiency economy for community-based adaptation to climate change: Lessons learned from Thai case studies. *Kasetsart Journal of Social Sciences* 2017;38(1):56-61.
- Kundzewicz ZW, Hegger DLT, Matczak P, Driessen PJP. Opinion: Flood-risk reduction: Structural measures and diverse strategies. *Proceedings of the National Academy of Sciences of the United States of America* 2018;115(49):12321-5.
- Lempérière F. Dams and floods. *Engineering* 2017;3(1):144-9.
- Leonard K. WAMPUM Adaptation framework: Eastern coastal Tribal Nations and sea level rise impacts on water security. *Climate and Development* 2021;13(9):842-51.
- Likert R. The method of constructing and attitude scale. In: Fishbein M, editor. *Readings in Attitude Theory and Measurement*. New York: John Wiley and Sons; 1967. p. 90-5.
- Maliva R. Adaptation options. In: Maliva R, editor. *Climate Change and Groundwater: Planning and Adaptations for a Changing and Uncertain Future: WSP Methods in Water Resources Evaluation Series No 6*. Cham: Springer International Publishing; 2021. p. 215-50.
- Marengo JA, Galdos MV, Challinor A, Cunha AP, Marin FR, Vianna Mds, et al. Drought in Northeast Brazil: A review of agricultural and policy adaptation options for food security. *Climate Resilience and Sustainability* 2022;1(1):Article No. 17.
- Mastrandrea MD, Heller NE, Root TL, Schneider SH. Bridging the gap: Linking climate-impacts research with adaptation planning and management. *Climatic Change* 2010;100(1):87-101.
- Mei X, Van Gelder PHAJM, Dai Z, Tang Z. Impact of dams on flood occurrence of selected rivers in the United States. *Frontiers of Earth Science* 2016;11(2):268-82.
- Ministry of Natural Resources and Environment (MNRE). *Climate Change Master Plan (CCMP) (2015-2050)*. The office of Natural Resources and Environmental Policy and Planning: MNRE; 2015.
- Mohr Carney M, Adams D, Mendenhall A, Ohmer M. The lens of community. *Journal of Community Practice* 2022;30(2):105-8.
- National Economic and Social Development Plan (NESDP). Draft: Thailand's 13th National Economic and Social Development Plan (2023-2027) [Internet]. 2021 [cited 2022 Oct 1]. Available from: <https://mocplan.ops.moc.go.th/th/content/category/detail/id/94/iid/6024>.
- Nonvide GMA. Does land security matter in adapting to climate change? An empirical evidence from Benin. *Climatic Change* 2023;176(10):Article No. 143.
- Nydrioti LSL, Katsiardi P, Assimacopoulos D. Stakeholder perceptions on climate change impacts and adaptation actions in Greece. *Euro-Mediterranean Journal for Environmental Integration* 2023;8(4):777-93.
- Orathai L, Anuwat W, Winitha C, Rapin Y. Enhancing the effectiveness of participatory management approach for local communities in the repeatedly flooded areas in the District of Warinchamrab, Ubon Ratchathani Province. *Local Administration Journal* 2019;12(1):87-110 (in Thai).
- Rambaree K, Sjöberg S, Turunen P. Ecosocial change and community resilience: The case of "Bönan" in global transition. *Journal of Community Practice* 2019;27(3-4):231-48.
- Rashidi MN, Begum RA, Mokhtar M, Pereira JJ. The conduct of structured interviews as research implementation method. *Journal of Advanced Research Design* 2014;1(1):28-34.
- Reid H. Ecosystem- and community-based adaptation: Learning from community-based natural resource management. *Climate and Development* 2016;8(1):4-9.
- Reynolds MP, Ortiz R. Adapting crops to climate change: A summary. In: Reynolds MP, editor. *Climate Change and Crop Production*. Wallingford UK: CABI; 2010. p. 1-8.
- Rivero RM, Mittler R, Blumwald E, Zandalinas SI. Developing climate-resilient crop: Improving plant tolerance to stress combination. *The Plant Journal* 2022;109(2):373-89.

- Romero Manrique D, Corral S, Guimarães Pereira Â. Climate-related displacements of coastal communities in the Arctic: Engaging traditional knowledge in adaptation strategies and policies. *Environmental Science and Policy* 2018;85:90-100.
- Shahid SA, Zaman M, Heng L. Soil Salinity: Historical perspectives and a world overview of the problem. In: Zaman M, Shahid SA, Heng L, editors. *Guideline for Salinity Assessment, Mitigation and Adaptation Using Nuclear and Related Techniques*. Cham: Springer International Publishing; 2018. p. 43-53.
- Singh R, Singh GS. Traditional agriculture: A climate-smart approach for sustainable food production. *Energy, Ecology and Environment* 2017;2(5):296-316.
- Smith AC, Tasnim T, Irfanullah HM, Turner B, Chausson A, Seddon N. Nature-based solutions in Bangladesh: Evidence of effectiveness for addressing climate change and other sustainable development goals. *Frontiers in Environmental Science* 2021;9:Article No. 737659.
- Steg L. Values, norms, and intrinsic motivation to act proenvironmentally. *Annual Review of Environment and Resources* 2016;41(1):277-92.
- Tee Lewis PG, Chiu WA, Nasser E, Proville J, Barone A, Danforth C, et al. Characterizing vulnerabilities to climate change across the United States. *Environment International* 2023;172: Article No. 107772.
- United States Agency for International Development (USAID). *Confronting the climate crisis in Southeast Asia* [Internet]. 2022 [cited 2024 Feb 6]. Available from: <https://www.usaid.gov/asia-regional/fact-sheets/confronting-climate-crisis-southeast-asia-regional-approach>.
- van Valkengoed AM, Perlaviciute G, Steg L. Relationships between climate change perceptions and climate adaptation actions: Policy support, information seeking, and behaviour. *Climatic Change* 2022;171(1-2):Article No. 10584.
- Vogel B, Henstra D, McBean G. Sub-national government efforts to activate and motivate local climate change adaptation: Nova Scotia, Canada. *Environmental, Developmental and Sustainability* 2020;22(2):1633-53.
- Yakah JA. *Mechanisms and Pathways for Climate-sensitive Transformational Change of Smallholder Agriculture in Ghana* [dissertation]. Accra, University of Ghana; 2016.
- Yamane T. *Statistics: An Introductory Analysis*. 3rd ed. New York: Harper and Row Publication; 1973.
- Young HR, Cornforth RJ, Gaye AT, Boyd E. Event Attributing science in adaptation decision-making: The context rain fall in urban Senegal. *Climate and Development* 2019;11(9):812-24.

Seagrass Community Structure and Ecosystem Carbon Stocks Along the Shoreline of Semujur Island, Bangka Belitung Province, Indonesia

Aldina Himmari Muliawati* and Devi N. Choesin

School of Life Sciences and Technology, Institut Teknologi Bandung, Ganeca Street 10, Bandung 40132, Indonesia

ARTICLE INFO

Received: 14 Nov 2023
Received in revised: 13 Feb 2024
Accepted: 19 Feb 2024
Published online: 2 Apr 2024
DOI: 10.32526/ennrj/22/20230325

Keywords:

Blue carbon/ Carbon storage/
Coastal ecosystem/ *Halodule
 uninervis*/ Organic carbon

* Corresponding author:

E-mail:
aldinahimmari@gmail.com

ABSTRACT

Seagrass meadows serve as vital blue carbon ecosystems, sequestering significant amounts of CO₂ and playing a crucial role in climate change mitigation. Semujur Island, located in the Bangka Belitung Province, exemplifies numerous small Indonesian islands boasting extensive seagrass meadows lining their shores. This research seeks to (1) describe the community structure of seagrass on Semujur Island, (2) assess the carbon storage within the seagrass ecosystem, and (3) analyze the relationship between seagrass community structure and carbon reserves across three distinct sites. According to the results of this study, there are eight species of seagrass on Semujur Island, i.e., *Cymodocea rotundata*, *Enhalus acoroides*, *Halodule uninervis*, *Halophila ovalis*, *Oceana serrulata*, *Syringodium isoetifolium*, *Thalassia hemprichii*, and *Thalassodendron ciliatum*. Diversity indices varied among sites, ranging from 1.48 to 1.72. Species evenness indices varied between 0.83 and 0.92, while dominance indices varied between 0.20 and 0.28. The highest estimated carbon stock was obtained at the site dominated by the species *H. uninervis* (75.11 MgC/ha); followed by the site dominated by *T. hemprichii* (50.55 MgC/ha). The correlation between seagrass community structure, including density and coverage, and carbon stocks demonstrated a moderate positive correlation, with coefficients of 0.430 and 0.528, respectively ($p < 0.05$). This research highlights the significance of integrating ecological dynamics into the management of seagrass ecosystems to enhance climate change mitigation efforts. Additionally, it offers valuable data as a reference for the restoration and conservation of seagrass ecosystems.

1. INTRODUCTION

Climate change is a global threat and challenge affecting countries around the world (James et al., 2023; Losciale et al., 2023). The situation is exacerbated by the rising levels of greenhouse gases, including CO₂, CH₄, and N₂O in the atmosphere, primarily driven by increased human activities (Cassia et al., 2018). Climate change mitigation endeavors have primarily focused on terrestrial vegetation, such as forests and plantations, as carbon sinks, often neglecting the potential contribution of coastal ecosystems (Bandh et al., 2023). Coastal ecosystems are renowned for their remarkable capacity to sequester and store carbon. Among the 'blue carbon ecosystems' in the tropical region, mangroves,

seagrass meadows, and tidal swamps play pivotal roles in this regard (Hilmi et al., 2021). In particular, seagrass ecosystems exhibit an impressive capability to store carbon, with an astonishing capacity of 830 MgC/ha, thereby surpassing the carbon absorption potential of terrestrial forests, which stands at 300 MgC/ha (Fourqurean et al., 2012). Seagrass meadows possess an outstanding capacity for carbon sequestration, accomplished through the daily removal of carbon from the atmosphere. This carbon is then stored within seagrass tissues (0-10% of total carbon) and sediments (90-99% of total carbon) (Tahir et al., 2023; Stankovic et al., 2021).

Indonesia is characterized by its extensive coastline which spans 81,290 km and ranks as the

second longest globally, surpassed only by Canada (Lasabuda, 2013). The nation has emerged as a significant contributor, accounting for approximately 17% of the world's blue carbon reserves, which are crucial for climate change mitigation purposes (Alongi et al., 2015). Nevertheless, this portrayal is deemed incomplete in fully representing Indonesia's coastal ecosystems. Thus, there is an imperative for comprehensive exploration, particularly concerning coastal ecosystems such as seagrass meadows, to augment Indonesia's role in advancing climate change mitigation efforts.

Semujuur Island, located within the administrative region of the Bangka Belitung Islands in Indonesia, is encircled by extensive and pristinely conserved seagrass ecosystems, thereby serving as a representative microcosm of the broader state of seagrass meadows in Indonesia. This unique ecological site remains relatively underexplored in scientific research, lacks formal protection status, and exists in proximity to human communities actively engaging in or near these seagrass habitats.

Different seagrass meadow locations are expected to exhibit differences in their community structure, potentially influencing their capacity to absorb and retain carbon. This hypothesis emphasizes the importance of examining the correlation between community structure and carbon storage, underscoring its significance for forthcoming management strategies of seagrass ecosystems. Consequently, this study aimed to achieve the following purposes: (1) describe the community structure of seagrass around Semujuur Island; (2) estimate carbon stocks in the seagrass

ecosystem; and (3) analyze the relationship between seagrass community structure and carbon stocks.

2. METHODOLOGY

2.1 Area of study

Field data collection was conducted from January to February 2023 in the waters around Semujuur Island, Bangka Belitung Islands (2°09'00" South Latitude and 106°19'12" East Longitude) (Figure 1(a)). Sampling was carried out at three separate sites of seagrass meadows (designated as Mead-1, Mead-2, and Mead-3) which differed in general environmental conditions (Figure 1(b)). Mead-1 is situated furthest from the shoreline of Semujuur Island, approximately 1.17 km away. It is characterized by clear water conditions, depths ranging from 90 to 135 cm, and a notable abundance of macroalgae. The sediment composition at this site comprises coarse sand interspersed with mixed corals, remnants of faunal shells, and rocks. In contrast, Mead-2 is positioned closer to the island's shoreline, characterized by turbid water conditions attributed to its proximity to human settlements. The water depth ranges from 40 to 60 cm, and the area exhibits a significant presence of plastic and other debris. Sediment composition predominantly consists of coarse sand, occasionally interspersed with fine sand, and remnants of faunal shells. Lastly, Mead-3 is located near a shallow area that emerges during low tide, revealing seagrass beds. It features clear water conditions and depths ranging from 60 to 90 cm, with some macroalgae present. The sediment composition comprises mainly fine sand mixed with remnants of faunal shells.

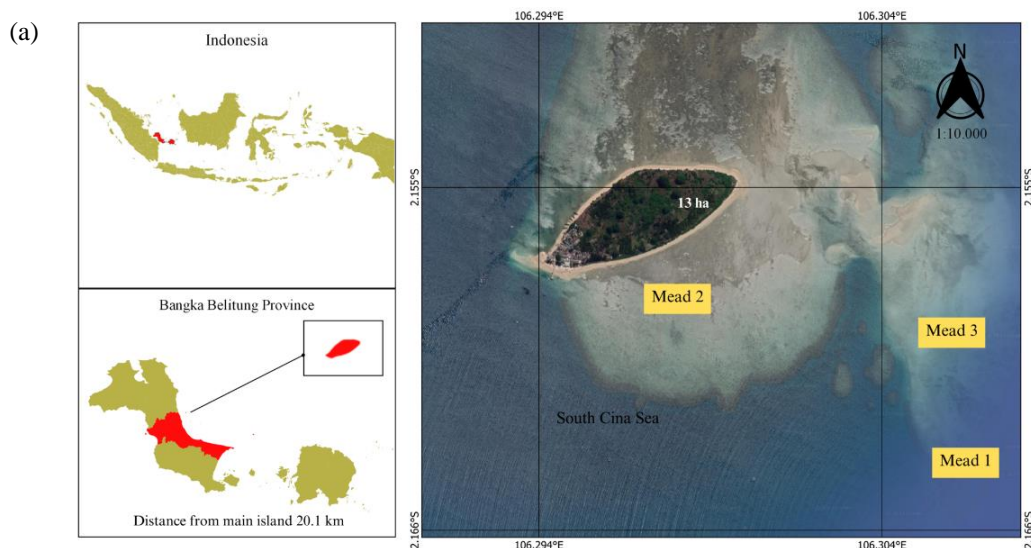


Figure 1. (a) Map of the study area in Semujuur Island and (b) Conditions of seagrass and sediment at the three meadow sites

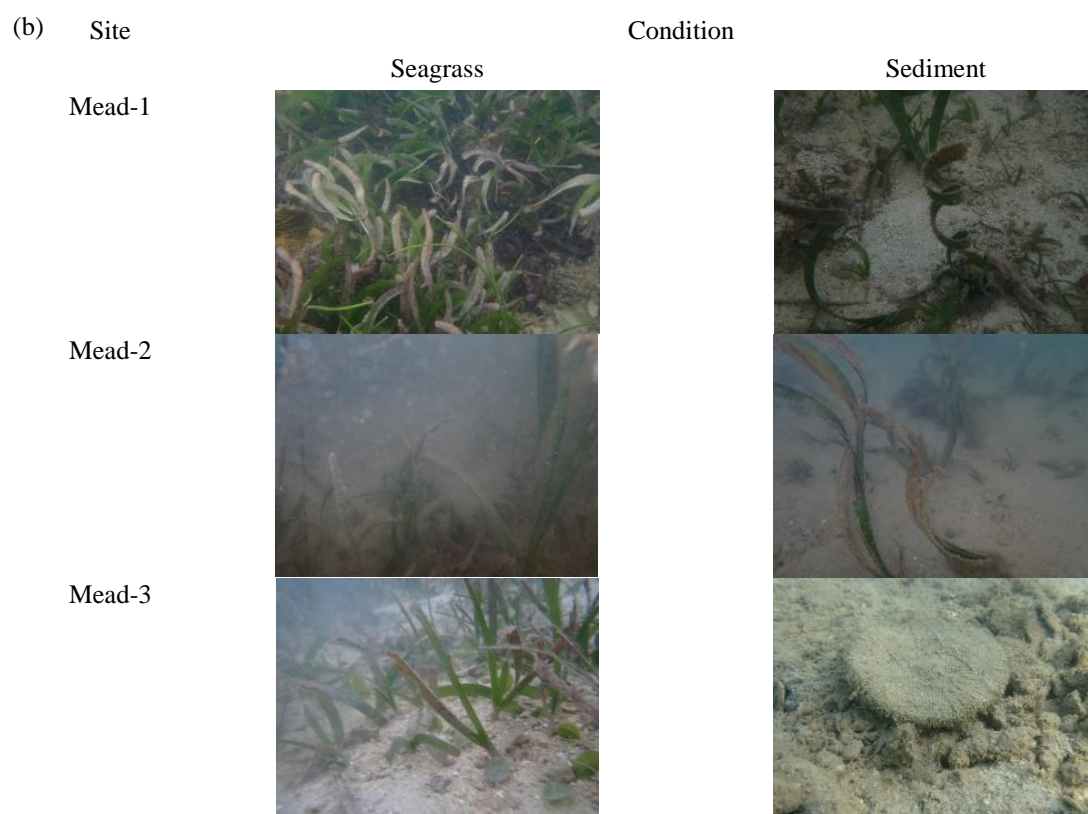


Figure 1. (a) Map of the study area in Semujur Island and (b) Conditions of seagrass and sediment at the three meadow sites (cont.)

Water quality measurements were found to vary among sites for certain parameters (Table 1). Water temperature, pH, and DO levels were assessed using a water quality meter (WQM, Combo Handeld AZ Instrument Model AZ 8603), while salinity was determined using a refractometer (ATC RZ 118). Total suspended solids (TSS) were quantified utilizing

a TSS meter within the Padjajaran University Integrated Laboratory. All parameters met the seawater quality standards for seagrass growth and development (Republic of Indonesia Government Regulation Number 22, 2021), except for turbidity in Mead-2 which exceeded the specified quality standard (TSS>5).

Table 1. Physico-chemical parameters of water at each site. Different superscripts within the same row indicate significant differences at $p<0.05$

	Site		
	Mead-1	Mead-2	Mead-3
Temperature (°C)	24.63±0.06 ^a	25.97±0.12 ^b	26.80±0.00 ^c
pH	8.35±0.00 ^a	8.44±0.05 ^b	8.41±0.02 ^{ab}
Dissolved oxygen (mg/L)	8.37±0.76 ^a	8.97±0.12 ^a	8.03±0.50 ^a
Salinity (‰)	30.33±0.58 ^b	28.00±0.00 ^a	28.33±1.15 ^a
Turbidity (FNU)	2.68±0.85 ^a	7.11±2.65 ^b	4.38±1.35 ^{ab}
Total suspended solid (mg/L)	12.33±11.15 ^a	14.00±9.00 ^a	19.00±19.92 ^a

2.2 Seagrass vegetation analysis

Vegetation analysis was undertaken to characterize the seagrass community structure at each site. This methodology was executed in accordance with the seagrass-watch protocol, as outlined by Rahmawati et al. (2019). Three parallel transect lines were delineated at each designated site, positioned

parallel to the shoreline and separated by 50 m. Seagrass species identification and assessment of coverage were conducted at intervals of 10 m along the transects, employing square quadrats measuring 50×50 cm. This process commenced from the 0-meter mark and continued to 100 m, encompassing a total of 11 quadrats per transect. Species abundance was

estimated within subplots measuring 25×25 cm within the quadrats. With three transects and 33 quadrat plots, the cumulative sampling area represented 10,000 m² or 1 hectare. Analysis of the collected data to

characterize the community structure at each site was performed utilizing the equations presented in [Table 2 \(Odum, 1993\)](#).

Table 2. Parameters and formula for seagrass vegetation analysis ([Odum, 1993](#))

Parameter	Formula	Description
Species density	$D = \frac{\sum ni}{Ai}$	D=seagrass density (ind/m ²) ∑ni=number of individuals of seagrass species (ind) Ai=transect area (m ²)
Shannon-wiener diversity index	$H' = - \sum_{i=1}^n (pi \ln pi)$	H'=diversity Index pi=the proportion of individuals of each species belonging to the i th species (ni) of the total number of individuals (N)
Simpson evenness index	$E = \frac{H'}{H_{max}}$	E=evenness Index H'=diversity Index H _{max} =log of number of seagrass species
Simpson dominance index	$D = \sum_{i=1}^n (pi)^2$	D=simpson Index pi=the proportion of individuals of each species belonging to the i th species (ni) of the total number of individuals (N)

2.3 Carbon stock measurement

Seagrass biomass data were collected by extracting samples from each observed seagrass species within every transect. This involved carefully prying to obtain all parts of the plant. During the sampling process, 5-10 individuals of each identified seagrass species were collected, or an approximate weight of 200 grams per species was obtained. These samples were meticulously cleaned to remove any attached organisms or debris. Subsequently, each seagrass plant was separated into its above-ground biomass (AGB), comprising leaves and sheaths, and below-ground biomass (BGB), consisting of roots and rhizomes. This facilitated a detailed and robust analysis of carbon distribution within the seagrass ecosystem, obtaining robust data and providing insights into the contribution of different plant components to carbon sequestration and storage dynamics. Subsequently, the seagrass samples were subjected to drying in a laboratory oven at 60°C for a period of 48-72 h until a constant weight was achieved ([Rahmawati et al., 2019](#)).

Regarding sediment sampling, sediment cores were extracted using PVC pipes measuring 50 cm in length and 5 cm (2 inches) in diameter. Three sediment samples were retrieved from each transect, totaling nine samples from each study site. The collected sediment cores were then stratified based on depth intervals (0-5 cm, 5-20 cm, and 20-50 cm). Following this, the samples underwent drying at 60°C for 48-72 h

until they reached a constant weight, rendering them ready for further analysis ([Rahmawati et al., 2019](#)).

Sediment compression factor was determined following the methods of [Rahmawati et al. \(2019\)](#), based on measurements of the total length of the PVC pipe used for sampling (A), the PVC length that penetrated the sediment/core length (E), the remaining PVC length which did not penetrate (B), the length of the sediment sample (D), and the part of the PVC pipe that was not filled with sediment (C). The formula used to determine the compaction correction factor is as follows:

$$\text{Compaction Correction Factor} = \frac{\text{Length of sediment sample (D)}}{\text{Depth of core (E)}}$$

The corrected sample (H') was calculated by multiplying the previously calculated correction factor by the length of the sediment sample without compaction (H). The results obtained were used to calculate bulk density.

$$\text{Corrected Sample (H')} = \text{Correction factor} \times \text{Length of sediment sample (H)}$$

Where; H'=length of sample collected; H=length of original sample (the length of sample without compaction).

Total biomass was calculated using the following equation:

$$B = W \times D$$

Where; B=total seagrass biomass (g/m²); W=individual biomass of seagrass species (g/ind); D=seagrass species density (ind/m²) (Rahmawati et al., 2019).

After obtaining the value of seagrass biomass, organic carbon was then measured using the dry ashing method (loss on ignition). The loss of sedimentary organic matter in the combustion process was determined using the following equation:

$$LOI = \left(\frac{W_o - W_t}{W_o} \times 100 \right)$$

Where; LOI=loss on ignition percentage (%); W_o=seagrass/sediment initial weight (g); W_t=seagrass/sediment final weight (g) (Rahmawati et al., 2019).

Organic content was analyzed using the following equation:

$$C_{org} = 0.43 \times LOI - 0.33$$

Where; C_{org}=organic carbon content percentage (%) (Rahmawati et al., 2019).

Carbon stocks in sediments were calculated using the following equation:

$$\text{Carbon storage in sediment (g } C_{org}/\text{cm}^3) = \text{DBD(dry bulk density)} \times C_{org} (\%)$$

Where; DBD=dry bulk density (g/cm³) (Rahmawati et al., 2019).

The total carbon stock in sediments was calculated per sample using the following equation (Rahmawati et al., 2019):

$$\text{Total of carbon storage in sediment (g } C_{org}/\text{cm}^2) = \text{carbon storage in sediment (g } C_{org}/\text{cm}^3) \times \text{sediment thickness (cm)}$$

2.4 Correlation analysis

A correlation analysis was performed using SPSS software to investigate the relationship between the community structure and carbon stock within the seagrass ecosystem. The Pearson correlation test, with a significance level set at 0.05, was employed to calculate the coefficient and assess the significance of the correlation. The correlation coefficient (r) has a value between $-1 \leq r \leq 1$. A correlation coefficient between 0 and +1 indicates positive correlation, while a coefficient between -1 and 0 indicates a negative correlation and is interpreted as outlined in Table 3 (Schober et al., 2018).

Table 3. Interpretation of r-value in Pearson Test (Schober et al., 2018)

No.	r Value	Interpretation
1	0.00-0.10	Negligible correlation
2	0.10-0.39	Weak correlation
3	0.40-0.69	Moderate correlation
4	0.70-0.89	Strong correlation
5	0.90-1.00	Very strong correlation

3. RESULTS AND DISCUSSION

3.1 Seagrass community structure

3.1.1 Species richness

Eight seagrass species were observed along the shorelines of Semujur Island. However, the composition of species varied slightly among the three surveyed sites (Table 4); this, in turn, indicated that not all species were uniformly distributed across the sites. A total of six to seven seagrass species were documented in each site. Notably, the presence of *T. ciliatum* and *O. serrulata* was exclusive to Mead-1, suggesting a more constrained spatial range for these species, with their distribution influenced by substrate and abiotic factors. Notably, *T. ciliatum* and *O. serrulata* are recognized for their preference for hard substrate habitats, particularly comprising dead coral fragments and exposure to strong wave actions and currents (Verheij, 1993; Short and Coles, 2001; Priosambodo, 2007). Mead-1 is located farthest from the shoreline and is therefore more exposed to waves and currents. The suitability between the ecological preferences of these two species and the prevailing environmental conditions and substrate type at Mead-1 explains their limited presence at this particular site.

Cymodocea rotundata was recorded in both Mead-2 and Mead-3, which are characterized by substrate that is ideally suited for the growth and development of this species, i.e., composed of a mixture of sand particles intermingled with the remnants of faunal shells. A study conducted by Rawung et al. (2018) found that this species can grow and develop well in such substrate conditions. Additionally, these sites were relatively shallow, and become exposed during low tide, producing conditions that favor the growth of *C. rotundata*. According to Bchir et al. (2019), *C. rotundata* thrives in sunlit waters and falls within the category of cosmopolitan seagrass species, capable of thriving in a wide range of habitats. This adaptation is consistent with the environmental conditions found in Mead-2 and Mead-3, where *C. rotundata* was observed. These

sites offer an optimal depth range, approximately 40 to 110 cm, which is shallower compared to Mead-1. The adequate depth in Mead-2 and Mead-3 provides

the requisite conditions for the growth and development of *C. rotundata*, as it ensures effective light penetration.

Table 4. Seagrass species richness at each site

Species	Mead-1	Mead-2	Mead-3
<i>Cymodocea rotundata</i> Asch. and Schweinf	-	+	+
<i>Enhalus acoroides</i> (Linnaeus F.) Royle, 1839	+	+	+
<i>Halodule uninervis</i> (Forssk) Asch	+	+	+
<i>Halophila ovalis</i> (R. Brown) Hooker f., 1858	+	+	+
<i>Oceana serrulata</i> (R. Brown) Byng and Christenh	+	-	-
<i>Syringodium isoetifolium</i> (Asch.) Dandy	+	+	+
<i>Thalassia hemprichii</i> (Ehrenberg) Ascherson, 1871	+	+	+
<i>Thalassodendron ciliatum</i> (Forssk.) Hartog	+	-	-
Total number of species	7	6	6

Description: (+)=species present, (-)=species absent

3.1.2 Species density

Seagrass species density is affected by a variety of site-specific factors, including water depth, turbidity, current velocity, and substrate type. The mean seagrass densities observed at Mead-1, Mead-2, and Mead-3 were 560 individuals/m², 241.34 individuals/m², and 602.67 individuals/m², respectively. The higher seagrass densities at Mead-1

and Mead-3 can be attributed to *H. uninervis* and *E. acoroides*, whereas *T. hemprichii* exhibited the highest density at Mead-2. The variation in species density observed across the data collection sites (Figure 2) is likely attributable to differences in environmental and sediment conditions among these sites.

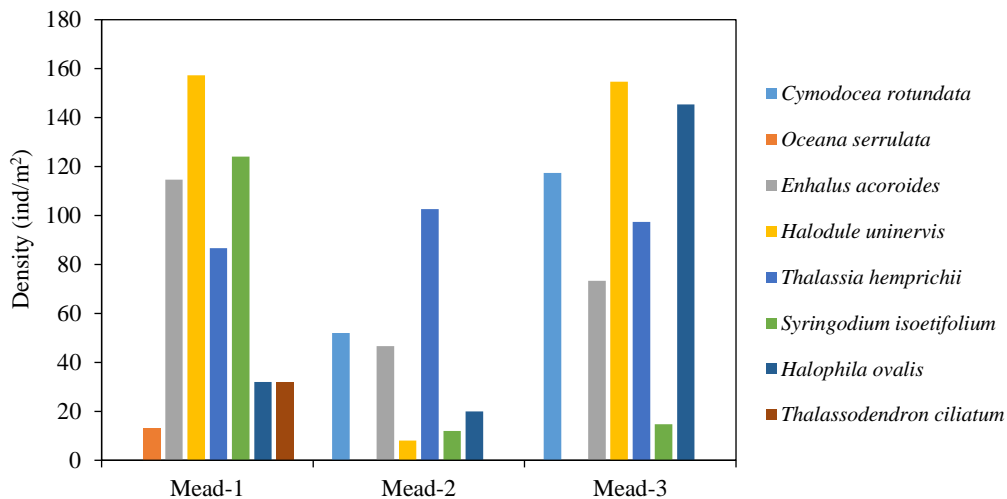


Figure 2. Species density at each site

Compared to the other seagrass species, *H. uninervis* exhibited notably higher densities at both Mead-1 and Mead-3. *H. uninervis*, a species widely distributed in the Indo-Pacific Region, thrives in intertidal and subtidal zones and demonstrates a robust capacity to flourish in high-salinity environments while maintaining resilience in the face of various

disturbances (Ravilla et al., 2020). Its ability to coexist with other seagrass species contributes to its abundance at the two sites. Meanwhile, Mead-2 exhibited the highest species density of *T. hemprichii*, a species which is typically found in muddy sediments, sensitive to turbidity and thrives in fine sandy substrates enriched with coral remains (Vermaat

et al., 1997; Terrados et al., 1998; Lefaan, 2012). The prevalence of *T. hemprichii* at Mead-2 can be ascribed to the specific environmental conditions present at this site. Previous studies (Waycott, 2011; Kilminster et al., 2015) have suggested that this species struggles to endure prolonged sun exposure and is susceptible to the impacts of rainwater. The discrepancies in species abundance observed among the sites have led to the development of distinct community structures, consequently influencing the potential for carbon sequestration and storage within the seagrass meadows. This variability in seagrass community structure across Semujur Island’s waters is also mirrored in the diversity, evenness, and dominance indices calculated for each site (Table 5). These indices offer valuable insights into the degree of diversity in seagrass community structure as well as its concomitant effect on the sequestration and storage of carbon stocks in the seagrass ecosystem.

Table 5. Diversity, evenness, and dominance indices of seagrass at three sites

Site	Diversity (H')	Evenness (J)	Dominance (C)
Mead-1	1.72	0.88	0.20
Mead-2	1.48	0.83	0.28
Mead-3	1.65	0.92	0.20

The diversity, evenness, and dominance indices provide insights into the composition and structure of seagrass communities at the different sites. Mead-1 exhibits the highest diversity, attributed partly to its greater species richness compared to the other sites, likely influenced by more favorable environmental

conditions for seagrass growth. Mead-2 shows the highest dominance index, mainly due to the prevalence of *T. hemprichii*, yet it maintains a moderately balanced level, suggesting diverse seagrass communities coexist. Mead-3 demonstrates the highest evenness index, indicating a more equitable distribution of species abundance. This equitable distribution at Mead-3 can benefit the ecological community by enhancing resilience against disturbances. Higher evenness may promote the establishment of a more resilient community less susceptible to environmental disruptions (Fitrian et al., 2017). These differences in community structure, as reflected by the indices, are anticipated to impact the carbon sequestration and storage capabilities of the respective seagrass meadows.

3.2 Seagrass ecosystem carbon stock

3.2.1 Biomass carbon stock

The assessment of seagrass dry weight and organic carbon content per species revealed that *E. acoroides* exhibited the highest dry weight at 2.99 grams dry weight per individual (Figure 3). This could be attributable to the large size of *E. acoroides*, which should enhance its carbon sequestration and storage capacity in comparison to other seagrass species, as noted by Citra et al. (2020). The significantly higher dry weight recorded for *E. acoroides* is indicative of its potential to contribute significantly to the total community biomass and, consequently, augment carbon storage within a seagrass meadow, as shown by the findings of Nugraha et al. (2019).

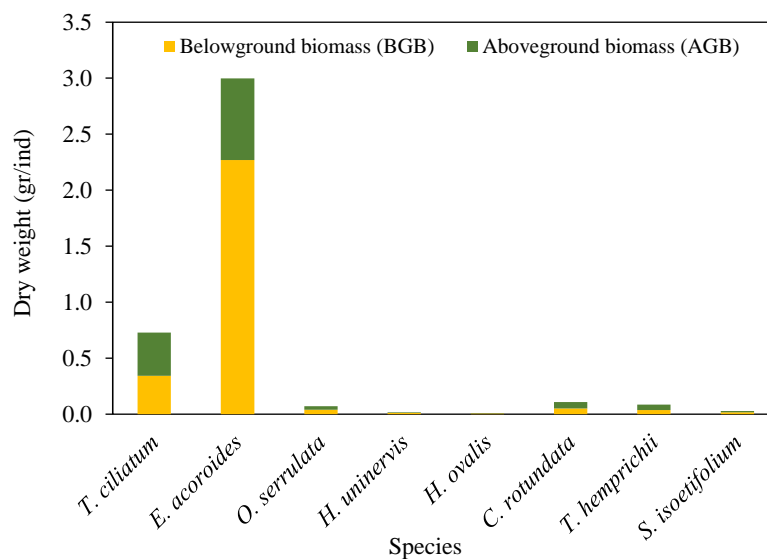


Figure 3. Dry weight of each seagrass species

Additionally, the comparison of dry weight results between aboveground biomass (AGB) and belowground biomass (BGB) reveals a significantly higher dry weight in BGB compared to AGB (Figure 3). This discrepancy is likely attributed to the inclusion of roots and rhizomes in BGB, which possess a higher capacity for carbon storage due to the accumulation of carbon resulting from the photosynthesis process. Furthermore, the positioning of roots and rhizomes beneath the sediment provides them with greater protection against environmental factors, thereby reducing the risk of disturbance and damage (Wahyudi et al., 2016).

Seagrass acts as an energy source for both the seagrass itself and the surrounding ecosystem by playing a pivotal role in the absorption of carbon dioxide (CO₂) and the production of glucose

(C₆H₁₂O₆). The mechanism of carbon sequestration, facilitated by seagrass, is intricately tied to the growth and proliferation of seagrass biomass. An examination of the organic carbon content across various seagrass species yielded consistent outcomes, indicating a homogeneous distribution of carbon within seagrass tissues (Kumala, 2020). The findings of the current study further validate that numerous seagrass species, irrespective of their size, present on Semujur Island possess comparable abilities to store organic carbon (%C_{org}) (Figure 4). This suggests that seagrass species, regardless of their size, exhibit efficient capabilities for storing organic carbon. Consequently, regions with thriving seagrass populations assume a crucial role in the sequestration and retention of carbon, surpassing areas lacking seagrass growth for this critical ecological function.

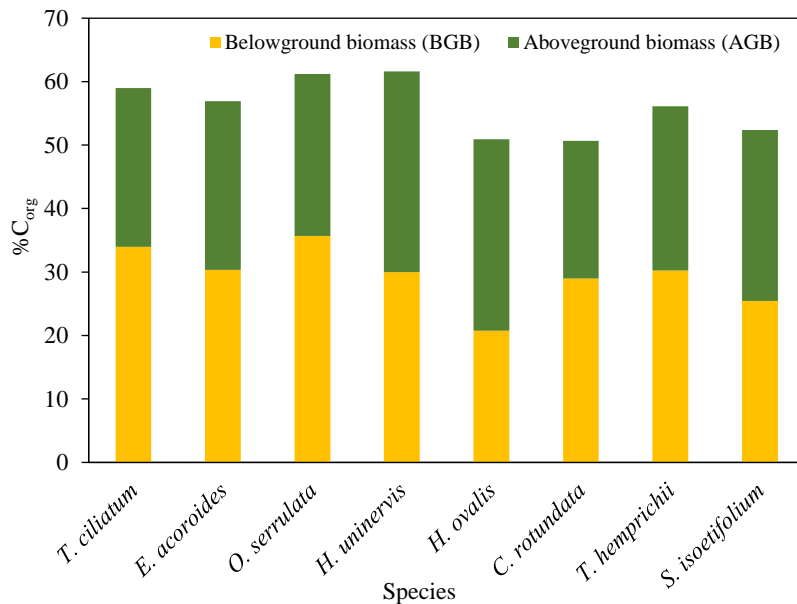


Figure 4. Carbon organic content (%C_{org}) of each seagrass species

3.2.2 Sediment carbon stock

Seagrass ecosystems, pivotal for their carbon sequestration and retention functions, are intimately linked with sediment deposition, acting as primary carbon reservoirs crucial for long-term carbon storage. These sediments, integral to seagrass habitats, serve as optimal sites for carbon storage, effectively sequestering carbon reserves within the substrate, even amidst seagrass degradation and decomposition (Kennedy and Bjork, 2009). As highlighted by Faust et al. (2021), carbon retention within these sediments can endure for extensive periods, potentially spanning

millennia. The containment of carbon within sediments presents a significant opportunity for prolonged preservation and ongoing accumulation, contingent upon the sustainability and upkeep of existing seagrass ecosystems (Kiswara and Ulumudin, 2009). Dry bulk density (DBD) and sediment organic carbon content (%C_{orgs}) stand as crucial parameters employed to assess sediment carbon within seagrass ecosystems. Table 6 presents the measurements of these two parameters for the three sites on Semujur Island wherein the sediment organic carbon content is data averaged from the whole core.

Table 6. Sediment dry bulk density and organic carbon content in each site

Site	Sediment	Dry bulk density (g/cm ³)	Sediment organic carbon content (%C _{orgs})
Mead-1	Coarse sand	0.74±0.21	0.62±0.11
Mead-2	Coarse and fine sand	0.63±0.25	0.83±0.37
Mead-3	Fine sand	1.04±0.35	0.72±0.12

According to these findings following sediment analysis, Mead-3 exhibited the highest dry bulk density (DBD) at 1.04±0.35 g/cm³, whereas Mead-2 recorded the highest sediment carbon organic content (C_{orgs}) at 0.83±0.37 %C_{orgs}. Differences in measurements can be ascribed to varying sediment conditions at each site. Sites characterized by fine sand sediment demonstrate an augmented ability for nutrient absorption compared to those with coarse sand sediment. The particle size of the underlying substrate plays a pivotal role in the organic matter binding process, with sediments containing smaller (finer) particle sizes exhibiting a heightened affinity for organic matter binding (Cyle et al., 2016). As a result, the distinct sediment conditions across the three sites can profoundly influence their respective capacities for carbon storage.

3.2.3 Total carbon stocks

Quantifying the total carbon stock in a particular location entails summing up the organic carbon within the entire seagrass biomass and the underlying sediment. The total carbon sequestered by seagrass and subsequently stored in sediment exhibited variations among sites. It is noteworthy that the site with the highest biomass carbon stocks does not necessarily correspond to the highest total carbon stocks (Figure 5). This observation can be linked to the specific characteristics of seagrass, sediment properties, and the overall environmental conditions unique to each site. Notably, Mead-3 emerges as the site with the highest total carbon stocks among the three sites under investigation, totaling 75.11 MgC/ha. This outcome may be attributed to a combination of factors, including significant seagrass biomass (due to the highest density), the presence of fine sand sediments with heightened carbon-absorbing capabilities, and the prevalence of optimal environmental conditions at Mead-3.

The data pertaining to carbon stocks within the seagrass ecosystem underscore the significant role of sedimentary carbon in the overall carbon stocks on Semujur Island. Sediment's capacity for carbon storage contributes approximately 90% of the total ecosystem carbon stocks in line with the findings of Stankovic et al. (2021). This outcome compellingly illustrates the crucial role played by seagrass ecosystems in carbon sequestration and subsequent storage within sediments. Consequently, areas or sites surrounded by seagrass meadows surpass those devoid of such vegetation in terms of their carbon storage potential. This attribute becomes particularly valuable when considering its utility in climate change mitigation, emphasizing the importance of preserving and maintaining these ecosystems.

In comparison with global and regional data (Indonesia) (Table 7), carbon stock values on Semujur Island fall within the range of the global average but exhibit lower values when contrasted with the regional average. The lower carbon stock measurements on the island may be attributed to specific contextual factors. Semujur Island, being a small landmass situated at a considerable distance from the main island, lacks vital carbon-contributing ecosystems such as mangrove habitats and tidal swamps. As highlighted by Ricart et al. (2020), a significant proportion of the most substantial carbon inputs, ranging from 70% to 90%, originate from allochthonous sources (external to the ecosystem), with autochthonous sources (internal to the ecosystem) accounting for only 10% to 30%. Field observations suggest that the carbon source within the seagrass ecosystem of Semujur Island is primarily internal, in stark contrast to other locations benefiting from external carbon sources. It is for this reason that the observed carbon stocks here are not as pronounced when compared with areas where additional external carbon sources enhance the ecosystem's carbon accumulation and storage.

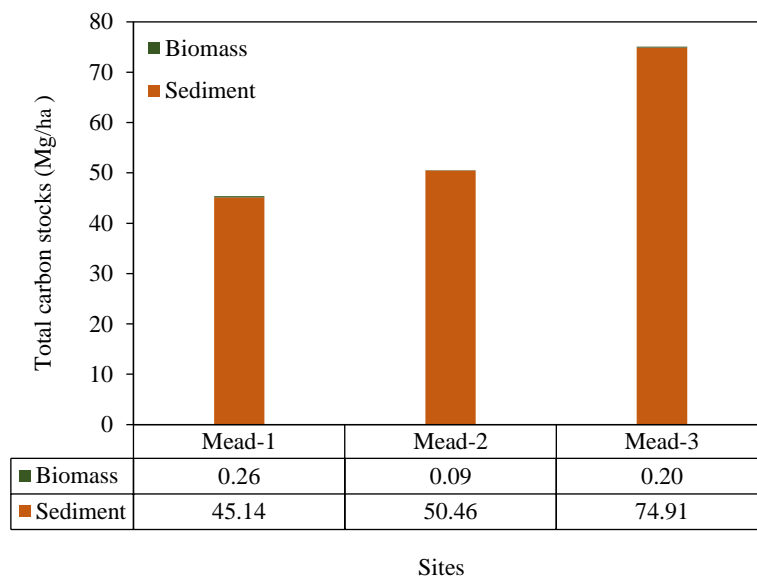


Figure 5. Total carbon stocks in the seagrass ecosystem of Semujur Island

Table 7. Comparison of carbon stock results with other studies

	Carbon stock (MgC/ha)		
	AGB	BGB	Sediment
Present study			
1. Mead-1	0.06	0.20	45.14
2. Mead-2	0.02	0.07	50.46
3. Mead-3	0.05	0.15	74.91
Global data (Fourqurean et al., 2012)	0.75 (0.001-5.548)	1.76 (0.001-17.835)	139.70 (9.10-628.10)
Regional data			
1. Java (Alongi et al., 2015)	0.66	1.75	62.40
2. South Sulawesi (Alongi et al., 2015)	0.26	0.55	148.40
3. East Kalimantan (Alongi et al., 2015)	0.01	0.02	243.30
4. Bali (Graha et al., 2016)	0.18	0.29	21.00
5. Lombok (Rahman et al., 2023)	0.14	0.30	48.40

3.3 Correlation between seagrass community structure and carbon stock

Notably, a correlation analysis was undertaken to explore the association between seagrass density and coverage with the acquired measurements of total carbon stock (sediment and biomass). According to Citra et al. (2020), elevated density and coverage have the potential to augment biomass within seagrass meadows, consequently influencing carbon storage. As it is clear that ecosystem carbon stocks are made up of primarily sediment carbon, further analysis in this study focused on the correlation between seagrass community structure and sediment carbon stock as a proxy for ecosystem carbon stocks. Sediment at different depths were used in the correlation analysis to see the relationship between community structure

aboveground and the amount of carbon stored in sediment of varying depths.

The outcomes of this analysis unveiled a moderate correlation (0.430) between density and carbon stock, as well as between seagrass cover and carbon stock (0.528) (Table 8). These correlation findings suggest that the relationship between density and coverage with carbon stock is not notably robust. Initially anticipated to provide deeper insights into the link between community structure and total carbon stocks, this analysis reveals that multiple factors influence this relationship, and the findings of this study do not align with initial expectations. The portrayal of seagrass community structure through density and coverage in this investigation does not seem to serve as a robust predictive tool. The moderate

correlations observed between community structure and carbon stock may partly stem from the limited dataset available for analysis. However, it is logical to infer that elevated density and coverage should bolster a seagrass meadow's ability for carbon absorption and storage. This logical inference can guide management strategies aimed at preserving, enhancing, or restoring

existing seagrass meadows to optimize their carbon sequestration potential. For a more comprehensive understanding of the relationship between community structure and carbon stocks, future research endeavours should encompass a broader array of potential influencing factors.

Table 8. Correlation between seagrass community structure and carbon stocks for each stratification

Carbon stock at each water depth (MgC/ha)	Community structure	
	Seagrass density	Seagrass coverage
Depth 0-5 cm	0.426	0.528
Depth 5-20 cm	0.430	0.480
Depth 20-50 cm	0.377	0.308
Depth 50-100 cm	0.341	0.261

4. CONCLUSION

This research, focusing on the community structure of seagrass meadows surrounding Semujur Island, revealed notable variations among the different sites, influenced by factors such as seagrass size, density, species composition, and environmental conditions. Mead-3 particularly stands out, exhibiting the highest ecosystem carbon stock (75.11 MgC/ha), attributed to its distinctive community structure dominated by large species like *E. acoroides* and *T. hemprichii*, alongside sediment comprising partly fine sand. This study emphasizes the significance of considering ecological relationships in the management of seagrass ecosystems for effective climate change mitigation. Additionally, the findings offer valuable data as a reference for the restoration and conservation endeavors of seagrass ecosystems, indicating a correlation between higher seagrass density and coverage with increased carbon storage capacity within the ecosystem.

ACKNOWLEDGEMENTS

This research was funded by an international research program grant from Institut Teknologi Bandung (ITB) in 2022-2023 (Program Riset Internasional ITB LPPM.PN-10-42-2022, contract No. 4949/IT1.B07.1/TA.00/2022). We would like to thank Amadeus Devin Gouw, Irsyad Riyan Putranto, Mahardika Zahran Kristanto, Dian Rosleine, Okto Supratman, the Laboratory staff of Aquatic Resources Management Laboratory of Bangka Belitung University, and all other parties who have helped bring this research into fruition.

REFERENCES

- Alongi DM, Murdiyarsa D, Fourqurean JW, Kauffman JB, Hutahaean A, Crooks S, et al. Indonesia's blue carbon: A globally significant and vulnerable sink for seagrass and mangrove carbon. *Wetlands Ecology and Management* 2015;24(1):3-13.
- Bandh SA, Malla FA, Qayoom I, Mohi-Ud-Din H, Butt AK, Altaf A. Importance of blue carbon in mitigating climate change and plastic/microplastic pollution and promoting circular economy. *Sustainability* 2023;15:Article No. 2682.
- Bchir R, Djellouli AS, Zitouna N, Aurelle D, Pergent G, Pergent-Martini C, et al. Morphology and genetic studies of *Cymodocea* seagrass genus in Tunisian Coasts. *International Journal of Experimental Botany* 2019;88(2):171-84.
- Cassia R, Nocioni M, Correa-Aragunde N, Lamattina L. Climate change and the impact of greenhouse gasses: CO₂ and NO_x, friends and foes of plant oxidative stress. *Frontiers in Plant Science* 2018;9:Article No. 00273.
- Citra FA, Suryanti S, Muskananfolia MR. The potential stocks and carbon uptake by seagrass meadows at Pari Island, Kepulauan Seribu, Indonesia. *IOP Conference Series: Earth and Environmental Science* 2020;530(1):Article No. 012022.
- Cyle KT, Hill N, Young KM, Jenkins TC, Hancock DW, Schroeder PA, et al. Substrate quality influences organic matter accumulation in the soil silt and clay fraction. *Soil Biology and Biochemistry* 2016;103:138-48.
- Faust JC, Tessin A, Fisher BJ, Zindorf M, Papadaki S, Hendry KR, et al. Millennial scale persistence of organic carbon bound to iron in Arctic marine sediments. *Nature Communications* 2021;12:Article No. 275.
- Fitrian T, Agus K, Rosmi NP. Seagrass community structure of Tayando-Tam Isand, Southeast Moluccas, Indonesia. *Biodiversitas* 2017;18(2):788-94.
- Fourqurean JW, Duarte CM, Kennedy H, Marbà N, Holmer M, Mateo MA, et al. Seagrass ecosystems as a globally significant carbon stock. *Nature Geoscience* 2012;5(7):505-9.
- Graha YI, Arthana IW, Karang IWGA. Seagrass carbon storage in the Sanur Beach area, Denpasar City. *Ecotrophic* 2016;10(1):46-53.
- Hilmi N, Chami R, Sutherland MD, Hall-Spencer JM, Lebleu L, Benitez MB, et al. The role of blue carbon in climate change

- mitigation and carbon stock conservation. *Frontiers in Climate* 2021;3:Article No. 710546.
- James RK, Keyzer LM, van de Velde SJ, Herman PMJ, van Katwijk MM, Bouma TJ. Climate change mitigation by coral reefs and seagrass beds at risk: How global change compromises coastal ecosystem services. *Science of the Total Environment* 2023;857:1-11.
- Kennedy H, Björk M. *Seagrass Meadows*. Switzerland: IUCN; 2009. p. 53.
- Kilminster K, McMahon K, Waycott M, Kendrick GA, Scanes P, McKenzie L, et al. Unravelling complexity in seagrass systems for management: Australia as a microcosm. *Science of The Total Environment* 2015;534:Article No. 17674.
- Kiswara W, Ulumuddin YI. The Role of Coastal Vegetation in the Global Carbon Cycle: Mangroves and Seagrass as Carbon Sinks. Workshop Ocean and Climate Change. IPB: Coordinating Ministry for People's Welfare and BRKP; 2009 (in Indonesian).
- Kumala ASN. Relationship between Community Structure and Carbon Stock of Seagrass Ecosystems on Karimunjawa and Kemujan Islands, Jepara, Central Java [dissertation]. Bandung, Institut Teknologi Bandung (ITB); 2020.
- Lasabuda R. Development of coastal and ocean areas from the perspective of the Indonesian Archipelagic State. *Platax Scientific Journal* 2013;1(2):92-101.
- Lefaan PT. Stability of seagrass habitat judging from species composition and density. *Natural Journal* 2012;8(1):17-21.
- Losciale R, Day JC, Rasheed MA, Heron SF. The vulnerability of world heritage seagrass habitats to climate change. *Global Change Biology* 2023;30:e17113.
- Nugraha AH, Kawaroe M, Srimariana ES, Jaya I, Apdillah D, Deswati SR. Carbon storage in seagrass meadow of Teluk Bakau-Bintan Island. *IOP Conference Series: Earth and Environmental Science* 2019;278(1):Article No. 012051.
- Odum EP. *Fundamental of Ecology*. Yogyakarta, Indonesia: Gadjah Mada University Press; 1993 (in Indonesian).
- Priosambodo D. Distribution of seagrass types in South Sulawesi. *Bionature Journal* 2007;8(1):8-17.
- Rahman FA, Qayim I, Wardianto Y. Carbon stored on seagrass beds in Gili Maringkik, Lombok, Indonesia. *Biotropia* 2023;30(1):63-73.
- Rahmawati S, Hernawan UE, McMahon K, Prayudha B, Prayitno HB, Wahyudi AJ, et al. Blue Carbon in Seagrass Ecosystem: Guideline for the Assessment of Carbon Stock and Sequestration in Southeast Asia. Yogyakarta: UGM Press; 2019 p. 12-43.
- Ravilla L, Navaith AS, Kalaivani P, Vanitha V. A review on *Halodule uninervis*: A potent seagrass. *International Journal of Research in Pharmaceutical Sciences* 2020;11(1):875-79.
- Rawung S, Tilaar FF, Rodoverhenuwu AB. Inventory of seagrass in marine field station waters, faculty of fisheries and marine sciences, UNSRAT, East Likupang District, North Minahasa Regency. *Platax Scientific Journal* 2018;6(2):38-45.
- Republic of Indonesia Government Regulation Number 22. Implementation of Environmental Protection and Management: SK No 085459 A. Jakarta; Indonesia: President of Republic Indonesia; 2021 (in Indonesian).
- Ricart AM, York PH, Bryant CV, Rasheed MA, Ierodiaconou D, Macreadie PI. High variability of blue carbon storage in seagrass meadows at the estuary scale. *Scientific Reports* 2020;10:Article No. 5865.
- Schober P, Boer C, Schwarte LA. Correlation coefficients: Appropriate use and interpretation. *Anesthesia and Analgesia* 2018;126(5):1763-68.
- Short FT, Coles RG. *Global Seagrass Research Methods*. Elsevier; 2001. p. 473.
- Stankovic M, Ambo-Rappe R, Carly F, Dangan-Galon F, Fortes MD, Hossain MS, et al. Quantification of blue carbon in seagrass ecosystems of Southeast Asia and their potential for climate change mitigation. *Science of The Total Environment* 2021;783:Article No. 146858.
- Tahir I, Mantiri DMH, Rumengan AP, Wahidin N, Lumingas LJJ, Kondoy KIF, et al. Variation of carbon content in sediments of seagrass ecosystems based on the presence of seagrass species on Mare Island, Indonesia. *AACL Bioflux* 2023;16(2):887-98.
- Terrados J, Duarte CM, Fortes MD, Borum J, Agawin NSR, Bach S, et al. Changes in community structure and biomass of seagrass communities along gradients of siltation in SE Asia. *Estuarine, Coastal and Shelf Science* 1998;46(5):757-68.
- Verheij E. Marine Plants on the Reefs of the Spermonde Archipelago, SW Sulawesi, Indonesia: Aspect of Taxonomy, Floristics and Ecology. *Rijksherbarium/Hortus Botanicus Leiden*; 1993. p. 320.
- Vermaat JE, Agawin NSR, Fortes MD, Uri JS, Duarte CM, Marbà N, et al. The capacity of seagrasses to survive increased turbidity and siltation: The significance of growth form and light use. *AMBIO: A Journal of the Human Environment* 1997;26(8):499-504.
- Wahyudi AJ, Rahmawati S, Prayudha B, Iskandar MR, Arfianti T. Vertical carbon flux of marine snow in *Enhalus acoroides* - dominated seagrass meadows. *Regional Studies in Marine Science* 2016;5:27-34.
- Waycott M, McKenzie LJ, Mellors JE, Elisson JC, Sheaves MT, Collier C, et al. Vulnerability of mangroves, seagrass, and intertidal flats in the tropical Pacific to climate change. In: Bell JD, Johnson JE, Hobday AJ, editors. *Vulnerability of Fisheries and Aquaculture in the Pacific to Climate Change*. New Caledonia: Secretariat of the Pacific Community Noumea; 2011.

Characteristics of Fine Particulate Matter (PM_{2.5}) Chemical Composition in the North Jakarta Industrial Area

Zeni Anggraini^{1,2*}, Muhayatun Santoso², and Asep Sofyan¹

¹Department of Environmental Engineering, Bandung Institute of Technology, Bandung, Indonesia

²National Research and Innovation Agency (BRIN), South Tangerang, Indonesia

ARTICLE INFO

Received: 27 Nov 2023
Received in revised: 31 Mar 2024
Accepted: 18 Apr 2024
Published online: 9 May 2024
DOI: 10.32526/ennrj/22/20230300

Keywords:

Air pollution/ PM_{2.5}/ Black carbon/
Chemical elements/ SuperSASS

* Corresponding author:

E-mail:
anggrainizeni@gmail.com

ABSTRACT

Air pollution around industrial area has become a serious concern for both the public and local government. Thus, research on PM_{2.5} characterization is urgently needed. This study identifies the concentration and chemical characteristics of PM_{2.5} to provide an in-depth understanding of the composition of these particles around the largest industrial complex in North Jakarta. Sixty samples of PM_{2.5} were collected from residential sites around industrial areas in North Jakarta. Samples were collected on Teflon filters using a SuperSASS instrument during the period from February to July 2023, representing the wet and dry seasons. Mass concentrations of PM_{2.5}, black carbon, and 19 chemical elements were determined. The average mass concentration of PM_{2.5} in the wet and dry seasons was $27.81 \pm 11.82 \mu\text{g}/\text{m}^3$ and $46.63 \pm 14.37 \mu\text{g}/\text{m}^3$, respectively. Although the concentration of PM_{2.5} was lower during the wet season, the concentrations of black carbon and certain elements did not decrease significantly. This shows that pollutants play an important role in both seasons in the study location. Sulfur is the most abundant element with the average concentration in the dry season ($2,727.89 \text{ ng}/\text{m}^3$) higher than in the wet season ($1,983.18 \text{ ng}/\text{m}^3$). The PM_{2.5} mass reconstruction results show that ammonium sulfate and black carbon have the largest portion of PM_{2.5} mass. The results are expected to be used as a scientific reference in studying air pollution problems in this region and assist in formulating air protection policies to reduce PM_{2.5} emissions.

1. INTRODUCTION

PM_{2.5} is considered the most harmful pollutant because it can enter the lung alveoli and blood circulation (Xie et al., 2021). A comprehensive study on the increase in PM_{2.5} concentrations during the dry season in Southeast Asia was reported by Nguyen et al. (2020). Previous research estimated that PM_{2.5} exposure caused 4.2 million deaths, equivalent to 7.6% of total global mortality (Cohen et al., 2017). Several epidemiological studies revealed a more consistent correlation of PM_{2.5} exposure with acute respiratory infection and decreased lung function (Wang et al., 2021; Yan et al., 2022). In 2016, the prevalence of Acute Respiratory Infection (ARI) in Indonesia reached 25%, with the proportion of infant deaths reaching 32.10% of all under-five deaths (Putra

and Wulandari, 2019). Based on Riskesdas data, the prevalence of ARI in the Special Capital Region of Jakarta (DKI Jakarta) in 2018 was 8.49% and North Jakarta was ranked second with the highest number of ARI cases (Ministry of Health of the Republic of Indonesia, 2018).

North Jakarta is a region within the DKI Jakarta Province that has seen a significant increase in industrial activity and urbanization. Marunda is one of the most densely populated areas in North Jakarta which has a strategic location about 10 km from Tanjung Priok port. The port plays an important role in the sustainability of economic activities and the transportation sector in this region. High activity in the transportation and industrial sectors is expected to increase PM_{2.5} concentrations. In recent years, people

living around the Marunda Industrial Area have felt a decrease in air quality. In 2015, cases of ARI in infants recorded at the local health centers reached 60 cases per 1000 and continue to increase (Anggraeni and Iriani, 2017). Several studies have found that the incidence of ARI cases is related to the chemical composition of PM_{2.5}, which contains harmful substances, such as heavy metals, organic compounds, inorganic chemical elements, and black carbon that have a negative impact on the human respiratory system (Darrow et al., 2014; Nascimento et al., 2020; Peng et al., 2009). In order to establish efficient air pollution control strategies, it is important to assess air quality and characterize the chemical composition of PM_{2.5} in the Marunda Industrial Area during seasonal changes.

2. METHODOLOGY

2.1 Sampling site

The Marunda Industrial Area, which covers most of North Jakarta, is a leading industrial center in DKI Jakarta due to its rapid industrial development. Marunda Industrial Area accommodates various production facilities and types of industries, such as coal loading and unloading, manufacturing, and processing. PM_{2.5} samples were collected from 2 February 2023 to 29 July 2023. The Indonesian Agency for Meteorology, Climatology, and

Geophysics (BMKG) defines that the wet season in Indonesia usually occurs from December to March, while the dry season occurs from June to September, with transitional periods from April to May and October to November. During the transition period in April, the effect of the east monsoon starts to strengthen, indicating the onset of the dry season from April to September (Aldrian and Dwi Susanto, 2003). The wet season is influenced by the northwest monsoon which brings more water vapor, resulting in increased rainfall. Conversely, the southeast monsoon in the dry season brings warm and dry air, resulting in less rainfall (Kusumaningtyas et al., 2018). Therefore, this study defines February-March as the wet season and April-July 2023 as the dry season.

Sampling of PM_{2.5} from ambient air in residential locations near the Marunda Industrial Area was conducted using a SuperSASS filter-based instrument (Super Speciation Air Sampling System; Met One Instrument, Inc., USA). Air was collected through an inlet with a flow rate of ±6.7 Lpm. The SuperSASS was operated for 24 h with a 3-days sampling interval following the EPA schedule. SuperSASS was installed on the rooftop of D2 Marunda Flat (coordinates -6°05'48.14" S and 106°57'39.42" E) at the height of ±20 m above ground level as shown in Figure 1.

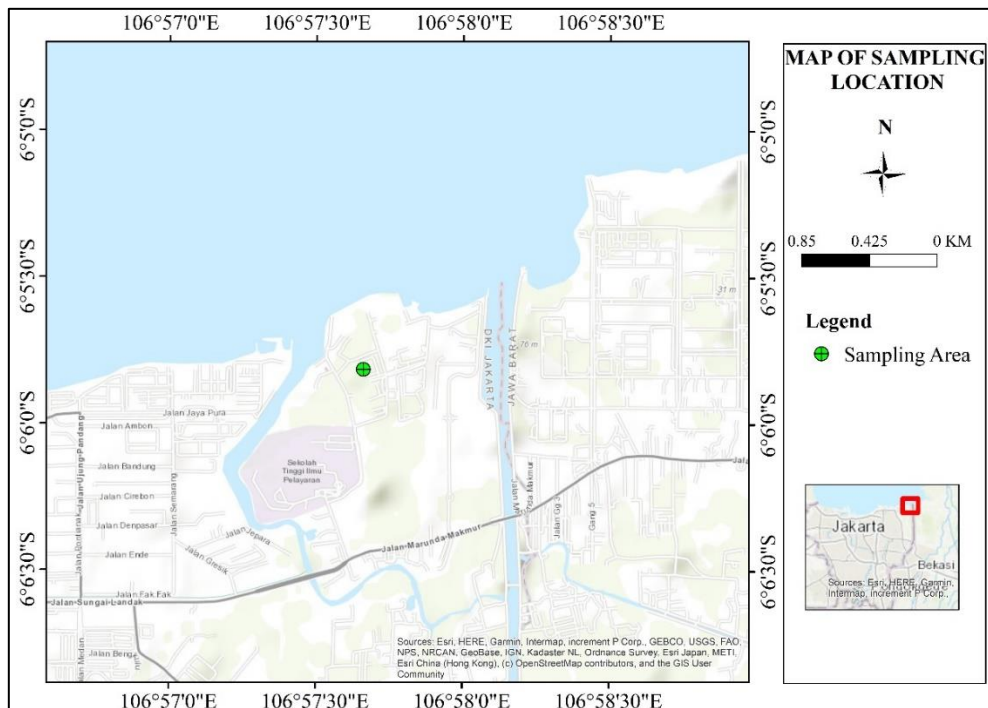


Figure 1. Map of PM_{2.5} sampling location

2.2 Mass concentrations of PM_{2.5} and black carbon analysis

Sixty samples were collected on Polytetrafluoroethylene (Teflon) filters with a diameter of 47mm. Before and after PM_{2.5} collection, the filters were conditioned at a temperature of 20±5°C and a maximum relative humidity of 50±5% for at least 24 h for gravimetric mass determination using a Mettler Toledo XP6 electronic microbalance. PM_{2.5} mass concentration was determined from the difference in mass before and after exposure divided by the volume of air passing through the filter. The black carbon (BC) concentrations in the PM_{2.5} samples collected on the filter was analyzed using a Smoke Stain Reflectometer (type EEL 43M, Diffusion Systems, Ltd). The black carbon particles will absorb most of the light from the device directed to the filter sample. The amount of light that is not absorbed will be reflected into the detector and the reflectance value is proportional to the concentration of black carbon on the filter (Begum et al., 2012).

2.3 Elemental characterization

Energy Dispersive X-ray Fluorescence (ED-XRF) Spectrometry is suited for airborne particle elemental analysis due to its simple, fast sample preparation and multi-element analysis in a single measurement (Canepari et al., 2009; Owoade et al., 2015). ED-XRF PANalytical Epsilon 5 was used for the analysis of 19 chemical elements (Na, Mg, Al, Si, S, Cl, K, Cr, Fe, Ni, Cu, As, Pb, Ca, Ti, V, Mn, Zn, and Br). Before the XRF was used, a calibration curve was created using the MicroMatter Single Element Standard which establishes a linear relationship between X-ray intensity and element concentration. The XRF instrument's accuracy was assessed using the measurement of Standard Reference Material (SRM) NIST 2783.

2.4 Reconstructed mass (RCM)

The measured PM_{2.5} mass was reconstructed from the sum of the analyzed chemical components to determine the relative contribution of various components to the PM_{2.5} mass. In this study, the RCM calculation is based on the following equation (Santoso et al., 2020a):

$$\text{RCM} = \text{Ammonium sulfate} + \text{Elemental carbon} + \text{Crustal matter} + \text{Sea salt} + \text{Smoke} + \text{Trace elements} \quad (1)$$

2.4.1 Ammonium sulfate

Ammonium sulfate ((NH₄)₂SO₄) is a dissolved secondary sulfate. Chan et al. (1997) explained, the mass of dissolved sulfate measured is strongly correlated with sulfur (S). Therefore, the mass of ammonium sulfate can be calculated as follows (Malm et al., 1994):

$$\text{Ammonium sulfate} = 4.125 [\text{S}] \quad (2)$$

2.4.2 Elemental carbon

The mass of elemental carbon is assumed to be the same as the mass of black carbon (BC), thus no multiplying factor is required (Watson et al., 2005).

$$\text{Elemental carbon} = [\text{Black Carbon}] \quad (3)$$

2.4.3 Crustal matter

Crustal matter is the sum of Al, Si, Ca, Fe, and Ti contained as oxides and a multiplying factor of 1.16 is required to exclude MgO, Na₂O, K₂O, and H₂O contained in the crustal mass (Chan et al., 1997; Rahman et al., 2019).

$$\text{Crustal matter} = 1.16 \left(\frac{1.90 [\text{Al}] + 2.15 [\text{Si}] + 1.41 [\text{Ca}]}{+ 1.67 [\text{Ti}] + 2.09 [\text{Fe}]} \right) \quad (4)$$

2.4.4 Sea salt

Na⁺ and Cl⁻ are the main components of sea salt present in fine particles in the air (Watson et al., 2012). In this study, the contribution of sea salt was estimated using the following equation (Ho et al., 2003).

$$\text{Sea salt} = 2.54 [\text{Na}] \quad (5)$$

2.4.5 Smoke

Potassium (K) can be associated as a trace element for smoke sources. However, K is also present in the crustal elements, which are assumed to have an average K/Fe ratio of 0.6. The equation used to estimate the mass of smoke in PM_{2.5} mass is given below (Oanh et al., 2006):

$$\text{Smoke} = [\text{K}] - 0.6 [\text{Fe}] \quad (6)$$

2.4.6 Trace elements

Trace elements not included in previous calculations can be added into the mass reconstruction analysis. Although their presence is only a small fraction (0.5-1.6%) of the total particulate mass, these elements are necessary to identify pollution sources and have a significant impact on the environment due to their toxicity (Chow et al., 2015).

2.5 Data analysis

Meteorological data in the form of wind direction and wind speed data from Air Quality Monitoring System (AQMS) near the research location were processed by creating a windrose to understand the wind distribution patterns around the Marunda Industrial Area. WRPlot View is the software used in the study to create windroses. Statistical analysis was performed using RStudio 2023.06.2+561 and Microsoft Excel 2019. All data were reported as mean ± standard deviation (SD). Data were analyzed using an independent t-test to determine whether or not there was an effect of season on the concentration and chemical composition of PM_{2.5} in the Marunda area. Independent t-test results with a p-value <0.05 were considered significant.

3. RESULTS AND DISCUSSION

3.1 Mass characteristics of PM_{2.5}

Rainfall during the study in February, March, April, May, June, and July was 370, 262, 47.6, 12.9, 29.4, and 93 mm, respectively. February and March, the wet season, receive an abundance of precipitation exceeding 100 mm, whereas April through July receive less than 100 mm. Figure 2 shows the time series of 24-hour average PM_{2.5} concentrations during the sampling period. The results show that from February to July 2023, some daily average PM_{2.5}

concentration data exceeded the national quality standard (55 µg/m³), especially from May to July which is the dry season period (Republic of Indonesia Government Regulation, 2021). Compared to WHO global air quality guidelines and National Ambient Air Quality Standard (NAAQS), PM_{2.5} levels in Marunda Industrial Area during the sampling period exceeded 74.57% and 94.92%, respectively, with the largest percentage occurring in the dry season (USEPA, 2006; WHO, 2021).

The seasonal variations in Indonesia have a significant influence on PM_{2.5} level of concentration. The fluctuating daily average PM_{2.5} concentrations shown in Figure 2 are most likely influenced by meteorological conditions. In the wet season, the average (±SD) PM_{2.5} mass concentration at the study location was 27.81±11.82 µg/m³, which was lower than the average concentration of 46.63±14.37 µg/m³ reported during the dry season. The decrease in PM_{2.5} concentration during the wet season can be due to the decrease in stagnant weather and the presence of strong winds from the southwest and northwest. These high-speed winds contribute, disperse, and carry away PM_{2.5} dust particles (Chirasophon and Pochanart, 2020). The independent t-test results show a statistically significant difference in PM_{2.5} mass concentration (p-value=6.14×10⁻⁶, α<0.05) between the two seasons.

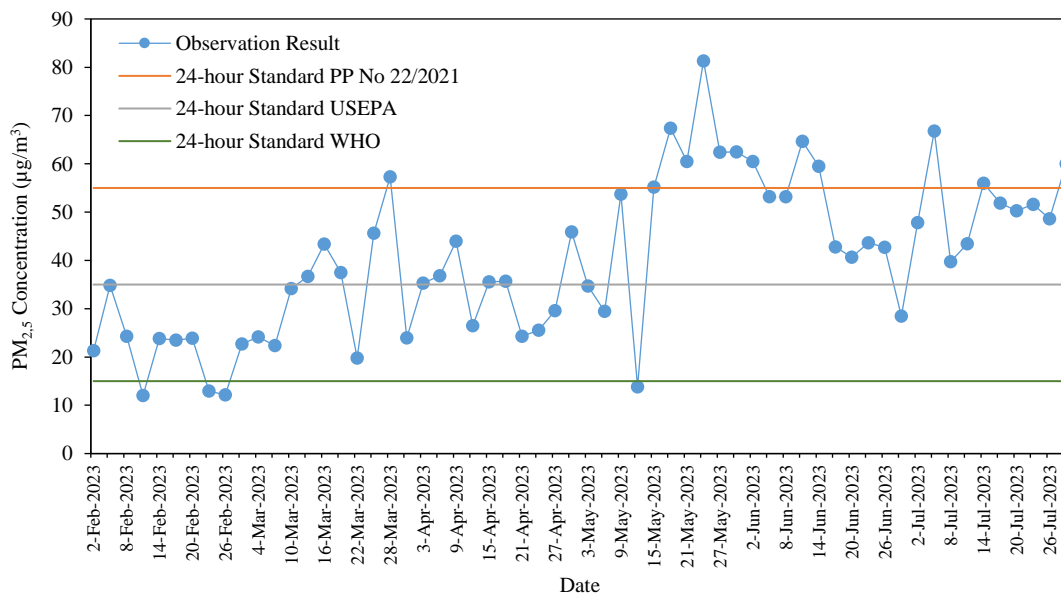


Figure 2. Daily mass concentrations of PM_{2.5} during the sampling period

May has the highest mass average concentration of PM_{2.5}, as shown in Figure 3. This is likely due to the relatively low precipitation in May relative to other

months. While the lowest concentration occurs in February when rainfall is abundant. These results are in line with research conducted by Istiana et al. (2023)

in Central Jakarta, a region situated at a considerable distance from the coast and serving as the epicenter of government and commerce. Despite the fact that air samples were collected in different areas, the findings from sampling in North Jakarta and Central Jakarta exhibit a comparable trend, with lower levels of PM_{2.5} concentrations observed during the wet season compared to the dry season. This phenomenon arises due to the role of rainfall in effectively removing

pollutants from the atmosphere. Rainfall accomplishes this by capturing pollutant particles and incorporating them into raindrops, which are then deposited onto various surfaces. Conversely, during the dry season, the eastern monsoon brings drier air and less rainfall, which restricts wet deposition. As a result, PM_{2.5} particles accumulate and their concentration in the air increases (Narita et al., 2019).

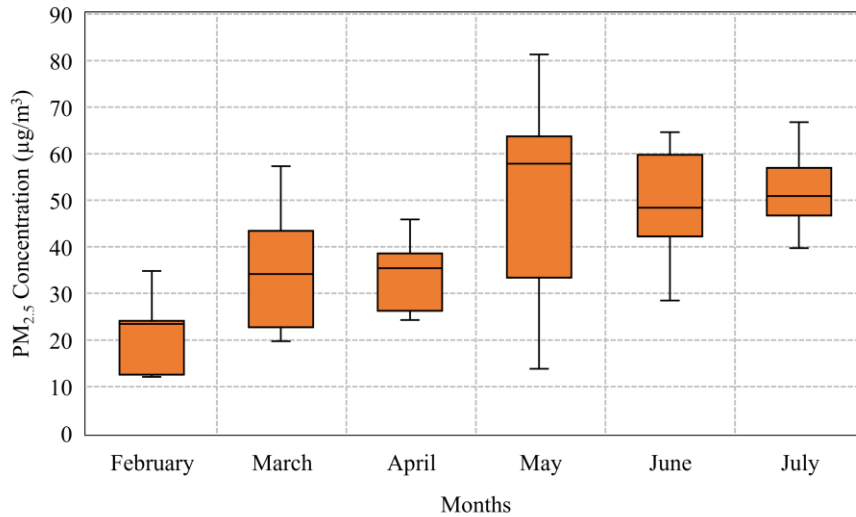


Figure 3. Monthly variations in PM_{2.5} concentrations at the study location

The results of this study are still above the average PM_{2.5} concentration value in industrial locations on Java Island, such as Waru Sidoarjo (18.26 µg/m³) and Surabaya (16.00 µg/m³) (Humairoh et al., 2020; Santoso et al., 2020b). This indicates that Marunda is more polluted than Waru and Surabaya. The PM_{2.5} concentrations observed in the three industrial districts are influenced by variations in population, topography, type of industry, and amount of data. The exponential increase in population, industrialization, and vehicular activity in Marunda has had a significant impact on air quality, mostly due to the presence of PM_{2.5} particles. Various kinds of public transportation, such as Bus Rapid Transit (BRT) and microtrans, have been constructed in the Marunda region. Nevertheless, these endeavors are inadequate to surmount the escalation in the quantity of automobiles and other activities that contribute to the emission of PM_{2.5} pollutants in Marunda and its neighboring regions.

Windrose in Figure 4 shows that in the wet season, the prevailing wind originates from the northwest quadrant, accounting for approximately 25.75% of the total wind direction, while the

southwest quadrant contributes around 12.02%. In contrast, during the dry season, the dominant wind blows from the northeast quadrant by 24.45% with weak winds from all directions. The average wind speed in the wet season is 1.43±0.98 m/s and 1.06±0.92 m/s in the dry season. The ambient temperature for each season was 27.55±1.78°C in the wet season and 28.60±2.50°C in the dry season. The relative humidity measured in the wet season and dry season were 69.18±15.92% and 65.03±32.19%, respectively. Variations in meteorological conditions between seasons have an impact on pollution levels and dispersion (Sasmita et al., 2019).

3.2 Characteristics of PM_{2.5} chemical composition

3.2.1 Black carbon (BC)

Black carbon (BC) particles have a significant impact on climate change and are linked to adverse effects on human health (Ambade et al., 2022). The observed concentration of BC in PM_{2.5} at the study location ranged from 1.90 to 11.39 µg/m³ (N=60). The average values during the wet season (February-March) and dry season (April-July) were 5.42±2.23 µg/m³ and 6.16±1.83 µg/m³, respectively. Figure 5

shows that the average concentration in May was the highest compared to the other months. There was no statistically significant variation in the average concentration between the wet and dry seasons (p -value=0.18, $\alpha > 0.05$). The presence of BC concentrations in $PM_{2.5}$ in urban locations, serves as a tracer of anthropogenic emissions from diesel-engine vehicles in places with high traffic volume (Wang et al., 2009). The Marunda Industrial Area, located in an essential position between ports and industries, has

high levels of transportation activities, primarily involving big vehicles predominantly powered by diesel engines. The average black carbon concentration at the location during the sampling period ($5.91 \mu\text{g}/\text{m}^3$) was above the average value reported by Santoso et al. (2020a) in Central Jakarta. The high concentration of BC is likely a result of the works on the Marunda Access Bridge, which contributed to increased traffic congestion.

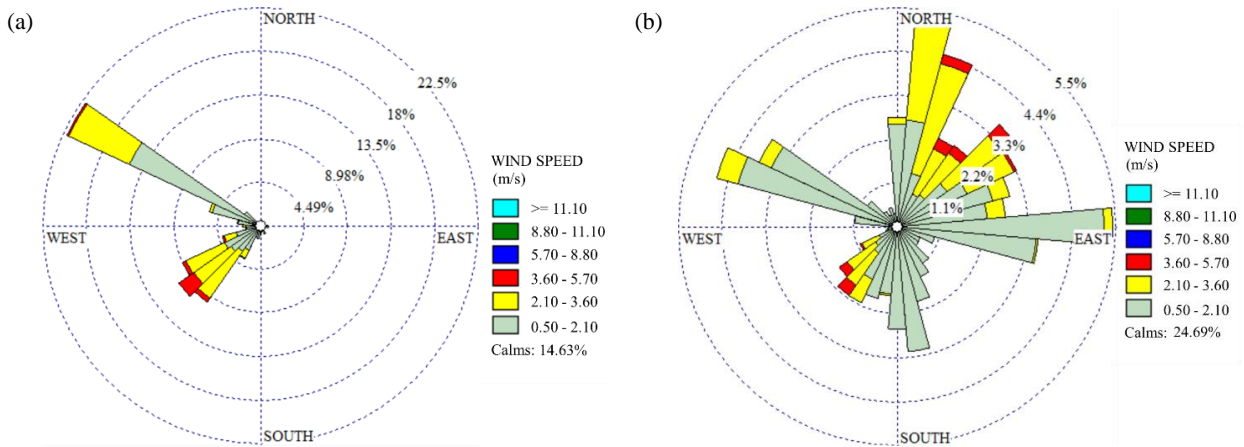


Figure 4. Wind directions and wind speeds in (a) wet season, (b) dry season

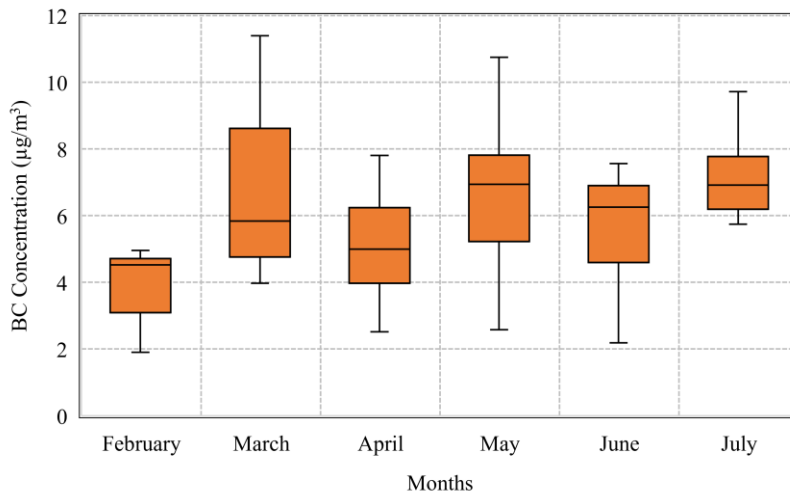


Figure 5. Monthly variations in black carbon concentration at the study location

3.2.2 Trace elements

Although the SRM NIST 2783 was not created by collecting $PM_{2.5}$ on a Polytetrafluoroethylene (Teflon) filter, it can still provide information about instrument performance. The results of elemental validation of the SRM NIST 2783 Air Particulate on Filter Media conducted by Kusmartini (2023) using the same PANalytical Epsilon 5 Energy Dispersive X-

Ray Fluorescence (ED-XRF) spectrometer used in this study, as shown in Table 1, show that the ED-XRF accuracy described as % recovery is in the range of 92-101%, and the measurement precision expressed as relative standard deviation (%RSD) is less than 10%. These validation results indicate that the analysis meets the quality requirements. (Lei et al., 2020).

Table 1. Validation results

Elements	Analysis results (ng/cm ²)	Certified value (ng/cm ²)	% Recovery	% RSD
	Concentration	Concentration		
Mg	863.00	865.00	99.70	1.49
Al	2337.00	2330.00	100.30	0.49
Si	5723.00	5884.00	97.30	0.38
S	105.00	105.00	99.70	1.19
K	536.00	530.00	101.10	1.52
Ca	1313.00	1325.00	99.00	0.65
Ti	150.00	150.00	100.10	0.98
Mn	32.00	32.00	100.40	3.00
Fe	2608.00	2661.00	98.00	2.90
Cu	40.00	41.00	99.60	0.33
Zn	166.00	180.00	92.30	0.82
As	1.20	1.18	101.70	0.57
Pb	31.00	32.00	96.90	6.24

During the sampling period, the average concentration of the 19 trace elements measured was 5,752.71 ng/m³, representing 14.25% of the total PM_{2.5} mass concentration obtained. Table 2 shows that sulfur (S) was the dominant element in the PM_{2.5} samples obtained from the Marunda Industrial Area. Its average concentration was higher during the dry season compared to the wet season. The presence of sulfur in PM_{2.5} is a result from the combustion of fossil fuels, such as coal and high-sulfur vehicle fuels (Santoso et al., 2020a). In Indonesia, heavy diesel vehicles, particularly trucks and other large vehicles that frequently operate near industrial or main roads, commonly utilize fuels that contain sulfur levels of up to 2,500 ppm. The high sulfur concentration is probably due to the sampling location vicinity near industrial facilities that utilize coal as a fuel source, as well as its close proximity to Marunda’s largest arterial road, which has frequent vehicle traffic.

Zinc (Zn) and Lead (Pb) were the heavy metals with the largest contribution to the total element concentration in PM_{2.5}. Zn and Pb have a significant

impact on DNA and chromosome damage (Cavanagh et al., 2009; de Kok et al., 2005). Zinc originates primarily from the non-metallic smelting industry and vehicle tire wear (Farahani et al., 2021). Compared to the lead (Pb) levels observed in downtown Jakarta as reported by Santoso et al. (2020a), the average lead concentration at the study location was 1.5 times greater, but still below 24-hour ambient air quality guidelines. The chemical elements Na, Al, Si, S, K, Cr, Fe, As, Ti, and Br showed significant seasonal variations (p-value<0.05). The increase in concentrations of elements classified as anthropogenic sources, such as S, K, Cr, and Br, from the wet season to the dry season is thought to be related to the activities of local pollutant sources, such as industry, vehicles and biomass burning (Liu et al., 2023). Meanwhile, Na, Al, Si, Fe, As, and Ti are likely associated with soil dust originating from construction activities around the study location. These elements show a significant decrease in concentration from the wet to the dry season.

Table 2. PM_{2.5} elements concentration (ng/m³) in wet season (February-March) and dry season (April-July)

Elements	Wet season		Dry season	
	Average±SD	Range	Average±SD	Range
Na	1,215.38±317.91	574.88-1,763.77	855.59±565.19	135.94-3,399.61
Mg	70.85±73.93	3.43-287.39	47.96±36.33	1.46-214.92
Al	362.87±454.31	8.78-2,639.77	116.46±202.53	13.54-1,291.21
Si	479.67±420.05	83.43-1,600.05	224.32±263.25	23.34-1,727.28
S	1,983.18±815.90	842.27-4,097.98	2,727.89±657.45	970.96-4,233.99
Cl	273.48±457.93	25.08-2,160.28	127.24±95.35	16.15-417.34

Table 2. PM_{2.5} elements concentration (ng/m³) in wet season (February-March) and dry season (April-July) (cont.)

Elements	Wet season		Dry season	
	Average±SD	Range	Average±SD	Range
K	356.18±120.75	170.22-616.10	597.25±232.80	188.03-1,137.99
Cr	5.26±1.99	1.86-11.29	6.82±2.79	2.14-16.38
Fe	445.79±190.69	85.75-791.30	229.67±151.99	39.37-705.08
Ni	3.84±1.71	0.87-8.47	3.15±1.69	0.32-6.87
Cu	23.06±21.00	1.38-93.27	23.93±21.45	1.31-114.56
As	18.80±10.20	0.99-35.52	13.33±8.49	2.18-35.69
Pb	106.04±105.60	6.18-446.02	59.07±53.59	4.93-245.46
Ca	181.94±136.65	43.53-532.50	142.25±72.47	13.17-443.46
Ti	30.41±23.16	2.99-92.35	14.67±16.25	2.98-104.15
V	0.79±0.46	0.23-1.97	0.73±0.32	0.26-2.07
Mn	46.96±22.35	3.53-87.15	49.99±45.21	1.49-212.54
Zn	371.06±225.81	45.14-807.49	349.74±337.81	18.17-2,122.09
Br	17.98±10.60	3.86-40.65	42.16±36.39	7.08-170.53

3.3 Reconstructed mass (RCM)

Figure 6 shows the reconstructed PM_{2.5} concentration based on average values during the wet and dry seasons. Based on the sum of six components, ammonium sulfate and black carbon account for the majority of PM_{2.5} mass in both seasons. Organic compounds and secondary nitrates are examples of unaccounted-for masses in this investigation. In Marunda, ammonium sulfate mass contributed the most (31.19%) to PM_{2.5} mass during the wet season compared with the dry season. The increase in relative humidity in the atmosphere increases the synthesis of (NH₄)₂SO₄ through chemical reactions, resulting in a larger concentration during the wet season. The ammonium sulfate found in this study was most likely caused by industrial and vehicular emissions. The research region is near an industrial sector that burns coal as its primary fuel, contributing to sulfur emissions into the atmosphere. In addition to industry, sulfur sources are expected to originate from the presence of ports on the northeast and northwest sides of the study area, which complicates matters with high volumes of heavy vehicle and ship emissions. In the wet season, black carbon accounts for 20.00% of PM_{2.5} mass, while in the dry season, it accounts for 13.63%. Bangkok and Bandung, both cities with high traffic volumes, similarly have higher amounts of black carbon contribution in the wet season than in the dry (Oanh et al., 2006).

Sea salt is a chemical component that contributes to 13.22% of the reconstructed PM_{2.5} mass during the wet season. The sampling location is less than one kilometer from the sea, where increased wind

speeds assist in facilitating the transportation of sea salt particles to coastal areas. Consequently, the concentration of sea salt in PM_{2.5} increases (Yin et al., 2005). The contribution of crustal matter is less than that of ammonium sulfate, sea salt, and unaccounted mass, indicating that crustal matter is more abundant in the coarse fraction than in the fine fraction, as reported by Oanh et al. (2006) in their investigation of six metropolitan cities in Asia. The mass of sea salt and crustal matter differed significantly in both seasons, with p-values of 2.2×10⁻⁶ and 0.2×10⁻², respectively. During the sampling period, the average smoke concentration was 342.69 ng/m³, with the dry season contributing 0.97% more PM_{2.5} mass. In Jakarta, source apportionment of pollutants identified biomass burning as one of the greatest contributors to PM_{2.5} levels. Due to insufficient waste collection, open dumping and burning of waste in open areas remains a frequent practice in large urban areas such as Jakarta (Santoso et al., 2013). During the dry season, the practice of open burning is more prevalent, resulting in smoke plumes. Smoke plumes are lifted into the air and carried by the wind, increasing PM_{2.5} concentrations in the atmosphere.

4. CONCLUSIONS

PM_{2.5} mass concentration levels in the Marunda Industrial Area, North Jakarta, have significantly exceeded WHO and US EPA daily averages, especially in the dry season. Daily PM_{2.5} trends indicate exposure to values ranging from 12.04 to 81.30 µg/m³, potentially harmful to sensitive groups' health. Sulfur was the species with the highest

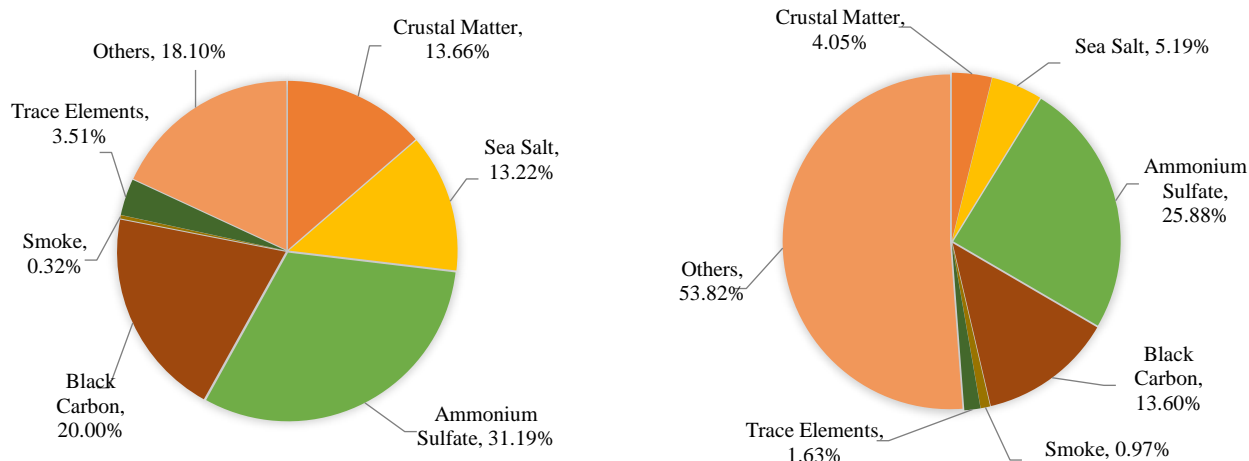


Figure 6. Reconstructed mass of PM_{2.5} (a) wet season, (b) dry season

concentration, and ammonium sulfate contributed to the largest proportion of the PM_{2.5} samples. Industrial activities involving coal are considered to be the source of excessive sulfur levels and a rise in ammonium sulfate in the atmosphere. Overall, this study demonstrates how climatic factors and pollutant sources contribute to PM_{2.5}. These findings can be used by local authorities to develop initiatives designed to lower the potential risk of PM_{2.5}.

ACKNOWLEDGEMENTS

This work was funded by National Research and Innovation Agency (BRIN) under the first batch of Riset Dan Inovasi Untuk Indonesia Maju (RIIM) program in 2022/2023, with contract number No: B-811/II.7.5/FR/6/2022 and No: B-2103/III.2/HK.04.03/7/2022.

REFERENCES

- Aldrian E, Dwi Susanto R. Identification of three dominant rainfall regions within Indonesia and their relationship to sea surface temperature. *International Journal of Climatology: A Journal of the Royal Meteorological Society* 2003;23(12):1435-52.
- Ambade B, Sankar TK, Sahu LK, Dumka UC. Understanding sources and composition of black carbon and PM_{2.5} in urban environments in East India. *Urban Science* 2022;6(3):Article No. 60.
- Anggraeni SN, Iriani DU. Indoor air quality and symptoms of acute respiratory infection in children under five in Marunda Public Flats North Jakarta. *Proceeding of the 1st International Integrative Conference on Health, Life and Social Sciences (ICHLaS 2017)*; 2017 Nov 11-12; Titan Conference Centre, South Tangerang; Indonesia; 2017.
- Begum BA, Hossain A, Nahar N, Markwitz A, Hopke PK. Organic and black carbon in PM_{2.5} at an urban site at Dhaka, Bangladesh. *Aerosol and Air Quality Research* 2012;12(6): 1062-72.
- Canepari S, Perrino C, Astolfi ML, Catrambone M, Perret D. Determination of soluble ions and elements in ambient air suspended particulate matter: Inter-technique comparison of XRF, IC and ICP for sample-by-sample quality control. *Talanta* 2009;77(5):1821-9.
- Cavanagh J-AE, Trought K, Brown L, Duggan S. Exploratory investigation of the chemical characteristics and relative toxicity of ambient air particulates from two New Zealand cities. *Science of the Total Environment* 2009;407(18):5007-18.
- Chan YC, Simpson RW, Mctainsh GH, Vowles PD, Cohen DD, Bailey GM. Characterisation of chemical species in PM_{2.5} and PM₁₀ aerosols in Brisbane, Australia. *Atmospheric Environment* 1997;31(22):3773-85.
- Chirasophon S, Pochanart P. The long-term characteristics of PM₁₀ and PM_{2.5} in Bangkok, Thailand. *Asian Journal of Atmospheric Environment* 2020;14(1):73-83.
- Chow JC, Lowenthal DH, Chen L-WA, Wang X, Watson JG. Mass reconstruction methods for PM_{2.5}: A review. *Air Quality, Atmosphere and Health* 2015;8:243-63.
- Cohen AJ, Brauer M, Burnett R, Anderson HR, Frostad J, Estep K, et al. Estimates and 25-year trends of the global burden of disease attributable to ambient air pollution: An analysis of data from the Global Burden of Diseases Study 2015. *The Lancet* 2017;389(10082):1907-18.
- Darrow LA, Klein M, Flanders WD, Mulholland JA, Tolbert PE, Strickland MJ. Air pollution and acute respiratory infections among children 0-4 years of age: An 18-year time-series study. *American Journal of Epidemiology* 2014;180(10):968-77.
- Farahani VJ, Soleimanian E, Pirhadi M, Sioutas C. Long-term trends in concentrations and sources of PM_{2.5}-bound metals and elements in central Los Angeles. *Atmospheric Environment* 2021;253(8):Article No. 118361.
- Ho KF, Lee SC, Chan CK, Jimmy CY, Chow JC, Yao XH. Characterization of chemical species in PM_{2.5} and PM₁₀ aerosols in Hong Kong. *Atmospheric Environment* 2003; 37(1):31-9.
- Humairoh GP, Syafei AD, Santoso M, Boedisantoso R, Assomadi AF, Hermana J. Identification of trace element in ambient air case study: Industrial Estate in Waru, Sidoarjo, East Java. *Aerosol and Air Quality Research* 2020;20(9):1910-21.
- Istiana T, Kurniawan B, Soekirno S, Nahas A, Wihono A, Nuryanto DE, et al. Causality analysis of air quality and meteorological parameters for PM_{2.5} characteristics determination: Evidence from Jakarta. *Aerosol and Air Quality Research* 2023;23(9):Article No. 230014.

- de Kok TM, Hogervorst JG, Briedé JJ, van Herwijnen MH, Maas LM, Moonen EJ, et al. Genotoxicity and physicochemical characteristics of traffic-related ambient particulate matter. *Environmental and Molecular Mutagenesis* 2005;46(2):71-80.
- Kusmartini I. Chemical Characterization of Fine Particulates (PM_{2.5}) using X-Ray Fluorescence and Ion Exchange Chromatography Methods [dissertation]. Bandung, Bandung Institute of Technology; 2023 (in Bahasa).
- Kusumaningtyas SDA, Aldrian E, Wati T, Atmoko D, Sunaryo S. The recent state of ambient air quality in Jakarta. *Aerosol and Air Quality Research* 2018;18(9):2343-54.
- Lei X, Chen R, Wang C, Shi J, Zhao Z, Li W, et al. Necessity of personal sampling for exposure assessment on specific constituents of PM_{2.5}: Results of a panel study in Shanghai, China. *Environment International* 2020;141:Article No. 105786.
- Liu S, Wu T, Wang Q, Zhang Y, Tian J, Ran W, et al. High time-resolution source apportionment and health risk assessment for PM_{2.5}-bound elements at an industrial city in northwest China. *Science of the Total Environment* 2023;870:Article No. 161907.
- Malm WC, Sisler JF, Huffman D, Eldred RA, Cahill TA. Spatial and seasonal trends in particle concentration and optical extinction in the United States. *Journal of Geophysical Research: Atmospheres* 1994;99(D1):1347-70.
- Ministry of Health of the Republic of Indonesia. Indonesia Basic Health Research (RISKESDAS) 2018. Jakarta, Indonesia: The National Institute of Health Research and Development; 2018.
- Narita D, Oanh NTK, Sato K, Huo M, Permadi DA, Chi NNH, et al. Pollution characteristics and policy actions on fine particulate matter in a growing Asian economy: The case of Bangkok Metropolitan Region. *Atmosphere* 2019;10(5): Article No. 227.
- Nascimento AP, Santos JM, Mill JG, de Almeida Albuquerque TT, Júnior NCR, Reisen VA, et al. Association between the incidence of acute respiratory diseases in children and ambient concentrations of SO₂, PM₁₀, and chemical elements in fine particles. *Environmental Research* 2020;188:Article No. 109619.
- Nguyen GTH, Shimadera H, Uranishi K, Matsuo T, Kondo A. Numerical assessment of PM_{2.5} and O₃ air quality in Continental Southeast Asia: Impacts of future projected anthropogenic emission change and its impacts in combination with potential future climate change impacts. *Atmospheric Environment* 2020;226:Article No. 117398.
- Oanh NTK, Upadhyay N, Zhuang Y-H, Hao Z-P, Murthy DVS, Lestari P, et al. Particulate air pollution in six Asian cities: Spatial and temporal distributions, and associated sources. *Atmospheric Environment* 2006;40(18):3367-80.
- Owoade KO, Hopke PK, Olise FS, Ogundele LT, Fawole OG, Olaniyi BH, et al. Chemical compositions and source identification of particulate matter (PM_{2.5} and PM_{2.5-10}) from a scrap iron and steel smelting industry along the Ife-Ibadan highway, Nigeria. *Atmospheric Pollution Research* 2015;6(1):107-19.
- Peng RD, Bell ML, Geyh AS, McDermott A, Zeger SL, Samet JM, et al. Emergency admissions for cardiovascular and respiratory diseases and the chemical composition of fine particle air pollution. *Environmental Health Perspectives* 2009;117(6): 957-63.
- Putra Y, Wulandari SS. Factors causing acute respiratory infection events. *Health Journal* 2019;10(1):Article No. 37 (in Bahasa).
- Rahman MS, Akhter S, Rahman R, Choudhury TR, Jolly YN, Akter S, et al. Identification of sources of PM_{2.5} at Farmgate Area, Dhaka using reconstructed mass calculation and statistical approaches. *Nuclear Science and Applications* 2019;28(1-2):13-23.
- Republic of Indonesia Government Regulation. Republic of Indonesia Government Regulation No.22 of 2021 concerning Implementation of Environmental Protection and Management [Internet]. 2021 [cited 8 Feb 2023]. Available from: <https://peraturan.bpk.go.id/Details/161852/pp-no-22-tahun-2021>.
- Santoso M, Lestiani DD, Damastuti E, Kurniawati S, Kusmartini I, Atmodjo DPD, et al. Long term characteristics of atmospheric particulate matter and compositions in Jakarta, Indonesia. *Atmospheric Pollution Research* 2020a;11(12): 2215-25.
- Santoso M, Lestiani DD, Kurniawati S, Damastuti E, Kusmartini I, Atmodjo DPD, et al. Assessment of urban air quality in Indonesia. *Aerosol and Air Quality Research* 2020b;20(10): 2142-58.
- Santoso M, Lestiani DD, Markwitz A. Characterization of airborne particulate matter collected at Jakarta roadside of an arterial road. *Journal of Radioanalytical and Nuclear Chemistry* 2013;297(2):165-9.
- Sasmita A, Andrio D, Hasibuan P. Mapping the distribution of particulates from burning solid waste from the palm oil processing industry, in Kampar Regency, Riau. *Journal of Science and Technology* 2019;18(2):57-67 (in Bahasa).
- United States Environmental Protection Agency (USEPA). NAAQS Table [Internet]. 2006 [cited 2023 Nov 14]. Available from: <https://www.epa.gov/criteria-air-pollutants/naaqs-table>.
- Wang F, Chen T, Chang Q, Kao Y-W, Li J, Chen M, et al. Respiratory diseases are positively associated with PM_{2.5} concentrations in different areas of Taiwan. *PLoS One* 2021;16(4):e0249694.
- Wang X, Westerdahl D, Chen LC, Wu Y, Hao J, Pan X, et al. Evaluating the air quality impacts of the 2008 Beijing Olympic Games: On-road emission factors and black carbon profiles. *Atmospheric Environment* 2009;43(30):4535-43.
- Watson JG, Chow JC, Chen L-WA. Summary of organic and elemental carbon/black carbon analysis methods and intercomparisons. *Aerosol and Air Quality Research* 2005; 5(1):65-102.
- Watson JG, Chow JC, Lowenthal DH, Chen L-WA, Wang X, Biscay P. Reformulation of PM_{2.5} Mass Reconstruction Assumptions for the San Joaquin Valley. Reno, Nevada: Desert Research Institute; 2012.
- World Health Organization (WHO). WHO Global Air Quality Guidelines: Particulate Matter (PM_{2.5} and PM₁₀), Ozone, Nitrogen Dioxide, Sulfur Dioxide and Carbon Monoxide. Geneva, Switzerland: World Health Organization; 2021.
- Xie W, You J, Zhi C, Li L. The toxicity of ambient fine particulate matter (PM_{2.5}) to vascular endothelial cells. *Journal of Applied Toxicology* 2021;41(5):713-23.
- Yan M, Ge H, Zhang L, Chen X, Yang X, Liu F, et al. Long-term PM_{2.5} exposure in association with chronic respiratory diseases morbidity: A cohort study in northern China. *Ecotoxicology and Environmental Safety* 2022;244:Article No. 114025.
- Yin J, Allen AG, Harrison RM, Jennings SG, Wright E, Fitzpatrick M, et al. Major component composition of urban PM₁₀ and PM_{2.5} in Ireland. *Atmospheric Research* 2005;78(3-4):149-65.

Exergy Analysis of Waste-to-Energy Technologies for Municipal Solid Waste Management

Nuhu Caleb Amulah*, Mohammed Ben Oumarou, and Abba Bashir Muhammad

Department of Mechanical Engineering, Faculty of Engineering, University of Maiduguri, P.M.B 1069, Maiduguri, Nigeria

ARTICLE INFO

Received: 27 Jan 2024
Received in revised: 3 Apr 2024
Accepted: 19 Apr 2024
Published online: 30 Apr 2024
DOI: 10.32526/enrj/22/20240023

Keywords:

Exergy/ Municipal solid waste/
Incineration/ Anaerobic digestion/
Plasma gasification/ Landfill

* Corresponding author:

E-mail:
amulahn@unimaid.edu.ng

ABSTRACT

In recent years, there have been increasing concerns over the detrimental effects of irreversible linear patterns of material and energy consumption, which have led to an enormous generation of municipal solid waste (MSW). Concepts like waste-to-energy (WtE) and recycling have gained increasing recognition and support as responses to these challenges. This study assessed the exergetic potential of four WtE technologies (landfill gas-to-energy, anaerobic digestion, incineration, and plasma gasification) in the context of the MSW characteristics of Maiduguri, Borno State. The population of Maiduguri, waste generation rate, waste composition, and the ultimate and proximate analysis of the MSW were used for the assessment. Exergetic potential in the form of electrical energy generation and three exergy-based indicators (exergy efficiency, exergy defect, and improvement potential) were evaluated for each WtE option. The results reveal that anaerobic digestion and plasma gasification are viable options based on the exergetic potential and the measured exergy performance indicators. These findings offer valuable insights for policymakers and waste management authorities, facilitating informed decisions to address environmental concerns and promote resource-efficient urban development in Maiduguri and similar regions.

1. INTRODUCTION

The global transition of the economy towards more efficient and stable manufacturing processes was marked by unprecedented industrialization, food production, population growth, material use, and waste generation. By the latter part of the 20th century, the dangers of unrestrained environmental pollution and overexploitation of natural resources had become the subject of discourse among researchers and policymakers.

Municipal solid waste (MSW) is an emblematic by-product of industrial society; it is the mixture of solid waste that is disposed daily by both urban and rural populations (Nanda and Berruti, 2021). The composition of MSW varies greatly depending on various factors such as culture, economy, geography, time, etc. Figure 1 shows the composition of MSW for the world, Africa, Nigeria, and Maiduguri. In each of the locations, organic waste which includes food waste

and green waste accounts for over 40% of the total waste generated, making it the most prevalent type of MSW.

MSW remains one of the key challenges of the 21st century. For instance, of the 174 million tonnes of waste generated in Sub-Saharan Africa, 69% of the waste is openly dumped and often burned. About 24% of the waste is disposed in some form of a landfill and 7% is recycled or recovered (Kaza et al., 2018). In Nigeria, only 20-30% of the waste generated is being collected and managed properly (Esohe, 2023). This raises a fundamental question: how can MSW be effectively managed to safeguard both public health and the environment? The importance of this question can hardly be overestimated. It bears directly upon the connection between humans, resources and the environment. This is because the characteristic of waste can be likened to a notion of a resource, which can be described as material that possesses value in its

use and is a reflection of human evaluation (Jones and Hollier, 1997). As awareness of these challenges grows, the traditional perspective of viewing MSW as a burden is slowly being replaced by approaches that seek to derive value from it by converting it into useful products using waste-to-energy (WtE) technologies and other approaches (Hadidi and Omer, 2017; Jadhao et al., 2017; Bakas et al., 2018). Various technological alternatives exist for the disposal and treatment of MSW including recycling, landfill gas-to-energy (LFGTE), composting, anaerobic digestion, gasification, incineration, and pyrolysis.

A 2003 MSW composition analysis in Maiduguri revealed that organic material comprised 25.80%, plastics 18.10%, metals 9.10%, paper and cardboard 7.50%, glass 4.30%, and others 35.20% of the total waste stream (Dauda and Osita, 2003). Compared with Figure 1, organic waste composition increased to 55.21%, and plastic waste increased to 32.56%. These shifts indicate a growing abundance of organic and plastic waste, both of which are viable feedstocks for WtE technologies like anaerobic digestion, incineration, LFGTE and plasma gasification.

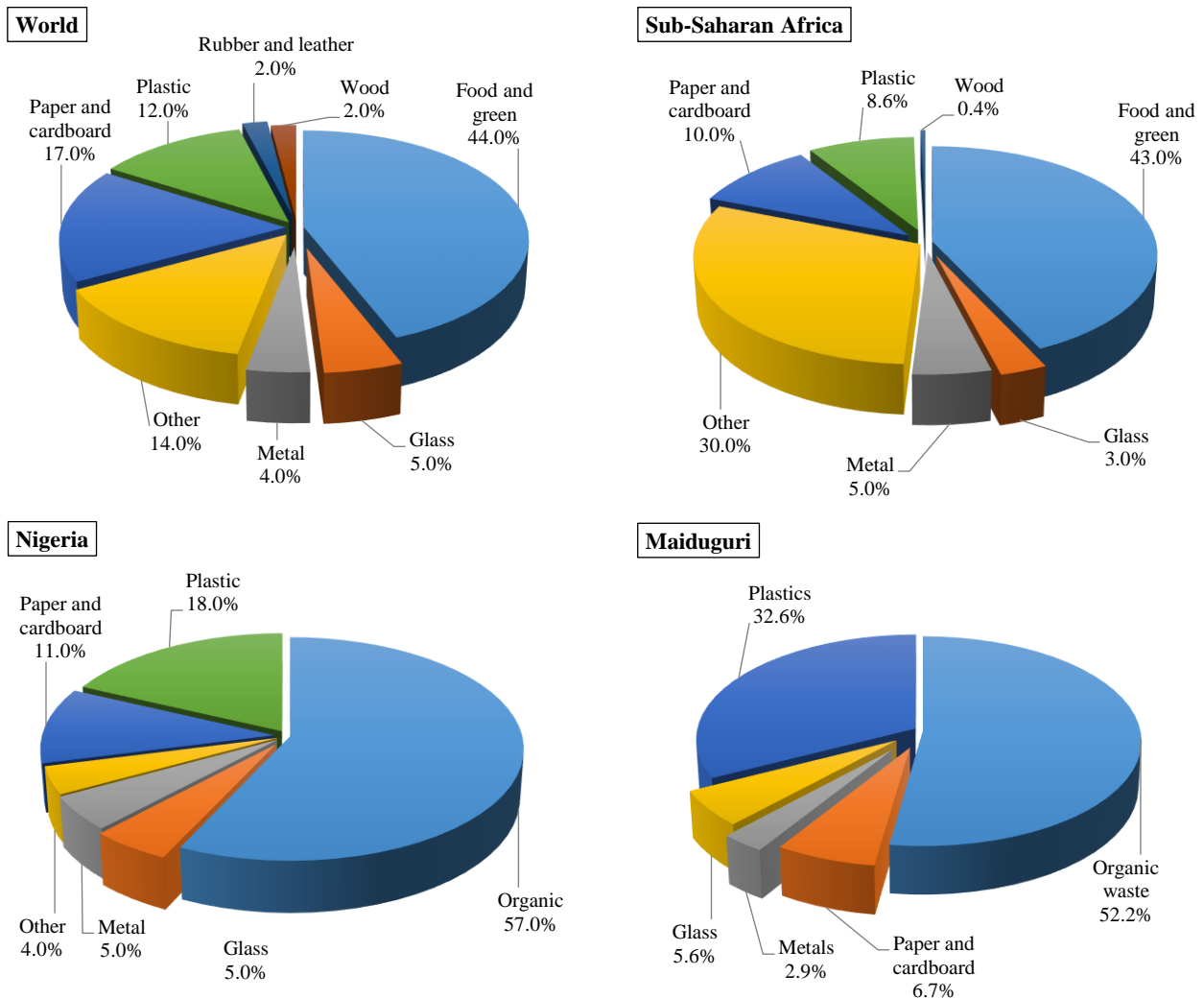


Figure 1. Waste composition for different locations. World and Sub-Sahara's charts were reproduced from Kaza et al. (2018), Nigeria's chart was reproduced from Kofoworola (2016), and Maiduguri's chart was based on data from Oumarou et al. (2017).

From social, economic, and environmental viewpoints, MSW management systems employing these contemporary technologies offer a wide range of benefits. However, the sustainability of these systems is often debated due to the diverse techniques available for weighing them (Soltanian et al., 2022). These

techniques include life cycle assessment (LCA), techno-economic analysis, material flow analysis (MFA), and thermodynamic methods.

Among the many sustainability assessment techniques, exergy analysis appears to provide the basis for developing comprehensive methodologies

for sustainability. This is attributed to its ability to identify and measure the thermodynamic inefficiencies of the MSW management system (Aghbashlo et al., 2019; Cavalcanti et al., 2019; Chen et al., 2022; Soltanian et al., 2022). Exergy is the maximum possible work that can be obtained from a system through a series of reversible operations that bring it into thermodynamic equilibrium with its surroundings. Exergy makes it possible to account for losses in the quality of resources and to meaningfully compare different types of energy, as well as to compare energy with material resources (Magnanelli et al., 2018), and is only defined with respect to a reference environment (see Gaudreau et al. (2012) for discussion on reference environments and their characteristics). The objective of this study is to evaluate the exergetic potential of converting MSW into useful work through various WtE technologies in Maiduguri, Nigeria. Findings from the study will benefit policymakers, waste management authorities, and communities in Maiduguri by providing insights

into the most efficient and sustainable methods for managing MSW and meeting energy needs.

2. METHODOLOGY

2.1 Study area

Maiduguri is the largest city in North-eastern Nigeria and serves as the capital of Borno State, Nigeria. It is located at 11.8311° N, 13.1510° E (see Figure 2). The city has experienced rapid growth in population due to rural-urban migration and the Boko Haram insurgency which has displaced millions of people from the neighbouring villages. The city serves as a commercial centre with links to Niger, Cameroon and Chad. It is composed of two local government areas, namely, Maiduguri Metropolitan Council and Jere Local Government Area.

The waste composition of Maiduguri constitutes the key input in this study. The typical waste composition for Maiduguri is shown in Figure 1, and the ultimate and proximate analysis of MSW utilised in this study is shown in Table 1.

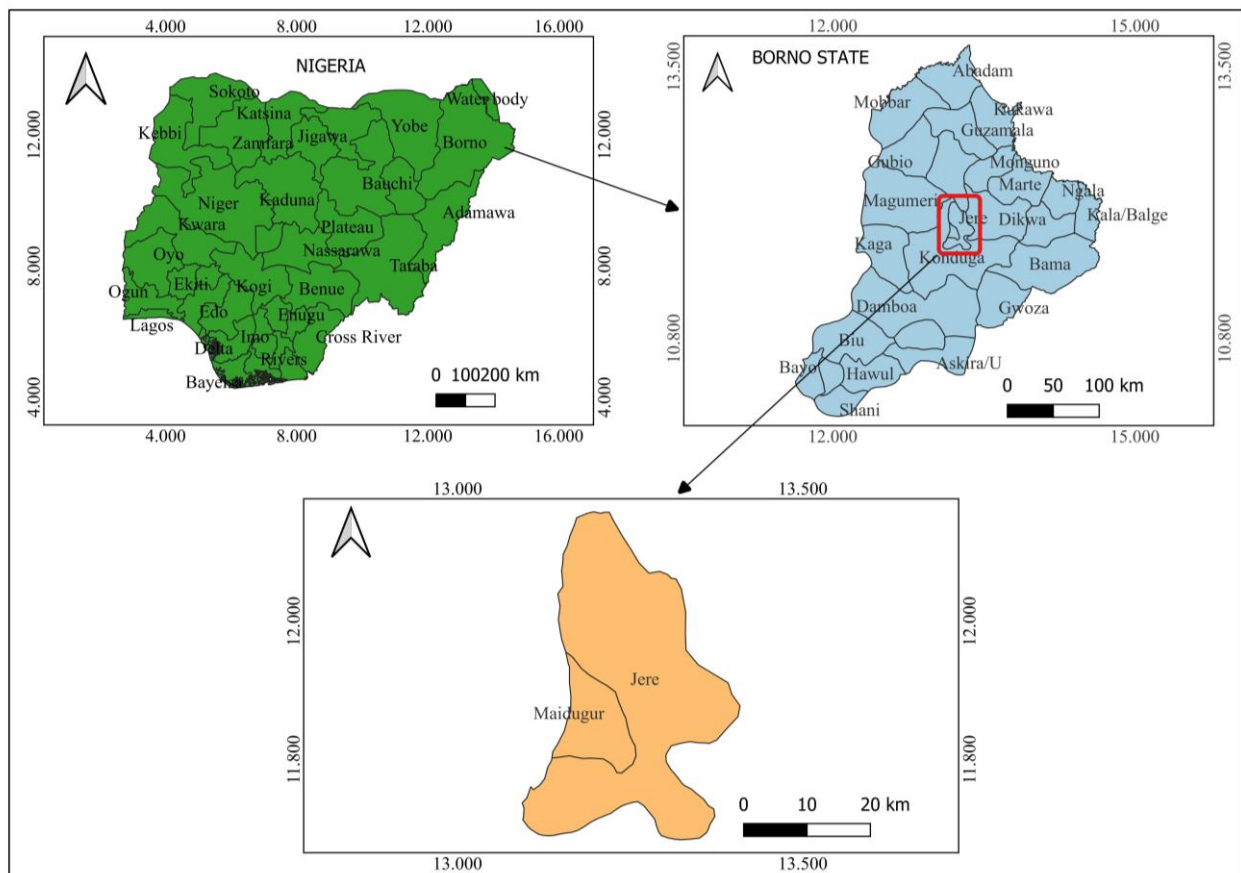


Figure 2. Map of the study area

Table 1. Results of the ultimate and proximate analysis of MSW (dry basis, weight percentage) (Oumarou et al., 2012)

Ultimate analysis	Carbon	Hydrogen	Nitrogen	Sulphur	Oxygen
	20.99	0.490	1.84	0.07	23.95
Proximate analysis	Moisture	Volatile matter	Ash	Fixed carbon	
	21.83	25.12	30.83	22.22	

2.2 Estimation of annual MSW generated

The amount of waste generated in tonnes/year by the population, P(n), is estimated using Equation 1.

$$W = P_0(1 + r)^n \times W_{\text{genR}} \times \frac{365}{1000} \quad (1)$$

Equation 2 is used to determine the amount of MSW input into each system.

$$W_{\text{in}} = W \times W_f \quad (2)$$

Where; P_0 is the base year population, r is the average annual population growth rate, W_{genR} is the waste generation in kg/capita/day and W_f is the fraction of the MSW that is sent to the WtE system.

2.3 Exergy analysis of WtE technologies

The reference state established in this study is characterised by a temperature (T_0) of 298.15 K and a pressure (P_0) of 101.3 kPa. Two components of exergy are considered: physical exergy, which is related to changes in temperature, pressure and concentration; and chemical exergy, which is linked to changes in the chemical composition of substances (Sato, 2004). Physical exergy is expressed as (Jadhao et al., 2017):

$$\text{Ex}_{\text{ph}} = (h - h_0) - T_0(s - s_0) = \int_{T_0}^T c_p dT - T_0 \int_{T_0}^T \frac{dT}{T} \quad (3)$$

Where; h is the specific enthalpy (J/kg K), s is the specific entropy (J/kg K), T is temperature (K), h_0 , s_0 and T_0 describe the state of the reference environment. The total chemical exergy is determined from the standard chemical exergy values of the elements using Equation 4 (Jadhao et al., 2017).

$$\text{Ex}_{\text{ch},i} = \Delta G_i^0 + \sum_i \gamma_i \text{Ex}_{\text{q},i}^0 \quad (4)$$

Where; γ_k represents the mole quantities, $\text{Ex}_{\text{q},i}^0$ is the standard chemical exergy (kJ/mol) of the i^{th} reference species and G is the Gibbs free energy (kJ/mol). The chemical exergy of the feed MSW is based on the ultimate analysis data presented in Table 1 and the waste composition shown in Figure 1. The values for the standard exergy of each element are

obtained from Rivero and Garfias (2006) (see Table S2 of the supporting information (SI)).

Three exergy-based indicators are used to evaluate the performance of the products of each WtE technology: the total exergy efficiency, which is expressed in Equation 5; the improvement potential (Equation 6), which measures the amount of exergy that can be saved by improving the performance of the process; and the exergy defect (Equation 7), which represents the proportion of exergy lost within a system.

$$\epsilon = \frac{\text{Ex}_{\text{out}}}{\text{Ex}_{\text{in}}} = 1 - \frac{\text{Ex}_{\text{d}}}{\text{Ex}_{\text{in}}} \quad (5)$$

$$\text{IP} = (1 - \epsilon)(\text{Ex}_{\text{in}} - \text{Ex}_{\text{out}}) = (1 - \epsilon)\text{Ex}_{\text{d}} \quad (6)$$

$$\delta = 1 - \epsilon \quad (7)$$

Where; ϵ is the exergy efficiency, Ex_{out} is the exergy of output, Ex_{in} is the exergy of input and Ex_{d} is the overall exergy lost or dissipated during the process.

2.3.1 Landfill gas-to-energy

The amount of CH_4 (m^3/year) is estimated using the Landfill Gas Emission Model (LandGEM) version 3.02 (Alexander et al., 2005). By this model, CH_4 is formed from decomposable material given by the first-order decomposition rate equation:

$$Q_{\text{CH}_4} = \sum_{i=1}^n \sum_{j=0.1}^1 kL_0 \left(\frac{W_{\text{in}}}{10}\right) e^{-kt_{ij}} \quad (8)$$

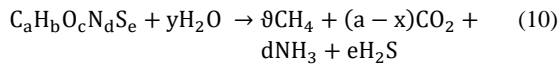
Where; i is the 1-year time increment, n is [year of the calculation] - [initial year of waste acceptance], j is the 0.1-year time increment, k is the methane generation rate (/year) and L_0 is the methane generation potential (m^3/tonne). The total exergy associated with the collected CH_4 is estimated using Equations 3 and 4. It is assumed that 33% of this exergy gets converted to electricity using an internal combustion engine. The exergy-based performance of this technology is estimated using Equations 5-7.

2.3.2 Anaerobic digestion

The volume of CH₄ obtained (m³/tonne) from the anaerobic digestion of MSW is estimated using Equation 9 (Huang and Fooladi, 2021):

$$V_{CH_4} = \frac{16\theta}{aM_C + bM_H + cM_O + M_N} \times \frac{1000}{\rho_{CH_4}} \quad (9)$$

Where; ρ_{CH_4} is the density of methane (see Table S1 of the SI). The other parameters are obtained from the Buswell equation which is expressed as:



Where; $\theta = \frac{1}{8}(4a + b - 2c - 3d - 2e)$ and $y = \frac{1}{4}(4a + b - 2c + 3d + 3e)$. The subscripts a, b, c, d, e are constants parameters with approximate values given by (Achinas and Euverink, 2016):

$$a = \frac{m_C}{M_C} = \frac{m_C}{12.01} \quad (11a)$$

$$b = \frac{m_H}{M_H} = \frac{m_H}{1.01} \quad (11b)$$

$$c = \frac{m_O}{M_O} = \frac{m_O}{16.00} \quad (11c)$$

$$d = \frac{m_N}{M_N} = \frac{m_N}{14.01} \quad (11d)$$

Where; m_C , m_H , m_O , and m_N represent the mass of carbon, hydrogen, oxygen and nitrogen, respectively.

The methane production from the digester is lower than the theoretical value because not all of the organic matter decomposes in the digester. Secondly, some of the organic matter in the waste is utilized in the synthesis of cell tissue for microorganisms, which obstructs microbial decomposition (Ogunjuyigbe et al., 2017; Cudjoe et al., 2020). Hence, the actual quantity of methane (m³) produced from the digester is estimated using:

$$V_{CH_4(Act)} = V_{CH_4} \times 0.85 \times W_{in} \quad (12)$$

The total exergy associated with the electricity generated from collected CH₄ is estimated using a conversion efficiency of 26%.

2.3.3 Incineration

The exergy flow is evaluated across three units of operation which are the dryer, incinerator, and turbine. The schematic of the exergy flow across these units is shown in Figure 3. A detailed description of the exergy analysis of this process is provided in the SI.

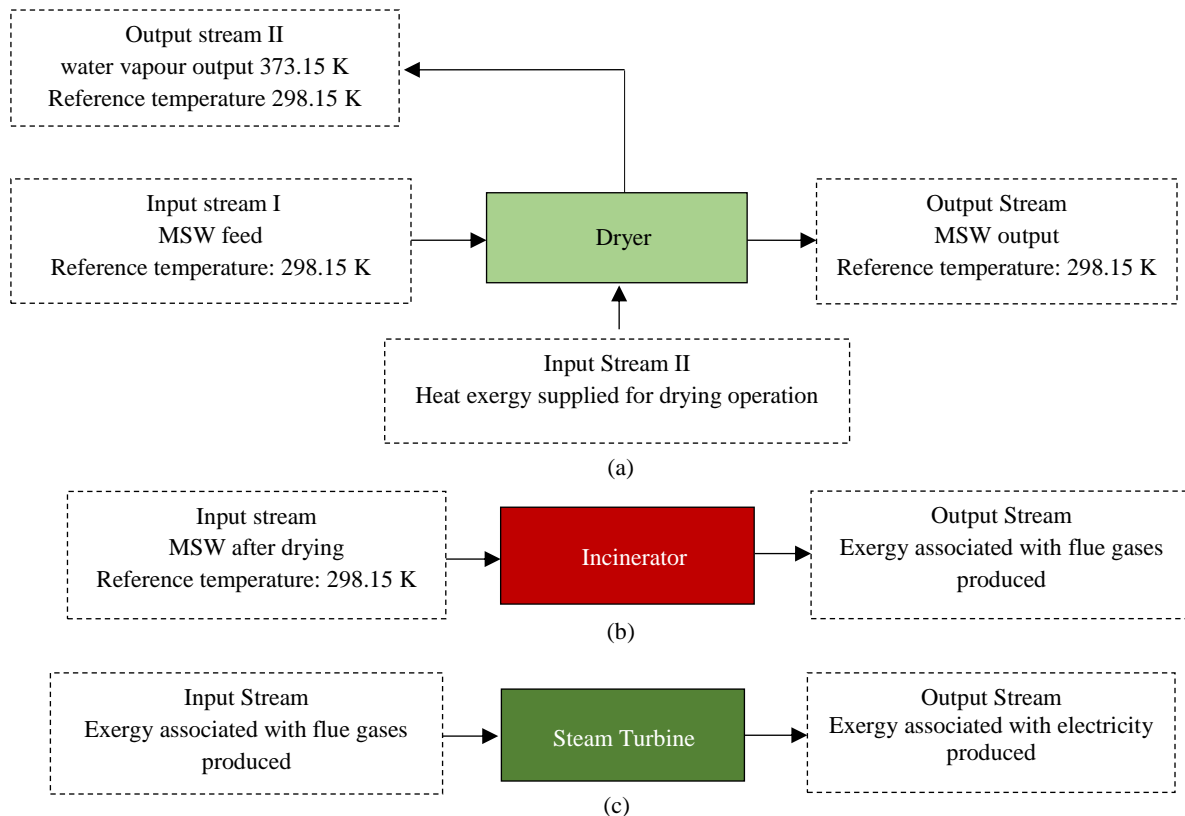


Figure 3. Exergy flow in incineration process

2.3.4 Plasma gasification

The flow of exergy in plasma gasification of MSW is shown in Figure 4. Because the initial moisture content of the Feed MSW and the allowable moisture content post-drying for both incineration and plasma gasification are identical, the exergy flow calculations across the dryer is the same in both processes. The first input stream to the plasma furnace is the chemical exergy associated with the tonnes of

MSW. The second input is air at the reference temperature.

For plasma gasification, a plasma torch powered by an electric arc is needed to ionize the gas and catalyse MSW into syngas. The electricity consumption for a plasma torch per tonne of MSW is about 180 kWh (Jadhao et al., 2017). Exergy associated with this electricity is the third input stream to the plasma furnace (see Figure 5).

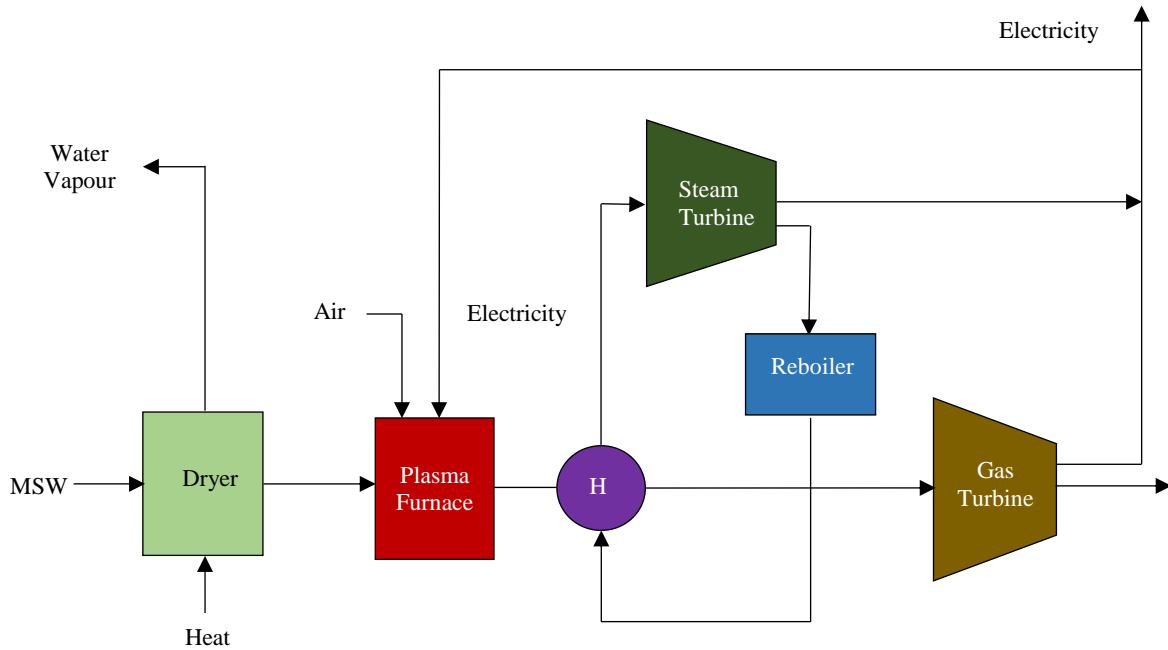


Figure 4. Plasma Gasification of MSW

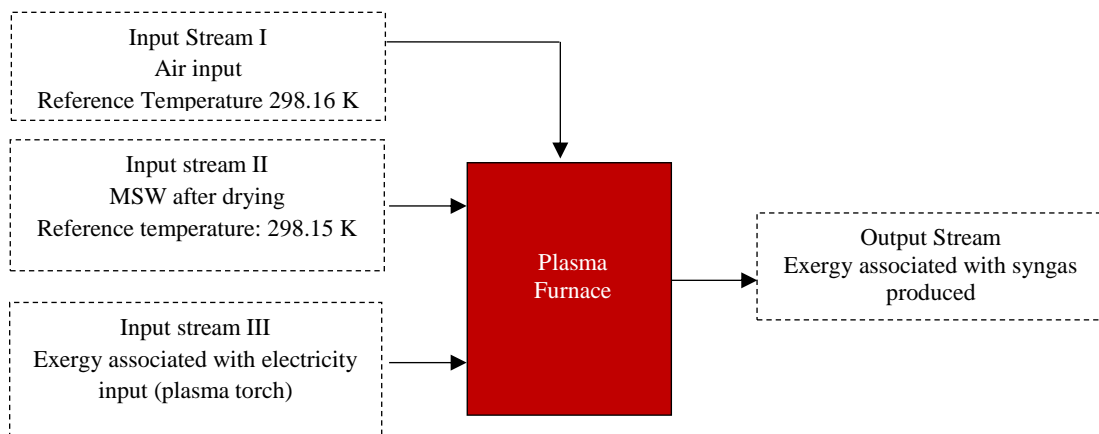


Figure 5. Exergy flow across plasma furnace in plasma gasification of MSW

It is assumed that the plasma gasification products burn and achieve equilibrium before leaving the plasma furnace, therefore, an equilibrium model is utilised in this study. The composition of the syngas produced is predicted based on the equilibrium model

established by Zainal et al. (2001) and was slightly adjusted with updated thermodynamic data from Yaws (2003). A detailed description of this process is provided in the SI.

3. RESULTS AND DISCUSSION

3.1 Waste generation

The two primary factors driving MSW generation potential in this study are population size (which depends on the population growth rate) and per capita waste generation rates. The waste generation for the year 2023 was estimated to be 2.63×10^5 tonnes using a waste generation rate of 0.53 kg/capita/day, base-year population of 1,328,100 and an annual growth rate of 2.40%. The MSW generation prediction model is based on the assumption that the type and amount of waste generated will not change over time.

Table 2. Chemical exergy associated with feed MSW

	Composition %	Molar mass (g/mol)	Mass (Tonnes)	Ex_q^0 (kJ/mol)	Ex_{ch}^0 (kJ)
Carbon	20.99	12.01	32028.74	410.27	1.09×10^{12}
Hydrogen	0.49	1.01	747.69	236.12	1.75×10^{11}
Nitrogen	1.84	14.01	2806.14	0.67	1.34×10^8
Sulphur	0.07	32.07	103.76	609.30	1.97×10^9
Oxygen	23.95	16.00	36549.99	3.92	8.95×10^9
Total					1.28×10^{12}

3.2 Exergy analysis of WtE technologies

Figure 6 illustrates CH_4 , CO_2 , and total LFG yearly volume rate emissions based on the LandGEM model, and its input parameters are methane generation rate of 0.07/year, methane generation potential of $170 \text{ m}^3/\text{tonne}$. According to the model, all of the LFG is made up of CH_4 methane and CO_2 carbon dioxide as well as trace amounts of non-methanogenic organic carbons and other pollutants. It is assumed that the LFG generation starts as soon as it is dumped, and the rate of gas of CH_4 generation reaches its peak within the first 10 years. Figure 6 shows that the production of LFG follows a characteristic trend in

However, this is not always the case, as MSW generation is affected by several other factors such as economic development and technological advancements. As a result, there is a lot of uncertainty in MSW generation predictions. This uncertainty is especially pronounced for processes that rely on the composition and quantity of MSW, such as anaerobic digestion and LFG production. Table 2 presents the estimate of the chemical exergy associated with 2.63×10^5 tonnes/year of MSW generated. The total chemical exergy of 1.28×10^{12} kJ serves as the input exergy of feed MSW for each of the WtE technologies.

which it attains its peak about 10 years after the initial waste acceptance, subsequently entering a phase of decline as the waste undergoes decomposition. CH_4 generation commences from a baseline of zero in the year 2023 and exhibits an incremental trajectory, reaching its peak in 2029 with a volume $8.47 \times 10^6 \text{ m}^3$, after which the rate declines gradually. The average CH_4 collected is $5.86 \times 10^6 \text{ m}^3/\text{year}$ and the exergy efficiency and other performance indicators associated with the electricity generated from landfilling are given in Table 5. The output exergy for the LFGTE option is 4.94×10^4 GJ, representing only 3.8% of the input exergy.

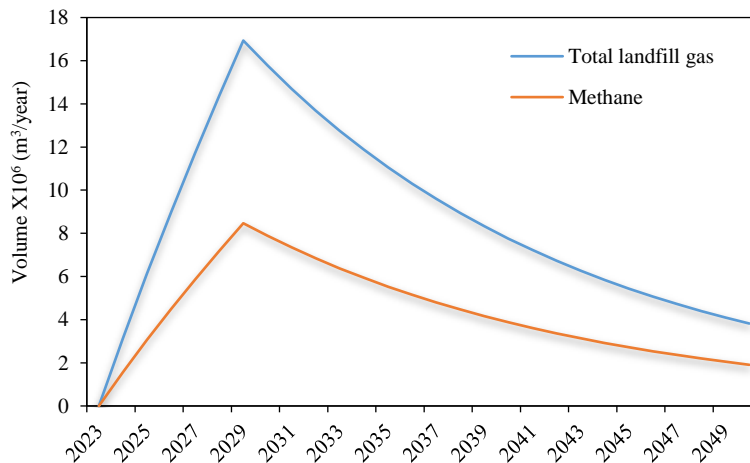


Figure 6. LFG generation from landfill

For anaerobic digestion, the feed MSW into the recovery system is 134,138.43 tonnes representing the organic fraction of MSW. The CH₄ collected as estimated from the Buswell equation, is 2.19×10⁷ m³/year. The exergy flow of the process is shown in Figure 7. The total exergy loss in the digester is 5.36×10⁵ GJ, representing 41.88% of the total exergy input. The most substantial exergy loss is observed in the IC engine which accounts for 42.97% of the total exergy input and 73.92% of the exergy of the CH₄ generated by the anaerobic digester.

The exergy content of the flue gases resulting from the incineration of MSW is presented in Table 3. It is worth highlighting an observation: the chemical exergy values of these flue gases are higher when compared to their physical exergy values. This disparity can be attributed to the specific condition of these gas streams, as both their temperature and pressure closely align with those of the reference state. This results in an increase in their chemical exergy, implying the significant role that temperature and pressure conditions play in influencing the exergy content of these gases during the incineration process.

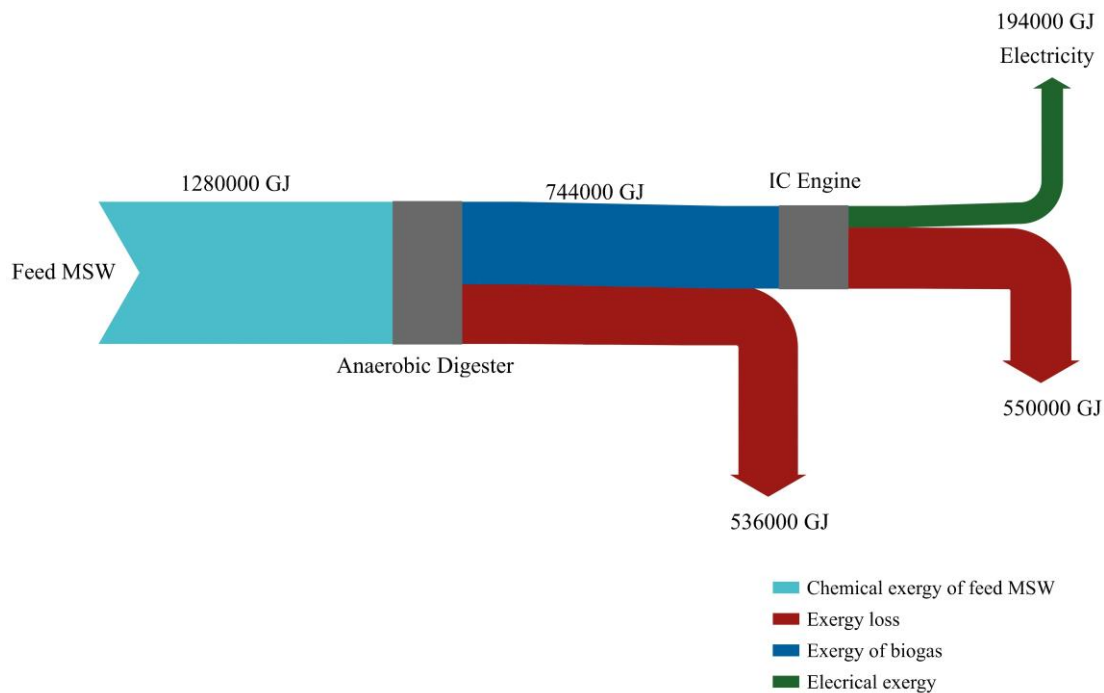


Figure 7. Flow of exergy in anaerobic digestion process

Table 3. Exergy associated with flue gases from incineration

Flue gases	Quantity emitted (kmol)	Ex _{ph} (kJ)	Ex _{ch} (kJ)
CO ₂	2.67×10 ⁶	5.74×10 ¹⁰	1.97×10 ¹¹
H ₂ O	7.40×10 ⁵	1.23×10 ¹⁰	4.45×10 ¹⁰
NO	2.00×10 ⁵	2.80×10 ⁹	2.73×10 ¹⁰
SO ₂	3.241×0 ³	7.18×10 ⁷	1.14×10 ⁹
HCl	0.00	0.00	0.00
Total		7.26×10 ¹⁰	2.70×10 ¹¹

In Figure 8, a visual representation is provided for the exergy flow within the incineration process. The most substantial exergy losses occur in the incinerator, as 73.29% of the exergy initially introduced into the incinerator is lost. This phenomenon is due to, firstly, the low carbon

composition of the MSW and, secondly, the substantial entropy generation resulting from the inherently highly irreversible combustion process that takes place within the incinerator. Also, approximately 13.86% of the total exergy that is supplied to the drying system is lost.

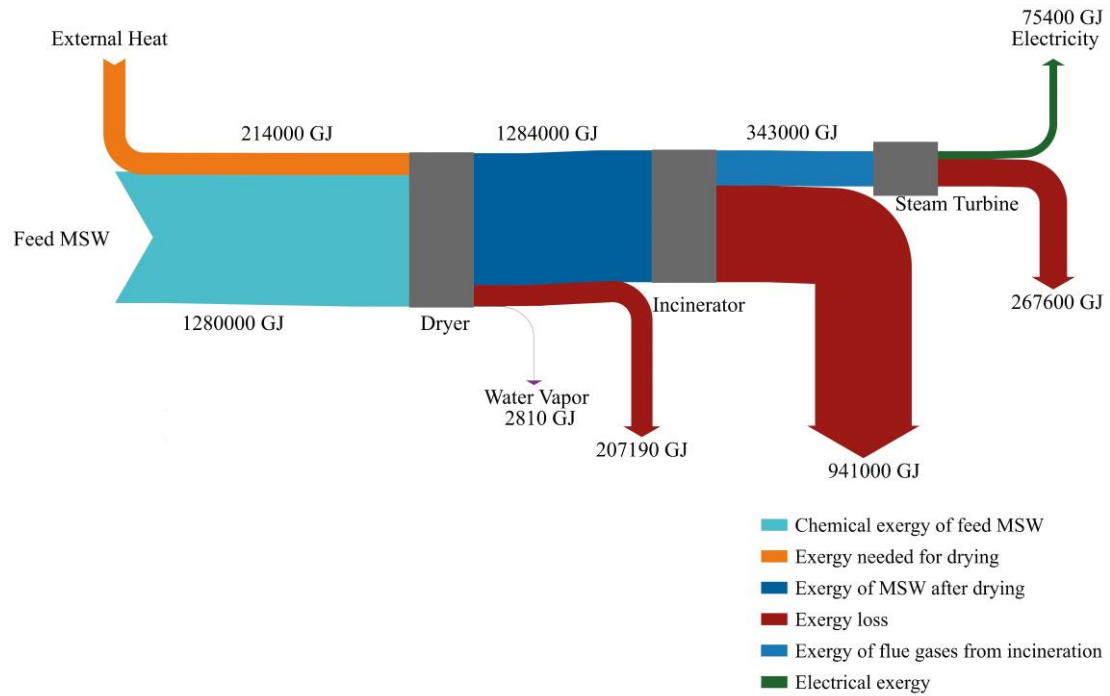


Figure 8. Exergy flow in incineration of MSW

The equilibrium model was employed to predict the products of the plasma gasification process. Initially, the MSW was assumed to have a high moisture content of 42%, which is unsuitable for the plasma process. However, the MSW was dried in the dryer to a permissible moisture content of up to 21.83% based on the results of the proximate analysis. This dried MSW is then introduced into the plasma furnace at ambient temperature and pressure. An electric current is passed through specifically designed electrodes to generate plasma gas. While various gases like oxygen and helium can be used between the electrodes to form plasma, air is assumed as the input gas in this study (see Figure 4) due to its cost-

effectiveness. Using the estimated values of the volumetric/molar composition of the syngas and the total moles of syngas from the equilibrium model, the moles of each constituent were estimated. The resulting physical and chemical exergy of each constituent are presented in Table 4.

Analysis of the exergy flows in this process revealed the magnitude and location of exergy losses, as shown in Figure 9. The highest exergy loss was identified to occur within the plasma furnace where 65.49% of the exergy supplied to it is dissipated. This exergy lost within the plasma furnace is notably lower than that observed in the incinerator since the MSW is exposed to higher temperatures in the plasma furnace.

Table 4. Exergy associated with syngas from plasma gasification of MSW

Constituents	Quantity (kmol)	Ex _{ph} (kJ)	Ex _{ch} (kJ)
CO	2.65×10 ⁶	4.64×10 ¹⁰	1.44×10 ¹¹
CO ₂	4.73×10 ³	1.32×10 ⁸	1.80×10 ⁸
N ₂	1.69×10 ⁶	2.86×10 ¹⁰	8.90×10 ¹⁰
H ₂	3.53×10 ⁶	5.74×10 ¹⁰	1.93×10 ¹¹
CH ₄	1.26×10 ⁴	4.51×10 ⁸	5.20×10 ⁸
Total		1.33×10 ¹¹	4.27×10 ¹¹

Table 5 provides a comparative analysis of the four technologies using some exergy-based performance metrics. It shows that anaerobic digestion accounts for the highest exergy efficiency. This is due to the high percentage of organic waste in the waste

stream. Even though plasma gasification technology requires electricity for its operation, it exhibits the greatest conversion potential as compared to incineration and LFGTE because it generates more net electricity. The low exergy efficiencies of the

thermochemical processes are due to the low carbon content in the MSW, as [Jadhao et al. \(2017\)](#) state that the exergy efficiency for such processes is roughly linearly proportional to the carbon content of the feed

MSW. [Table 5](#) also shows the inverse relationship between exergy efficiency and exergy defect, i.e., the lower the efficiency, the larger the fraction of exergy that is lost within a system.

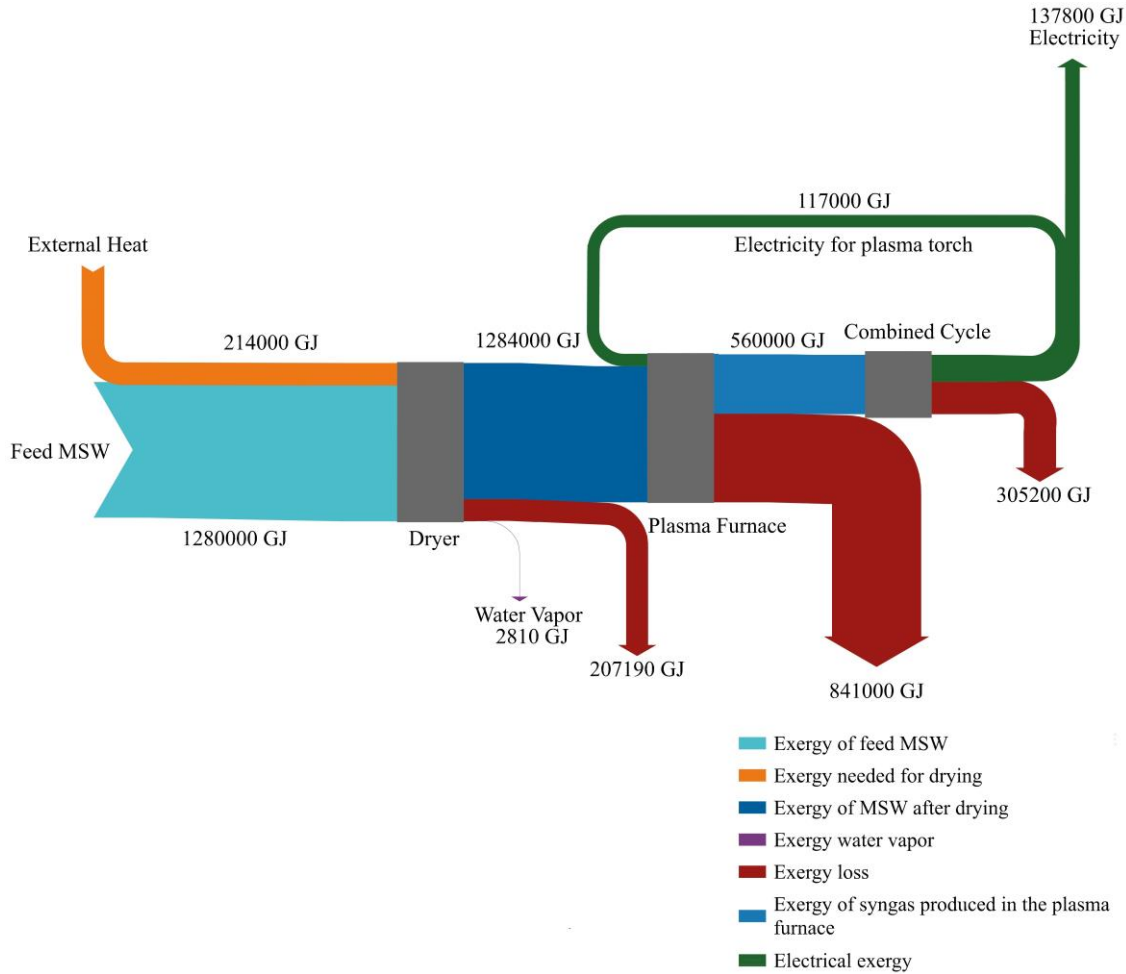


Figure 9. Flow of exergy in plasma gasification of MSW

Table 5. Energy-based performance indicators for WtE options

	ϵ (%)	IP (GJ)	δ	Ex_d (GJ)
LFGTE	3.80	1.96×10^6	0.96	1.24×10^6
Anaerobic digestion	15.16	9.21×10^5	0.85	1.09×10^6
Incineration	5.05	1.35×10^6	0.95	1.42×10^6
Plasma gasification	9.22	1.23×10^6	0.91	1.36×10^6

The improvement potential values which indicate the possible improvements of each WtE option are also outlined in [Table 5](#). It shows that the LFGTE option has the highest improvement potential and anaerobic digestion has the lowest due to its higher exergy efficiency. Optimizing the waste feedstock with a higher proportion of organic material will help improve the efficiency of these options. For incineration and plasma gasification, it has been noted

herein that the incinerator and the plasma furnace account for the highest exergy destruction. Thus, enhancing the performance of this unit can have a significant impact on improving the overall efficiency of the entire process. [Fellaou and Bounahmidi \(2018\)](#) noted that the best way to decrease the irreversibility of a process or system is to decrease the difference between the total exergy output and input values. The irreversibility due to combustion can however, not be

avoided completely. Irreversibility due to combustion can be reduced to a minimum value by working with MSW with high carbon content or using better fuel. In this regard, Oumarou et al. (2012) suggest that supplementary fuels such as sugarcane straw or weeds can be added to the MSW.

4. CONCLUSION

This study evaluated the exergy potential of converting MSW into useful energy through four WtE technologies in Maiduguri, Nigeria. The four technologies evaluated were landfill gas-to-energy, anaerobic digestion, incineration, and plasma gasification. The main conclusions are drawn as follows:

1) Anaerobic digestion demonstrated the highest conversion potential, generating more net electricity compared to other options due to the high organic content of the waste stream.

2) Plasma gasification also showed relatively high exergy efficiency due to its operation at elevated temperatures in the plasma furnace.

3) Incineration and landfill gas-to-energy exhibited lower exergy efficiencies.

Analysis of exergy losses identified the incinerator and plasma furnace as the primary sources of exergy losses in the incineration and plasma gasification processes, respectively. Therefore, maximizing the performance of these units through advanced technologies or optimized operating conditions could significantly enhance overall system efficiency. Additionally, incorporating supplementary fuels with high carbon content, as suggested by prior studies, could further improve the performance of thermochemical WtE options.

While anaerobic digestion and plasma gasification emerged as promising options based on different metrics, the optimal choice for Maiduguri will depend on specific local considerations including cost, available infrastructure, and environmental impacts. Further research focusing on improving the performance of critical units, exploring alternative fuels, and conducting techno-economic and environmental impact analysis would be valuable in determining the most sustainable and efficient WtE solution for Maiduguri and similar localities.

SUPPLEMENTARY MATERIAL

Supporting information is provided for this paper. The supporting information includes additional

tables of variables used and methodological details that contribute to a comprehensive understanding of the research outcomes.

REFERENCES

- Achinas S, Euverink GJ. Theoretical analysis of biogas potential prediction from agricultural waste. *Resource-Efficient Technologies* 2016;2(3):143-7.
- Aghbashlo M, Tabatabaei M, Soltanian S, Ghanavati H. Biopower and biofertilizer production from organic municipal solid waste: An exergoenvironmental analysis. *Renewable Energy* 2019;143:64-76.
- Alexander A, Burklin C, Singleton A. Landfill gas emissions model (LandGEM) version 3.02 user's guide [Internet]. 2005 [cited 2023 Jul 14]. Available from: <https://www3.epa.gov/ttnca1/dir1/landgem-v302-guide.pdf>.
- Bakas I, Laurent A, Clavreul J, Saraiva AB, Niero M, Gentil E, et al. LCA of solid waste management systems. In: Hauschild MZ, Rosenbaum RK, Olsen SI, editors. *Life Cycle Assessment: Theory and Practice*. Cham, Switzerland: Springer Nature; 2018. p. 887-926.
- Cavalcanti EJ, Carvalho M, Ochoa AA. Exergoeconomic and exergoenvironmental comparison of diesel-biodiesel blends in a direct injection engine at variable loads. *Energy Conversion and Management* 2019;183:450-61.
- Chen L, Xiao K, Hu F, Li Y. Performance evaluation and optimization design of integrated energy system based on thermodynamic, exergoeconomic, and exergoenvironmental analyses. *Applied Energy* 2022;326:Article No. 119987.
- Cudjoe D, Han MS, Nandiwardhana AP. Electricity generation using biogas from organic fraction of municipal solid waste generated in provinces of China: Techno-economic and environmental impact analysis. *Fuel Processing Technology* 2020;203:Article No. 106381.
- Dauda M, Osita OO. Solid waste management and re-use in Maiduguri, Nigeria [Internet]. 2003 [cited 2024 Mar 20]. Available from: <https://hdl.handle.net/2134/30546>.
- Esohe B. The Current state of waste management in Nigeria and the challenges of transitioning to a circular economy [Internet]. 2023 [cited 2023 Jul 2]. Available from: <https://www.linkedin.com/pulse/current-state-waste-management-nigeria-challenges-circular-braimah/>.
- Fellaou S, Bounahmidi T. Analyzing thermodynamic improvement potential of a selected cement manufacturing process: Advanced exergy analysis. *Energy* 2018;154:190-200.
- Gaudreau K, Fraser RA, Murphy S. The Characteristics of the exergy reference environment and its implications for sustainability-based decision-making. *Energies* 2012;5(7): 2197-213.
- Hadidi LA, Omer MM. A financial feasibility model of gasification and anaerobic digestion waste-to-energy (WTE) plants in Saudi Arabia. *Waste Management* 2017;59:90-101.
- Huang W, Fooladi H. Economic and environmental estimated assessment of power production from municipal solid waste using anaerobic digestion and landfill gas technologies. *Energy Reports* 2021;7:4460-9.
- Jadhao SB, Shingade SG, Pandit AB, Bakshi BR. Bury, burn, or gasify: Assessing municipal solid waste management options in Indian megacities by exergy analysis. *Clean Technologies and Environmental Policy* 2017;19:1403-13.

- Jones GA, Hollier G. Resources, Society and Environmental Management. United Kingdom: SAGE Publications Ltd; 1997.
- Kaza S, Yao L, Bhada-Tata P, Van Woerden F. What a Waste 2.0: A Global Snapshot of Solid Waste Management to 2050. Washington, DC: World Bank; 2018.
- Kofoworola OF. Comparative assessment of the environmental implication of management options for municipal solid waste in Nigeria. International Journal of Waste Resources 2016;7(1):Article No. 1000259.
- Magnanelli E, Berglihn OT, Kjelstrup S. Exergy-based performance indicators for industrial processes. International Journal Energy Research 2018;42:3989-4007.
- Nanda S, Berruti F. Municipal solid waste management and landfilling technologies: A review. Environmental Chemistry Letters 2021;19:1433-56.
- Ogunjuyigbe ASO, Ayodele TR, Alao MA. Electricity generation from municipal solid waste in some selected cities in Nigeria: An assessment of feasibility, potential and technologies. Renewable and Sustainable Energy Reviews 2017;80:149-62.
- Oumarou MB, Dauda M, Sulaiman AT, Babagana MT. Characterization and generation of municipal solid wastes in Northeastern Nigeria. Continental Journal of Renewable Energy 2012;3(1):1-7.
- Oumarou MB, Shodiya S, Ngala GM, Bashir MA. Artificial neural network modelling of the energy content of municipal solid wastes in Northern Nigeria. Arid Zone Journal of Engineering, Technology and Environment 2017;13(6):840-7.
- Rivero R, Garfias M. Standard chemical exergy of elements updated. Energy 2006;31(15):3310-26.
- Sato N. Chemical Energy and Exergy: An Introduction to Chemical Thermodynamics for Engineers. Elsevier Science and Technology Books; 2004.
- Soltanian S, Kalogirou SA, Ranjbari M, Amiri H, Mahian O, Khoshnevisan B, et al. Exergetic sustainability analysis of municipal solid waste treatment systems: A systematic critical review. Renewable and Sustainable Energy Reviews 2022;156:Article No. 111975.
- Yaws CL. Yaw's Handbook of Thermodynamic and Physical Properties of Chemical Compounds. Beaumont, Texas: Lamar University; 2003.
- Zainal ZA, Ali R, Lean CH, Seetharamu K. Prediction of performance of a downdraft gasifier using equilibrium modeling for different biomass materials. Energy Conversion and Management 2001;42(12):1499-515.

Willingness to Pay Estimation for the Restoration of Water Quality of a Eutrophic Lake

Mc Jervis Soltura Villaruel

Department of Science and Technology Philippines, Research Unit - Philippine Science High School - Main Campus, Quezon City, Philippines

ARTICLE INFO

Received: 8 Feb 2024
Received in revised: 21 Apr 2024
Accepted: 26 Apr 2024
Published online: 7 May 2024
DOI: 10.32526/ennrj/22/20240035

Keywords:

Contingent valuation/ Economic value/ Ecosystem service/ Tadolac Lake/ Water quality regulation/ Willingness to pay

* Corresponding author:

E-mail: mjsvillaruel@pshs.edu.ph

ABSTRACT

Lakes are recognized as highly susceptible to the impacts of various anthropogenic activities, making them one of the most vulnerable aquatic ecosystems. These ecosystems frequently experience degradation due to the lack of policies recognizing the importance of their often overlooked regulating ecosystem services. A contingent valuation approach was employed to assess the stakeholders' willingness to pay (WTP) for the restoration of the water quality of a eutrophic lake using the case of Tadolac Lake, situated within the municipality of Los Baños, Laguna Province, Philippines. The findings of the study revealed that households in the area expressed a WTP of Php 95.88/household/month or Php 1,150.56/household/year (1 USD=55.89 Php), with 72.30% of respondents indicating their readiness to support efforts to improve the water quality of Tadolac Lake. The likelihood of a positive response significantly varied depending on factors such as the offered price, gender, educational attainment, duration of residency, household size, income, and the method of questionnaire administration (cheap talk vs. non-cheap talk). These results underscore the community's favorable disposition towards investing in improving Tadolac Lake's water quality. This valuation study contributes a fresh perspective on lake management strategies. Moreover, it emphasizes the importance of environmental education regarding social-ecological dynamics as a crucial requirement for crafting comprehensive policies that will steer sustainable management of natural lake resources.

1. INTRODUCTION

Lake ecosystems are crucial in sustaining and supporting human well-being, serving as sources of potable water, fisheries, recreation, and aesthetic pleasure (Dudgeon et al., 2006; Nakano et al., 2016). However, urbanization and population growth have increased pollution from wastewater discharge, solid waste accumulation, and nutrient runoff into lakes (Bashir et al., 2020). This influx of pollutants has compromised the water quality in many lakes, causing oxygen depletions, algal bloom, and biodiversity loss. Such degradation threatens the ecological balance and jeopardizes the livelihoods of those who rely on the lake for their sustenance and economic activities (Sinclair et al., 2023).

The economic significance of a lake's benefits is contingent upon alterations in its water quality and/or quantity (Jala and Nandagiri, 2015). Quantifying the economic implications of gains or losses from ecosystems can enhance comprehension of the advantages of improving environmental quality and the expenses linked to their decline (Wegner and Pascual, 2011). Nonetheless, the value of ecosystem services for human well-being remains undervalued in decisions about ecosystem utilization, governance, and rehabilitation (Rounsevell et al., 2018). Consequently, the economic appraisal of sustainable lake management has been largely overlooked in scientific inquiry (Gebremedhin et al., 2018).

The Contingent Valuation Method (CVM) is a commonly used method for assessing the economic value of environmental goods and services that lack market value, such as the conservation of lakes and their ecosystems (Grazhdani, 2015). It entails directly questioning the respondents' willingness to pay for a particular environmental improvement or the compensation they would demand to tolerate a decline (Khong et al., 2019). Willingness to pay (WTP) reveals the perceived value that individuals place on ecosystem services provided by various ecosystems (Clinch, 2004). Ecosystem services comprise a broad spectrum of benefits humans can obtain from ecosystems, such as clean water, recreational opportunities, biodiversity support, and cultural values (Costanza et al., 1997). By understanding people's WTP, policymakers and resource managers can better prioritize conservation efforts, allocate resources effectively, and make informed decisions about land use and development (Dahal et al., 2018). For example, in lake conservation, WTP estimates can provide insight into the economic benefits of maintaining water quality, preserving aquatic habitats, and promoting sustainable recreational activities. This information is crucial for justifying investments in conservation efforts, designing user fees or taxes to fund preservation initiatives, and demonstrating the importance of lakes to local communities and economies (Kumar and Martinez-Alier, 2011).

WTP determination through the CVM approach was also utilized in other studies to evaluate the economic value of ecosystem services provided by lakes. For instance, Janko and Zemedu (2015) assessed the fisherman's willingness to pay for fisheries management. They found that educational attainment, income, and the respondent's perception of lake fishery management significantly influenced their willingness to pay, showing positive correlations. Likewise, Van Oijstaeijen et al. (2020) employed monetary valuation and labor-days payment mechanisms to gauge farmers' preferences for controlling water hyacinth in Lake Tana, Ethiopia. They found that local farmers were willing to contribute over half a million euros annually to eradicate this invasive plant. Šebo et al. (2019) utilized CVM to gauge the value of enhancing lake water quality in Slovakia. In addition, Bueno et al. (2016) similarly employed CVM to assess the worth of urban lake rehabilitation in the Philippines, focusing on water quality improvement. While numerous studies using the CVM to evaluate improvements in lake

water quality have emerged recently, such research remains scarce in the Philippines. Bueno et al. (2016) study is the only available published study in the country where the CVM approach was utilized to investigate stakeholders' WTP in restoring lake water quality. Therefore, addressing the research gap in this area is crucial in establishing a foundational understanding of how stakeholders can contribute to implementing restoration efforts and sustainable water management practices.

Tadlac Lake, situated in Los Baños, Laguna, Philippines, holds significant ecological and socio-economic importance within its local community. Historically, the lake has been a crucial resource for residents, enabling fishing activities primarily through *Oreochromis* (Tilapia) aquaculture. Nevertheless, the unregulated expansion of fishing operations led to eutrophication and deterioration of the lake's water quality. A massive fish kill occurred in December 1999 during the lake's annual turnover, followed by the complete eradication of the remaining fish population in February 2000. The Laguna Lake Development Authority (LLDA), along with the Barangay Council and the Barangay Fisheries and Aquatic Resource Management Council (BFARMC), initiated efforts to rehabilitate the lake by imposing a ban on aquaculture in the area (Santos-Borja, 2008). This ban remains in effect to this day. However, according to the study conducted by Villaruel and Camacho (2022), the lake's eutrophic condition persists despite some improvements in water quality. This could be attributed to the influx of organic matter from residential and commercial establishments along the lake's shoreline. Consequently, this situation underscores the necessity to implement additional or alternative measures to restore the lake's water quality.

Maintaining the good water quality of lakes is essential for their ecological importance and the numerous benefits they provide to society. A healthy lake supports sustainable aquaculture practices and preserves natural biodiversity, making it more attractive for recreational activities and tourism. Assessing residents' WTP in restoring the water quality of a eutrophic lake can offer valuable perspectives on the perceived worth of the lake's ecosystem services and gauge support for conservation and restoration initiatives. Additionally, such exploration could offer insights into the factors influencing willingness to pay, thus aiding policymakers and government officials in refining communication strategies and environmental

protection policies for lake conservation. Hence, this study seeks to determine the economic value of a eutrophic lake's water quality regulation service using the case of Tadalac Lake. This was done by eliciting WTP from its stakeholders. Furthermore, the study also investigates the factors that could influence residents' WTP. Gaining insights into the WTP for water quality restoration in Tadalac Lake can provide valuable understanding regarding the perceived value of lake restoration efforts. A thorough comprehension of the stakeholders' WTP in Tadalac Lake and the factors influencing it can serve as a blueprint for analogous conservation and restoration globally. The findings of this study could provide a comprehensive viewpoint essential for advancing sustainable water management practices on a global scale.

2. METHODOLOGY

2.1 Theoretical framework of contingent valuation method

The CVM was employed to assess the economic worth of an ecological service that lacks a market price. CVM, a technique for estimating values of goods without existing markets, involves structured surveys asking respondents about their willingness to pay for hypothetical changes in environmental goods or services (Mendelsohn and Olmstead, 2009). Widely employed for freshwater ecosystems due to its adaptability and capacity to estimate nonmarket values

(Van Houtven et al., 2007; Zhen et al., 2011), CVM has been shown to estimate values for non-point source pollution such as domestic effluents (Grazhdani, 2015). It entails directly questioning the respondents' willingness to pay for a particular environmental improvement or the compensation they would demand to tolerate a decline (Khong et al., 2019). This study assessed stakeholders' preferences regarding water quality restoration in Tadalac Lake by proposing a theoretical wastewater treatment facility, thereby determining their WTP.

2.2 Sampling site and sample size

The study covered Tadalac Lake in Los Baños, Laguna (Figure 1). Currently, the lake is not open for aquaculture activity, but fishing and recreational activities are allowed there. The stakeholders of the lake include the residents of the Barangay (village) Tadalac living near the lake. The appropriate sample size was computed from the total population of the stakeholders using Slovin's formula. The interview was conducted exclusively with household heads, such as the wife, husband, or any adult member responsible for income generation and decision-making about the family's finances. The head of the household is described as any adult family member who contributes to the household's earnings and has the authority to make financial decisions on behalf of the household (Indab, 2008).

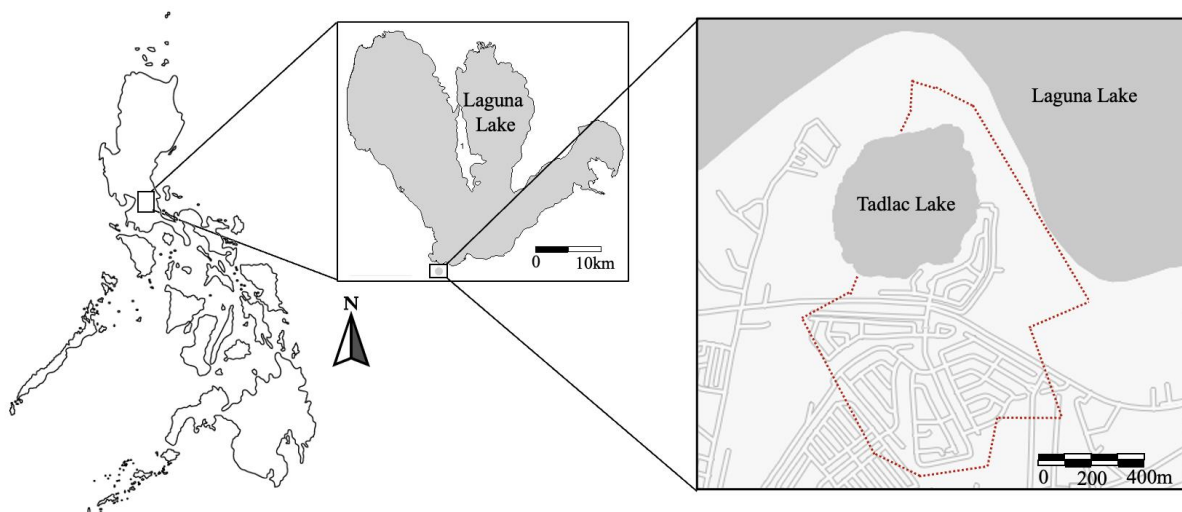


Figure 1. Tadalac Lake map highlighting Brgy. Tadalac (14.1824°N, 121.2061°E). The area within the red dotted line is the jurisdiction of Brgy Tadalac. Residents residing in this area are the respondents of the study.

2.3 Questionnaire structure

The survey was done by face-to-face interview. The questionnaire formulated (See Supplementary data) is divided into three categories: socio-

demographic profile, knowledge, attitude, and perception on the lake, and WTP elicitation questions. The first part of the questionnaire involves the socio-demographic profile of the respondents, including the

name, age, gender, marital status, educational attainment, and number of people in the household. The second part involves questions about the uses of the lake and aims to determine the provisional services that the stakeholders derive from the lake. The last part of the questionnaire involves questions that will elucidate how the stakeholders value the lake in terms of its provisioning services (water, fish, etc).

A focus group discussion was also held with the barangay officials and residents to acquire significant information and stakeholders' perceptions regarding the status of the lake. The information acquired was used in the finalization of the questionnaire. Before conducting the survey, pretesting of the survey questionnaire was carried out to assess the appropriateness and efficiency of the participating institutions, payment scheduling, technical, and political viability of the program, and the clarity of the scenario and questions employed. The pretesting facilitated the identification of any questionnaire sections that were ambiguous or challenging for respondents to comprehend. Accordingly, necessary revisions were implemented before the commencement of the main survey. Furthermore, all questionnaires were translated into Filipino for easier understanding.

After the questionnaires were finalized, they were categorized into two groups: the cheap talk (CT) questionnaire and the non-cheap talk (NCT) questionnaire. For the cheap talk questionnaire, the respondents were informed that other respondents would also pay the same amount of a particular bid. Meanwhile, respondents were not told that other respondents would pay the same bid amount for the non-cheap talk questionnaire. The cheap talk mechanism was used since it can affect the frequency of respondents who will say yes to a specific bid (Aadland and Caplan, 2006).

2.4 Payment scheme

The question regarding willingness to pay (WTP) was presented in a format where respondents had to choose between two options: whether they were willing to pay a specific amount. If a respondent is willing to pay, they were asked about their preferred payment scheme: monthly, quarterly, or yearly. Eight (8) bids in Philippine Peso (Php) currency were used to ascertain the stakeholder's WTP. The bids are Php 20, Php 40, Php 60, Php 80, Php 100, Php 120, Php 140, and Php 160. The bid amount was distributed equally to the CT and NCT questionnaires. The same

number of NT and NCT questionnaires were used in the survey to avoid strategic bias.

2.5 Determination of mean willingness to pay (MWTP) and factors affecting it

The CVM was adopted in the study to determine the stakeholders' WTP for the water quality restoration of Tadalac Lake. The MWTP was calculated using the formula in the study of Hanemann (1994):

$$MWTP = \frac{1}{|\beta|} \ln(1 + e^{\alpha})$$

Where; β represents the coefficient of the bid price, while α serves as a constant. This constant is determined either by the absence of additional independent variables or by the combination of the estimated constant and the sum of all other independent variable coefficients multiplied by their means (Donovan and Nicholls, 2003), i.e.

$$\alpha_0 + \sum_{j=1}^k \beta_j \bar{X}_j$$

Where; α_0 represents the constant of the logistic model, while the coefficients β_j 's do not account for the coefficient of the bid price.

Besides the bid price, various other variables may impact respondents' WTP. Thus, the function below incorporates all such factors anticipated to influence WTP among Tadalac residents:

$$WTP_2 = F(X_1, X_2, X_3, X_4, D_1, D_2, D_3, D_4)$$

Factors that could affect the WTP were X_1 (respondent's age), X_2 (educational attainment), X_3 (bid prices), and X_4 (respondent's income). This formula also incorporated dummy variables, with 1 and 0 serving as the respective placeholders for them: D1: gender (0=male; 1=female respondents); D2: respondents' educational level (1=had at least a college degree; 0=secondary school completer or lower educational level)

The respondent's WTP and the factors influencing their WTP were calculated using logistic regression. Logistic regression was also done using SPSS ver. 20.

3. RESULTS AND DISCUSSION

3.1 Socio-economic profile of the respondents

Table 1 shows the respondents' socio-economic profile. Most respondents are female, with 69.79% (n=268), while male respondents account only for

30.21% (n=116). The respondent gender demographic contrasts the general population census, indicating that the Philippine population comprises 50.14% males and 49.86% females. The ages of the respondents were presented into age classes. Majority of the respondents belong to the age class 30-39 with 37.50% (n=144), followed by age class 50-59 with 18.75% (n=72), then 40-49 (14.58%), followed by age class 20-29 and 60-69 both having a 12.50% (n=48). The age class with the lowest number of respondents are the brackets of 70-79 and 80-89, with 3.13% and 1.04%, respectively. For educational attainment, it follows the result of the study conducted by [Weinstein in 2010](#) that most of the graduates in the rural areas in the Philippines are at secondary level and do not pursue tertiary education. Most of the respondents are graduates of high school (44.79%; n=171), followed by college and vocational degree holders with 37.50% (n=68), and last are elementary graduates with 17.70% (n=36). Most respondents have lived in the barangay Tadalac for 31-40 years (23.96%), followed by respondents living in the area for 0-10 years (20.83%). The respondents living for 21-30 years in Tadalac are the 3rd highest with 15.63%. This is followed by 13.54% of respondents living in the barangay for 41-50 years and 12.50% living for 51-60 years. Respondents living for 11-20

years come next (8.33%) and last live for 61-70 years in the area (5.21%). Regarding household size, 53.13% of the participants were from small households (1-4 members per household), whereas 46.88% resided in larger families (5-8 members per household). A large proportion stated that their dependents were 2-3 individuals (58.33%), while 23.96% of the respondents indicated that their dependents were only 0-1 persons. Among the respondents, a cumulative 272 (70.83%) reported average monthly income of Php 10,000 or less. This income falls significantly below the income benchmark of Php 13,797 established by the Philippine Statistics Office in 2023 to cover the essential monthly needs, both food and non-food, of a family consisting of five members ([Mapa, 2023](#)). Merely 3.12% of the respondents declared an income exceeding Php 30,001. With Laguna Lake and Tadalac Lake within proximity, the majority of the respondents earned through fishing and farming (27.08%; n=104), followed by non-farm businesses such as sari-sari (small) store, tricycle operators, and others (20.83%; n=80). In terms of house ownership, the majority of the respondents own their house (65.63%; n=252), with the bungalow type being the most common among the respondents (67.71%; n=260).

Table 1. Socio-economic profile of the respondents inhabiting Tadalac Lake (n=384)

Variable	Response	Frequency	Percentage (%)
Gender	Female	268	69.79
	Male	116	30.21
Age	20-29	48	12.50
	30-39	144	37.50
	40-49	56	14.58
	50-59	72	18.75
	60-69	48	12.50
	70-79	12	3.13
	80-89	4	1.04
Educational attainment	Elementary	36	17.70
	High School	172	44.79
	College, vocational school, and above	68	37.50
Years living in Tadalac	0-10	80	20.83
	11-20	32	8.33
	21-30	60	15.63
	31-40	92	23.96
	41-50	52	13.54
	51-60	48	12.50
	61-70	20	5.21
Household size	1-4	204	53.13
	5-8	180	46.88

Table 1. Socio-economic profile of the respondents inhabiting Tadalac Lake (n=384) (cont.)

Variable	Response	Frequency	Percentage (%)
Number of dependents	0-1	92	23.96
	2-3	224	58.33
	4-5	64	16.67
	6 above	4	1.04
Household income (Php)	0-10,000	272	70.83
	10,001-20,000	80	20.83
	20,001-30,000	20	5.21
	30,001-40,000	4	1.04
	40,001-50,000	4	1.04
	50,001-60,000	4	1.04
Source of income	Farming/Fishing	104	27.08
	Hired labor	48	12.50
	Private employee	60	15.63
	Government employee	48	12.50
	Resort employee	8	2.08
	Non-farm business	80	20.83
	Other	36	9.38
Ownership of the house	Own	252	65.63
	Rent	56	14.58
	Share	20	5.21
	Caretaker	12	3.13
	Squat	20	5.21
	Others	24	6.25
Kind of the house	Bungalow	260	67.71
	Nipa Hut	44	11.46
	Apartment	52	13.54
	Others	28	7.29

3.2 Knowledge, attitudes, and practices in Tadalac Lake

Knowledge, attitudes, and perceptions of the respondents about the lake were summarized and presented in [Table 2](#). The majority of the respondents believed that they obtained benefits from the lake (78.13%). Sightseeing, recreation, washing clothes, and fishing were identified as the primary benefits they derive from the lake. Less than 50% of the respondents agreed that the lake was cleaned after the massive fish occurred in 1999 (about 42.17%; n=164). Moreover, they believed that the protection of the lake was necessary and that it was the responsibility of the residents to take care of it.

An overwhelming favorable rating (yes=96.88%) was achieved when the respondents were asked if it was good that the lake would be maintained clean. Furthermore, the majority of the respondents also agreed to the removal of the fish cages in the lake (63.54%). Fish cages were removed

from the lake after the massive fish kill in 1999 as part of the rehabilitation of the lake. The lake is still closed for aquaculture, although there are few fish cages. Also, respondents (57%) agreed that the lake’s periphery should be free from any establishments like resorts and houses to improve its water quality.

3.3 Determination of willingness to pay and factors influencing it

Of the 384 respondents surveyed, 361 were deemed valid, with 23 protest bidders excluded ([Table 3](#)). Protest bids are frequently submitted by respondents who may hold a value for the commodity that is either higher or lower than the average but decline to pay due to ethical or other considerations ([Halstead et al., 1992](#)). Most respondents (72.30%; n=252) agreed to pay the bid price they were randomly assigned. On the other hand, 100 respondents were unwilling to pay the bid price they were asked (27.70%) for the water quality improvement

intervention (Table 3). This finding clearly shows the overwhelming interest among residents of Brgy. Tadalac to support the improvements of the water quality of Tadalac Lake. The WTP of the respondents

reflects the value they place on the water regulation service provided by Tadalac Lake. The bid price signifies the sum they will pay for the suggested intervention (Reis et al., 2022).

Table 2. The respondents’ knowledge, attitude, and perception on Tadalac Lake

Variables (Questions)	Response	Frequency	Percentage
Recipient of the lake’s services (Do you benefit from the lake?)	Yes	300	78.13
	No	60	15.63
	Undecided	24	6.25
Benefits from the lake (In what ways do you benefit from the lake)	Recreation	60	15.63
	Sightseeing	160	41.67
	Drinking	16	4.17
	Washing clothes	60	15.63
	Fishing	40	10.42
	Watering plants	32	8.33
	Others	16	4.17
Is the protection of the lake necessary?	Yes	380	98.96
	No	4	1.04
	Undecided	0	0.00
Is it the responsibility of residents to take care of the lake?	Yes	376	97.92
	No	8	2.08
	Undecided	0	0.00
Do you think the lake was cleaned after the massive fish kill?	Yes	164	42.71
	No	140	36.46
	Undecided	80	20.83
Is it good to maintain the lake clean?	Yes	372	96.88
	No	4	1.04
	Undecided	8	2.08
Are you in favor of the removal of the fish cages in the lake?	Yes	244	63.54
	No	96	25.00
	Undecided	44	11.46
Is it good that there are no establishments along the bank of the lake, such as resorts and houses?	Yes	220	57.29
	No	112	29.17
	Undecided	52	13.54
If you compare the lake’s condition during the 1990s, can you say that the lake was cleaner before?	Yes	120	31.25
	No	196	51.04
	Undecided	68	17.71
Are you in favor of opening the lake for aquaculture again?	Yes	124	32.29
	No	220	57.29
	Undecided	40	10.42

Table 3. Distribution of respondents who gave positive and negative WTP*

Willingness to pay	Frequency	Percentage
Positive (Yes to the Bids)	261	72.30
Negative (No to the Bids)	100	27.70
Total	361	100.00

*protest bidders – 23

Logistic regression was utilized to assess the MWTP. In the regression model (Table 4), the likelihood of voting “yes” (coded as 1) or “no” (coded as 2) was analyzed in relation to bid prices exclusively. The bid price variable demonstrated statistical significance at a 95% confidence level, with a negative coefficient consistent with economic expectations. This suggests that as bid prices increase, the likelihood

of the respondents' WTP diminishes (Luangmany et al., 2009).

The MWTP was calculated using the formula $Mean_{(bids)} = \alpha/\beta$. Employing the parametric method, the MWTP was determined to be -0.767/-0.008, resulting in Php 95.88. This signifies that the average maximum WTP for the water quality restoration of Tadalac Lake stands at Php 95.88 per household per month. For a year, this totals to Php 1,150.56 per household. This trend is mostly likely affected by the respondents' income, which is one of the major significant determinants of WTP. As shown in Table 5, the frequency of individuals who voted yes at lower bid prices (Php 20-100) was higher than those who voted yes at higher bid price levels (Php 120-160). Moreover, respondents whose monthly household income was Php 10,000 or less voted for a lower bid

price. As the bid price increases, families from lower monthly income brackets tend to vote less in favor of the higher bid price. Conversely, respondents earning Php 10,001 and above monthly are more inclined to vote for a higher bid price. This is very prominent at Php 120, Php 140, and Php 160 bid prices. Furthermore, this finding is supported by the logistic regression model (Table 6) in which household income is one of the significant variables that determined the probability of the respondents' WTP (correlation coefficient 0.281; $p < 0.001$). This outcome aligns with the previous findings of Xiong et al. (2018), Mumbi and Watanabe (2020), and Hao et al. (2023), who similarly identified income and bid price as notable determinants impacting WTP, wherein respondents with a higher income were more willing to pay than their counterparts.

Table 4. Results of the regression analysis using only bids as a factor

Model 1 (Bids only)			
Variable	Coefficient	T-ratio	P-value
Constant	-0.767	2.383	0.0001
Bid	-0.008	0.251	0.0001

Table 5. The frequency of respondents who voted yes grouped according to their monthly income per price bid (n=384)

Monthly income per household	Bid price (Php)							
	20	40	60	80	100	120	140	160
0-10,000	36	32	12	32	24	4	-	-
10,001-20,000	-	-	11	4	12	20	21	16
20,001-30,000	4	-	16	-	-	-	-	-
30,001-40,000	-	-	-	4	4	-	-	-
40,001-50,000	-	4	-	-	-	-	1	4
Total	40	36	39	40	40	24	22	20

Aside from the bid price and monthly household income, other variables that affect the respondents' willingness to vote in favor of a particular bid were also presented in Table 6. Gender, educational attainment, years of stay in Tadalac, household size, and cheap talk or non-cheap talk questionnaire were the significant variables that influenced the WTP of the respondents.

It was observed that female respondents account for 64.78% (n=184) of individuals who voted yes for the bids asked, while males account for 35.21% (n=100) only (Table 7). Gender difference affects decision-making attitudes (Villanueva-Moya and

Exposito, 2020). Minasyan and Tovmasyan (2020) argued that women were participating in many of the decision-making activities on par with men. Women have an influence on monetary decision-making. Klesment and Bavel (2022) stated that women are predominantly involved in financial decision-making within marital contexts. In the Philippines, the monetary expenses are often decided by women in the household as they are the ones who handle and keep the money on behalf of the family. Therefore, it is highly probable that women would respond positively to WTP requests, given their role in managing household finances.

Table 6. Correlation analyses between respondents' WTP and their socio-economic profile, method of interview (with or without cheap talk), price of the bid, knowledge, attitude, and perception (excluding protest bidders)

Variables	Correlation coefficient	Significance level	Remarks
Socio-economic Profiles			
a) Bids	-0.008	0.0001	Significant
b) Gender	-8.144	0.0100	Significant
c) Age	0.103	0.0520	Not significant
d) Educational attainment	-6.652	0.0060	Significant
e) Years stay in Tadalac	-0.169	0.0110	Significant
f) Household size	1.276	0.0190	Significant
g) Number of dependents	-0.268	0.3420	Not significant
h) Household income (Php)	0.281	0.0001	Significant
i) Source of income	2.609	0.1010	Not significant
j) Ownership of the house	15.546	1.0000	Not significant
k) Kind of the house	3.010	0.3200	Not significant
l) Cheap or non-cheap talk	5.195	0.0130	Significant
Attitude			
a) Recipient of the lake's services (Do you benefit from the lake?)	19.942	0.9990	Not significant
Knowledge			
a) Is the protection of the lake necessary?	0.453	0.8130	Not significant
b) Is it the responsibility of residents to take care of the lake?	19.59	1.0000	Not significant
c) Do you think the lake was cleaned after the massive fish kill?	0.766	0.4150	Not significant
Perception			
a) Is it good to maintain the lake clean?	-1.248	0.4580	Not significant
b) Are you in favor of the removal of the fish cages in the lake?	-3.056	0.0260	Not significant
c) Is it good that there are no establishments along the bank of the lake, such as resorts and houses?	3.410	0.0640	Not significant
d) If you will compare the condition of the lake during the 1990's, can you say that the lake is still clean?	1.137	0.3650	Not significant
e) Are you in favor of opening the lake for aquaculture again?	0.765	0.5180	Not significant

The level of education influences decision-making, and the higher an individual's educational attainment, the more concern they have about the events in their environment (Klein, 1999; Kanyoka et al., 2008; Xiong et al., 2018). Educational attainment is a significant variable that affects the WTP of the respondents. Respondents who finished secondary education, tertiary, vocational, or postgraduate degrees responded positively to the bid they were asked. Similar findings were observed by Tziakis et al. (2009) in Northwest Crete, Lamsal et al. (2015) in Nepal, and Makwinja et al. (2019) in Malawi. They found that respondents with higher educational attainment were most likely willing to pay for conservation programs.

Most respondents living in Brgy Tadalac for 31

to 40 years exhibited the highest number of individuals who agreed to pay for the bid prices they were asked for. The number of years the respondents lived in an area significantly affects their knowledge and awareness of the area (Xiong et al., 2018). They are more concerned about the status and improvement of their environment. Citizens who have resided in the area longer can give more concrete answers about the area's status before and after. For example, those respondents who lived in the area longer can determine if the condition of the lake at present is better than before. Meanwhile, respondents who are new to the area might give a vague and unrelated answer about the topic. Hence, the knowledge, attitude, and perception about the lake might vary depending on the years the respondent is present.

Table 7. Frequency of individuals who voted yes for every significant variable

Significant variable	Percentage and frequency
Gender	Female=64.78% (n=184)
	Male=35.21% (n=100)
Educational attainment	Elementary=19.72% (n=56)
	High school=56.34% (n=160)
	College, Vocational and Postgraduate=23.94% (n=68)
Years of stay in Brgy. Tadlac	0-10=19.72% (n=56)
	11-20=11.17% (n=32)
	21-30=12.68% (n=36)
	31-40=23.94% (n=68)
	41 - 50 = 9.86% (n=28)
	51-60=12.68% (n=36)
Household size	1-4=59.15% (n=168)
	5-8=40.85% (n=116)
Cheap talk (CT) or non-cheap talk (NCT)	CT=52.11% (n=148)
	NCT=47.89% (n=136)
Removal of fish cages in the lake	Yes=69.01% (n=196)
	No=23.94% (n=68)
	Undecided=7.04% (n=20)

Household size also influences a household's response to a specific bid price. The household size determines the adequacy or sufficiency of the family's income source (Kolstoe et al., 2022). Families with numerous dependents often face inadequate income sources, leading them to prioritize fulfilling basic needs, as indicated by Attree (2005) and Hosany and Hamilton (2023). Hence, the larger families size, the lower the probability of WTP. This condition was also perceived in the study's findings wherein more respondents from small household sizes tend to be more willing to pay for the bid prices (Table 7). This trend is also evident in the studies of Moffat et al. (2011), Zelalem and Beyene (2012), and Yifei et al. (2018), wherein they observed that as family size increases, the household tends to have a negative attitude toward willingness to pay.

The type of questionnaire used had a significant influence on the respondents' WTP as more respondents voted 'yes' using the cheap talk questionnaire (52.11%) than the non-cheap talk questionnaire (47.89%) (Table 7). With the cheap talk questionnaire, participants were informed that others would also be paying the same specified bid. This approach was utilized because it could influence other participants' WTP, as they might opt to match the bid they are presented with, knowing that others will do the same. Cummings and Taylor (1999) initially

explored the cheap talk about stated preferences. They incorporated lines within the survey questionnaire to address the issue of hypothetical bias, urging participants to consider the real opportunity costs associated with hypothetical alternatives carefully. Cheap talk breaks the typical anonymity between the survey researchers and the respondents. Employing cheap talk would also mitigate the demand effects during the survey. Demand effects could be anything that may influence the respondents' behavior in the survey (Carlsson et al., 2018). Research on WTP by Lusk (2003), Carlsson et al. (2005), Pontoni et al. (2018), and Lopez-Becerra and Alcon (2021) similarly indicated that employing a cheap talk questionnaire could positively influence attitudes toward willingness to pay.

3.4 Reasons for willingness and unwillingness to pay

Respondents who accepted the proposed bid were asked about their rationale for accepting a randomly asked bid (Table 8). Among them, 60.92% (n=173) expressed willingness to pay due to their belief in the project's capacity to "restore the clean water of the lake." It was followed by "conserving the lake will benefit the future generation" (22.18%). The aesthetic value of the lake was also a factor in why respondents were positive for WTP (9.15%). High

attribution to the aesthetic and restoration of the water quality is probably due to ecotourism. Tadalac Lake is currently being used as a recreational and swimming site of Laresio Resort. Maintaining the lake’s aesthetic value and good water condition will help the residents, especially those working in the resort, generate income for their families. Notably, according to the barangay officials, most of the resort employees are residents of Brgy. Tadalac.

Conversely, 61% of the respondents who said ‘no’ to the bid price stated that the government should fund the water quality restoration program for the lake. According to some respondents, the previous lake rehabilitation was carried out by the local government

unit (LGU) and Laguna Lake Development Authority (LLDA); therefore, the government should again take responsibility for further restoring the lake’s water quality. In addition, 21% of the respondents who said no pointed out that they don’t have the capacity and the money to pay. Another factor that limits the respondents to say ‘yes’ to a given bid is the bid price. Eighteen percent (18%) indicated that they found the offered bid price too high, leading them to decline. Among those who refused, a majority (68%) reported a monthly income of ≤ Php 10,000. These results align with [Carter and Barrett \(2006\)](#) assertion that poverty diminishes willingness to pay for conservation investments.

Table 8. Frequency of individuals who voted yes for every significant variable

Reasons for ‘Yes’	Frequency	Percentage
Restore the clean water of the lake	173	60.92
Conserving the lake will benefit future generations	63	22.18
Aesthetic value	26	9.15
Others	14	4.93
No answer	8	2.82
Reasons for ‘No’	Frequency	Percentage
The government should fund the restoration	61	61.00
The bid price is too high	18	18.00
I don’t have the capacity and the money to pay	21	21.00

3.5 Policy implications

The study’s findings affirm the positive willingness of respondents to pay for water quality restoration of Tadalac Lake. Should government agencies and policymakers consider formalizing a payment scheme, the study’s WTP results could provide a foundation. However, it’s crucial to consider factors influencing the stakeholders’ WTP, such as poverty, as it may impede households’ WTP and their readiness to engage in environmental conservation efforts. [Gibson et al. \(2016\)](#) suggested that assessing public preferences through WTP can be challenging when dealing with populations facing severe financial constraints. Thus, exploring alternative payment methods, such as installment payment options or labor contributions, might be more viable. Although this study focused on a specific locality (Tadalac Lake), its findings could serve as a model or basis for implementing institutionalized environmental user fees in other lake restoration initiatives by considering all the factors that could influence the WTP identified in this study.

4. CONCLUSION

This study assessed the economic value of Tadalac Lake’s water quality regulating ecosystem service by determining the stakeholders’ WTP to enhance the lake’s water quality. Considering various pertinent variables and factors, the calculated WTP stood at Php 95.88 per household per month or a sum of Php 1,150.56 per household annually. Primary motivations for this willingness to pay included the desire for the lake’s water to be restored to cleanliness and a sense of responsibility towards conserving it for future generations. Financial inability and the expectation of government funding for restoration were critical reasons for unwillingness to pay. Factors affecting households’ WTP included the offered price, gender, level of education, duration of residence, household size, income, and the method of questionnaire administration.

The elicited WTP for Tadalac Lake’s regulatory service prompts a fresh angle in the ongoing discourse surrounding the lake’s utilization, with the overarching objective being an all-encompassing

estimate of its total economic value (TEV). Assessing the TEV of Tadlac Lake is crucial for devising and executing appropriate policies for sustainable management that reconcile ecological preservation with the utilization of aquatic resources.

ACKNOWLEDGEMENTS

I would like to thank the officials of Barangay Tadlac, particularly Kagawad Nilo, for their assistance during the data collection process for this study. I would also like to thank my Ecology students under the BS Biology program of PUP - Manila batch 2017 for their survey assistance. The Research Ethics Board of the University of the Philippines Los Baños has confirmed that the study is exempted from obtaining ethical approval as the research is merely observational as long the participants in the survey gave their consent to be interviewed.

REFERENCES

- Aadland D, Caplan AJ. Cheap talk reconsidered: New evidence from CVM. *Journal of Economic Behavior and Organization* 2006;60(4):562-78.
- Attree P. Low-income mothers, nutrition and health: A systematic review of qualitative evidence. *Maternal and Child Nutrition* 2005;1(4):227-40.
- Bashir I, Lone FA, Bhat RA, Mir SA, Dar ZA, Dar SA. Concerns and threats of contamination on aquatic ecosystems. *Bioremediation and Biotechnology* 2020;7:1-26.
- Bueno EA, Ancog R, Obalan E, Cero AD, Simon AN, Malvecino-Macalintal MR, et al. Measuring households' willingness to pay for water quality restoration of a natural urban lake in the Philippines. *Environmental Processes* 2016;3(4):875-94.
- Carlsson F, Frykblom P, Lagerkvist CJ. Using cheap talk as a test of validity in choice experiments. *Economic Letters* 2005;89(2):147-52.
- Carlsson F, Kataria M, Lampi E. Demand effects in stated preference surveys. *Journal of Environmental Economics and Management* 2018;90:294-302.
- Carter MR, Barrett CB. The economics of poverty traps and persistent poverty: An asset-based approach. *Journal of Development Studies* 2006;42(2):178-9.
- Clinch JP. Cost-benefit analysis applied to energy. In: Cutler J, editor. *Encyclopedia of Energy*. Elsevier Science; 2004. p. 715-25.
- Costanza R, d'Arge R, de Groot R, Farber S, Grasso M, Hannon B, et al. The value of the world's ecosystem services and natural capital. *Nature* 1997;387:253-60.
- Cummings RG, Taylor LO. Unbiased value estimates for environmental goods: A cheap talk design for the contingent valuation method. *The American Economic Review* 1999;89(3):649-65.
- Dahal RP, Grala RK, Gordon JS, Petrolia DR, Munn IA. Estimating the willingness to pay to preserve waterfront open spaces using contingent valuation. *Land Use Policy* 2018;78:614-26.
- Donovan GH, Nicholls DL. Consumer preferences and willingness to pay for character-marked cabinets from Alaska birch. *Forest Product Journal* 2003;53(11-12):27-32.
- Dudgeon D, Arthington AH, Gessner MO, Kawabata ZI, Knowler DJ, Lévêque C, et al. Freshwater biodiversity: Importance, threats, status and conservation challenges. *Biological Reviews of the Cambridge Philosophical Society* 2006; 81(2):163-82.
- Grazhdani D. Contingent valuation of residents' attitudes and willingness-to-pay for non-point source pollution control: A case study in AL-Prespa, Southeastern Albania. *Environmental Management* 2015;56:81-93.
- Gebremedhin S, Getahun A, Anteneh W, Bruneel S, Goethals P. A drivers-pressure-state impact-responses framework to support the sustainability of fish and fisheries in Lake Tana, Ethiopia. *Sustainability* 2018;10(8):Article No. 2957.
- Gibson J, Rigby D, Polya D, Russell N. Discrete choice experiments in developing countries: Willingness to pay versus willingness to work. *Environmental and Resource Economics* 2016;65:697-721.
- Halstead JM, Luloff AE, Steven TH. Protest bidders in contingent valuation (CV). *Northeastern Journal of Agricultural and Resource Economics* 1992;21(2):160-9.
- Hanemann WM. Valuing the environment through contingent valuation. *Journal of Economic Perspective* 1994;8(4):19-43.
- Hao Q, Xu S, Liao Y, Qiao D, Shi H, Xu T. Determinants of residents' willingness to pay for water quality improvements in Haikou, China: Application of CVM and ISM approaches. *Water* 2023;15(7):Article No. 1305.
- Hosany ARS, Hamilton RW. Family responses to resource scarcity. *Journal of the Academy of Marketing Science* 2023;51:1351-81.
- Indab A. Willingness to pay for whale shark conservation in Sorsogon, Philippines. In: Olewiler N, Francisco H, Ferrer A, editors. *Marine and Coastal Ecosystem Valuation, Institutions, and Policy in Southeast Asia*. Singapore: Springer; 2016. p. 93-128.
- Jala, Nandagiri L. Evaluation of the economic value of Pilikula Lake using travel cost and contingent valuation methods. *Aquatic Procedia* 2015;4:1315-21.
- Janko AM, Zemedu L. Fishermen's willingness to pay for fisheries management: The case of Lake Ziway, Ethiopia. *International Journal of Fisheries and Aquatic Studies* 2015;2(6):320-5.
- Kanyoka P, Farolfi S, Morardet S. Households preferences and willingness to pay for multiple use water services in rural areas of South Africa: An analysis based on choice modeling. *WaterSA* 2008;36:715-24.
- Khong TD, Loch A, Young MD. Inferred valuation versus conventional contingent valuation: A salinity intrusion case study. *Journal of Environmental Management* 2019;243: 95-104.
- Klein J. The relationship between level of academic education and reversible and irreversible processes of probability decision making. *Higher Education* 1999;37:323-39.
- Makwinja R, Kosamu IBM, Kaonga CC. Determinants and values of willingness to pay for water quality improvement: Insights from Chia lagoon, Malawi. *Sustainability* 2019;11(17):Article No. 4690.
- Klesment M, Bavel JV. Women's relative resources and couples' gender balance in financial decision-making. *European Sociological Review* 2022;38(5):739-53.

- Kumar P, Martinez-Alier J. The economics of valuing ecosystem services and biodiversity: An international assessment. *Economic and Political Weekly* 2011;46(24):76-80.
- Kolstoe S, Naald BV, Cohan A. A tale of two samples: Understanding WTP differences in the age of social media. *Ecosystem Service* 2022;55:Article No. 101420.
- Lamsal P, Atreya K, Pant KP, Kumar L. An analysis of willingness to pay for community-based conservation activities at the Ghodaghodi Lake Complex, Nepal. *International Journal of Biodiversity Science, Ecosystem Services and Management* 2015;11(4):341-8.
- Lopez-Becerra EI, Alcon F. Social desirability bias in the environmental economic valuation: An inferred valuation approach. *Ecological Economics* 2021;184:Article No. 106988.
- Luangmany D, Voravong S, Thanthathap K, Souphonphacdy D, Baylatry M. Valuing Environmental Services using Contingent Valuation Method. Ho Chi Minh City, Vietnam: Economy and Environment Partnership for Southeast Asia; 2009.
- Lusk J. Effects of cheap talk on consumer willingness-to-pay for golden rice. *American Journal of Agricultural Economics* 2003;85(4):840-56.
- Mapa CDS. Preliminary 2023 First Semester Official Poverty Statistics [Internet]. 2023 [cited 2024 Apr 11]. Available from: <https://psa.gov.ph/statistics/poverty>.
- Mendelsohn R, Olmstead S. The economic valuation of environmental amenities and disamenities: Methods and applications. *Annual Reviews of Environment and Resource* 2009;34(1):325-47.
- Minasyan D, Tovmasyan G. Gender differences in decision-making and leadership: Evidence from Armenia. *Business Ethics and Leadership* 2020;4(1):6-16.
- Moffat B, Motlaleng GR, Thukuza A. Households willingness to pay for improved water quality and reliability of supply Chobe Ward, Muan. *Botswana Journal of Economics* 2011;8(12):45-61.
- Mumbi AW, Watanabe T. Differences in risk perception of water quality and its influencing factors between lay people and factory workers for water management in River Sosiani, Eldoret Municipality Kenya. *Water* 2020;12:Article No. 2248.
- Nakano S, Yahara T, Nakashizuka T. Aquatic Biodiversity Conservation and Ecosystem Services. Singapore: Springer. 2016.
- Pontoni F, Creti A, Joets M. Economic and environmental implications of hydropower concession renewals: A case study in Southern France. *Revue Economique* 2018;2(60):241-66.
- Reis JVD, Leitao MDMVBR, Galvincto JD. Willingness to pay for water ecosystem services in a river basin of the in South America largest semi-arid region. *Nova Economia* 2022;32(1):293-318.
- Rounsevell M, Fischer M, Torre-Marin Rando A, Mader A. The regional assessment report on biodiversity and ecosystem services for Europe and Central Asia [Internet]. 2018 [cited 2024 Feb 7]. Available from: <https://www.ipbes.net/assessment-reports/eca>.
- Santos-Borja A. Multi-stakeholder's efforts for the sustainable management of Tadalac Lake, the Philippines [Internet]. 2008 [cited 2024 Feb 7]. Available from: https://satoyama-initiative.org/case_studies/multistakeholders_efforts-for-the-sustainablemanagement-of-tadalac-lake-the-philippines/.
- Šebo J, Gróf M, Šebová M. A contingent valuation study of a polluted urban lake in Košice, Slovakia: The case of the positive distance effect. *Journal of Environmental Management* 2019;243:331-9.
- Sinclair JS, Fraker ME, Hood JM, Reavie ED, Ludsins SA. Eutrophication, water quality, and fisheries: A wicked management problem with insights from a century of change in Lake Erie. *Ecology and Society* 2023;28(3):Article No. 10.
- Tziakis I, Pachiadakis I, Moraitakis M, Xideas K, Theologis G, Tsagarakis KP. Valuing benefits from wastewater treatment and reuse using contingent valuation methodology. *Desalination* 2009;237:117-25.
- Van Houtven, Powers GJ, Pattanayak K. Valuing water quality improvements in the United States using meta-analysis: Is the glass half-full or half-empty for national policy analysis? *Resource and Energy Economics* 2007;29:206-28.
- Van Oijstaeijen W, Van Passel S, Cools J, de Bisthoven LJ, Hugé J, Berihun D, et al. Farmers' preferences towards water hyacinth control: A contingent valuation study. *Journal of Great Lakes Research* 2020;46:1459-68.
- Villanueva-Moya L, Expósito F. Spanish women were making risky decisions in the social domain: The mediating role of femininity and fear of negative evaluation. *Frontiers in Psychology* 2020;11:Article No. 561715.
- Villaruel MJS, Camacho MVC. Phytoplankton community dynamics in Tadalac Lake, Los Baños Laguna, Philippines. *Journal of Fisheries and Environment* 2022;46(3):55-71.
- Wegner G, Pascual U. Cost-benefit analysis in the context of ecosystem services for human well-being: A multidisciplinary critique. *Global Environmental Change* 2011;21(2):492-504.
- Weinstein J. The Problem of Rural Education in the Philippines [Internet]. 2010 [Cited 2024 Feb 7]. Available from: <https://joshweinstein.wordpress.com/2010/03/02/the-problem-of-education-in-the-philippines/>.
- Xiong K, Kong F, Zhang N, Lei N, Sun C. Analysis of the factors influencing willingness to pay and payout level for ecological environment improvement of the Ganjiang River basin. *Sustainability* 2018;10:Article No. 2149.
- Yifei Z, Li S, Luo Y. Evaluation of households' willingness to accept the ecological restoration of rivers flowing in China. *Environmental Progress and Sustainable Energy* 2018; 38(4):1-10.
- Zelalem L, Beyene F. Willingness to pay for improved rural water supply in Goro-Gutu District of Eastern Ethiopia: An application of contingent valuation. *Journal of Economics and Sustainable Development* 2012;3(14):145-59.
- Zhen L, Li F, Huang H, Dilly O, Liu J, Wei Y, et al. Households' willingness to reduce pollution threats in the Poyang Lake Region, Southern China. *Journal of Geochemical Exploration* 2011;110(1):15-22.

Phenolated Alkali Lignin/Magnetite Composite as an Adsorbent for Methyl Violet 6B in Wastewater

Mary Sheenalyn P. Rodil*, Corazon D. Sacdalan, Rissabell R. Robero, Maria Evytha L. Salinas, and Trixie N. Santander

Technological University of the Philippines, Manila, Philippines

ARTICLE INFO

Received: 20 Sep 2023
Received in revised: 2 May 2024
Accepted: 8 May 2024
Published online: 20 May 2024
DOI: 10.32526/ennrj/22/20230256

Keywords:

Adsorption kinetics/ Dye removal/
Isotherm models/ Optimization/
Reusability/ Thermodynamic

* Corresponding author:

E-mail:
marysheenalyn_rodil@tup.edu.ph

ABSTRACT

Methyl violet 6B (MV6B), found in wastewater, poses hazardous effects to aquatic ecosystems and human health; therefore, it must be removed immediately. In response, this study pioneered the development of a dye adsorbent by incorporating phenolated alkali lignin (PAL) into magnetite (Fe_3O_4), offering a solution for MV6B removal. Lignin was extracted from coconut husk through alkali extraction, chemically modified using phenolation, and integrated onto the magnetite surface. SEM and FTIR spectroscopy were used to characterize the adsorbent, and various parameters were optimized, along with evaluations of the adsorption kinetics and isotherm models, as well as the adsorbent's reusability. PAL was successfully deposited onto the magnetite based on the characterization. The experimental results revealed that the optimal conditions for the removal of MV6B using PAL/ Fe_3O_4 composite are pH 4, a temperature of 313 K, a dosage of 0.10 g PAL/ Fe_3O_4 per 15 mL of MV6B, and a contact time of 150 minutes. MV6B's equilibrium removal rate was 95.1%, with an adsorption capacity at equilibrium of 6.42 mg/g. The adsorption of MV6B followed a pseudo-second-order kinetic model and the Freundlich model isotherm. A thermodynamic study showed that the adsorption process was spontaneous and exothermic. PAL/ Fe_3O_4 was highly reusable after three cycles without the need for desorption. Hence, this study has demonstrated that the PAL/ Fe_3O_4 adsorbent is practical, economical, and efficient for wastewater treatment.

1. INTRODUCTION

Widespread industrialization and urbanization have led to an upsurge in groundwater and surface water pollution, which has become a top priority and a global crisis. This environmental crisis is exacerbated by the presence of dyes derived from industrial processes such as paper production, textile manufacturing, tanning operations, and paint industries. According to a World Bank report, the textile industry is responsible for between 17% and 20% of water contamination during the textile finishing and dyeing processes (Saini, 2017). As an effluent, these dyes can discharge in an aquatic environment from 2% for basic dyes to 50% for reactive dyes (Sharma et al., 2021). These dyes pose a threat not only to the integrity of

wastewater and the environment but also to the balance of marine ecosystems and the well-being of the communities living in close proximity. Even at low concentrations, these dyes wield the potential to inflict significant and lasting harm upon the environment. The complex chemical structures and synthetic origins of many dyes used in industry make them resilient and difficult to remove.

One of the standard dyes heavily used by different industries is methyl violet 6B (MV6B). MV is a carcinogenic organic dye with long-lasting deleterious effects that pose hazards to humans, marine life, and the environment (Foroutan et al., 2019). MV has been classified as a hazardous recalcitrant substance, exhibiting limited biodegradability.

Citation: Rodil MSP, Sacdalan CD, Robero RR, Salinas MEL, Santander TN. Phenolated alkali lignin/magnetite composite as an adsorbent for methyl violet 6B in wastewater. *Environ. Nat. Resour. J.* 2024;22(3):257-269. (<https://doi.org/10.32526/ennrj/22/20230256>)

Conventional wastewater treatment systems are unable to effectively remove MV from the wastewaters, resulting in its dispersal into the environment (Casas et al., 2009). Various methods of removing dyes have been studied in order to reduce the adverse effects on the environment. These consist of membrane filtering, solvent extraction, biofilm utilization, coagulation-flocculation, bacterial treatment, electrochemical oxidation, and photocatalytic degradation. However, some of these methods can be expensive, energy-intensive, lead to the formation of secondary pollutants and require careful disposal of the generated sludge.

Due to its simple design, low cost, wide applicability, effectiveness and minimal environmental impact, another method used to clean wastewater contaminated with dyes is the utilization of adsorbents. Numerous analyses determined that polymeric adsorbent is effective in elimination of the different dyes (Bensalah, 2024). Lignin is one kind of polymer capable of treating dye-contaminated wastewater. By altering, carbonizing, and compositing lignin, numerous researchers have produced a variety of lignin-derived adsorption materials, with potential uses in the wastewater treatment industry (Wang et al., 2022). In this recent study, lignin was modified through phenolation and magnetite was incorporated for faster magnetic separation. This process can lead to a novel lignin-based material, the phenolated alkali lignin/magnetite (PAL/Fe₃O₄) composite. Its ability to adsorb aqueous MV6B was evaluated, analyses of kinetic models, isotherm models and thermodynamic parameters were also carried out.

2. METHODOLOGY

2.1 Fabrication of phenolated alkali lignin/magnetite (PAL/Fe₃O₄) composite

Alkali lignin is extracted using 123 g of coconut husk, which was air-dried, crushed into powder, and sieved through a 60-mesh filter. A mixture of 7.5% (w/v) NaOH solution and coconut husk powder in a 1:10 (w/v) ratio was prepared and refluxed for 1.5 h at 90±2°C. A cloth was used to filter the warm refluxed mixture. The filtrate was then cooled to room temperature. Following the cooling process, the filtrate, which appeared as a black liquor, was acidified using 2 M and 0.50 M H₂SO₄ until the pH reached a value of 2. The precipitate was filtered and repeatedly rinsed with distilled water until the pH became neutral, then dried (Panamgama and Peramune, 2018).

To synthesize the PAL, 9 g of extracted lignin and 36 g of phenol were dissolved in 90 mL of a 72% H₂SO₄ solution and continuously stirred for 6 h at 60°C. To dilute the H₂SO₄ to a 3% concentration, 2,070 mL of distilled water was added to the mixture, which was then heated for an additional hour at 125°C. The PAL was subsequently centrifuged at 10,000 rpm for 10 min. After being washed three times with distilled water, the PAL was dried for 6 h at 105°C.

For integration of Fe₃O₄ onto the surface of PAL, 18.2 g of FeCl₃·6H₂O and 12.6 g of FeSO₄·7H₂O were dissolved in 100 mL water and heated until the temperature reached 90°C (Benhalima et al., 2023a). Subsequently, 30 mL of 26% NH₄OH and 3 g of PAL in 600 mL of distilled water were added to the mixture. The pH was adjusted to 10 using 2 M and 0.10 M NaOH. The mixture was stirred at 300 rpm for 30 min at 80°C. The resulting PAL/Fe₃O₄ composite was subjected to centrifugation at 10,000 rpm for 10 min, followed by three rinses with distilled water, and finally, oven-dried at 50°C.

2.2 Characterization of phenolated alkali lignin/magnetite (PAL/Fe₃O₄) composite

The surface morphology of the PAL/Fe₃O₄ composite underwent examination through scanning electron microscopy, with a voltage of 10.0 kV and a magnification of 10.6 mm × 500 and 10.0 k SE (Hitachi Model- SU3800; Tokyo, Japan). Fourier Transform Infrared Spectroscopy (Shimadzu IRTracer-100; Kyoto, Japan) in the wave number region from 400 cm⁻¹ to 4,000 cm⁻¹ was applied to analyze the alkali lignin, PAL, and PAL/Fe₃O₄ composite, giving evidence on chemical bond rearrangements and structural modifications.

2.3 Optimization of parameters in the adsorption of MV using PAL/Fe₃O₄ composite

Initially, the pH of 15 mL of a 45 mg/L MV6B solution was adjusted to levels 4, 6, 8, and 10 using 0.10 M HCl and 0.10 M NaOH. Afterward, 0.15 g of PAL/Fe₃O₄ composite adsorbent was introduced into each solution for 30 min. The adsorbent was subsequently isolated with a magnet, and the final MV6B concentration was determined at 592 nm using a UV-Vis spectrophotometer (UH5300 spectrophotometer; Tokyo, Japan). Next, under optimal pH conditions, four flasks each containing 15 mL of a 45 mg/L MV6B solution and 0.15 g of PAL/Fe₃O₄ were heated at a temperature of 293 K, 303 K, 313 K, and 323 K. After heating and reaching equilibrium, the

adsorbent was separated, and the MV6B concentration was measured as previously described. Following this, while maintaining the optimal pH and temperature, the study investigated the effect of varying the dosage of PAL/Fe₃O₄ composite (0.05 g, 0.10 g, 0.15 g, and 0.20 g). Each dosage was added to 15 mL of the 45 mg/L MV6B solution. Lastly, under the optimal conditions of pH, temperature, and dosage, 15 mL of a 45 mg/L MV6B solution was exposed to varying contact times, ranging from 5 min to 150 min. After each specified time interval, the adsorbents were separated, and the absorbance of the aqueous solution was recorded. The adsorption capacity at equilibrium (q_e , mg/g) and the removal efficiency R (%) were calculated from the following Equations (1) and (2), respectively:

$$q_e = \frac{C_o - C_f}{w} \times V \quad (1)$$

$$\% R = \frac{C_o - C_f}{C_o} \times 100 \quad (2)$$

Where; C_o and C_f stand for the initial and final concentrations of the adsorbate (mg/L), V represents the volume of the solution (L), w is the mass of the adsorbent (g), and $\% R$ symbolizes the percentage of removal (Benhalima and Ferfera-Harrar, 2019).

2.4 Adsorption kinetic study

The adsorption of MV6B using PAL/Fe₃O₄ composite was investigated within 5 min to 150 min at optimal pH, temperature, and adsorbent dosage. The data underwent kinetic study, employing both the pseudo-first order (PFO) and pseudo-second order (PSO) models, following Equations (3) and (4), respectively.

$$\ln(q_e - q_t) = \ln q_e - K_1 t \quad (3)$$

$$\frac{t}{q_t} = \frac{1}{K_2 q_e^2} + \frac{t}{q_e} \quad (4)$$

Where; q_e represents the adsorption capacity at equilibrium (mg/g), q_t stands for adsorption capacity at time t (mg/g), K_1 denotes the rate constant of the PFO model (min^{-1}), and K_2 symbolizes the rate constant of the PSO model (min^{-1}) (Benhalima et al., 2017).

2.5 Adsorption isotherm model

MV6B solutions spanning concentrations from 20 mg/L to 90 mg/L were prepared. Subsequently, 15 mL of each solution was combined with 0.10 g

PAL/Fe₃O₄. These mixtures were conditioned at pH 4 and a temperature of 313 K. Following this, the equilibrium concentrations were ascertained and subjected to analysis utilizing the Langmuir, Freundlich, and Temkin isotherm models, following Equations (5), (6), and (7), respectively.

$$\frac{C_e}{q_e} = \frac{C_e}{q_m} + \frac{1}{K_L q_m} \quad (5)$$

$$\log(q_e) = \log(K_F) + \frac{1}{n} \log(C_e) \quad (6)$$

$$q_e = B \ln(K_T) + \frac{RT}{b} \ln C_e \quad (7)$$

Where; C_e represents the concentration of adsorbate at equilibrium (mg/L), while q_e denotes the adsorption capacity at equilibrium (mg/g). The parameter q_m refers to the maximum adsorption capacity of the adsorbent (mg/g). K_L was used to symbolize the Langmuir isotherm constant (L/mg), and K_F represents the Freundlich isotherm constant (L/mg). The variable n signifies the degree of adsorption favorableness, b represents the heat of adsorption (J/mol), and B stands for the Temkin constant (RT/b), where R is the universal gas constant (8.314 J/mol·K), T is the absolute temperature (K), and K_T signifies the Temkin constant (Benhalima et al., 2017).

2.6 Thermodynamic study

To obtain an understanding of how temperature affects the adsorption process, the thermodynamic parameters, such as Gibbs free energy change (ΔG°), standard enthalpy change (ΔH°), and standard entropy change (ΔS°), were evaluated. These were done at a temperature of 293 K, 303 K, and 313 K. The following equations were utilized in the calculation of these parameters:

$$\Delta G^\circ = -RT \ln K_d \quad (8)$$

$$\ln K_d = -\frac{\Delta H^\circ}{RT} + \frac{\Delta S^\circ}{R} \quad (9)$$

Where; K_d represents the concentration ratio of the MV6B adsorbed to the MV6B remained in solution at equilibrium. R is the universal gas constant (8.314 J/mol·K), while T is the absolute temperature in Kelvin. To find the values of ΔH° (in kJ/mol) and ΔS° (in J/mol·K), respectively, $\ln K_d$ was plotted linearly against ($1/T$). The slope and intercept of the resulting graph were computed (Benhalima et al., 2017).

2.7 Reusability of phenolated alkali lignin/magnetite (PAL/Fe₃O₄) composite

After the first adsorption of MV6B using 0.10 g of PAL/Fe₃O₄ under optimal conditions, the adsorbent was recovered using magnets and dried. The reusability of PAL/Fe₃O₄ was evaluated through three successive cycles without employing a desorption process. The the removal efficiency R (%) were calculated from Equation 2.

3. RESULTS AND DISCUSSION

3.1 Fabrication of phenolated alkali lignin/magnetite composite (PAL/Fe₃O₄) composite

Figure 1 illustrates the fabricated alkali lignin (a), phenolated alkali lignin (PAL) (b), and the PAL/magnetite composite (PAL/Fe₃O₄) (c) utilized in this study. Coconut husk underwent alkaline lignin

extraction using a 7.5% NaOH (w/v) solution to increase the pore volume and surface area of lignin. The resulting solid residue was separated from the black liquor and processed to obtain 77 g of deep brown alkali lignin from an initial 123 g sample. This alkali lignin was phenolated in an acidic medium at an elevated temperature, involving the condensation of its aromatic rings with phenol to increase the phenolic hydroxyl groups (Taleb et al., 2020). The resulting phenolated alkali lignin (PAL) served as a multidentate ligand for binding to iron oxide through coordination. This binding transformed the iron oxide surface, enhancing PAL's attachment. Incorporating magnetite into the composite was done to functionalize the adsorbent, improving adsorption efficiency and enabling faster magnetic separation (Liu et al., 2020; Touihri et al., 2021).

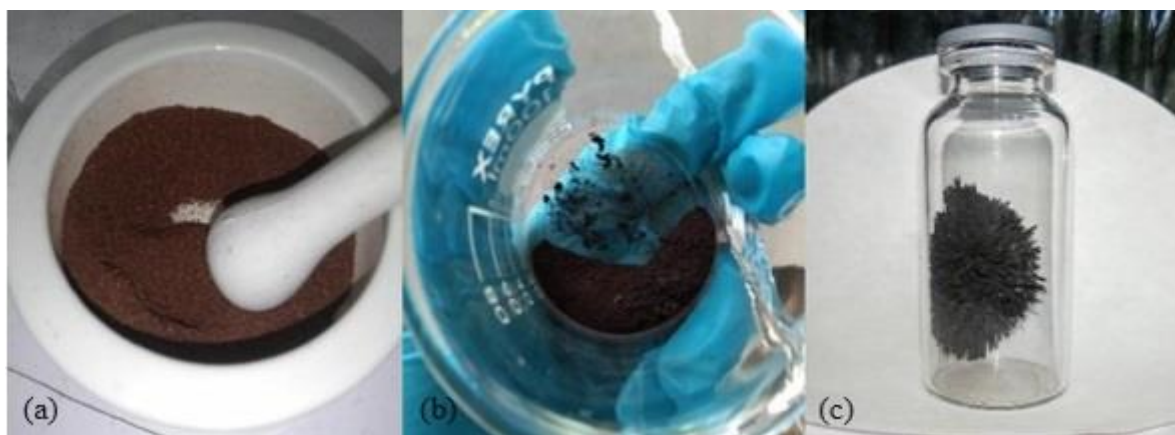


Figure 1. Fabricated of (a) alkali lignin, (b) PAL, and (c) PAL/Fe₃O₄ composite

3.2 Characterization of phenolated alkali lignin/magnetite Composite (PAL/Fe₃O₄) composite

3.2.1 Fourier transform infrared (FTIR) spectroscopy

Figure 2 presents the FTIR spectrum of the adsorbent, which comprises lignin, PAL, and PAL/Fe₃O₄.

In the lignin spectrum, O-H stretching vibrations are present at 3,321 cm⁻¹. The spectrum exhibits characteristic C=C stretching vibrations at 1,604 cm⁻¹, indicative of aromatic rings within the lignin structure. Peaks in the region around 1,035 cm⁻¹ represent aromatic C-H in-plane deformation (Chaudhari, 2016). In contrast, phenolated alkali lignin (PAL) retains the aromatic rings found in unmodified lignin, displaying strong absorption peaks in the 1,500-1,600 cm⁻¹ range, attributable to C=C stretching vibrations within the

aromatic rings. Compared to lignin spectra, PAL exhibits a broader absorption band at 3,232 cm⁻¹, supporting the increased presence of phenolic functional groups, which are products of the phenolation process, in PAL (Younesi-Kordkheili and Pizzi, 2021). Distinct peaks between 1,593 cm⁻¹ and 1,500 cm⁻¹ in the spectra represent the bending vibrations of hydroxyl groups (OH) in lignin. The C-O stretching vibrations of these groups, appearing as a band at 1,118.71 cm⁻¹, serve as their defining characteristics. Peaks in the 2,850-2,916 cm⁻¹ range, corresponding to C-H stretching vibrations, particularly in aliphatic and methoxy groups, indicate that the lignin has undergone changes. Since aliphatic groups in lignin are unusual, the development of these peaks in the spectra is likely due to the influence of modifications.

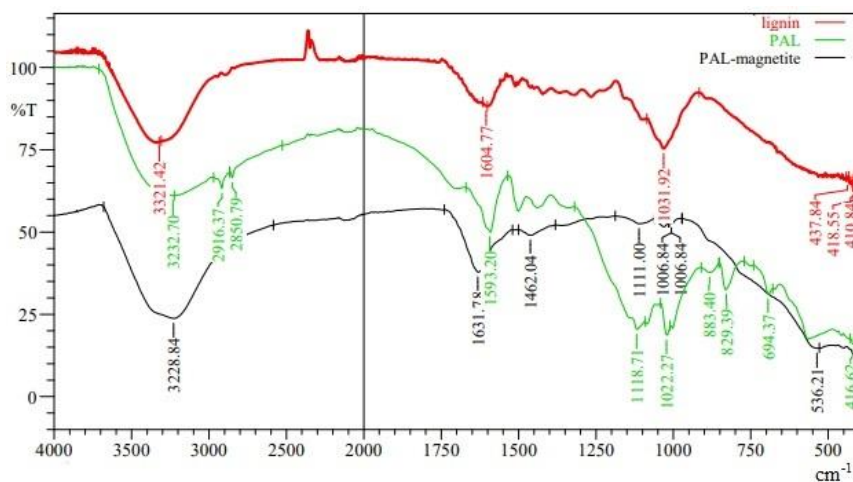


Figure 2. FTIR spectra of alkali lignin, PAL, and PAL/Fe₃O₄ composite

In the PAL/Fe₃O₄ spectrum, a spectral band at 3,228 cm⁻¹ is broader than in PAL, confirming the presence of a substantial O-H group. Distinct peaks are evident at 1,006 cm⁻¹ and 1,111 cm⁻¹, which can be directly attributed to the elongation of C-O bonds within the phenolic hydroxyl group. These peaks serve as clear indicators of the chemical interaction between PAL and magnetite. The spectrum also exhibits a peak at 536 cm⁻¹, signifying the intense vibration of Fe-O bonds originating from magnetite. This pronounced Fe-O band underscores the presence of magnetite in the composite (Benhalima et al., 2023a).

3.2.2 Scanning electron microscopy (SEM)

Figure 3 displays the SEM images showcasing the surface morphology of PAL/Fe₃O₄ at magnifications of 500x and 10000x.

The images show that the adsorbent exhibits a rough surface, with some particles displaying a granulated appearance and compact grain structures of varying sizes. This heterogeneous structure of the adsorbent particles can be attributed to the uneven adhesion of PAL to magnetite, resulting in the creation of numerous adsorption sites, which are important to improve the adsorbent's capacity and effectiveness when interacting with dye molecules (You et al., 2022).

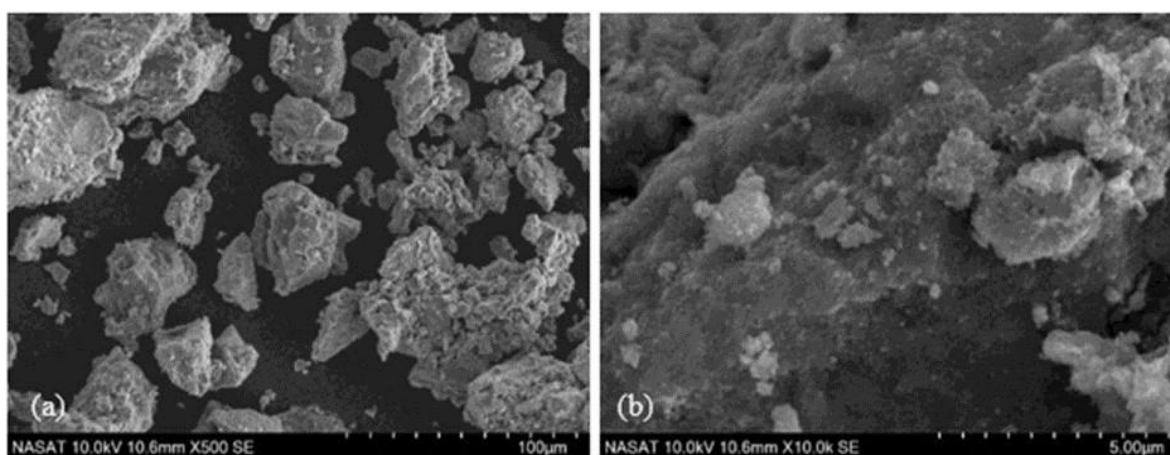


Figure 3. SEM images of PAL/Fe₃O₄ with magnifications of (a) 500x and (b) 10000x

3.3 Parameter optimization for the removal of MV6B via adsorption

Figure 4 displayed the results of the parameter optimization for the removal of MV6B.

The adsorption efficiency values decrease with rising pH from 4 to 10. At low pH, MV6B, and PAL

undergo protonation due to the high concentration of H⁺ ions in the acidic environment. However, given that phenolated alkali lignin is a polymeric substance with a complex structure, their interaction does not primarily depend on electrostatic attraction between their charged moieties (Meng et al., 2020). The

interaction can be driven by hydrophobic interactions facilitated by their aromatic structures, along with strong π - π stacking interactions. Additionally, despite their positive charges, potential hydrogen bonding between functional groups such as hydroxyl (-OH) groups in PAL and nitrogen atoms in MV6B and charge-induced interactions can contribute to their binding. At basic pH, alterations in solubility, conformation, and aromatic ring alignment in PAL

and MV6B can reduce the exposure of hydrophobic regions, disrupt π - π stacking interactions and weaken hydrogen bonding. However, the adsorption efficiency persists at high level because of the strong affinity of MV6B onto negatively charged adsorbents. In alkaline media, the phenolate ions are generated and thus enhance electrostatic attraction affinity toward the cationic dye.

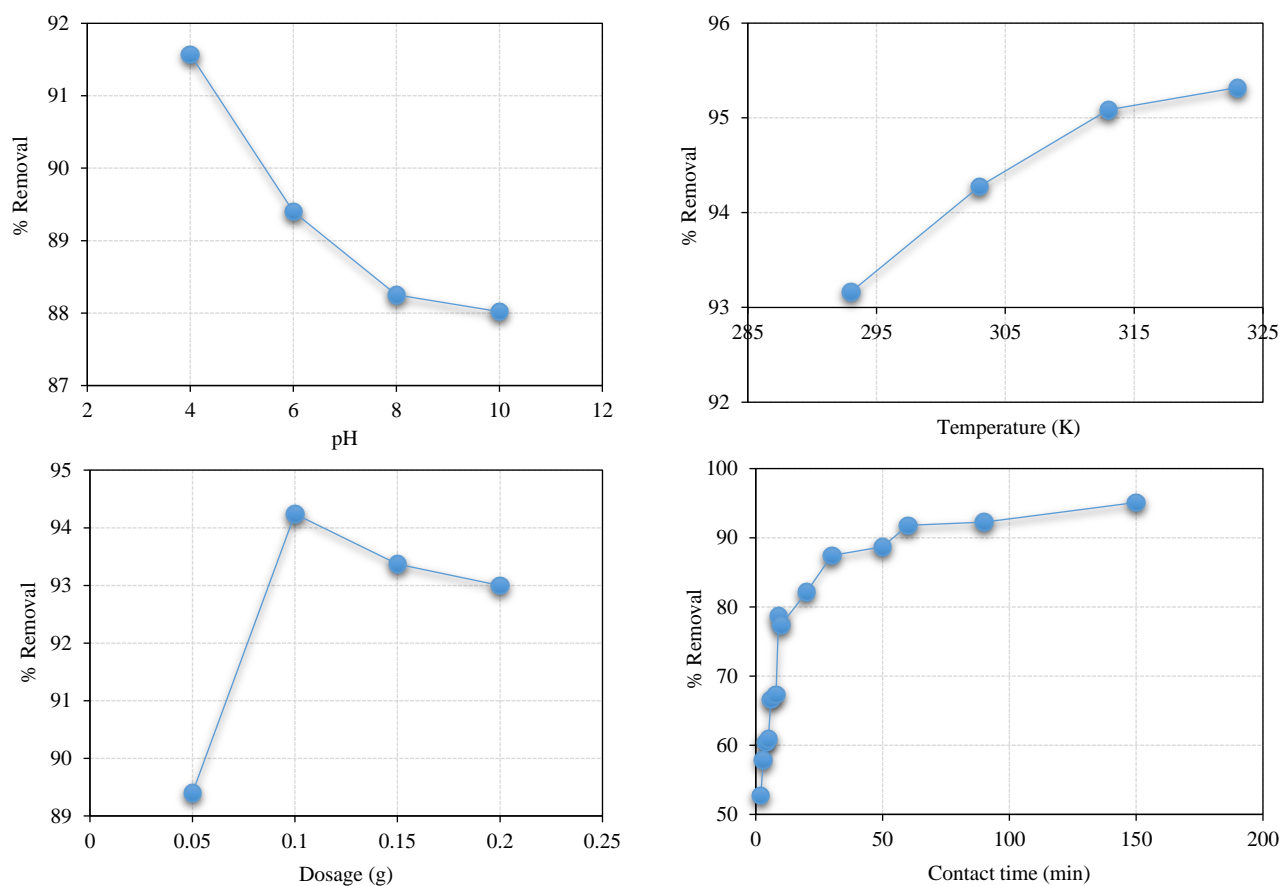


Figure 4. The effects of pH, temperature, dosage, and contact time on the adsorption of MV6B using PAL/Fe₃O₄

The adsorption efficiency increases as the temperature rises from 293 K to 323 K, indicating that adsorption is an endothermic reaction. The adsorption at 313 K and 323 K is not significantly different, suggesting that the adsorption of MV6B plateaus after the temperature surpasses 313 K. Furthermore, the most efficient adsorption was observed at 0.10 g PAL/Fe₃O₄. As the amount increases beyond 0.10 g, the capacity to adsorb decreases due to the minor agglomeration of the adsorbents. This agglomeration covers the active sites, preventing the binding of MV6B (Chen and Chen, 2018).

Under ideal conditions of pH, temperature, and PAL/Fe₃O₄ dosage, the optimal contact time for

MV6B adsorption is 150 min. The adsorption efficiency increases as time progresses, followed by a plateau in adsorption efficiency, which results from the saturation of available adsorption sites by MV6B.

3.4 Adsorption kinetics

Figure 5 depicts the linear fitting of pseudo-first-order model and the pseudo-second-order kinetic model of the adsorption of MV6B using PAL/Fe₃O₄ composite. The relevant parameters of the models including equilibrium rate constant, adsorption capacity at equilibrium and correlation coefficients are shown in Table 1.

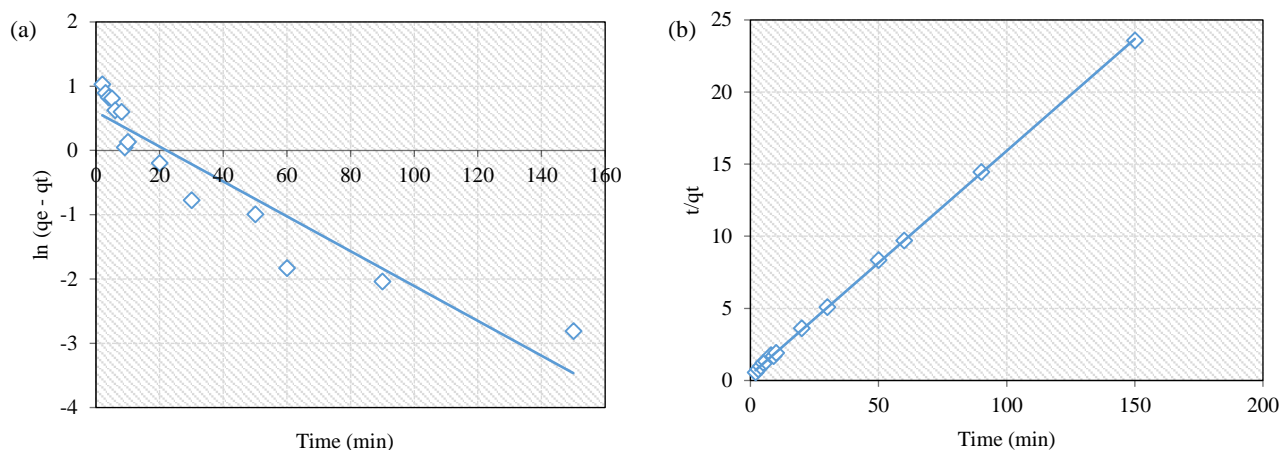


Figure 5. Linear fitting of the (a) pseudo-first and (b) pseudo-second-order kinetic model of the adsorption of methyl violet using PAL/Fe₃O₄ composite

Table 1. Parameters of pseudo-first and pseudo-second-order kinetic model of the adsorption of methyl violet using PAL/Fe₃O₄

Parameters	Pseudo-first-order	Pseudo-second-order
Equilibrium rate constant, K	$-1.75 \times 10^{-4}/\text{min}$	$6.04 \times 10^{-2} \text{ g}/\text{mg} \cdot \text{min}$
q_e , experimental	6.42 mg/g	6.42 mg/g
q_e , calculated	1.95 mg/g	6.44 mg/g
R^2	0.913	0.999

It could be clearly seen that pseudo-second-order model best described the adsorption kinetics with higher correlation coefficient ($R^2=0.999$) versus the pseudo-first-order model ($R^2=0.913$), indicating a chemisorption process. The kinetics study implied chemical interactions between the MV6B and PAL/Fe₃O₄ surface, as shown in Figure 6, characterized

by electrostatic attraction, hydrophobic interactions facilitated by their aromatic structures, along with strong $\pi-\pi$ stacking interactions and hydrogen bonding. Chemical adsorption assumes a dominant role in magnetic lignin compared to diffusion (Fang et al., 2021; Benhalima et al., 2023b; Benhalima et al., 2024).

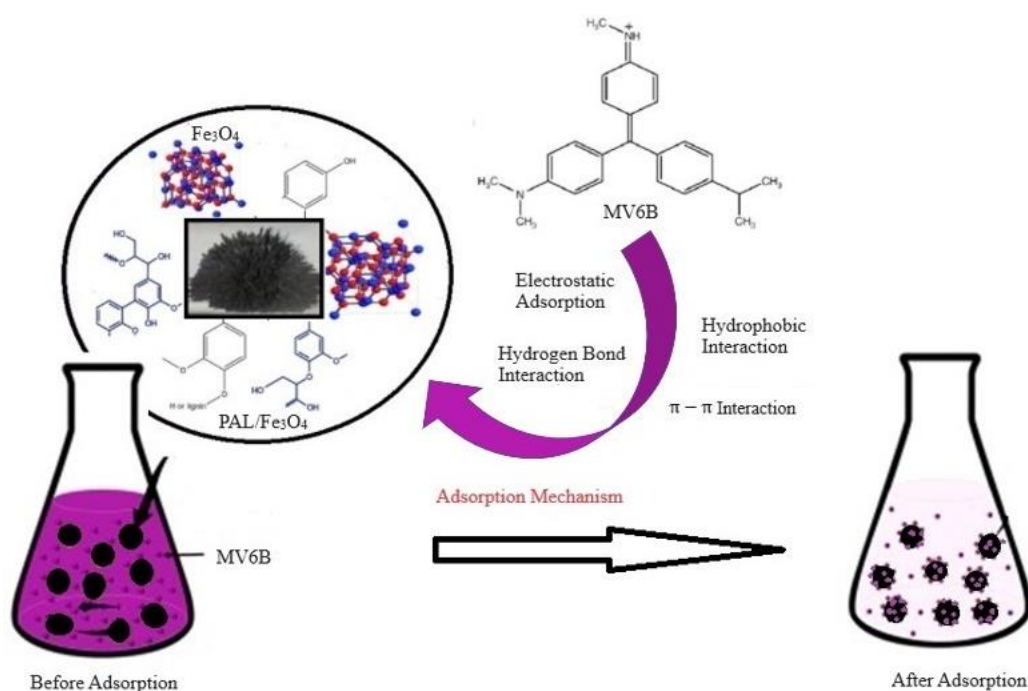


Figure 6. Adsorption mechanism of MV6B on PAL/Fe₃O₄ composite adsorbent

3.5 Adsorption isotherm

An adsorption isotherm defines the interaction between the adsorbate and the adsorbent and provides the capacity of the adsorbent to adsorb. The Langmuir isotherm model is used to describe monolayer adsorption, which occurs when all available active sites are occupied, reaching maximum adsorption and saturation (Liu et al., 2019). The Temkin isotherm predicts that the heat of adsorption for all molecules reduces linearly with increasing coverage (Ringot et al., 2007). On the other hand, the Freundlich isotherm

gives an expression for the surface heterogeneity, the exponential distribution of active sites, and their energy (Ayawei et al., 2015). Figure 7 shows the linear fitting of the Langmuir, Temkin, and Freundlich isotherm model of the adsorption of MV6B using PAL/Fe₃O₄ composite while Table 2 provides the parameters for each model such as maximum monolayer adsorption capacity (q_m), binding energy (B_T), equilibrium constant (K_L or K_T), and the Freundlich constant (K_F), along with correlation coefficients (R^2).

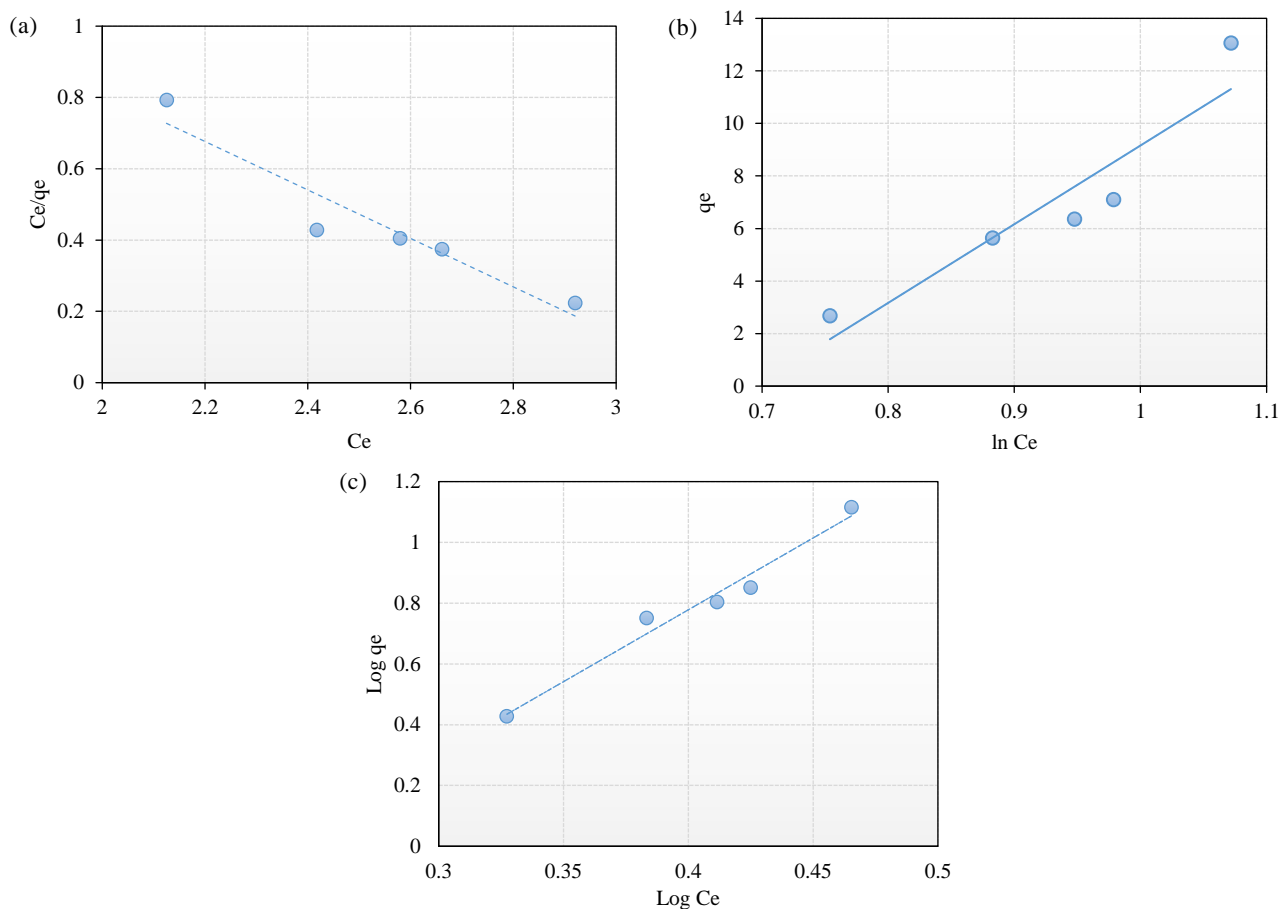


Figure 7. Linear fitting of the (a) Langmuir, (b) Temkin, and (c) Freundlich isotherm model of the adsorption of MV6B using PAL/Fe₃O₄

Table 2. Parameters of Langmuir, Temkin, and Freundlich isotherm model

Langmuir isotherm	Temkin isotherm	Freundlich isotherm
q_m (mg/g)=-1.470	B_T (J/mol)=29.96	n =0.212
K_L (L/mg)=-0.312	K_T (L/mg)=0.4994	K_F (L/mg)=0.0771
R_L =-0.0917	R^2 =0.872	R^2 =0.971
R^2 =0.909		

The Langmuir isotherm model employs the separation factor (R_L) to assess the favorability of an isotherm. When $0 < R_L < 1$, it is considered favorable; when $R_L > 1$, it is unfavorable; $R_L = 1$ indicates linearity,

and $R_L = 0$ implies irreversibility (Ayawei et al., 2017). As indicated in Table 2, the R_L value obtained is -0.0917, signifying that the Langmuir isotherm for MV6B adsorption using PAL/Fe₃O₄ is unfavorable.

This is supported by a correlation coefficient of 0.9099. On the other hand, the Temkin model's calculated R^2 was 0.8718, thus cannot adequately describe MV6B's adsorption. The positive BT values for MV6B (29.96 J/mol) demonstrate an endothermic reaction, with a K_T value of 0.4995 L/mg.

In the Freundlich model, the adsorption phenomenon is considered favorable when $n < 1$, unfavorable when $n > 1$, linear adsorption when $n = 1$ and irreversible when $n = 0$ (Chiban et al., 2011). The adsorption favorability value, n , is 0.212 which implies favorable adsorption. The Freundlich model best described the adsorption isotherm with higher

correlation coefficient ($R^2 = 0.971$) versus the other two models, indicating that the adsorption sites are non-identical. Furthermore, Freundlich model describes multilayer adsorption, which means the quantity of adsorbate adsorbed escalates with an increase in solution concentration. The determined adsorption capacity constants exhibited a value of 0.0771 L/mg.

3.5 Thermodynamic Study

The thermodynamic parameters which provide understandings into the energetics of the adsorption of MV6B on PAL/Fe₃O₄ were presented in Table 3.

Table 3. The thermodynamic parameters for MV6B adsorption on PAL/Fe₃O₄ at different temperatures

Temperature (K)	K_d	$\ln K_d$	Thermodynamic parameters		
			ΔG° (kJ/mol)	ΔH° (kJ/mol)	ΔS° (J/mol·K)
293	1.362463	0.309294	-0.75382753	1.60	5.76
303	1.647635	0.499341	-1.258534079		
313	1.934874	0.660042	-1.718439123		

The negative values of ΔG° and the positive value of ΔH° indicate that the adsorption of the MV6B was spontaneous and endothermic. The spontaneity increase from 293 to 313 K, signifying more driving forces and thus greater adsorption capacity at higher temperatures. In chemisorption process, this suggests that the formation of chemical bonds between the MV6B and PAL/Fe₃O₄ is energetically favorable, leading to the adsorption of the species onto the surface. Positive ΔS° values indicate that the MV6B

become more disordered upon adsorption onto the PAL/Fe₃O₄ surface.

3.6. Reusability of PAL/Fe₃O₄ composite in the adsorption of MV6B

The reusability of PAL/Fe₃O₄ shown in Figure 8 was evaluated through repeated adsorption cycles without desorption. The optimal conditions, determined from the evaluated parameters, are as follows: $C_0 = 45$ mg/L, pH=4, and a dosage of 0.10 g/15 mL at 313 K.

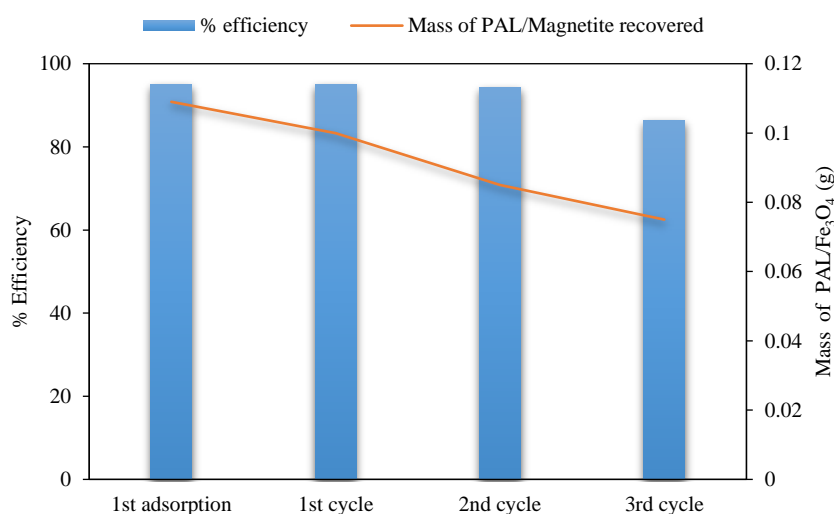


Figure 8. Reusability of PAL/Fe₃O₄ composite in the adsorption of MV6B dye

The adsorption capacity of PAL/Fe₃O₄ experienced a minimal decline between the first and second adsorption cycles. However, by the third cycle, the percent removal decreased to 86.53%, due to weight loss of the adsorbent during recovery and the potential saturation of adsorption sites owing to prior adsorption processes. As PAL is modified by Fe₃O₄, it can be recovered by magnetic substances after adsorption and has good reuse performance. Similarly, the study of [Canbaz \(2023\)](#), highlights the potential of magnetite-containing adsorbents as reusable and environmentally friendly alternatives in wastewater treatment. The results align with the Freundlich model, which predicts efficient dye uptake without a significant desorption process. The Freundlich model suggests multilayer adsorption, which could explain the absence of desorption. Thus, PAL/Fe₃O₄ exhibits

impressive reusability while retaining its adsorption capacity, making it a practical and cost-effective option for wastewater treatment.

[Figure 9](#) displays the UV-visible analysis of the MV6B solution before and after adsorption, providing insights into the repeatability of the process. Following the adsorption process, reduction in the intensity of the 592 nm peak is evident, signifying a decrease in the concentration of MV6B within the solution. There is no significant shift in the position of the absorption peak, which suggests that there was no substantial degradation of MV6B during the adsorption process.

The MV6B after adsorption was also analyzed using Shimadzu IRTracer-100 FTIR to ensure the absence of secondary pollution including phenol, result was shown in [Figure 10](#).

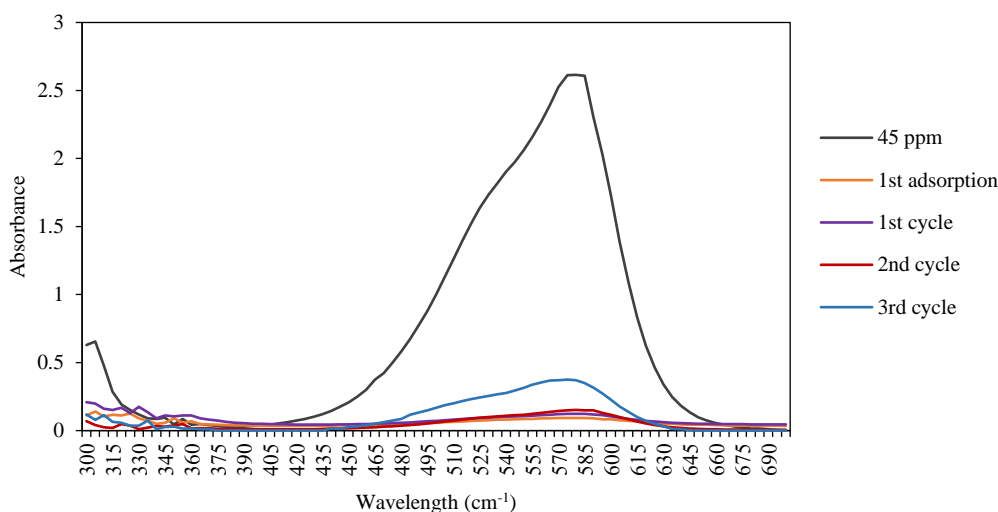


Figure 9. UV-visible spectrum of MV6B after several adsorptions at 592 nm

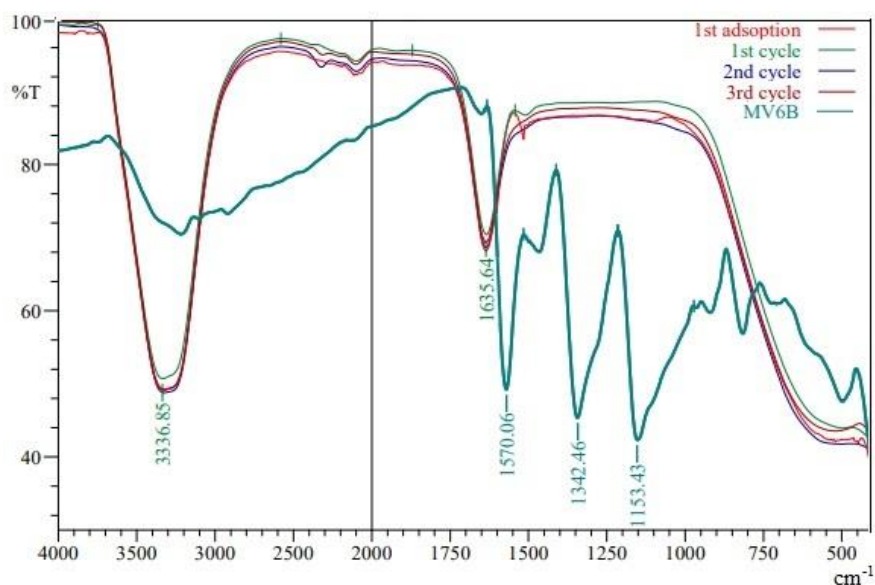


Figure 10. FTIR spectra of MV6B after adsorption using PAL/Fe₃O₄

The IR peaks indicated the presence of water. The peaks around $3,400\text{ cm}^{-1}$ indicates strong absorption due to the stretching of the O-H bonds in water molecules. The peaks that appears around $1,600\text{-}1,700\text{ cm}^{-1}$ corresponds to the bending motion of the water molecule. No bending vibration of C-H bonds in the aromatic ring appeared at $1,300\text{-}1,500\text{ cm}^{-1}$, indicating the absence of phenol.

3.7 Comparison of adsorption capacities of various adsorbents for the removal of MV dye

Table 4. Comparison of adsorption capacities of different adsorbents for methyl violet dye exclusion

Adsorbents	Adsorption capacity (mg/g)	References
Fe ³⁺ cross-linked ternary carboxymethyl cellulose/polyaniline/TiO ₂ photocomposites	159.08	Benhalima et al. (2024)
Polypyrrole-modified biopolymers	88.5	Benhalima et al. (2023b)
Ag-NPs-loaded cellulose derived from peanut-husk agro-waste	7.0928	Aljeddani et al. (2023)
Pectin hydrogel@Fe ₃ O ₄ -bentonite	909.091	Beigi et al. (2023)
Cationic ion exchange resin Amberlite®IRC-50	10.0	Bensalah et al. (2023)
Bio-adsorbent from date seeds	59.5	Ali et al. (2022)
Coconut husk powder	454.54	Sultana et al. (2022)
Microporous coconut shell activated carbon	320.5	Kamdod and Kumar (2022)
Egg shell	25.73	Khadam et al. (2022)
Mesoporous aluminosilica monoliths	554.85	Al-Hazmi et al. (2022)
NaOH-activated aerva javanica leaf	315.2	AL-Shehri et al. (2021)
Activated carbon from lemon wood/Fe ₃ O ₄ magnetic nanocomposite	35.3	Foroutan et al. (2021)
Phenolated alkali lignin/magnetite composite	6.42	Present Study

4. CONCLUSION

This study demonstrates that the phenolated alkali lignin/magnetite composite is an effective adsorbent for methyl violet, exhibiting excellent adsorption capacity and reusability. This adsorbent proves to be a practical and cost-effective solution for the treatment of methyl violet-contaminated wastewater. The equilibrium removal rate of methyl violet is recorded at 95.1%, with an adsorption capacity at equilibrium of 6.42 mg/g. The adsorption of methyl violet follows a pseudo-second-order kinetic model, and the Freundlich isotherm model. This suggests that the adsorption is multilayered, and the PAL/magnetite composite contains heterogeneous adsorption sites.

ACKNOWLEDGEMENTS

The College of Science at Technological University of the Philippines deserves the authors' sincere gratitude for providing the materials for the effective completion of this study.

A comparative study of adsorbents synthesized in this study with various types of adsorbents documented in the literature for methyl violet removal is presented in [Table 4](#).

Based on the data provided in [Table 4](#), the prepared composites in this study have lower adsorptive capacity as compared with other adsorbents for methyl violet dye exclusion. This discovery emphasizes the need for more research to optimize the present composites' adsorption capacities to increase their efficacy in dye removal applications.

REFERENCES

- Aljeddani G, Alghanmi R, Hamouda R. Study on the isotherms, kinetics, and thermodynamics of adsorption of crystal violet dye using Ag-NPs-loaded cellulose derived from peanut-husk agro-waste. *Polymers* 2023;15(22):Article No. 4394.
- Al-Hazmi G, Akhdhar A, Shahat A, Elwakeel K. Adsorption of Gentian violet dye onto mesoporous aluminosilica monoliths: Nanoarchitectonics and application to industrial wastewater. *International Journal of Environmental Analytical Chemistry* 2022. DOI: <https://doi.org/10.1080/03067319.2022.2104641>.
- Ali N, Jabbar N, Alardhi S, Majdi H, Albayati T. Adsorption of methyl violet dye onto a prepared bio-adsorbent from date seeds: Isotherm, kinetics, and thermodynamics studies. *Heliyon* 2022;8(8):Article No. 10276.
- AL-Shehri H, Almudaifer E, Alorabi A, Alanazi H, Alkorbi A, Alharthi F. Effective adsorption of crystal violet from aqueous solutions with effective adsorbent: Equilibrium, mechanism studies and modeling analysis. *Environmental Pollutants and Bioavailability* 2021;33(1):214-26.
- Ayawei N, Angaye S, Wankasi D, Dikio E. Synthesis, characterization and application of Mg/Al layered double hydroxide for the degradation of congo red in aqueous solution. *Open Journal of Physical Chemistry* 2015;5(3):56-70.

- Ayawei N, Ebelegi A, Wankasi D. Modelling and interpretation of adsorption isotherms. *Journal of Chemistry* 2017;2017:Article No. 3039817.
- Beigi P, Ganjali F, Hassanzadeh-Afrouzi F, Salehi M, Maleki A. Enhancement of adsorption efficiency of crystal violet and chlorpyrifos onto pectin hydrogel@Fe₃O₄-bentonite as a versatile nanoadsorbent. *Scientific Reports* 2023;13:Article No. 10764.
- Benhalima T, Ferfera-Harrar H. Eco-friendly porous carboxymethyl cellulose/dextran sulfate composite beads as reusable and efficient adsorbents of cationic dye methylene blue. *International Journal of Biological Macromolecules* 2019;132:126-41.
- Benhalima T, Ferfera-Harrar H, Lerari D. Optimization of carboxymethyl cellulose hydrogels beads generated by an anionic surfactant micelle templating for cationic dye uptake: Swelling, sorption and reusability studies. *International Journal of Biological Macromolecules* 2017;105(1):1025-42.
- Benhalima T, Ferfera-Harrar H, Saha N, Saha P. Fe₃O₄ imbuing carboxymethyl cellulose/dextran sulfate nanocomposite hydrogel beads: An effective adsorbent for methylene blue dye pollutant. *Journal of Macromolecular Science, Part A* 2023a;60(6):442-61.
- Benhalima T, Chicha W, Ferfera-Harrar H. Sponge-like biodegradable polypyrrole-modified biopolymers for selective adsorption of basic red 46 and crystal violet dyes from single and binary component systems. *International Journal of Biological Macromolecules* 2023b;253(8):Article No. 127532.
- Benhalima T, Mokhtari M, Ferfera-Harrar H. Synergistic adsorption/photodegradation effect for effective removal of crystal violet dye and acetamiprid pesticide using Fe³⁺ cross-linked ternary carboxymethyl cellulose/polyaniline/TiO₂ photocomposites. *Journal of Water Process Engineering* 2024;57:Article No. 104670.
- Bensalah J. Removal of the textile dyes by a resin adsorbent polymeric: Insight into optimization, kinetics and isotherms adsorption phenomenally. *Inorganic Chemistry Communications* 2024;161:Article No. 111975.
- Bensalah B, Idrissi A, Faydy M, Doumane G, Staoui A, Hsissou R, et al. Investigation of the cationic resin as a potential adsorbent to remove MR and CV dyes: Kinetic, equilibrium isotherms studies and DFT calculations. *Journal of Molecular Structure* 2023;1278:Article No. 134849.
- Canbaz G. Fe₃O₄@Granite: A novel magnetic adsorbent for dye adsorption. *Processes* 2023;11(9):Article No. 2681.
- Casas N, Parella T, Vicent T, Caminal G, Sarrà M. Metabolites from the biodegradation of triphenylmethane dyes by *Trametes versicolor* or laccase. *Chemosphere* 2009; 75(10):1344-9.
- Chaudhari A. Nitrobenzene oxidation for isolation of value added products from industrial waste lignin. *Journal of Chemical, Biological and Physical Sciences* 2016;6(63):501-13.
- Chen J, Chen H. Removal of anionic dyes from an aqueous solution by a magnetic cationic adsorbent modified with DMDAAC. *New Journal of Chemistry* 2018;42:7262-71.
- Chiban M, Soudani A, Sinan F, Persin M. Single, binary and multi-component adsorption of some anions and heavy metals on environmentally friendly *Carpobrotus edulis* plant. *Colloids Surf B Biointerfaces* 2011;82(2):267-76.
- Fang L, Wu H, Shi Y, Tao Y, Yong Q. Preparation of lignin-based magnetic adsorbent from kraft lignin for adsorbing the congo red. *Frontiers in Bioengineering and Biotechnology* 2021;9:Article No. 691528.
- Foroutan R, Mohammadi R, Farjadfar S, Esmaeili H, Ramavandi B, Sorial G. Eggshell nano-particle potential for methyl violet and mercury ion removal: Surface study and field application. *Advanced Powder Technology* 2019;30(10):2188-99.
- Foroutan R, Peighambari S, Peighambari S, Pateiro M, Lorenzo J. Adsorption of crystal violet dye using activated carbon of lemon wood and activated carbon/Fe₃O₄ magnetic nanocomposite from Aqueous Solutions: A kinetic, equilibrium and thermodynamic study. *Molecules* 2021; 26(8):Article No. 2241.
- Kamdod A, Kumar M. Adsorption of methylene blue, methyl orange, and crystal violet on microporous coconut shell activated carbon and its composite with chitosan: Isotherms and kinetics. *Journal of Polymers and the Environment* 2022;30:5274-89.
- Khadam S, Javed T, Jilani M. Adsorptive exclusion of crystal violet dye from wastewater using eggshells: Kinetic and thermodynamic study. *Desalination and Water Treatment* 2022;268:99-112.
- Liu G, Liao L, Dai Z, Qi Q, Wu J, Ma L, et al. Organic adsorbents modified with citric acid and Fe₃O₄ enhance the removal of Cd and Pb in contaminated solutions. *Chemical Engineering Journal* 2020;39:Article No. 125108.
- Liu L, Luo X, Ding L, Luo S. Application of nanotechnology in the removal of heavy metal from water. In: Liu L, Luo X, Ding L, Luo S, Deng F, editors. *Nanomaterials for Nanomaterials for the Removal of Pollutants and Resource Reutilization*. Elsevier; 2019. p. 83-147.
- Meng X, Scheidemantle B, Li M, Wang Y, Zhao X, Toro-González M, et al. Synthesis, characterization, and utilization of a lignin-based adsorbent for effective removal of azo dye from aqueous solution. *ACS Omega* 2020;5(6):2865-77.
- Panamgama A, Peramune P. Coconut coir pith lignin: A physicochemical and thermal characterization. *International Journal of Biological Macromolecules* 2018;113:1149-57.
- Ringot D, Lerzy B, Chaplain K, Bonhoure J, Auclair E, Larondelle Y. In vitro biosorption of ochratoxin A on the yeast industry by-products: Comparison of isotherm models. *Bioresource Technology* 2007;98(9):1812-21.
- Saini R. Textile organic dyes: Polluting effects and elimination methods from textile waste water. *International Journal of Chemical Engineering Research* 2017;9(1):121-36.
- Sharma J, Sharma S, Soni V. Classification and impact of synthetic textile dyes on Aquatic Flora: A review. *Regional Studies in Marine Science* 2021;45:Article No. 101802.
- Sultana S, Islam K, Hasan M, Khan H, Khan M, Deb A, et al. Adsorption of crystal violet dye by coconut husk powder: Isotherm, kinetics and thermodynamics perspectives. *Environmental Nanotechnology, Monitoring and Management* 2022;17:Article No. 100651.
- Taleb F, Ammar M, Mosbah M, Salem R, Moussaoui Y. Chemical modification of lignin derived from spent coffee grounds for methylene blue adsorption. *Scientific Reports* 2020;10:Article No. 11048.
- Touihri M, Guesmi F, Hannachi C, Hamrouni B, Sellaoui L, Badawi M, et al. Single and simultaneous adsorption of Cr (VI) and Cu (II) on a novel Fe₃O₄/pine cones gel beads nanocomposite: Experiments, characterization and isotherms modeling. *Chemical Engineering Journal* 2021;416:Article No. 129101.

- Wang T, Jiang M, Yu X, Niu N, Chen L. Application of lignin adsorbent in wastewater Treatment: A review. *Separation and Purification Technology* 2022;302:Article No. 122116.
- You X, Zhou R, Zhu Y, Bu D, Cheng D. Adsorption of dyes methyl violet and malachite green from aqueous solution on multi-step modified rice husk powder in single and binary systems: Characterization, adsorption behavior and physical interpretations. *Journal of Hazardous Materials* 2022; 430:Article No. 128445.
- Younesi-Kordkheili H, Pizzi A. A Comparison among lignin modification methods on the properties of lignin-phenol-formaldehyde resin as wood adhesive. *Polymers* 2021; 13(20):Article No. 3502.

Demography, Structure, and Composition of a Low-Disturbance Forest in Luzon, Philippines

Jeri E. Latorre^{1*}, John Michael M. Galindon², Nestor A. Bartolome Jr.³, Melizar V. Duya¹,
and Lillian Jennifer V. Rodriguez¹

¹Institute of Biology, University of the Philippines Diliman, Quezon City 1101, Philippines

²National Grid Corporation of the Philippines, Quezon City 1101, Philippines

³First Gen Hydro Power Corporation, Ortigas Avenue, Pasig City 1604, Philippines

ARTICLE INFO

Received: 5 Sep 2023
Received in revised: 10 Apr 2024
Accepted: 7 May 2024
Published online: 21 May 2024
DOI: 10.32526/ennrj/22/20230235

Keywords:

Forest dynamics/ Tree size/ Tree recruitment/ Tree mortality/ Tree growth/ Forest restoration

* Corresponding author:

E-mail: lvrodriguez@up.edu.ph

ABSTRACT

Tropical forests continue to face deforestation in countries such as the Philippines. To look at the long-term behavior of forests in response to intrinsic and extrinsic factors, continual monitoring of forest dynamics is needed. To do this, we established a 2-ha permanent tropical forest plot in a low-disturbance area in Maluyon, Philippines. We addressed three main questions: 1) How does the plot change through time? 2) How do different species in the plot change through time? 3) Would the responses differ by tree size? We measured, mapped, and identified all trees ≥ 1 cm in diameter in 2011. In 2015, we re-measured surviving trees and measured, mapped, and identified recruits. A total of 177 tree species were found in the plot. The forest exhibited a mean growth rate of 0.054 cm/year, mortality rate of 0.011%/year, and recruitment rate of 0.019%/year. Overall growth and mortality rates were lower in Maluyon than in other plots, possibly due to the forest's high tree density and low disturbance. Species-specific rates revealed the presence of both the growth-survival and the stature-recruitment trade-offs. Size class analysis showed higher growth rates in large-sized than in small-sized trees. In contrast, small-sized trees exhibited a higher mortality rate compared to large-sized trees, likely due to density dependence. Key findings of the study may be utilized to increase the success rate of restoration efforts in this watershed. Using a mix of fast-growing, generalist species with high survival rates (e.g., *Allophylus cobbe* and *Anisoptera thurifera*) is highly recommended.

1. INTRODUCTION

Tropical forests are among the largest reservoirs of the world's biodiversity, supporting roughly 60% of the Earth's total species (Andresen et al., 2018; Handley, 2018). They have the highest gross primary productivity out of all the terrestrial biomes and account for one-fourth of terrestrial carbon (Beer et al., 2010; Pinmongkhonkul et al., 2023). Across different regions, forest structures vary depending on the biotic and abiotic forces they are exposed to (Davies et al., 2021). These environmental stresses impact forest growth and productivity, mortality, and species demographics (McDowell et al., 2020). As such, continual monitoring of forest dynamics provides

much-needed information on the long-term behavior of forests (Davies et al., 2021).

In the Philippines, tropical forest ecosystems have drastically reduced over time. Early reports show that, in 1934, the country had roughly 17 million hectares worth of forest vegetation (Bautista, 1990). However, from 1980 to 1987, deforestation in the Philippines averaged approximately 157,000 hectares per year, with illegal operations persisting into the 21st century (Kummer, 1992; Lopez, 2020). In addition, the Philippines ranks first worldwide for countries with the highest disaster risk index due to frequent tropical cyclones (Atwii et al., 2022). As of 2015, available forest cover had reduced to 7 million

Citation: Latorre JE, Galindon JMM, Bartolome Jr NA, Duya MV, Rodriguez LJV. Demography, structure, and composition of a low-disturbance forest in Luzon, Philippines. Environ. Nat. Resour. J. 2024;22(3):270-282. (<https://doi.org/10.32526/ennrj/22/20230235>)

hectares, constituting a sharp, 59% decrease in less than a century (Forest Management Bureau, 2018).

Combining the expanding threat of land conversion and the increase of stronger typhoons, it is predicted that these environmental stresses affecting the country's remaining forest ecosystems would only worsen over time (Yih et al., 1991). This entails the need to conduct extensive studies to examine long-term distributional patterns of Philippine tropical forests.

Despite the clear importance of tropical forests and their alarming vulnerability in the country, Philippine forests remain biologically under-surveyed to this day (Pang et al., 2021). In-depth studies of Philippine forest responses are limited, with a majority of these sites surveyed following major anthropogenic or natural disturbances. For example, regenerating forest sites were studied in Leyte Island to determine the impact of major slash-and-burn farming (known locally as *kaingin*) on forest composition and structure (Mukul et al., 2020). Another forest dynamics plot in the Philippines, the Palanan Forest Dynamics Plot in Isabela, Luzon island was monitored following its exposure to typhoons (Pasion et al., 2022; Yap et al., 2016). These studies show that major disturbances indeed pose a heavy influence on forest structure. But what happens in these forests when there are no major disturbances? Studies on Philippine forests with little to no disturbances are needed to characterize the baseline dynamics in intact rainforests. Thus, we established the Maluyon Permanent Forest Dynamics Plot, a low-disturbance plot located in Nueva Ecija, Luzon Island, Philippines. Characterized as an uneven-aged forest with mountainous terrain, the area has a monthly temperature range of 23.21°C to 31.1°C, an average annual relative humidity of 83.37%, and an annual average rainfall of 176.65 cm (Lasco et al., 2010).

Three major questions were addressed in the study: (1) How does the plot change through time?, (2) How do the populations of different species in the plot change through time?, and (3) Would the changes differ by tree size?

The study first analyzed plot-level changes in community-weighted functional traits (e.g., species abundance and basal area) and demographic rates. Secondly, the demographic rates of each species were evaluated by determining their corresponding recruitment rate, growth rate, and mortality rate during the 4-year interval between the 2011 and 2015 forest censuses. The plot's overall forest dynamics were then assessed using demographic rates per size class.

Corresponding findings from the study were used to discuss whether these demographic shifts are also manifested by forests across the globe. This opens up another emerging field of interest covered by forest dynamics, which is the generation of models for predicting forest behavior. These generalized models would be able to curate pre-determined inferences of changes in the functional composition and structure of forests in response to periodic, environmental stresses - thereby enforcing optimized interventions in response to timely environmental issues such as deforestation and climate change.

In summary, the study was able to generate (1) plot-level forest changes, (2) demographic rates for all species found in the plot, and (3) demographic changes per size class.

2. METHODOLOGY

2.1 Plot establishment and monitoring

The Maluyon Permanent Forest Dynamics Plot (MPFDP) is a 2-ha lowland tropical rainforest plot located in Mt. Maluyon of the Pantabangan-Carranglan Watershed Forest Reserve in Pantabangan, Nueva Ecija, Luzon island, Philippines (15°52'25.25"N, 121°03'32.75"E, Figure 1). The plot was established in 2011 as part of the Biodiversity Conservation and Monitoring Program of the First Gen Hydro Power Corporation. Following the ForestGEO Network's protocol (Condit, 1998), all free-standing stems ≥ 1 cm diameter at breast height (DBH) within the plot were measured, tagged, mapped, and identified to species- (or morphospecies-) level. Individuals whose complete scientific names were not known were assigned unique descriptors instead. Site mapping was conducted by dividing the plot into 20×20 m² quadrats with 5×5 m² sub-quadrats each. The corresponding x-y coordinates of each individual tree were then obtained through in situ mapping.

The MPFDP was then re-censused in 2015. All surviving stems were measured at their original points of measurement. All new stems ≥ 1 cm diameter at breast height (DBH) (termed as recruits) were measured, tagged, mapped, and identified to species- (or morphospecies-) level.

The study area has high tree endemism at 61%, among which 28% of the species were classified as rare. The presence of anthropogenic disturbances in the watershed, such as illegal logging, slash-and-burn farming, and livestock grazing - all of which were performed solely by locals - had also been previously

documented (Pabico et al., 2021). As of 2011, there have been no anecdotes or documentation that the

MPFDP has been impacted by typhoons or other natural disturbances.

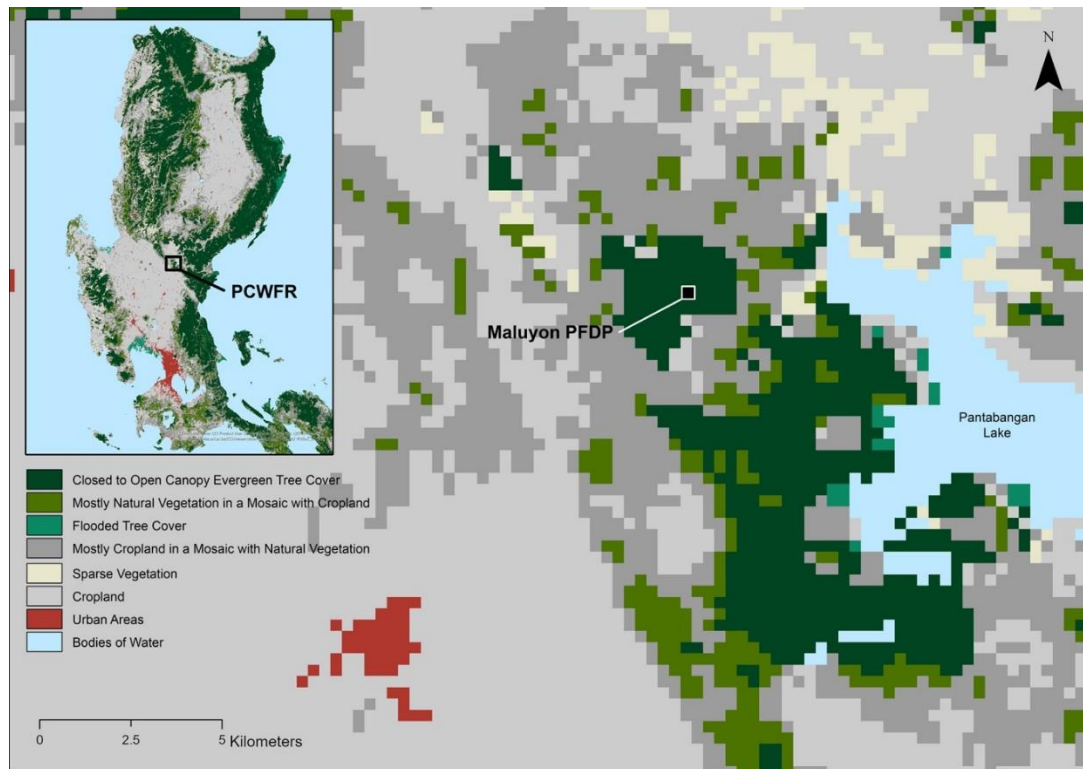


Figure 1. Location map of the Maluyon Permanent Forest Dynamics Plot (PFDP), established in 2011 inside the Pantabangan-Carranglan Watershed Forest Reserve (PCWFR), Nueva Ecija, Philippines. Inset: Luzon Island, Philippines.

2.2 Data management

Each tree individual entry logged into the database should have met the specified criteria. Only the main stem was used for data analysis because abundance, frequency, and demographic rates are based on individual tree data and also because we did not estimate aboveground biomass in this study.

Datasets were loaded into R, which served as the main software for data management and code execution (R Core Team, 2020). Tables for the 2011 and 2015 censuses were cleaned to ensure that the following data conditions were met: (1) each entry must be tagged as either alive (A), dead (D), or a recruit (“ ” in 2011, “A” in 2015) and (2) both datasets contained the same number of entries. Duplicates were further identified based on the uniqueness of each individual’s stem ID, and these were either manually deleted or tagged with a new unique stem ID.

2.3 Species abundance, basal area, and importance value

The study utilized the *fgeo* R package for data analysis and transformation (Lepore et al., 2019). Three traits were analyzed per species: 1) species

abundance, defined as the count of individuals for each unique species; 2) relative abundance, defined as the proportion of species abundance to the total number of sampled individuals; and 3) basal area, defined as the area occupied by trees at breast height.

We also computed the Importance Value Index (IVI), originally described by Curtis and McIntosh (1951) as the relative importance of a tree species within a stand. It is computed by summing up three separate values per tree species: relative frequency ((number of subplots where a species is present/50 subplots) \times 100%), relative abundance ((number of individual trees of a species/total number of individuals in the plot) \times 100%), and relative density ((total basal area of a species/total basal area in the plot) \times 100%). A tree species can have a maximum IVI value of 300 and more important species in the stand have higher IVI values (Curtis and McIntosh, 1951).

2.4 Demographic rates analysis

Forest dynamics patterns were analyzed by determining demographic rate changes in the 2-hectare MPFDP through the 4-year time interval of the two censuses. Trees were first grouped per species. The

growth, recruitment, and mortality rates were then calculated using the *fgeo* R package, whose corresponding equations for the demographic rates are as follows:

$$\text{Growth Rate} = \frac{\text{DBH}_{2015} - \text{DBH}_{2011}}{T}$$

$$\text{Mortality Rate} = \frac{\log[N_{2011}] - \log[N_S]}{T}$$

$$\text{Recruitment Rate} = \frac{\log[N_{2015}] - \log[N_S]}{T}$$

Where; DBH_{2015} =diameter at breast height measured in 2015 (in cm), DBH_{2011} =diameter at breast height measured in 2011 (in cm), T =time interval between censuses (in years), N_{2011} =total number of individual trees in 2011, N_{2015} =total number of individual trees in 2015, and N_S =total number of surviving individual trees in 2015.

To determine if tree size would affect tree response, demographic rates were also computed based on the following size class categories: (1) small ($1 \leq \text{DBH} \leq 10$ cm); (2) medium ($10 \text{ cm} < \text{DBH} \leq 20$ cm); and (3) large ($\text{DBH} > 20$ cm).

3. RESULTS

3.1 Forest composition and plot-level dynamics

Overall, a total of 177 tree species were recorded in the 2-ha Maluyon Permanent Forest Dynamics Plot (MPFDP), belonging to 91 families

and 97 genera. An initial tree community of 175 tree species was censused in 2011. However, this was reduced to 172 species by 2015. Five species from the 2011 census were not documented again in the next census (Table S1). However, two additional species were seen in 2015 (*Artocarpus blancoi* and *Canthium* sp. 1). Tree abundance increased from 10,658 tree individuals in 2011 to 10,686 recorded individuals in 2015 (accounting for 572 recruits and 544 tree deaths). The increase in tree abundance also led to an increase in tree density (Table 1). Tree density increased from 4,824 individuals per hectare in 2011 to 5,343 individuals per hectare in 2015.

The most abundant species in the plot were similar in 2011 and 2015 (Table S2). Species-specific basal areas also showed little change in both census years (Tables S3 and S4). *Camellia lanceolata* (Theaceae) was the most dominant tree species constituting 18.95% of all individuals in the initial census, and having the highest IVI (Table 2). Despite being only half as abundant as *C. lanceolata*, *Mangifera monandra* had the highest basal area totaling 29.82% of the basal area of the whole plot, and the second-highest IVI (Table 2).

Trees inside the plot showed an overall mean growth rate of 0.054 cm/year, a mean mortality rate of 0.011%/year, and a mean recruitment rate of 0.019%/year (Table 1).

Table 1. Forest demography in the Maluyon Permanent Forest Dynamics Plot

Census year	Tree density (individuals/ha)	Growth (cm/year)	Mortality (%/year)	Recruitment (%/year)
2011	4,824	0.054	0.011	0.019
2015	5,343			

3.2 Species-level demography

Demographic rates varied across species. A species from the genus *Aglaia* exhibited the highest increase in girth, with a growth rate of 0.650 ± 2.69 cm/year (Table 3). Five other species grew at least 0.2 cm/year (Table 3; *Elaeocarpus* sp. 01, *Lithocarpus* sp. 04, *Syzygium* sp. 10, *Ficus* sp., and *Palaquium heterosepalum*). On the other side of the growth spectrum, many species had no growth. Of the species that were represented by more than one individual, five species, *Ardisia philippinesis* (n=25), *Artocarpus* sp. 02, *Celtis luzonica*, *Leucosyke capitellata*, and

Mitrephora sp. 02 did not grow in diameter during the 4-year study period (Table 4).

The annualized mean mortality rate in the plot was low. Among species, an unidentified species had the highest mortality rate was 0.173%/year (Confidence Interval (CI): 0.025-0.590%/year) (Table 5). This was followed by *Claoxylon* sp. and *Calophyllum soulattri*, *Ficus congesta*, and *Sterculia ceramica* with a mean mortality rate of 0.101%/year. It was further observed that a total of 96 species had a mortality rate of 0 (Table S6). Among these, 81 species had populations of ≤ 10 individuals.

Table 2. Most abundant species in the Maluyon Permanent Forest Dynamics Plot in 2011. Species included in this table are those with more than 100 individuals/ha. DBH stands for diameter at breast height.

Species	Family	Relative abundance (%)	Basal area (cm ²)	Density (individuals/ha)	Maximum DBH (cm)	Mean DBH (cm)	Importance value index (IVI)
<i>Camellia lanceolata</i>	Theaceae	18.95%	33,900	1,010	18.4	3.91	20.99
<i>Mangifera monandra</i>	Anacardiaceae	9.00	230,600	480	65.6	11.77	11.30
<i>Cinnamomum mercadoi</i>	Lauraceae	7.89	40,600	421	30.2	5.81	9.94
<i>Allophylus cobbe</i>	Sapindaceae	3.70	46,500	197	54.3	7.65	5.60
<i>Garcinia rubra</i>	Clusiaceae	3.54	3,080	189	10.6	2.68	5.54
<i>Anisoptera thurifera</i>	Dipterocarpaceae	3.26	48,700	174	81.9	8.42	5.32
<i>Syzygium</i> sp. 02	Myrtaceae	2.77	47,800	148	34.6	11.00	4.07
<i>Atalantia racemosa</i>	Rutaceae	2.64	3,170	141	12.2	3.14	4.52
<i>Syzygium</i> sp. 01	Myrtaceae	2.24	10,900	120	31.5	5.48	3.13
<i>Palaquium bataanense</i>	Sapotaceae	2.19	13,300	117	40.7	6.13	4.12
<i>Memecylon sorsogonense</i>	Melastomataceae	2.15	670	115	5.2	1.81	4.15
<i>Aporosa symplocifolia</i>	Phyllanthaceae	1.93	5,920	103	14.2	5.18	3.46
Other species (n=163)		39.74	76,835.060	5,490			

As to recruitment rate, a species of *Celastrus* exhibited the highest annualized mean rate (0.275%/year, CI: 0.054-0.674%/year), followed by *Garcinia* sp. 03, *Aglaiia elliptica*, *Artocarpus* sp., *Heritiera sylvatica*, *Dysoxylum excelsum*, *Garcinia* sp. 04, and *Leucosyke capitellata* (Table 6). On the other hand, a total of 88 species in the plot had a recruitment rate of 0%/year (Table S7).

3.3 Variation in demographic rates according to size class

Large-sized trees had the highest growth rates (0.154±0.023 cm/year), followed by medium-sized (0.079±0.008 cm/year), and then small-sized trees (0.035±0.003 cm/year) (Figure 2). In terms of mortality, small-sized trees in the plot had the highest mortality rate among the size classes (0.014%/year), followed by medium-sized (0.009%/year) and large-sized trees (0.005%/year). The mortality rate of small-sized trees was significantly different from the other two. The annualized mean recruitment rate inside the plot was 0%/year for all size classes.

Table 3. Tree species with the highest growth rates in the Maluyon Permanent Forest Dynamics Plot. N=number of individual trees

Rank	Species	N	Rate (cm/year) ±95% confidence interval
1	<i>Aglaiia</i> sp. 05	2	0.650±2.69
2	<i>Elaeocarpus</i> sp. 01	4	0.538±0.485
3	<i>Lithocarpus</i> sp. 04	10	0.373±0.235
4	<i>Syzygium</i> sp. 10	1	0.250
5	<i>Ficus</i> sp.	2	0.21±0.91
6	<i>Palaquium heterosepalum</i>	4	0.2±0.3
7	<i>Syzygium densinervium</i>	73	0.177±0.259
8	<i>Artocarpus ovatus</i>	1	0.175
9	<i>Ficus</i> sp. 05	1	0.175
10	<i>Chionanthus</i> sp. 01	4	0.156±0.203
11	<i>Artocarpus</i> sp.	1	0.150
12	<i>Astronia williamsii</i>	12	0.14±0.11
13	<i>Terminalia macrantha</i>	62	0.14±0.061
14	<i>Radermachera pinnata</i>	5	0.14±0.20
15	<i>Allophylus cobbe</i>	381	0.13±0.017
16	<i>Elaeocarpus</i> sp.	41	0.112±0.101
17	<i>Actinodaphne ramosii</i>	25	0.111±0.063
18	<i>Shorea guiso</i>	44	0.11±0.05
19	<i>Ficus variegata</i>	3	0.108±0.345
20	<i>Maranthes corymbosa</i>	69	0.108±0.039

Table 4. Tree species with the lowest growth rates in the Maluyon Permanent Forest Dynamics Plot. Species with 0% mortality rates are indicated with an (*).

Rank	Species	N	Rate (cm/year) ±95% confidence interval
1	<i>Aglaiia</i> sp. 03*	1	0
2	<i>Alstonia scholaris</i> *	1	0
3	<i>Artocarpus</i> sp. 02*	2	0
4	<i>Celastrus</i> sp. 02*	1	0
5	<i>Celtis luzonica</i> *	2	0
6	<i>Dysoxylum</i> sp. 04*	1	0
7	<i>Monoon</i> cf. <i>klemmei</i>	6	0±0.088
8	<i>Ficus congesta</i>	1	0
9	<i>Ficus carpenteriana</i> *	1	0
10	<i>Leucosyke capitellata</i> *	2	0
11	<i>Melicope</i> sp. 01*	1	0
12	<i>Mitrephora</i> sp. 02	4	0

Table 4. Tree species with the lowest growth rates in the Maluyon Permanent Forest Dynamics Plot. Species with 0% mortality rates are indicated with an (*) (cont.).

Rank	Species	N	Rate (cm/year) \pm 95% confidence interval
13	<i>Palaquium</i> cf. <i>lanceolatum</i> *	1	0 \pm 0.186
14	<i>Ardisia philippinensis</i>	25	0
15	<i>Glochidion luzonense</i>	17	0.004 \pm 0.028
16	<i>Symplocos</i> sp. 03	22	0.004 \pm 0.013
17	<i>Clausena anisum-olens</i>	4	0.005 \pm 0.008
18	<i>Antidesma</i> sp.	11	0.006 \pm 0.017
19	<i>Glycosmis</i> cf. <i>parviflora</i>	18	0.007 \pm 0.015
20	<i>Ficus pseudopalma</i> *	3	0.007 \pm 0.031

Table 5. Tree species with the highest mortality rates in the Maluyon Permanent Forest Dynamics Plot. N=number of individual trees; D=number of deaths

Rank	Species	N ₂₀₁₁	D ₂₀₁₅	Annualized mean Rate (%/year)	Confidence interval	
					Lower	Upper
1	Unidentified species 09	2	1	0.173	0.025	0.590
2	<i>Claoxylon</i> sp.	12	4	0.101	0.037	0.238
3	<i>Calophyllum soulattri</i>	3	1	0.101	0.017	0.410
4	<i>Ficus congesta</i>	3	1	0.101	0.017	0.410
5	<i>Sterculia ceramica</i>	3	1	0.101	0.017	0.410
6	<i>Memecylon lanceolatum</i>	12	3	0.072	0.024	0.193
7	<i>Shorea astylosa</i>	9	2	0.063	0.017	0.203
8	<i>Mitrephora</i> sp. 02	5	1	0.056	0.011	0.256
9	<i>Ardisia pyramidalis</i>	128	24	0.052	0.035	0.077
10	<i>Dysoxylum</i> sp. 02	6	1	0.046	0.009	0.216
11	<i>Guioa discolor</i>	64	10	0.042	0.023	0.077
12	<i>Syzygium</i> sp. 02	295	43	0.039	0.029	0.053
13	<i>Glycosmis</i> cf. <i>parviflora</i>	21	3	0.039	0.013	0.107
14	<i>Microcos stylocarpa</i>	7	1	0.039	0.008	0.187
15	<i>Prunus marsupialis</i>	14	2	0.039	0.011	0.130
16	<i>Calophyllum</i> sp.	159	22	0.037	0.025	0.056
17	<i>Aglaia edulis</i>	23	3	0.035	0.012	0.098
18	<i>Archidendron clypearia</i>	55	7	0.034	0.016	0.069
19	<i>Lithocarpus</i> cf. <i>philippinensis</i>	119	14	0.031	0.019	0.052
20	<i>Lithocarpus</i> sp.	34	4	0.031	0.012	0.078

Table 6. Tree species with the highest recruitment rates in the Maluyon Permanent Forest Dynamics Plot. N=number of individual trees; R=number of recruits

Rank	Species	N ₂₀₁₅	R ₂₀₁₅	Annualized Mean Rate (%/year)	Confidence Interval	
					Lower	Upper
1	<i>Celastrus</i> sp. 02	3	2	0.275	0.054	0.674
2	<i>Garcinia</i> sp. 03	5	3	0.229	0.063	0.534
3	<i>Aglaia elliptica</i>	2	1	0.173	0.025	0.590
4	<i>Artocarpus</i> sp.	2	1	0.173	0.025	0.590
5	<i>Heritiera sylvatica</i>	2	1	0.173	0.025	0.590
6	<i>Dysoxylum excelsum</i>	2	1	0.173	0.025	0.590
7	<i>Garcinia</i> sp. 04	2	1	0.173	0.025	0.590
8	<i>Leucosyke capitellata</i>	4	2	0.173	0.040	0.480
9	<i>Calophyllum soulattri</i>	3	1	0.101	0.017	0.410

Table 6. Tree species with the highest recruitment rates in the Maluyon Permanent Forest Dynamics Plot. N=number of individual trees; R=number of recruits (cont.)

Rank	Species	N ₂₀₁₅	R ₂₀₁₅	Annualized mean rate (%/year)	Confidence interval	
					Lower	Upper
10	<i>Croton</i> sp. 01	3	1	0.101	0.017	0.410
11	<i>Elaeocarpus</i> sp. 01	6	2	0.101	0.026	0.309
12	<i>Calophyllum blancoi</i>	7	2	0.084	0.022	0.263
13	<i>Symplocos</i> sp. 03	30	8	0.078	0.038	0.148
14	<i>Mitrephora</i> sp. 02	5	1	0.056	0.011	0.256
15	<i>Champeria manillana</i>	61	12	0.055	0.031	0.094
16	<i>Chionanthus</i> sp. 02	11	2	0.050	0.014	0.165
17	<i>Memecylon lanceolatum</i>	11	2	0.050	0.014	0.165
18	<i>Tarrenoidea wallichii</i>	6	1	0.046	0.009	0.216
19	<i>Psychotria</i> sp. 01	32	5	0.042	0.018	0.096
20	<i>Sterculia comosa</i>	27	4	0.040	0.016	0.099

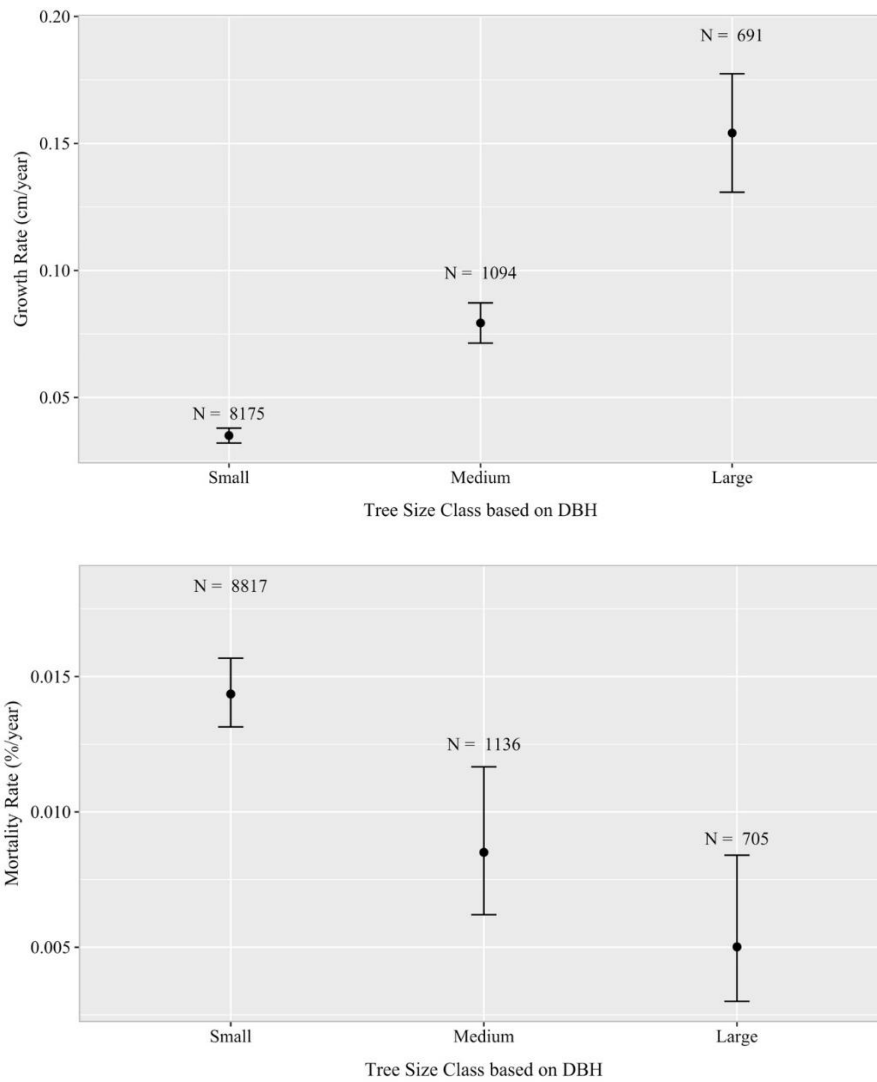


Figure 2. Demographic rates of tree individuals in the Maluyon Permanent Forest Dynamics Plot grouped per size class.

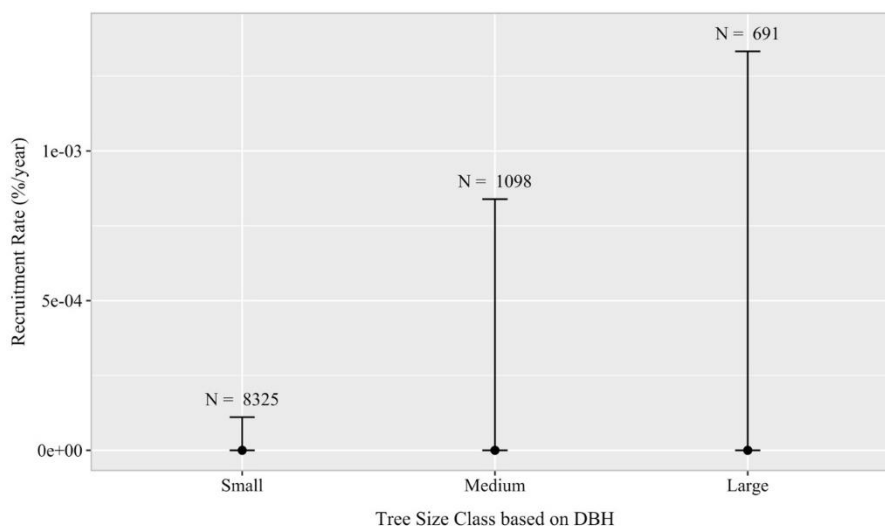


Figure 2. Demographic rates of tree individuals in the Maluyon Permanent Forest Dynamics Plot grouped per size class (cont.).

4. DISCUSSION

Forest dynamics provide a crucial understanding of how ecosystems behave with the changing climate. The response of forest communities to external and interspecific pressures provides vital knowledge on forest resiliency and possible adaptations amid these disturbances (Thompson et al., 2009). Here, a detailed discussion on the changes in plot-, species-, and stature-level responses in the Maluyon Permanent Forest Dynamics Plot (MPFDP) over 4 years is presented.

4.1 Plot-level demography

Forest dynamics is primarily described using three demographic rates: growth, mortality, and recruitment rates. Growth in the Maluyon plot was observed to be much slower in comparison to that of typhoon-prone forests. The Luquillo Plot in Puerto Rico and the Fushan Plot in Taiwan, for example, both exhibited growth rates greater than 0.10 cm/year (Hogan et al., 2018). This was also the case for the Palanan Plot in the Philippines, which exhibited even higher growth rates (0.117-0.164 cm/year) (Hogan et al., 2018). These rates are more than twice the average growth rate in Maluyon (Table 1). Across existing permanent forest plots, the Maluyon growth rate was instead closest to that of the Barro Colorado Island (BCI) forest in Panama during some census intervals, where the BCI forest exhibited growth rates of 0.025-0.080 cm/year (Hogan et al., 2018). Like the Maluyon Plot, the BCI forest is a tropical forest with no recorded strong tropical cyclones directly affecting it. Apart from the lack of tropical cyclones in the Maluyon area, the slower growth may be associated

with increased competition brought about by higher tree density. Across different tropical forests, tree growth was negatively affected by neighborhood crowding (Rozenaal et al., 2020). In 2015, tree density in the Maluyon Plot was 5,343 trees per hectare, whereas Palanan tree density in 2010 was 4,708 trees per hectare (Yap et al., 2016). Maluyon's tree density is also higher than that of the Luquillo Plot in 2016, which was 1,857 trees per hectare (Zimmerman, 2020). Higher tree density may lead to higher competition for resources in the Maluyon Plot, which may have led to its relatively slow growth rate.

As to mortality rate, the Maluyon Plot had a lower mean rate (0.011%/year) compared to the Palanan Plot ($2.05 \pm 0.03\%$ /year) (Yap et al., 2016; Hogan et al., 2018). Mortality rate in Maluyon was lower than that of other forests as well, such as the Kolombangara forest in the Solomon Islands (1.4-2.2%/year) and the CTFS-ForestGEO large forest dynamics plot in Virginia, USA (1.4-2.1%/year) (Gonzalez-Akre et al., 2016). This lower mortality in the Maluyon Plot in contrast to that of other forests may also be due to the lack of disturbances (Hogan et al., 2018). Lastly, recruitment rate in the Maluyon Plot (0.019%/year) was similar to the recruitment rates of other Asia-based plots during typhoon-free intervals. Particularly, recruitment rate was most similar to the Luquillo Plot (0.014-0.092%/year) and the Palanan Plot (0.016%/year) in periods where no typhoons were observed.

Overall, the presence of periodic, high-intensity forest disturbances seems to play a significant role in driving demographic rates among these forests. Moreover, similarities in climate seasonality,

biogeography, and geology may have a less significant role in shaping forest dynamics (Russo et al., 2021). This is clearly illustrated in the Maluyon and Palanan Plots, which are both located in Luzon Island, Philippines. The growth rate in Palanan is more than twice that of Maluyon, but their mortality and recruitment rates are similar during Palanan's non-typhoon interval. Nonetheless, there remains much opportunity to further investigate the broad set of factors that contribute to tree growth and survival, such as microclimate variations, functional trait shifts, and interspecific interactions (Monoy et al., 2016; De Frenne et al., 2021; Detto et al., 2022).

4.2 Species-level demography

Globally, tropical forest communities are largely structured according to two demographic trade-offs: (1) the growth-survival trade-off and (2) the stature-recruitment trade-off (Rüger et al., 2020; Russo et al., 2021; Kambach et al., 2022). These trade-offs postulate that plants can allocate their limited resources to (1) either fast growth or long survival and (2) either tall stature or increased recruitment. Combining these two trade-offs, Rüger et al. (2020) categorized species into five functional groups: Slow, Fast, Long-lived pioneer, Short-lived breeder, and Intermediate. Given the resulting species-specific demographic rates, these two trade-offs were evident in the Maluyon Plot.

At the extreme end of the growth-survival spectrum, there are "Slow" species in the Maluyon Plot that have the lowest growth rates and the highest survival rates (i.e., 0% mortality) (Tables 4 and S6). Eleven out of the 20 species in Table 4 have 0% mortality. These include *Ficus pseudopalma*, *Palaquium* cf. *lanceolatum*, *Leucosyke capitellata*, and *Celtis luzonica*. Three species in the Maluyon Plot are at the other end of this growth-survival spectrum. These are the "Fast" growers, with the highest mortality rates: *Archidendron clyperia* (growth rate: 0.078 cm/year, rank 18th in mortality), *Guoia discolor* (growth rate: 0.077 cm/year, rank 11th in mortality), and *Shorea astylosa* (growth rate: 0.071 cm/year, rank 7th in mortality).

Short-lived breeders are also well-represented in the Maluyon Plot. These are the species that attain low tree stature but compensate with high levels of recruitment (Rüger et al., 2020). Three species best represent this group in the plot: *Camellia lanceolata*, *Celastrus* sp. 02, and *Garcinia* sp. 03. The most abundant tree in the plot is *C. lanceolata* and it had an

additional 96 recruits in 2015. However, it only has a mid-range tree stature (maximum DBH: 18.40 cm). Its abundance is possibly linked to its ability to fruit and flower in the Philippines almost all year round (Galindon, pers. obs.). *Celastrus* sp. 02 had the highest recruitment rate but one of the lowest maximum DBH (1.7 cm). Similarly, *Garcinia* sp. 03 had the second-highest recruitment rate but one of the lowest maximum DBH (2.0 cm).

Like in the Maluyon Plot, the growth-survival and stature-recruitment trade-offs are also observed in the Palanan Plot, despite it being a disturbance-prone forest (Russo et al., 2021; Kambach et al., 2022). The establishment and monitoring of additional plots in other Philippine islands will give us a further understanding of the generality of these trade-offs in shaping Philippine forest diversity.

4.3 Variation in demographic rates according to size class

It was demonstrated that as tree size increased, growth rates increased, while mortality rates decreased. This pattern was also the case for the Mudumalai forest in India, where large-sized trees had the lowest mortality rates and small-sized trees exhibited the highest growth rates (Sukumar et al., 2004). Mortality rates across forests are said to be density-dependent, and further driven by the direct and indirect effects of anthropogenic perturbations (Lutz et al., 2014; Anderson-Teixeira et al., 2015). We see this in the MPFDP where small-sized trees had the highest size class population and the highest mortality rate. Conversely, large-sized trees had the lowest size class population, which may explain why they exhibited lower mortality.

Recruitment rate inside the plot was observed to be 0%/year for all size classes, thus suggesting a slow recruitment rate for the entire area. Particularly, small-sized trees had the lowest recruitment rate of the three size classes. This may be attributed to the overshadowing of tall, mature trees with large canopies, therefore limiting the availability of light for growth (Coomes and Allen, 2007).

4.4 Implications to forest conservation and restoration

The Maluyon Plot is an integral part of the Pantabangan-Caranglan Watershed Forest Reserve. It is an important conservation area because threatened forest species, such as *Shorea contorta* (Dipterocarpaceae) and *Palaquium батаанense*

(Sapotaceae), which are both included in the IUCN Red List of Threatened Species, are abundant inside the plot.

The extensive data from the plot can also be used to craft science-based forest restoration efforts because it is important to look into species characteristics, such as their survival rate and distribution, to evaluate their effectiveness in forest rehabilitation (Marod et al., 2022). Species to be selected for restoration programs should be native, representative of the flora in the area, and able to accelerate ecological succession (Elliott et al., 2022). Based on our data, the use of a mix of fast-growing, generalist species with high survival rates may be best suited for increasing the success rate of restoration of the denuded areas in the Pantabangan-Carranglan Watershed. Prospective candidates include *Camellia lanceolata*, *Mangifera monandra*, *Allophylus cobbe*, *Anisoptera thurifera*, and *Syzygium* sp. 01- all of which exhibited high abundance and growth in the MPFDP as seen in their respective spatial distribution maps (Figure 3). *Camellia lanceolata*, *A. thurifera*,

and *M. monandra* are seen to be well-distributed throughout the plot. On the other hand, *A. cobbe* and *Syzygium* sp. 01 are only concentrated in specific regions of the forest plot, which may suggest more specific conditions for these species to survive. All of these species rank among the top 20 most abundant tree species in the plot. The IVI of these trees are also among the highest of all recorded tree species, indicating their ecological importance and dominance within the plot. Notably, a study on forest management highlights that IVI is a valuable tool in prioritizing species for conservation (Yilma et al., 2021). These recommended native species are thus promising candidates for restoration efforts in the country. Apart from their high growth rates and IVI, these species were also observed to have high basal areas and are thus efficient carbon sinks. Their high carbon sequestration rates may be used to combat climate change. Lastly, *M. monandra*, *A. cobbe*, and *Syzygium* sp. 01 bear fleshy fruits that can attract frugivores and greatly contribute to facilitating the natural regeneration of the watershed (Elliott et al., 2022).

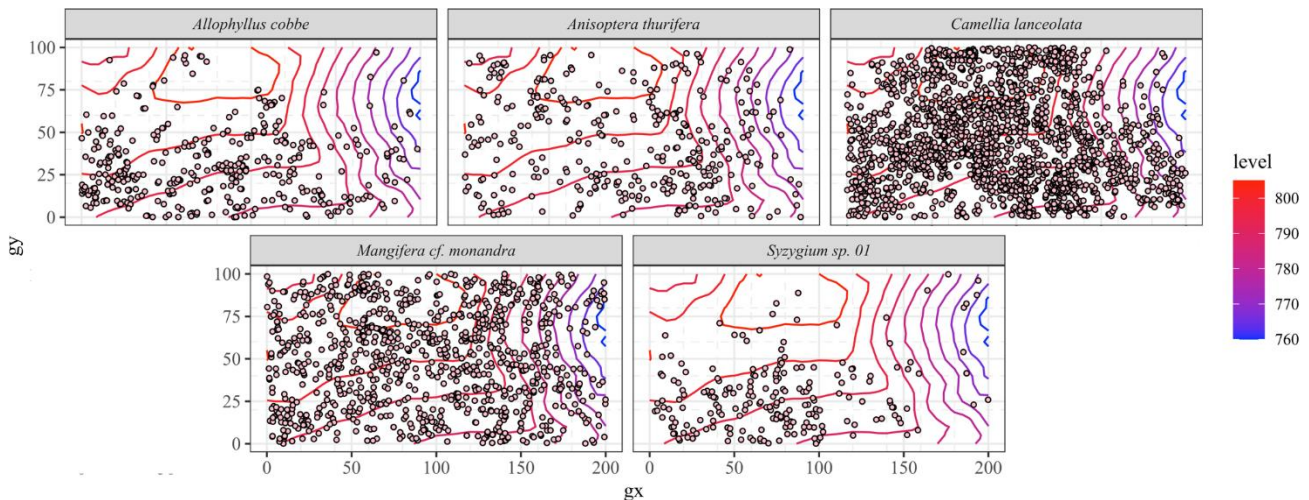


Figure 3. Spatial distribution maps of *Allophylus cobbe*, *Anisoptera thurifera*, *Camellia lanceolata*, *Mangifera monandra*, and *Syzygium* sp. 01 in the Maluyon Permanent Forest Dynamics Plot.

5. CONCLUSION

The Maluyon Permanent Forest Dynamics Plot harbors 177 tree species belonging to 91 families and 97 genera. Tree abundance and tree density increased to 10,686 recorded individuals and 5,343 individuals per hectare in 2015. Mean growth and mortality rates were lower in the Maluyon Plot in comparison to other forest dynamics plots. The slower, overall growth rate may be associated with less disturbance and high competition brought about by high tree density. Species-specific analysis revealed the presence of two

demographic trade-offs: the growth-survival and the stature-recruitment trade-offs. Demographic rates also varied as a function of size class. Small-sized trees had the lowest growth rate while large-sized trees had the highest growth rate. It was also observed that large-sized trees had lower mortality rates. Recruitment rates, on the other hand, were close to zero for all size classes. Monitoring of additional plots in other Philippine islands will give us a further understanding of the generality of these tropical forest dynamics patterns.

ACKNOWLEDGEMENTS

We would like to thank Dr. Sandra Yap, Claire Elmido, Jimmy Mangalindan Jr., and Dr. Perry Ong for their help with fieldwork and data management. We extend our gratitude to the Philippine Department of Environment and Natural Resources (DENR) Region III for issuing Wildlife Gratuitous Permit Nos. III-11-02 and III-15-02. We are also thankful for the generous funding and support from the First Gen Hydro Power Corporation. Lastly, we thank Dr. Mariano Roy Duya for providing comments on earlier versions of this manuscript.

REFERENCES

- Anderson-Teixeira KJ, Davies SJ, Bennett AC, Gonzalez-Akre EB, Muller-Landau HC, Wright SJ, et al. CTFS-ForestGEO: A worldwide network monitoring forests in an era of global change. *Global Change Biology* 2015;21(2):528-49.
- Andresen E, Arroyo-Rodríguez V, Escobar F. Tropical biodiversity: The importance of biotic interactions for its origin, maintenance, function, and conservation. In: Datillo W, Rico-Gray V, editors. *Ecological Networks in the Tropics: An Integrative Overview of Species Interactions from Some of the Most Species-Rich Habitats on Earth*. Springer International Publishing; 2018. p. 1-13.
- Atwii F, Sandvik KB, Kirch L, Paragi B, Radtke K, Schneider S, et al. *WorldRiskReport 2022: Focus: Digitalization* [Internet]. 2022 [cited 2023 Jul 30]. Available from: <https://reliefweb.int/report/world/worldriskreport-2022-focus-digitalization>.
- Bautista G. The forestry crisis in the Philippines: Nature, causes, and issues. *The Developing Economies* 1990;28(1):67-94.
- Beer C, Reichstein M, Tomelleri E, Ciais P, Jung M, Carvalhais N, et al. Terrestrial gross carbon dioxide uptake: Global distribution and covariation with climate. *Science* 2010; 329(5993):834-8.
- Condit R. *Tropical Forest Census Plots: Methods and Results from Barro Colorado Island, Panama and a Comparison with Other Plots*. Berlin, Heidelberg: Springer; 1998.
- Coomes DA, Allen RB. Effects of size, competition and altitude on tree growth. *Journal of Ecology* 2007;95(5):1084-97.
- Curtis JT, McIntosh RP. An upland forest continuum in the prairie-forest border region of Wisconsin. *Ecology* 1951;32(3):476-96.
- Davies SJ, Abiem I, Abu Salim K, Aguilar S, Allen D, Alonso A, et al. ForestGEO: Understanding forest diversity and dynamics through a global observatory network. *Biological Conservation* 2021;253:Article No. 108907.
- De Frenne P, Lenoir J, Luoto M, Scheffers BR, Zellweger F, Aalto J, et al. Forest microclimates and climate change: Importance, drivers and future research agenda. *Global Change Biology* 2021;27(5):2279-97.
- Detto M, Levine JM, Pacala SW. Maintenance of high diversity in mechanistic forest dynamics models of competition for light. *Ecological Monographs* 2022;92(2):e1500.
- Elliott S, Tucker NI, Shannon DP, Tiansawat P. The framework species method: Harnessing natural regeneration to restore tropical forest ecosystems. *Philosophical Transactions of the Royal Society B* 2022;378(1867):Article No. 20210073.
- Forest Management Bureau. *Philippine forestry statistics 2018* [Internet]. 2018 [cited 2021 Sept 11]. Available from: <https://forestry.denr.gov.ph/index.php/statistics/philippines-forestry-statistics>.
- Gonzalez-Akre E, Meakem V, Eng C-Y, Tepley AJ, Bourg NA, McShea W, et al. Patterns of tree mortality in a temperate deciduous forest derived from a large forest dynamics plot. *Ecosphere* 2016;7(12):e01595.
- Handley V. *Cultivating Biodiversity: Tropical Forests in the Philippines* - UC Botanical Garden [Internet]. 2018 [cited 2021 Apr 17]. Available from: <https://botanicalgarden.berkeley.edu/research-conservation/philippines-biodiversity>.
- Hogan JA, Zimmerman JK, Thompson J, Uriarte M, Swenson NG, Condit R, et al. The frequency of cyclonic wind storms shapes tropical forest dynamism and functional trait dispersion. *Forests* 2018;9(7):Article No. 404.
- Kambach S, Condit R, Aguilar S, Bruelheide H, Bunyavejchewin S, Chang-Yang C-H, et al. Consistency of demographic trade-offs across 13 (sub)tropical forests. *Journal of Ecology* 2022;110(7):1485-96.
- Kummer DM. Remote sensing and tropical deforestation: A cautionary note from the Philippines. *Photogrammetric Engineering and Remote Sensing* 1992;58(10):1469-71.
- Lasco RD, Cruz RVO, Pulhin JM, Pulhin FB. *Assessing Climate Change Impacts, Vulnerability and Adaptation: The Case of Pantabangan-Carranglan Watershed*. Laguna, Philippines; World Agroforestry Centre; 2010.
- Lepore M, Arellano G, Condit R, Davies S, Detto M, Gonzalez-Akre E, et al. *Fgeo: Analyze forest diversity and dynamics* [Internet]. 2019 [cited 2022 May 21]. Available from: <https://cran.r-project.org/web/packages/fgeo/index.html>.
- Lopez A. Over P8-M hot logs seized in Caraga in Q1 2020 [Internet]. 2020 [cited 2021 Jun 13]. Available from: <https://www.pna.gov.ph/articles/1102720>.
- Lutz JA, Larson AJ, Furniss TJ, Donato DC, Freund JA, Swanson ME, et al. Spatially nonrandom tree mortality and ingrowth maintain equilibrium pattern in an old-growth *Pseudotsuga-Tsuga* forest. *Ecology* 2014;95(8):2047-54.
- Marod D, Duengkae P, Sangkaew S, Racharak P, Suksavate W, Uthairatsamee S, et al. Population structure and spatial distribution of tree species in lower montane forest, Doi Suthep-Pui National Park, Northern Thailand. *Environment and Natural Resources Journal* 2022;20(6):644-63.
- McDowell NG, Allen CD, Anderson-Teixeira K, Aukema BH, Bond-Lamberty B, Chini L, et al. Pervasive shifts in forest dynamics in a changing world. *Science* 2020;368(6494):471-501.
- Monoy CC, Tomlinson KW, Iida Y, Swenson NG, Slik JWF. Temporal changes in tree species and trait composition in a cyclone-prone Pacific dipterocarp forest. *Ecosystems* 2016; 19:1013-22.
- Mukul SA, Herbohn J, Firn J. Rapid recovery of tropical forest diversity and structure after shifting cultivation in the Philippines uplands. *Ecology and Evolution* 2020;10(14): 7189-211.
- Pabico L, Duya M, Fidelino J, Ong P, Duya MR. Bird feeding guild assemblage along a disturbance gradient in the Pantabangan-Carranglan Watershed and Forest Reserve, Central Luzon Island, Philippines. *Philippine Journal of Science* 2021;150(S1):237-55.
- Pang S, De Alban JD, Webb E. Effects of climate change and land cover on the distributions of a critical tree family in the Philippines. *Scientific Reports* 2021;11:Article No. 276.

- Pasion BO, Duya MRM, Ong PS, Fernando ES. Twelve-year changes in palm populations from a tropical lowland forest in the Philippines. *Community Ecology* 2022;23(3):327-35.
- Pinmongkhonkul S, Boonriam W, Madhyamapurush W, Iamchuen N, Chaiwongsaen P, Mann D, et al. Species diversity, aboveground biomass, and carbon storage of watershed forest in Phayao Province, Thailand. *Environment and Natural Resources Journal* 2023;21(1):47-57.
- R Core Team. RStudio: Integrated Development for R [Internet]. 2020 [cited 2022 Apr 20]. Available from <http://www.rstudio.com/>.
- Rozendaal DMA, Phillips OL, Lewis SL, Affum-Baffoe K, Alvarez-Davila E, Andrade A, et al. Competition influences tree growth, but not mortality, across environmental gradients in Amazonia and tropical Africa. *Ecology* 2020;101(7):Article No. e03052.
- Rüger N, Condit R, Dent DH, DeWalt SJ, Hubbell SP, Lichstein JW, et al. Demographic trade-offs predict tropical forest dynamics. *Science* 2020;368(6487):165-8.
- Russo SE, McMahon SM, Detto M, Ledder G, Wright SJ, Condit RS, et al. The interspecific growth-mortality trade-off is not a general framework for tropical forest community structure. *Nature Ecology and Evolution* 2021;5:174-83.
- Sukumar R, Suresh HS, Dattaraja HS, Niranjana J. Mudumalai forest dynamics plot, India. In: Losos E, Leigh E, editors. *Tropical Forest Diversity and Dynamism: Findings from a Large-Scale Plot Network*. Chicago: University of the Chicago Press; 2004, p. 551-63.
- Thompson ID, Mackey B, McNulty S, Mosseler A. *Forest Resilience, Biodiversity, and Climate Change: A Synthesis of the Biodiversity/Resilience/ Stability Relationship in Forest Ecosystems*. Montreal: Secretariat of the Convention on Biological Diversity; 2009.
- Yap S, Davies S, Condit R. Dynamic response of a Philippine dipterocarp forest to typhoon disturbance. *Journal of Vegetation Science* 2016;27(1):133-43.
- Yih K, Boucher DH, Vandermeer JH, Zamora N. Recovery of the rain forest of southeastern Nicaragua after destruction by hurricane Joan. *Biotropica* 1991;23(2):106-13.
- Yilma G, Edaso A, Teshome S. Characterizing the existing woodland forest to determine forest habitat management options in Gamogofa zone, southern Ethiopia. *Plants and Environment* 2021;3(4):113-20.
- Zimmerman J. LFDP census 6 [Internet]. 2020. [cited 2022 May 21]. Available from: <https://luquillo.lter.network/forest-dynamics/>.

Formulation of Novel Microbial Consortia for Rapid Composting of Biodegradable Municipal Solid Waste: An Approach in the Circular Economy

P. A. K. C. Wijerathna^{1,2}, K. P. P. Udayagee³, F. S. Idroos¹, and Pathmalal M. Manage^{1*}

¹Centre for Water Quality and Algae Research, Department of Zoology, Faculty of Applied Sciences, University of Sri Jayewardenepura, Gangodawila, Nugegoda 10250, Sri Lanka

²Faculty of Graduate Studies, University of Sri Jayewardenepura, Gangodawila, Nugegoda 10250, Sri Lanka

³Department of Bio-Systems Technology, Faculty of Technology, University of Sri Jayewardenepura, Gangodawila, Nugegoda 10250, Sri Lanka

ARTICLE INFO

Received: 27 Sep 2023
Received in revised: 30 Apr 2024
Accepted: 8 May 2024
Published online: 21 May 2024
DOI: 10.32526/ennrj/22/20230270

Keywords:

Bacterial consortium/ Composting/
Hydrolytic enzymes/ Municipal
solid waste/ Waste management

* Corresponding author:

E-mail: pathmalal@sjp.ac.lk

ABSTRACT

Urbanization and rapid industrialization have led to the escalation of municipal solid waste generation and accumulation. Composting is widely recognized as a sustainable solution for solid waste management. However, its long-term investment is considered a disadvantage. The present research study discusses the rapid biotransformation of solid waste into valorized compost. Bacteria were isolated from soil, solid waste, and leachate samples from open dump sites. From the 18 different bacterial consortia created using potential isolates, the five most promising consortia were selected based on concurrent different enzyme production. These selected consortia were incorporated into typical compost bins with Municipal Solid Waste (MSW). Daily monitoring of enzymatic activity, pH, conductivity, bulk density, moisture, and temperature, along with other composting parameters, was conducted. The study's results demonstrated that consortium No. 5, comprising *Bacillus haynesii*, *Bacillus amyloliquefaciens*, and *Bacillus safensis*, exhibited significant ($p < 0.05$) enzyme activity of cellulase, amylase, lipase and proteinase enzymes during composting compared to the control and other treatment setups. Consortium No. 5 also facilitated rapid and successful composting, as evidenced by significant alterations of composting parameters by exhibiting a shorter average composting time, reducing it from 110 ± 10 days to 20 ± 3 days, showcasing the potential applicability of formulated bacterial consortium as a sustainable and greener approach to the global solid waste problem. The novelty of this study lies in the isolation of local bacterial strains from open dump sites soil, MSW, and MSW leachate samples, which were then utilized in the composting organic fraction of MSW, enhancing the potential for effective waste management.

1. INTRODUCTION

Rapid urbanization, industrialization and agricultural modernization-related anthropogenic activities cause a massive generation and accumulation of Municipal Solid Waste (MSW) globally. Simultaneously, the worldwide MSW generation in 2016 was about 2,010 MT, projected to grow to 3,400 MT by 2050 (Pal and Tiwari, 2023).

Consequently, the improper MSW management practices severely impacted natural ecosystems and public health circumstances in numerous ways (Wang et al., 2023; Wijerathna et al., 2023).

Recovering useful materials or energy from garbage has become standard in the circular economy. The need for environment-friendly solutions is increasing rapidly, yet recent technological

Citation: Wijerathna PAKC, Udayagee KPP, Idroos FS, Manage PM. Formulation of novel microbial consortia for rapid composting of biodegradable municipal solid waste: An approach in the circular economy. Environ. Nat. Resour. J. 2024;22(3):283-300. (<https://doi.org/10.32526/ennrj/22/20230270>)

advancements have elevated solid waste management to a stable foundation. Most waste is composed of easily recyclable organic materials, with estimates ranging from 40-50% (Goushterova et al., 2020). Composting is considered one of the popular eco-friendly and cost-effective approaches in which the organic waste converts into valorized stable humic soil amendments (Chen et al., 2021; Wang et al., 2023).

The application of high-quality compost for agricultural lands is beneficial to minimize the cost of chemical fertilizers, improve crop yield and enhance the soil structure (Goushterova et al., 2020). Conversely, still, traditional composting consists of the areas where the entire process could be improved to overcome the issues of low treatment efficiency and poor final product quality (Pal and Tiwari, 2023). The significant time requirement is one of the major limitations in traditional composting which both delays production and expands the land area required. Inoculation of the effective microbial consortium which has a greater organic waste degradation potential is a promising greener approach for efficient organic waste composting (Wang et al., 2023).

The full biotransformation of waste into valorized composts necessitates the synergistic action of various hydrolytic enzymes in microbes, allowing the development of such a thing an even better value (Shah et al., 2022; Koyama et al., 2022). Nevertheless, the lignocellulolytic oxidative enzymes in numerous fungal and bacterial species combine to depolymerize complex substrates which include cellulose, hemicellulose, and lignin in waste (Andlar et al., 2018; Kumar et al., 2022). Besides, the efficiency with which microorganisms break down organic waste correlates to their structural and functional stability (Andlar et al., 2018). For example, microorganisms in the soil around waste are constantly exposed to new substrates and chemicals, strengthening their natural defenses and making them more resilient. Keeping the waste breakdown rate comparable to garbage disposal may be possible by inoculating waste with potential microorganisms that secrete extracellular hydrolytic enzymes at higher levels, such as cellulase, amylase, protease, pectinase, and lipase (Sarkar and Chourasia, 2017).

The performance of a developed microbial consortium relies on factors which include the nature of the substrate, different climatic or environmental factors and the synergistic interactions with the existing microbial community (Kumar et al., 2022). Besides, numerous studies have been conducted on the

development of an efficient microbial consortium for enhancing composting and waste management (Koyama et al., 2022; Wang et al., 2023). However, still, the current available microbial solutions have been unable to answer all the issues in composting MSW efficient and sustainable manner.

The focus of the present study was to develop a novel bacterial consortium with locally isolated potential bacterial strains to enhance the composting process of organic MSW as a cost-effective greener approach (Kumar et al., 2022). Furthermore, this research study may lead to a promising waste management technology in meeting agenda 2030 by highlighting the importance of achieving SDGs 11 and 12, sustainable cities and communities and responsible consumption. Furthermore, the findings of this research would be beneficial in the real-world composting industry and society to meet critical factors of SDGs 9, 1, 3, 6, and 14; Industry, innovation and infrastructure, no poverty, good health and well-being, clean water and sanitization (Chen et al., 2021).

2. METHODOLOGY

2.1 Collection of samples for bacteria isolation

Sample sites were selected based on the accessibility to natural MSW whereby the onsite microbial community could predominantly be adapted to break down MSW by nature which could be isolated easily in large numbers. Three major dumps including Karadiyana (6°48'58.23"N, 79°54'9.27"E), Meethotamulla (6°56'18.65"N, 79°53'25.00"E) and Kerawalapitiya (7°30'33.63"N, 80°21'12.24"E) in Sri Lanka were selected for the isolation of bacteria from soil, solid waste and leachate. Leachate samples were collected into sterilized amber-coloured glass bottles, whereas soil and solid waste samples were collected into sterilized press-seal bags. The samples were transported to the lab in an ice box and immediately subjected to microbiological analysis (Gunaratne et al., 2024). Figure 1 illustrates the sampling locations of this study.

2.2 Isolation of bacteria from the soil, leachate, and solid waste

The isolation of bacteria was performed following the standard serial dilution method. One gram of the composite soil/solid waste sample or 1 mL of leachate sample were individually transferred to test tubes filled with 10 mL of sterilized saline water and mixed well, followed by subsequent tenfold dilution by transferring 1 mL solution to sterile 9 mL deionized

water. Finally, 100 μ L of the solution from each dilution was transferred onto a sterile solid nutrient agar medium (1.5%, pH 7) to prepare spread plates and then incubated at 37°C for 24 h. Bacterial

colonies with different morphological features were isolated, purified and stored at 4°C for future studies (Sarkar and Chourasia, 2017).

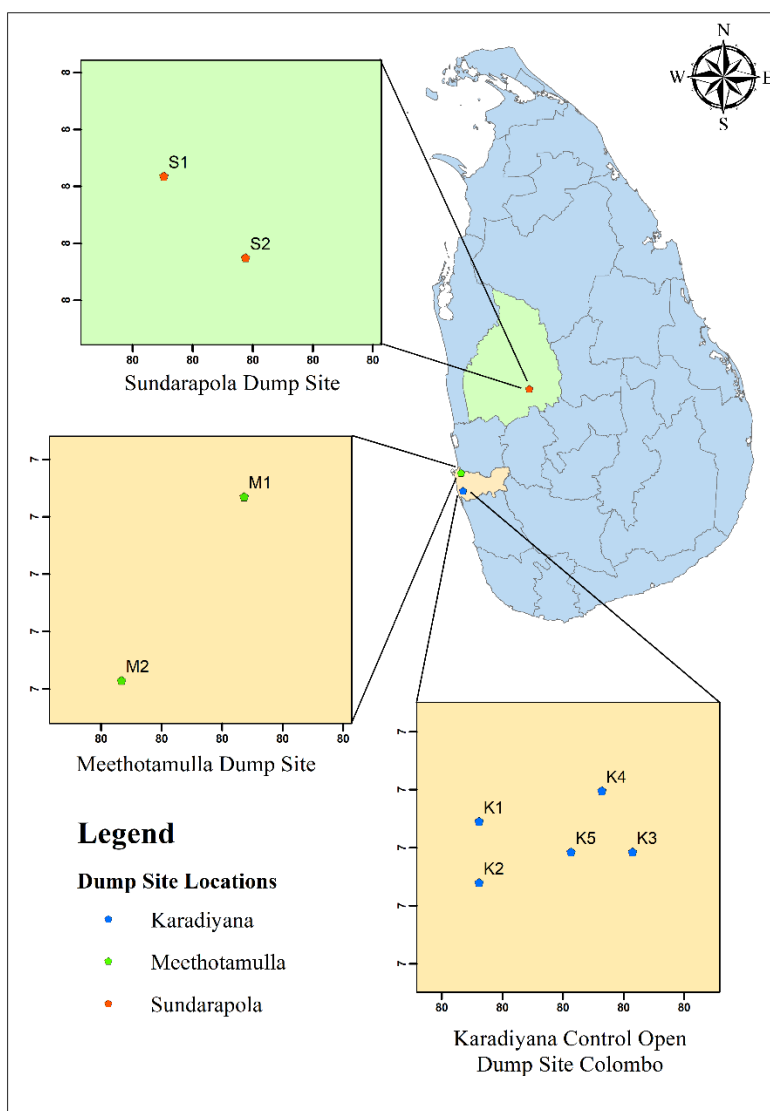


Figure 1. Sampling locations

2.3 Primary Screening of bacteria for extracellular enzymes production potential (enzyme assays)

The isolated microorganisms were subjected to the primary screening following the clear zone formation on different substrates. The cellulase enzyme producers were screened following the Congo Red method using Carboxyl Methyl Cellulose (CMC) as the substrate (Zhang et al., 2021; Harindintwali et al., 2020). The amylase-positive bacteria were screened following the starch-agar medium, and proteinase-positive bacteria were screened using skimmed milk agar medium. Finally, the lipase-positive bacteria were screened using the Phenyl Red

agar medium and olive oil as the substrate (Sarkar and Chourasia, 2017).

2.4 Secondary screening of different enzyme-producing bacteria

Secondary screening was conducted for all the positive (enzyme-producing) isolates obtained from primary screening to select the best enzyme-producing strains to be used for final consortia preparation. Four different enzyme assays were performed for selected bacteria from the primary screening to quantify the extracellular cellulase, amylase, lipase, and proteinase enzyme production.

The test tubes were heated at 100°C for 5 min and cooled to room temperature. Finally, the solutions were diluted by adding 5 mL of distilled water and absorbance values were recorded at 540 nm. The glucose standard curve was used to determine the amylase activity (Dhiman et al., 2021).

2.4.1 Amylase assay

The Di-Nitro Salicylic acid (DNS) method was used to determine amylase activity. A 1% starch broth was made and 50 mM phosphate buffer (pH 7) was prepared as a substrate. Tubes were filled with substrate, crude enzyme, and buffer following incubation for 30 min under 37°C. Then, the enzyme blank and 1 mL of DNS reagent were added into each test tube. The test tubes were heated at 100°C for 5 min and cooled to room temperature. Finally, the solutions were diluted by adding 5 mL of distilled water and absorbance values were recorded at 540 nm. The glucose standard curve was used to determine the amylase activity (Dhiman et al., 2021).

2.4.2 Cellulase assay

The standard DNS method was used to determine cellulase enzyme activity and the assay was carried out in the same manner as the amylase assay. Substrates for the assay were prepared by adding 1% of Carboxy Methyl Cellulose (CMC) broth in 50 mM phosphate buffer (pH 7) solution. Similar to the amylase assay, the substrate, crude enzyme extract and buffer solutions were mixed and heated in the same procedure of amylase assay. The absorbance values were recorded at 540 nm and the cellulase activity was measured using the glucose standard curve. One unit of enzyme activity is referred to as the amount of enzyme that releases one mole of reducing sugar per minute (U/mL/min) under assay conditions (Sarkar and Chourasia, 2017).

2.4.3 Protease assay

Protease enzyme activity was measured spectrophotometrically by Sigma's universal protease assay using Casein as the substrate. One per cent casein broth was prepared in 50 mM potassium phosphate buffer (pH 7.5) as the substrate. The crude enzyme, substrate and buffer were added to tubes and incubated at 37°C for 10 min. Finally, the absorbance was measured under 660 nm, and one unit of enzyme activity is defined as the amount of enzyme that releases 1 mol of tyrosine per minute under assay conditions (U/mL/min) (Patel et al., 2019).

2.4.4 Lipase assay

Lipase enzyme activity was measured titrimetrically using tributyrin oil as the substrate. First, 1 mL of the substrate was into a test tube containing 3 mL of 50 mM Tris-HCl buffer (pH 8). Next, 1 mL of the crude enzyme broth was mixed with the solution and incubated for 30 min at 37°C. After incubating, 1% phenolphthalein was mixed with the broth and titrated with 50 mM NaOH a pinkish colour developed. One unit of enzyme activity is defined as the amount of enzyme that releases 1 mol of fatty acid per minute under assay conditions (Sarkar and Chourasia, 2017).

2.5 Antagonistic effects

Eighteen consortia were formulated using the best potential isolates with the most significant single enzyme-producing ability for cellulase, proteinase, lipase and amylase enzymes. The antagonistic effects were checked for each consortium, and the cross-streaking method was used to test antagonisms. The incubated plates were examined for inhibition zones, which indicate the antagonistic effects of bacteria in the consortium. The consortia which did not show any antagonistic activity, were subjected to concomitant enzyme production (Zhimo et al., 2020).

2.5.1 Concomitant enzyme production by the consortium

The selected consortia were subjected to concomitant enzyme production by culturing in a modified medium containing specific cellulose, starch, protein and lipids substrates. After that, an equalized 1% broth consortium was inoculated in 50 mL of synthetic medium which contains 0.5% of each of mineral salts, CMC, starch, and skimmed milk. After that, the broth cultures were incubated for 7 days under 37°C at 150 rpm (Sarkar and Chourasia, 2017). The enzyme activity for each specific enzyme was carried out for the samples withdrawn every 24 h, and the concomitant enzyme production of each consortium was measured (Ma and Liu, 2019).

2.6 Preparation of consortia broth cultures and the field experimental setup for the compost study

Municipal solid waste was obtained from Maharagama municipal council, western province, Sri Lanka, for the field experiment. Standard-size (height 150 cm, diameter 45 cm) eighteen concrete compost bins were used for the field experiment, and the bins were placed on a flat open field area, labelled and each

one filled with 100 kg of composited municipal solid waste. The automated sensor set-up was established inside the compost bins to read the temperature and relative humidity of the compost bins' cap space every 30 min and all treatments were triplicated. The best five consortia (a, d, f, h, j) from the concomitant enzyme assay were selected for the composting field application set-up, and they were named C1, C2, C3, C4, and C5, respectively.

A loop full of bacteria in each consortia was separately inoculated to the 100 mL of sterilized nutrient broth medium and incubated at 30°C for 48 h under shaking conditions of 50 rpm. After the broth

cultures were separately centrifuged under 6,000 rpm for 10 min to remove the supernatant. The microbial pellet was washed twice with a sterilized saline solution to remove medium residues. The pellets were dissolved in sterilized saline water and equalized for 590 nm wavelength to 0.35 absorbance value using a UV visible spectrophotometer. The same volume of equalized (5 mL) of bacterial cell suspension of each bacterial type in the consortia was mixed to prepare the consortia broth and a 1% v/w of consortia broth was inoculated to the respective compost bins. Figure 2 shows the field experimental set-up of the composting study.



Figure 2. The experimental field set-up of the composting study

2.7 Characterization of solid waste and the final compost

2.7.1 Solid waste characterization

A composite sample was taken from fresh MSW and the experiments were carried out immediately. The solid waste was characterized by measuring the initial pH and conductivity using an aqueous mixture of 1:10 diluted (w/v) using a multipara meter (Model Star 2001-Thermo Scientific); Total Kjeldahl Nitrogen (TKN) concentrations were analyzed for a standard composite mixture of a solid waste sample using the standard methods (Awasthi et al., 2018).

The concentration of lipids, proteins, carbohydrates, starch and free sugars was analyzed according to standard methods (Awasthi et al., 2018). Further, the composite solid waste's bulk density was determined using a standard metalcore 100 cc cylinder. The Initial microbial count was recorded following the standard serial dilution method and the standard pour plate method on the Nutrient Agar Universal medium.

2.7.2 Characterization of the final compost

To determine the quality of the final compost sample, the TKN, total organic carbon (TOC), C:N ratio, total phosphate and total ash content were

measured in the final compost following the standard methods (Mahapatra et al., 2022; Parameswaran et al., 2024). The Germination Index (GI) was calculated in all samples following the equation given using green gram seeds.

$$GI = \frac{\text{Number of germinated seeds in sample} \times \text{Root length in the sample} \times 100}{\text{Number of germinated seeds in control} \times \text{Root length in control}}$$

2.7.3 Mesophilic and thermophilic viable cell count

The mesophilic and thermophilic bacteria were cultured on a nutrient agar medium by preparing a compost suspension by mixing 1 g of compost in 9 mL sterilized distilled water and a tenfold dilution series was prepared from the initial sample. The standard pour plate method was used to grow bacteria. The plates were incubated for 72 h at either 28°C or 55°C to determine the number of colony forming units (CFU) of mesophiles and thermophiles, respectively (Lin et al., 2022).

2.8 DNA extraction and identification of bacteria using 16S r RNA

The 16S rRNA identification was done only for the bacteria in the best-performed (C5) consortia. A

loop full of bacteria from each isolate was transferred to prepared sterilized nutrient broth media and incubated at 30°C for 48 h. After that, a 200 µL of each broth culture was transferred to sterilized Eppendorf tubes and centrifuged under 10,000 rpm for 2 min. The supernatant was discarded and the procedure was repeated until obtaining a clear bacterial pellet. The obtained bacterial pellet was filled with 200 µL of cell lysis solution (Promega®, Cat No: A7933) and mixed thoroughly. The DNA extraction was carried out using a two-times repeated freeze-thaw cycle followed by heating under 120°C for 10 min and freezing on ice for 10 min. The DNA solution was again centrifuged under 10,000 rpm for 2 min and the extracted DNA was transferred to a sterilized Eppendorf tube (Goushterova et al., 2020). The extracted DNA was subjected to the 16S rRNA gene sequencing, sending the bacterial DNA to Macrogen, Korea. The gene sequence was used to carry out BLAST with the NCBI Gene Bank database and aligned using multiple alignment software programs.

2.9 Figures and statistical analysis

Statistical analysis was carried out using the Minitab 17 version and a one-way ANOVA test was

used. Figures were created using MS Excel 2010 version.

3. RESULTS AND DISCUSSION

3.1 Isolation, primary, and secondary screening of bacteria

Following a 24-hour incubation at 37°C, a total of 226 morphologically different bacterial colonies were isolated from the soil, leachate, and solid waste sample. The isolated bacteria were screened for potential extracellular hydrolytic enzyme dynamic as a strong indicator which can determine the rate of biomass transformation during composting. Microbes secrete several hydrolytic enzymes, such as cellulase, protease, lipase, and amylase, which can degrade the predominant substrates of MSW (Zhang et al., 2021).

Figure 3 represents the positive results obtained for each enzyme plate assay. Based on the primary screening results, the CMC agar plate assay revealed the presence of 15 cellulase-positive bacterial strains. Similarly, the starch agar assay identified 15 amylase-positive bacterial strains and the skimmed milk agar assay revealed 15 proteinase-positive bacterial strains. Lastly, the lipase plate assay revealed 7 lipase-positive isolates.

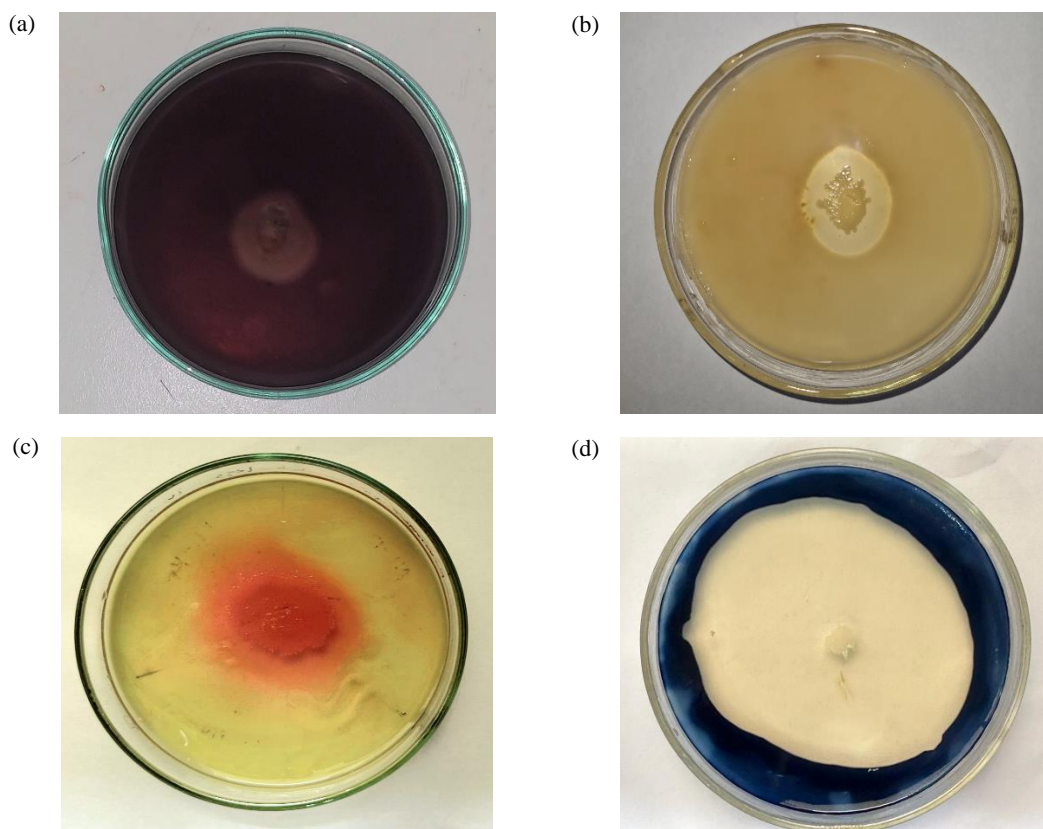


Figure 3. Positive isolates for the cellulase (a) *Bacillus amyloliquefaciens* strain BAC1-PP391056, proteinase; (b) *Bacillus haynesii* strain BHC1-PP391133; lipase (c) *Bacillus safensis* PP391033); and amylase (d) *Bacillus amyloliquefaciens* strain AMWC-PP391615 tests.

The number of lipase-positive isolates has recorded as a lower number compared to the cellulase, amylase and proteinase-positive isolates. This might be attributed to the predominant bacterial community in the dump site environment may have adapted to degrade carbohydrates and protein substrates (Harindintwali et al., 2020). Further, Chukwuma et al. (2023) have depicted the potentiality of lingo-cellulolytic bacteria *Bacillus* spp. from MSW landfill, which can break down biomass by producing hydrolytic enzymes.

According to the secondary screening results (Table 1) of the study, cellulase-positive bacterial isolates K11 and K50 exhibited the highest cellulase activity at 6.2 ± 0.2 U/mL/min and were selected for subsequent consortia formation. The highest amylase activity was observed in bacterial isolates K21 and K29, with values of 6.5 ± 0.1 U/mL/min and 6.2 ± 0.3

U/mL/min, respectively. Similarly, the most significant proteinase activity was found in bacterial strains K21 and K29, with measurements of 7.2 ± 0.2 U/mL/min and 6.5 ± 0.1 U/mL/min, respectively. Bacteria K29 and K17 exhibited the highest lipase activity, with values of 4.2 ± 0.2 U/mL/min and 3.8 ± 0.2 U/mL/min, respectively indicating the efficient degradation potential lipid substrates.

Similarly, Sarkar and Chourasia (2017) have researched bio-fortified compost using developed microbial consortia which were able to produce amylase, cellulase, and lipase activities of 4.18 U/mL/min, 2.35 U/mL/min, 15.62, and U/mL/min, respectively. Besides, the studies carried out by Zhang et al. (2021) have recorded the 0.8 U/mL/min of cellulase activity for the hydrolysis of lignocellulosic sugarcane bagasse.

Table 1. Enzyme activities of isolated bacterial strains

Positive isolates	Cellulase enzyme activity (U/mL/min)	Amylase enzyme activity (U/mL/min)	Proteinase enzyme activity (U/mL/min)	Lipase enzyme activity (U/mL/min)
KX2	3.5 ± 0.1	ND	5.8 ± 0.2	ND
K01	3.8 ± 0.2	3.5 ± 0.1	ND	ND
K05	4.2 ± 0.1	ND	ND	2.6 ± 0.2
K07	3.5 ± 0.1	ND	ND	ND
K04	3.2 ± 0.1	4.2 ± 0.1	6.8 ± 0.2	ND
K19	3.8 ± 0.1	ND	ND	ND
K20	2.5 ± 0.2	ND	3.2 ± 0.2	ND
K17	2.1 ± 0.2	ND	1.8 ± 0.2	3.8 ± 0.2
K18	1.5 ± 0.1	5.2 ± 0.1	4.5 ± 0.1	ND
K13	1.1 ± 0.1	ND	ND	ND
K14	5.2 ± 0.1	3.8 ± 0.1	ND	ND
K11	6.2 ± 0.3	ND	6.2 ± 0.3	ND
K50	6.2 ± 0.2	ND	5.2 ± 0.1	ND
K32	4.2 ± 0.1	4.2 ± 0.1	ND	ND
K21	ND	6.5 ± 0.1	7.2 ± 0.2	ND
K29	ND	6.2 ± 0.3	ND	4.2 ± 0.2
K30	ND	4.8 ± 0.1	ND	1.5 ± 0.1
K39	ND	1.6 ± 0.1	ND	ND
K37	ND	5.7 ± 0.1	ND	ND
KX2	ND	0	5.8 ± 0.2	ND

*Note - All the data were the average of the three replicates, ND - Not Detected

3.2 Antagonistic effects

The performance of a microbial consortium relies on several conditions including the microbial composition, metabolic mechanisms of microbes and the synergistic interactions of the individual strains in the microbial community (Blair et al., 2021). Particularly, the antimicrobial substances that are

secreted by some microorganisms can selectively kill or inhibit the growth of other bacteria in their vicinity (Lin et al., 2022).

Therefore, the effectiveness of bacterial consortia relies on the compatibility of the other bacteria in the same consortium. The results indicated that there was no antagonism exhibited between any

bacterial species in consortia A to J, respectively, based on the results of the antagonistic assay (Table 2) for all bacteria consortia. However, it revealed an adverse, antagonistic interaction in consortium K which caused the K50 species of bacteria to obstruct

the growth of K04 and K21. Producing hazardous substances may hamper growing conditions and degrade consortium performance. The consortia that showed no signs of antagonism were subjected to further study.

Table 2. Prepared different consortia and their antagonistic effects

Consortium No.	Bacterial combination	Antagonistic effects
A	K01, K04, K21, K29	ND
B	K01, K04, K21, K17	ND
C	K01, K04, K29, K17	ND
D	K01, KX2, K21, K29	ND
E	K01, KX2, K21, K17	ND
F	K01, KX2, K29, K17	ND
G	K50, K04, K21, K29	ND
H	K50, K04, K29, K17	ND
I	K50, KX2, K21, K 29	ND
J	K50, KX2, K21, K 17	ND
K	K50, K04, K21, K17	Detected
L	K50, KX2, K29, K17	ND

*Note - ND (Not Detected)

3.3 Screening of best potential bacterial consortia for field application

The concomitant production of each enzyme was used to select the best 5 consortia for the field application. According to Figure 4, the consortia a, d, f, h, j (denoted by C1-C5 respectively in the Table 3) were shown the highest concomitant enzyme production, whereas demonstrating the enzyme

activity of 21.2 ± 0.2 , 20.4 ± 0.2 , 15.3 ± 0.1 , 19.4 ± 0.1 , and 20.5 ± 0.2 U/mL/min, respectively. The most potential five consortia (Table 3) were separately inoculated to each composting setup and their respective composting rates were determined. Similarly, Al-Dhabi et al. (2019) have studied the concomitant enzyme production of developed consortia to enhance solid waste composting.

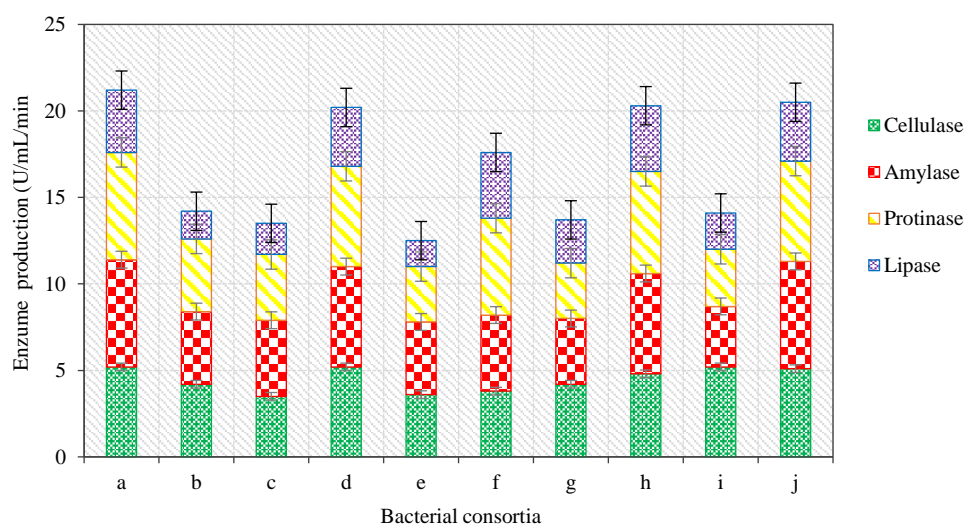


Figure 4. Concomitant enzyme production by formulated consortia (Note: All the data were the average of the three replicates)

Table 3. Selected potential bacterial consortia for the field study

Bacterial consortium	Bacterial species of the consortium
C-1	K01, K04, K21, K29
C-2	K01, KX2, K21, K29
C-3	K01, KX2, K29, K17
C-4	K50, K04, K29, K17
C-5	K50, KX2, K21, K17

3.4 Solid waste characterization

In Table 4, the basic characteristics of the municipal solid waste used in the composting study are presented. The data obtained from the waste samples indicated that they exhibited typical waste characteristics, and no extreme deviations were observed. This suggests that the waste samples used in the study were representative of municipal solid waste and can be considered suitable material for the composting process (Kumar et al., 2022).

Table 4. Preliminary characterization of the solid waste

Parameter	Mean value
pH	7.5±0.3
Electrical conductivity (µS/cm)	750.21±1.50 µS/cm
Moisture %	65±2 %
Ash content	62.5±3 %
Bulk density	285±10 kg/m ³
Total nitrogen	7.2±0.5 g/kg
Total phosphate	0.8±0.5 g/kg
Total lipid content	15.10±0.50 g/kg

Note - Data were the average of the three replicates

3.5 Changes in composting parameters

Compost maturity and stability are vital aspects of compost quality that are directly related to the degree of decomposition (Mahapatra et al., 2022). Figure 5 illustrates the fluctuations in temperature (a), pH (b), electrical conductivity (c), and moisture (d) during the composting process.

Temperature (Figure 5(a)) is one of the crucial factors that reflects microbial metabolism during composting. It affects the rate of reactions and contributes to pathogen and seed eradication, ensuring the sanitation of the composting process. The optimal temperature range for composting is typically considered to be 40-65°C (Sun et al., 2019). The composting process consists of four phases: the mesophilic phase (25-40°C), thermophilic phase (45-70°C), cooling phase (second mesophilic phase), and maturation phase (Awasthi et al., 2018).

In the study, a significant difference ($p < 0.05$) was observed between the five inoculated samples and

the control sample in terms of compost temperature. The highest temperature of $65.5 \pm 0.2^\circ\text{C}$ was recorded on the fourth day for the C5-added sample. Interestingly, the C5 consortium inoculated sample rapidly entered the thermophilic phase within two days, while the other samples indicated a slower transition pattern. Importantly, the control sample exhibited a meagre temperature increment rate, indicating a prolonged entry into the thermophilic phase with slower composting (Rashwan et al., 2021). A rapid enhancement in temperature throughout the early stage of composting leads to the speedy breakdown of degradable organic substrates relies on accelerated microbial metabolism. Additionally, several researchers have recorded the maximum temperature in the thermophilic phase as $60\text{-}70.2^\circ\text{C}$ that were similar to the present study (Sun et al., 2021; Chen et al., 2022). However, most of the composting studies have reported that the thermophilic phase has started after 5-7 days of composting (Finore et al., 2023; Wan et al., 2020). Importantly, the results of the present study were better compared to most of the previous studies indicating a rapid solid waste degradation due to the favorable synergistic interactions of bacteria in the C5 consortia with the environmental microbial community.

The pH levels depicted in Figure 5(b) followed the same pattern across all treatments, following a sudden pH drop which indicates the formation of organic acids and favourable conditions for the breakdown of lignin and cellulose by the mesophilic microorganisms. Notably, treatment C5 exhibited less time exceptional performance by reaching this phase within the first 2-3 days, whereas the control took 9-11 days. Furthermore, an increase in pH (6-9) indicates compost maturity. Treatment C5 reached the mature pH after five days, while the control took 17-19 days. The control sample showed a significantly slower composting dynamic compared to the treatments with added consortia. A significant correlation of pH was observed between C2 and C5 treatments compared to the control treatment ($p < 0.05$). Microbial activities are greatly influenced by the pH, and a neutral pH is optimum for composting. After day 3, when the thermophilic phase prevailed, the pH increased due to possible ammonia evolution (Sun et al., 2021; Awasthi et al., 2018; Wijerathna et al., 2024). Previous research revealed that the presence of H^+ induced a reduction in pH values after the maximum pH as ammonia and nitrification volatilized which relies on the results of the present study (Wan et al., 2020).

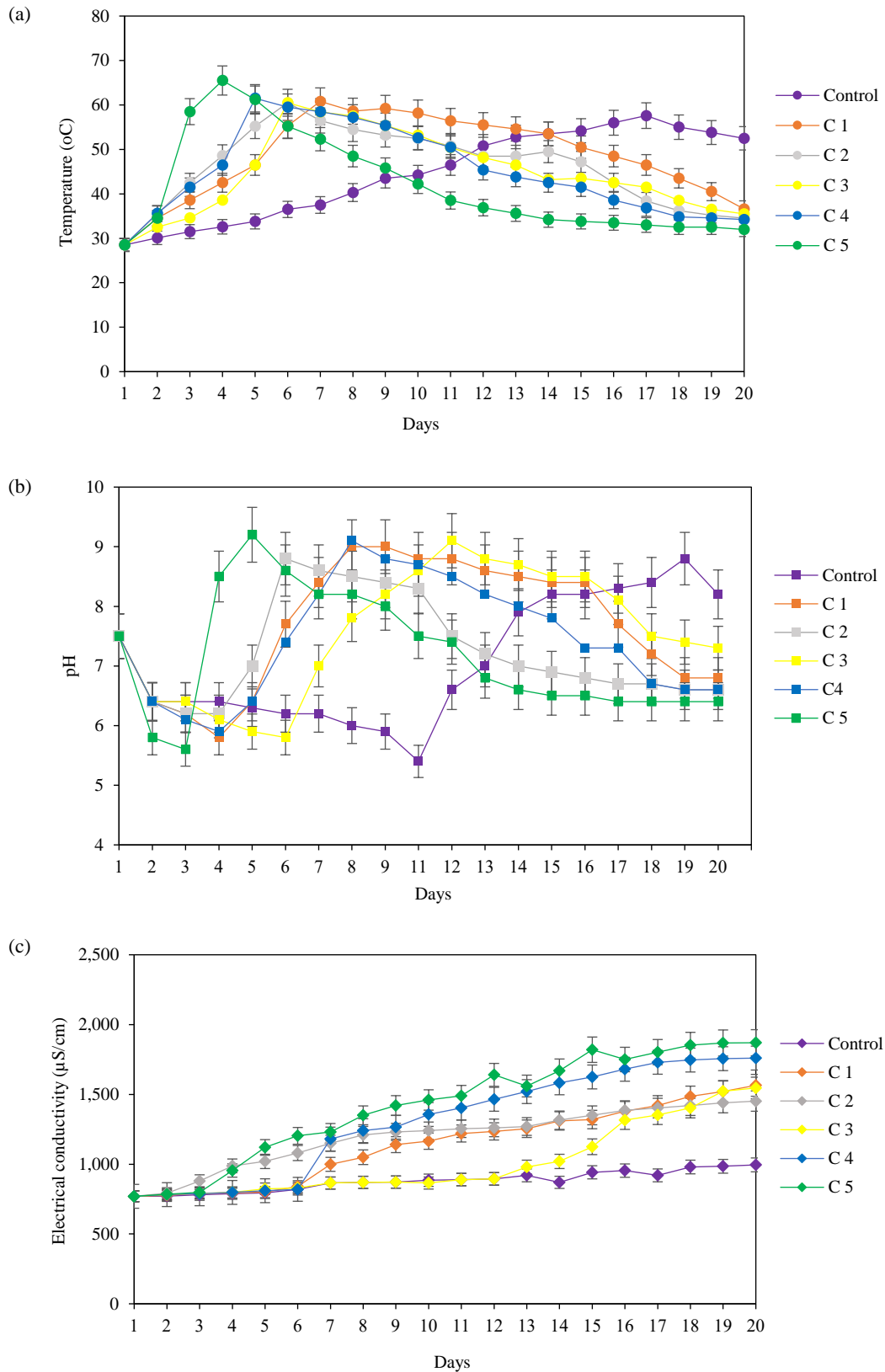


Figure 5. Changes of the temperature (a), pH (b), electrical conductivity (c), and moisture (d) during the composting period (*Note - All the data were the average of the three replicates)

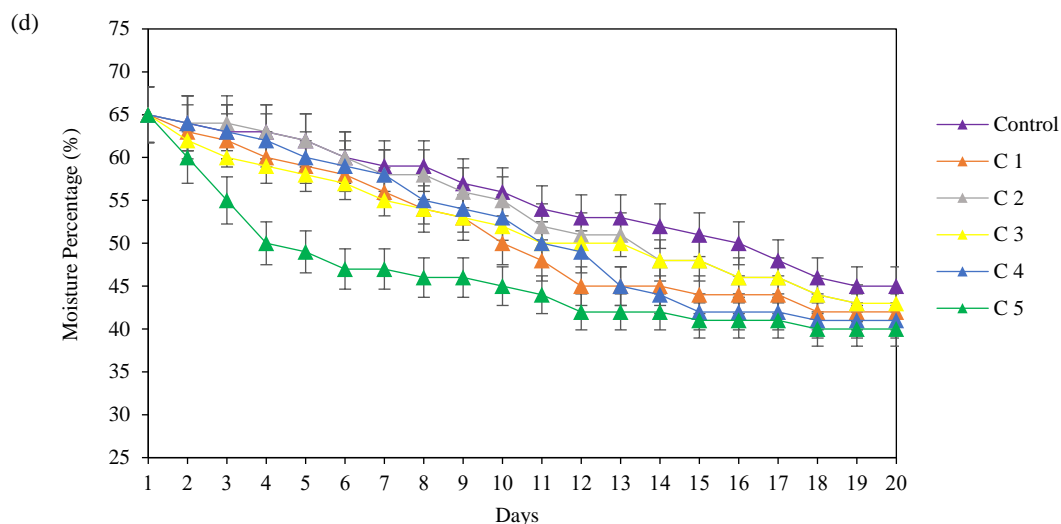


Figure 5. Changes of the temperature (a), pH (b), electrical conductivity (c), and moisture (d) during the composting period (*Note - All the data were the average of the three replicates) (cont.)

Electric conductivity (EC) reflects the level of salinity in the final compost product, which impacts nutrient availability for plant growth (Rashwan et al., 2021). Figure 5(c) illustrates that changes in EC which all the consortium-inoculated samples were significant ($p < 0.05$) compared to the control sample. The C5 inoculated treatments exhibited the highest EC, indicating rapid degradation of solid waste. During composting, the EC values increase due to the production of inorganic compounds and ion release (Rashwan et al., 2021). It is generally desirable for mature compost to have an EC value below 4 mS/cm, as excessive EC can hinder plant growth. In this study, all composts had EC values below 4 mS/cm, reflecting good compost quality (Rashwan et al., 2021).

Regarding moisture changes, all consortium-added samples displayed a significant moisture loss ($p < 0.05$) compared to the control throughout the composting period. The C5 samples showed the most rapid moisture loss due to their accelerated temperature increase during the thermophilic phase. Moisture is a crucial parameter closely associated with microbial activities (Awasthi et al., 2018). Initial moisture values below 30% can lead to accelerated dehydration and biologically unstable compost. On the other hand, moisture values above 80% can create anaerobic respiration conditions, reduce compost porosity, and cause leachate and unpleasant odour conditions (Awasthi et al., 2018).

Figure 6 depicts the changing pattern of bulk density over time for all the consortium-added samples compared to the control. The results reveal that the bulk density increased in all samples.

However, there were variations in the rate of bulk density increment among the different treatments. The control sample exhibited a relatively smaller increase in bulk density, while consortiums 4 and 5 showed a rapid increase during the first and second weeks of composting.

The increase in bulk density can be attributed to the mineralization of organic matter, resulting in a rapid reduction in the mass and volume of MSW. However, certain inert materials such as soil minerals, metals, and other inorganic constituents do not decompose and instead remain as part of the finished compost. These inert materials contribute to the increment in bulk density observed during composting (Kumar et al., 2022). Overall, the increasing bulk density observed in the consortium-added samples indicates the progress of composting and the transformation of organic waste into a denser, more stable compost product (Awasthi et al., 2018; Chen et al., 2022).

3.6 Hydrolytic enzyme dynamics during composting

The dynamics of hydrolytic enzymes during the composting period were analyzed in Figure 7. The study observed changes in α -amylase, cellulase, proteinase, and lipase concentrations over time and among different treatments.

According to Figure 7(a), all compost samples exhibited a rapid increase in α -amylase at the beginning of the composting process. This initial increment could be attributed to the presence of abundant starch content in the selected solid waste sample. The availability of starch created an optimal

environment for starch-degrading bacteria, leading to increased synthesis of the amylase enzyme. However, as the composting period progressed, the

concentration of α -amylase showed a declining rate in all treatments. This decline was likely due to the depletion of starch in the piles over time.

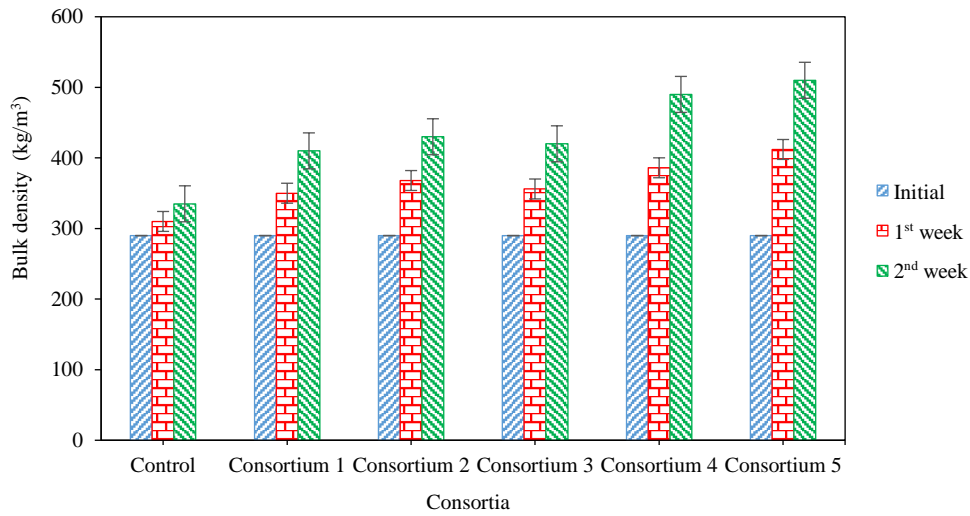


Figure 6. Changes in the bulk density (Note - All the data were the average of the three replicates)

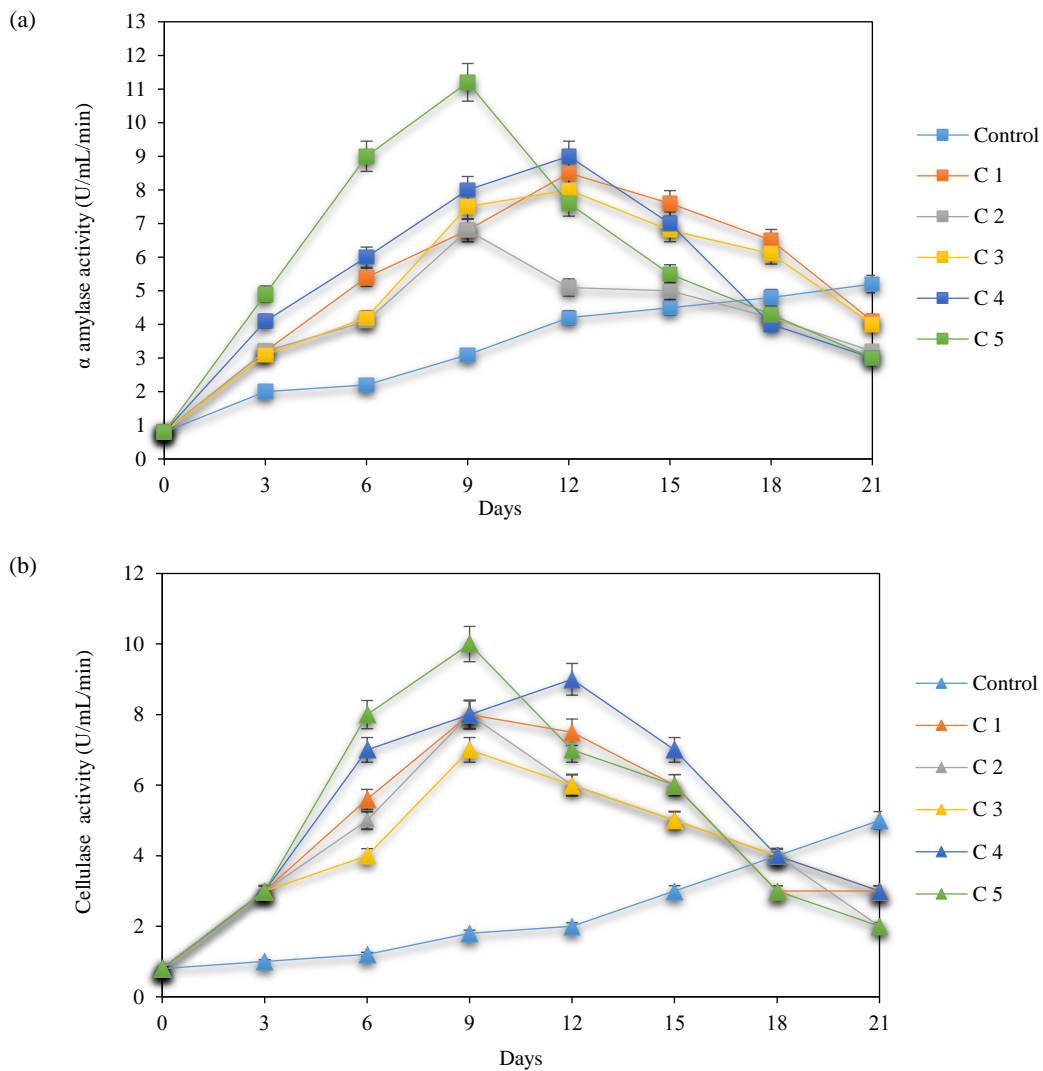


Figure 7. Hydrolytic enzyme dynamics during the composting period (Note - All the data were the average of the three replicates)

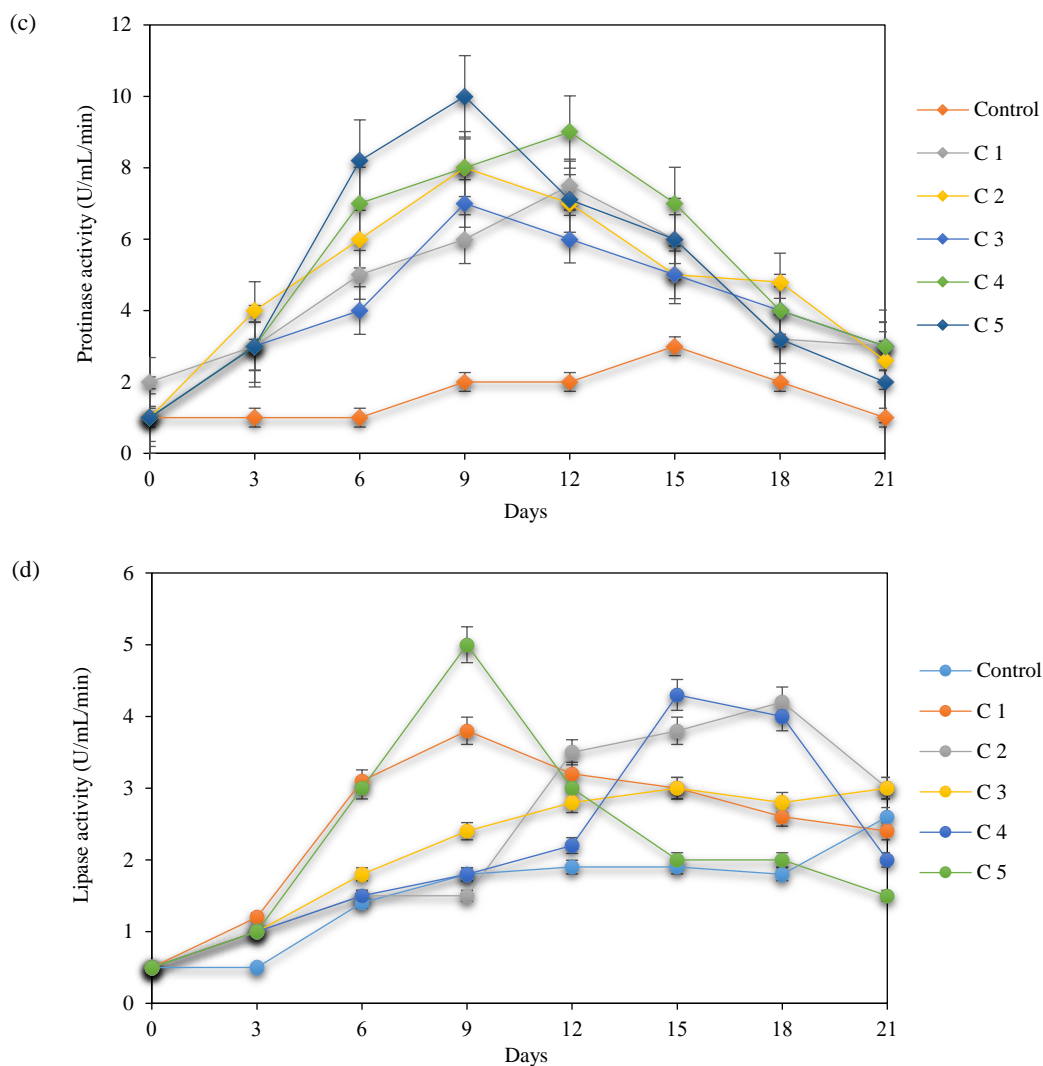


Figure 7. Hydrolytic enzyme dynamics during the composting period (Note - All the data were the average of the three replicates) (cont.)

Interestingly, the highest α -amylase enzyme activity was recorded in consortium C5 until the peak on the 9th day of composting. This finding suggests that consortium C5 exhibited hyperactivity in the presence of sufficient starch. In contrast, the control samples showed the lowest α -amylase activity until the other treatments peaked, but they demonstrated a steady and smooth increasing pattern throughout the study. Similarly, Pan (2021) recorded α -amylase activity of 3.7 U/mL/min from a thermostable bacillus sp. isolated from compost and observed a reduction of α -amylase activity with the increase of starch concentration, indicating substrate inhibition.

Figure 7(b) exhibits the cellulase activity of all consortia inoculated samples which indicates a rapid increase compared to the control. The control sample, however, displayed a prolonged rate of enzyme activity increase. Consortium C5 exhibited the highest cellulase activity peak at 10 U/mL/min on the 9th day of composting, while the other consortia-added

treatments showed lower peaks compared to C5. Cellulase is crucial for cellulose degradation and requires the involvement of both fungi and bacteria, such as cracking bacteria and *Aspergillus* sp. The reason for observing the highest cellulase activity on the 10th day may be attributed to the comparatively slower degradation rate of cellulase which is mostly completed in the middle and late phases of composting (Finore et al., 2023). Similarly, several researchers have measured the cellulase activity during organic waste composting (Dantoliya et al., 2022; Malik and Javed, 2021). Further, Lin et al. (2022) have observed a similar finding to the present study indicating that the cellulase activity was significantly higher during the thermophilic phase (>55°C) than the other phases. Further, the obtained results demonstrate that the C5 consortium has successfully accelerated the cellulose degradation of MSW by enhancing the cellulase activity.

Proteinase, an enzyme responsible for protein and peptide degradation in solid waste, also exhibited varying dynamics among the consortia treatments. The highest proteinase activity, 10 U/mL/min, was recorded from consortium C5 on the 9th day of composting. As the composting stages progressed, the availability of protein content gradually decreased, resulting in lower protease activity and eventually entering the stabilization phase. The control sample displayed the lowest proteinase production, with a maximum enzyme activity of 3 U/mL/min. Significant differences in proteinase activity were observed between the treatments, with consortia C1, C2, C3, and C4 showing increased activities of 8, 8, 7, and 8 U/mL/min, respectively. Similarly, Sarkar and Chourasia (2017) recorded the highest proteinase activity of 16 U/mL/min on the 4th day of MSW composting which showed a bit higher enzymatic activity values than those recorded in the present study. This may be due to the lower protein content in the collected MSW. However, accelerated Proteinase activity was observed during the thermophilic phase of composting, which indicated that protease plays an important role in the thermophilic phase, similar to the findings of Awasthi et al. (2018).

Moreover, lipase, responsible for breaking down lipid substances in solid waste, exhibited relatively low activity compared to other enzymes. The highest lipase activities were recorded from consortia C5, C4, C3, C2, and C1, with values of 5, 4, 3, 3, and 4.2 U/mL/min, respectively. Lipids are more complex to degrade compared to other substrate types, and their abundance in the compost piles could impair oxygen transfer efficiency and microbial dynamics. The lower lipase activity suggests a relatively lower amount of lipid substrates in the MSW. Similarly, Ng et al. (2019) isolated the *Enterococcus* sp., *Staphylococcus* sp., *Bacillus* sp., *Providencia* sp., and *Morganella* sp. activity up to 15.40 U/mL/min and 15.62 U/mL/min. The majority of collected MSW contained the lignocellulose substrates. This may have led to the relatively low lipase production in the present study.

When considering the total hydrolytic enzyme activity of all consortia, consortium C5 exhibited slightly higher activity compared to the control and other treatments (C1, C2, C3, and C4). These findings provide insights into the enzymatic dynamics during composting, highlighting the influence of different consortia on the degradation of organic components in MSW.

3.7 Changes in mesophilic and thermophilic bacterial population

Figure 8(a) and (b) provides insights into the dynamics of viable cell counts during the composting period. In terms of the mesophilic bacterial count, a significant difference ($p < 0.05$) was observed between all the consortium-added samples and the control sample. As the composting process progressed, the mesophilic bacterial count gradually decreased due to the rise in temperature during the thermophilic phase. Similar to the observation of Rich et al. (2018) the control sample exhibited a slower reduction rate in mesophilic viable cell count, which can be attributed to its slower composting rate and a more prolonged mesophilic phase during the composting process. The mesophilic bacterial population was roughly steady during the thermophilic phase. This is in line with the findings of Ince et al. (2020) and Shah et al. (2022) who found a decrease in bacteria during the thermophilic phase, followed by an increase as temperatures dropped.

The thermophilic bacterial count of all the consortium-added samples demonstrated a significant increase ($p < 0.05$) compared to the control sample. The thermophilic phase is characterized by elevated temperatures, which promote the degradation of complex waste substances into simpler monomers. Similar to the observations of Finore et al. (2023) the favourable environment in the consortium-added samples led to a higher population of thermophilic bacteria compared to the control, indicating more efficient decomposition and organic matter breakdown during composting.

Overall, the observations from Figure 8 highlight the effectiveness of the consortium-added samples in promoting bacterial activity and accelerating the composting process, particularly during the thermophilic phase. The higher thermophilic bacterial counts in the consortium-added samples suggest enhanced microbial activity and the potential for more efficient decomposition of organic waste materials (Finore et al., 2023).

3.8 Final compost characterization

Seed Germination Index (GI) (Table 5) is one of the important and sensitive indicators of compost quality that determine the phytotoxicity effect of the compost (Awasthi et al., 2018). The results indicate that the GI of the final compost ranged from 76 ± 3 to 110 ± 2 . If the GI value is 26-65, the substrate is

classified as phytotoxic; if the GI value is 66-100, the product is classified as non-phytotoxic, stable, and can be used in agricultural production; and if the GI value is greater than 101, the product is classified as phytonutrient-phyto stimulant and can be used as fertilizer (Meena et al., 2021). According to the data, the GI value of C2-C5 compost samples was in the acceptable range. However, C5 consortia inoculated compost demonstrated an exceptionally favourable GI value (110.25 ± 2.21) indicating the potential

applicability of the C5 compost as a fertilizer (Meena et al., 2021; Awasthi et al., 2018). Further, Total Kjeldahl Nitrogen (TKN) and total organic carbon (TOC) and C:N values of all the compost samples ranged from 1.82 ± 0.51 to 2.50 ± 0.25 , 14.40 ± 0.16 to 26.66 ± 0.50 , respectively. Moreover, the C5 final compost sample demonstrated the maximum TKN of 2.50 ± 0.25 indicating a good quality compost compared to the other samples (Awasthi et al., 2018).

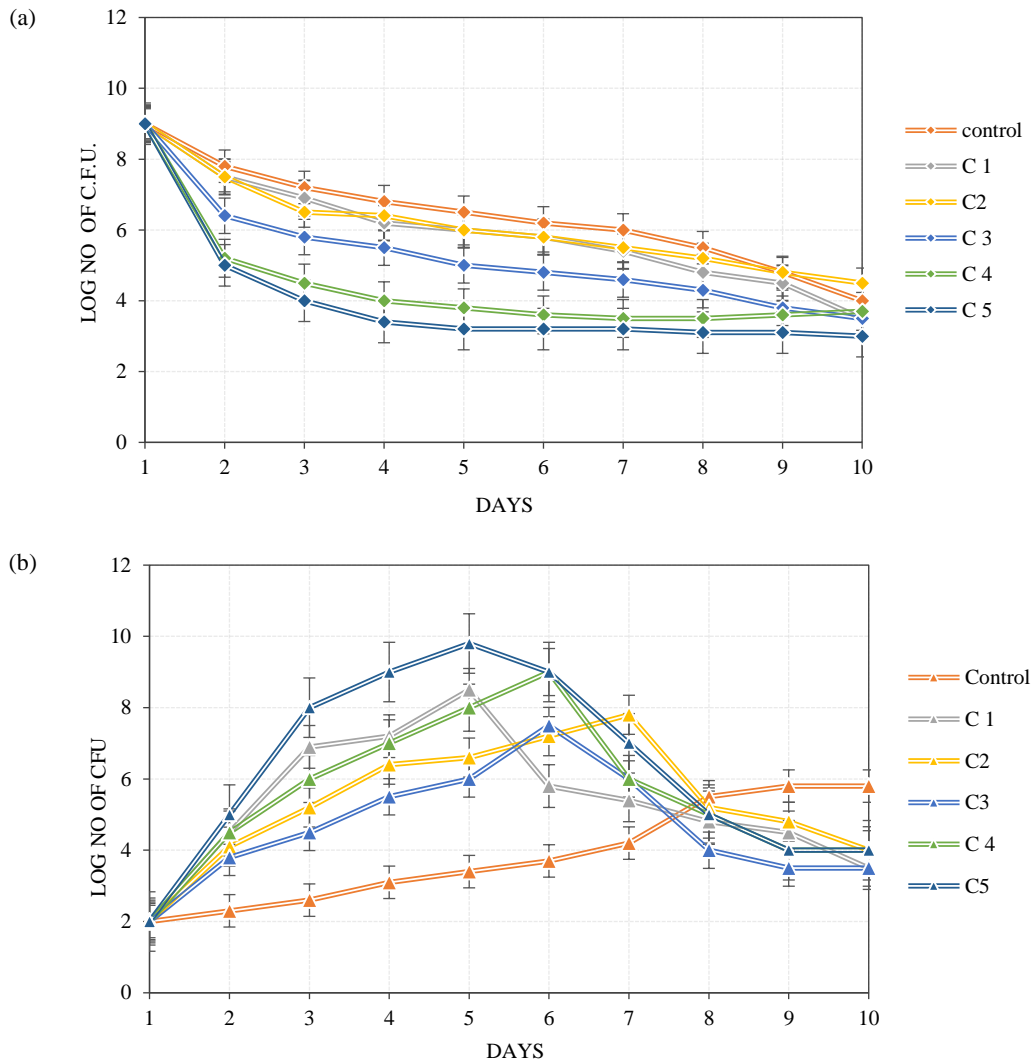


Figure 8. Mesophilic (a) and thermophilic (b) viable cell count during composting (Note - All the data were the average of the three replicates)

Table 5. Quality parameters of the final compost

Parameter	Compost sample					
	Control	C1	C2	C3	C4	C5
GI	76.53±3.21	72.43±4.25	80.15±3.51	84.51±2.22	84.50±2.31	110.25±2.21
TKN (g/kg)	1.82±0.51	2.22±0.42	2.10±0.25	2.20±0.52	2.00±0.25	2.50±0.25
TOC (g/kg)	48.25±0.52	45.23±0.45	44.15±0.52	46.12±0.22	40.25±0.50	36.34±0.50
C:N	26.66±0.50	20.42±0.52	20.90±0.34	20.90±0.32	20.00±0.15	14.40±0.16

3.8 Molecular identification

According to the 16S rRNA analysis results, the bacteria in the C5 consortium belong to the *Bacillus haynesii* strain BHC1 (PP391133), *Bacillus amyloliquefaciens* strain BAC1 (PP391056), and *Bacillus safensis* (PP391033) and *Bacillus amyloliquefaciens* strain AMWC (PP391615). Recently, a few studies have been carried out for *Bacillus* inoculation for the lignocellocis biomass degradation (Wang et al., 2023; Zainudin et al., 2022). Mei et al. (2020) studied biomass lignin degradation using *B. amyloliquefaciens* and have achieved successful results. Further, Zaccardelli et al. (2020) have stated that *B. amyloliquefaciens* can be

successfully applied to control plant soil-borne diseases. There are no records on the usage of *B. safensis* for lignocellocis waste degradation. Importantly, though the individual effect of *B. haynesii* and *B. amyloliquefaciens* on composting have been researched, the synergistic interaction of *B. haynesii* and *B. amyloliquefaciens* with *B. safensis* in the same consortia has not been studied. Additionally, Sahu et al. (2020) have recorded *B. haynesii* and *B. amyloliquefaciens* as plant growth-promoting bacterium while producing diverse growth-promoting substances. Figure 9 represents the phylogenetic relationship of the bacterial strains in the prepared C5 consortium.

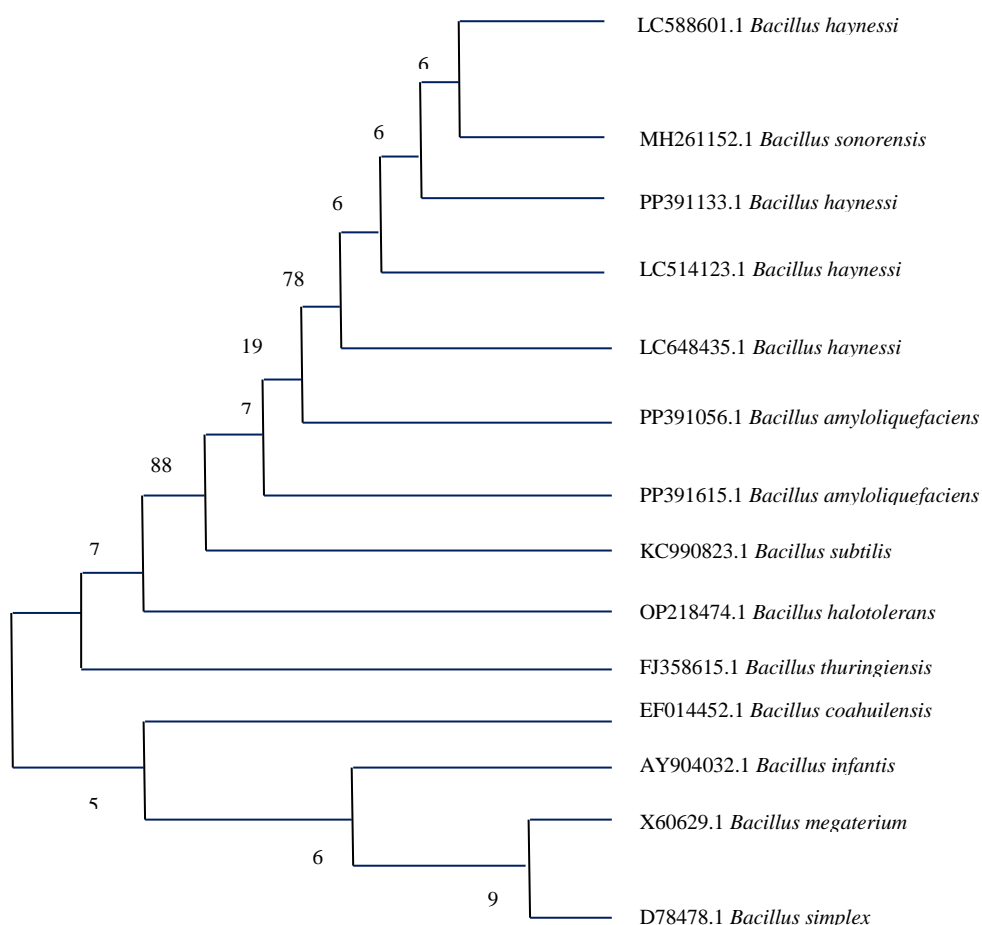


Figure 9. Phylogenetic analysis of the bacterial strains in the C5 consortium

The evolutionary history was inferred by using the Maximum Likelihood method and General Time Reversible model using MEGA11.

4. CONCLUSION

Four *Bacillus* sp. were contained in the prepared novel bacterial consortium (C5) which includes *B. haynesii* strain BHC1 (PP391133), *B.*

amyloliquefaciens strain BAC1 (PP391056), and *B. safensis* (PP391033), and *B. amyloliquefaciens* strain AMWC (PP391615). The consortium could significantly ($p < 0.05$) alter the composting parameters which include pH, temperature, EC, and bulk density, enzyme dynamics by rapidly converting MSW into compost within 20 ± 3 days. Further, the findings reveal that the prepared consortium has successfully reduced

the phyto toxicity of compost while enhancing the rate of compost maturity and stability. Therefore, the proposed novel consortium can be used as a potential green approach for sustainable MSW management.

ACKNOWLEDGEMENTS

The authors wish to thank for University of Sri Jayewardenepura, Nugegoda, Sri Lanka for financial assistance for this research under the university grant, Grant No: ASC/1/RE/SCI/2021/28.

REFERENCES

- Al-Dhabi NA, Esmail GA, Mohammed Ghilan AK, Valan Arasu M. Composting of vegetable waste using microbial consortium and biocontrol efficacy of *Streptomyces* sp. Al-Dhabi 30 is isolated from the Saudi Arabian environment for sustainable agriculture. *Sustainability* 2019;11(23):Article No. 6845.
- Andlar M, Rezić T, Mardetko N, Kracher D, Ludwig R, Santek B. Lignocellulose degradation: An overview of fungi and fungal enzymes involved in lignocellulose degradation. *Engineering in Life Sciences* 2018;18(11):768-78.
- Awasthi MK, Wang Q, Wang M, Chen H, Ren X, Zhao J, et al. In-vessel co-composting of food waste employing enriched bacterial consortium. *Food Technology and Biotechnology* 2018;56(1):83-9.
- Blair EM, Dickson KL, O'Malley MA. Microbial communities and their enzymes facilitate degradation of recalcitrant polymers in anaerobic digestion. *Current Opinion in Microbiology* 2021;64:100-8.
- Chen L, Li W, Zhao Y, Zhou Y, Zhang S, Meng L. Effects of compound bacterial agent on gaseous emissions and compost maturity during sewage sludge composting. *Journal of Cleaner Production* 2022;366:Article No. 133015.
- Chen Z, Li Y, Peng Y, Ye C, Zhang S. Effects of antibiotics on hydrolase activity and structure of microbial community during aerobic co-composting of food waste with sewage sludge. *Bioresource Technology* 2021;321:Article No. 124506.
- Chukwuma OB, Rafatullah M, Kapoor RT, Tajarudin HA, Ismail N, Siddiqui MR, et al. Isolation and characterization of Lignocellulolytic bacteria from municipal solid waste landfill for identification of potential hydrolytic enzyme. *Fermentation* 2023;9(3):Article No. 298.
- Dantoliya S, Joshi C, Mohapatra A, Shah D, Bhargava P, Bhanushali S, et al. Creating wealth from waste: An approach for converting organic waste into value-added products using microbial consortia. *Environmental Technology and Innovation* 2022;25:Article No. 102092.
- Dhiman VK, Chauhan V, Kanwar SS, Singh D, Pandey H. Purification and characterization of actinidin from *Actinidia deliciosa* and its utilization in inactivation of α -Amylase. *Bulletin of the National Research Centre* 2021; 45:Article No. 213.
- Finore I, Feola A, Russo L, Cattaneo A, Donato PD, Nicolaus B, et al. Thermophilic bacteria and their thermozymes in composting processes: A review. *Chemical and Biological Technologies in Agriculture* 2023;10(1):Article No. 7.
- Goushterova A, Nacheva L, Dinev N, Kabaivanova L. Addition of microbial inoculum as a way for compost improvement by enhancing the activities of hydrolytic enzymes. *Baltica* 2020;33(9):16-35.
- Gunaratne KBB, Wijerathna PAKC, Manage PM. Identification of *Salmonella* sp., *Shigella* sp., and Pathogenic *E. coli* in dug wells water around Karadiyana, Meethotamulla, and Kerawalapitiya open dump sites. *Proceedings of International Forestry and Environment Symposium*; 2024 Jan 5-6, (Vol. 28); Nugegoda, Sri Lanka: University of Sri Jayewardenepura; 2024.
- Harindintwali JD, Zhou J, Yu X. Lignocellulosic crop residue composting by cellulolytic nitrogen-fixing bacteria: A novel tool for environmental sustainability. *Science of the Total Environment* 2020;715:Article No. 136912.
- Ince O, Ozbayram EG, Akyol C, Erdem EI, Gunel G, Ince B. Bacterial succession in the thermophilic phase of composting of anaerobic digesters. *Waste Biomass Valorization* 2020; 11:841-9.
- Koyama M, Kakiuchi A, Syukri F, Toda T, Tran QNM, Nakasaki K. Inoculation of *Neurospora* sp. for improving ammonia production during thermophilic composting of organic sludge. *Science of the Total Environment* 2022;802:Article No. 149961.
- Kumar R, Kim TH, Basak B, Patil SM, Kim HH, Ahn Y, et al. Emerging approaches in lignocellulosic biomass pretreatment and anaerobic bioprocesses for sustainable biofuel production. *Journal of Cleaner Production* 2022;333:Article No. 130180.
- Lin H, Cheng Q, Sun W, Yang F, Ding Y, Ma J. Copper exposure effects on antibiotic degradation in swine manure vary between mesophilic and thermophilic conditions. *Science of the Total Environment* 2022;841:Article No. 156759.
- Ma Y, Liu Y. Turning food waste to energy and resources towards a great environmental and economic sustainability: An innovative integrated biological approach. *Biotechnology Advances* 2019;37(7):Article No. 107414.
- Mahapatra S, Ali MH, Samal K. Assessment of compost maturity-stability indices and recent development of composting bin. *Energy Nexus* 2022;6:Article No. 100062.
- Malik WA, Javed S. Biochemical characterization of Cellulase from *Bacillus subtilis* strain and its effect on digestibility and structural modifications of lignocellulose rich biomass. *Frontiers in bioengineering and biotechnology* 2021;9:Article No. 800265.
- Meena MD, Dotaniya ML, Meena MK, Meena BL, Meena KN, Dautaniya RK, et al. Maturity indices as an index to evaluate the quality of sulphur-enriched municipal solid waste compost using a variable byproduct of sulphur. *Waste Management* 2021;126:180-90.
- Mei J, Shen X, Gang L, Xu H, Wu F, Sheng L. A novel lignin degradation bacteria-*Bacillus amyloliquefaciens* SL-7 used to degrade straw lignin efficiently. *Bioresource Technology* 2020;310:Article No. 123445.
- Ng SM, Tey LH, Leong SY, Ng SA. Isolation, screening and characterization of the potential microbes to enhance the conversion of food wastes to bio-fertilizer. *Proceedings of AIP Conference*; 2019 Sep (Vol. 2157, No. 1); United States of America: American Institute of Physics (AIP); 2019.
- Pal DB, Tiwari AK. Sustainable Valorization of Agriculture and Food Waste Biomass: Application in Bioenergy and Useful Chemicals. Springer Nature; 2023.
- Pan I. Exploration for thermostable β -Amylase of a *Bacillus* sp. isolated from compost soil to degrade bacterial biofilm. *Microbiology Spectrum* 2021;9(2):e0064721.

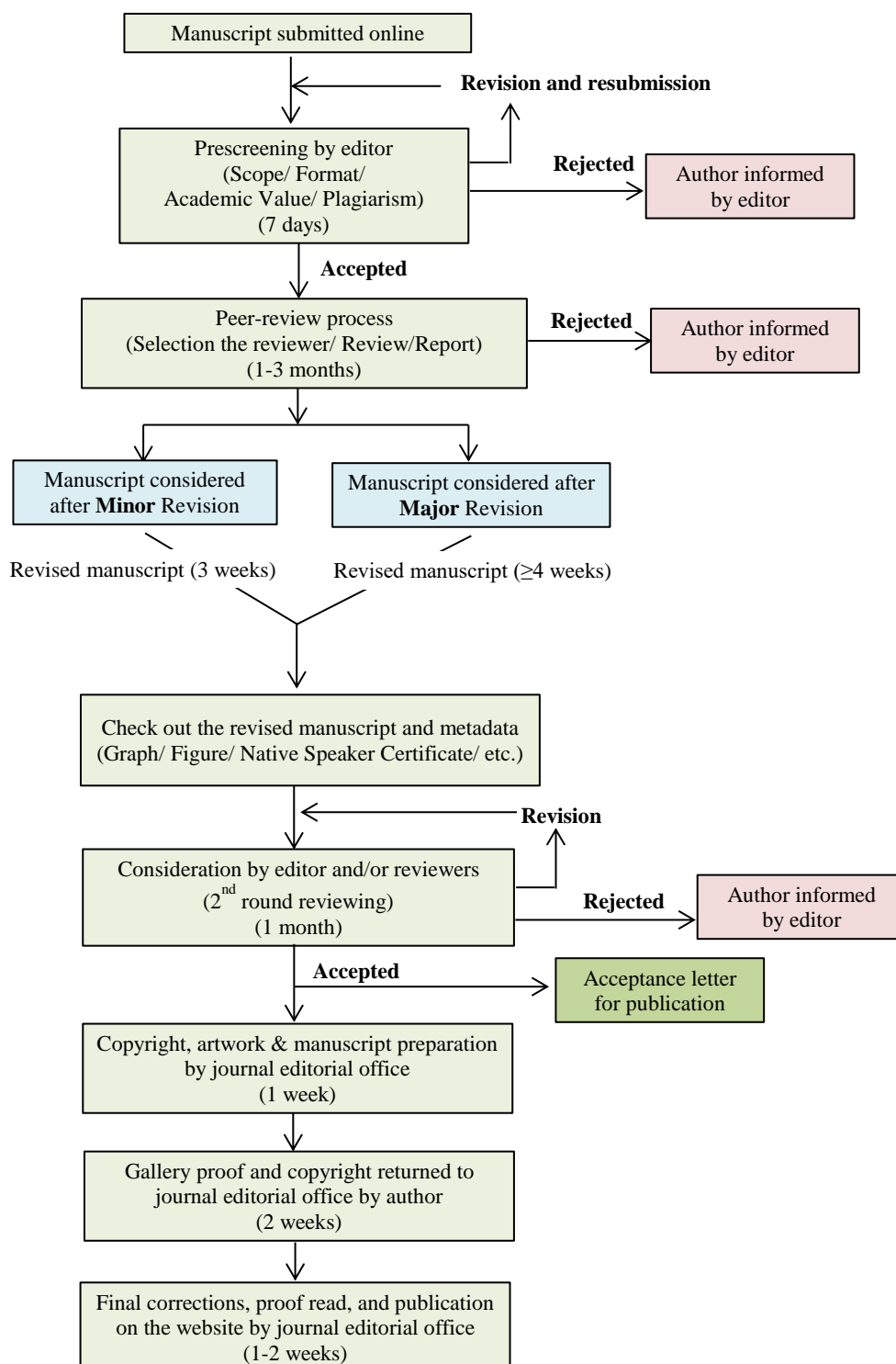
- Parameswaran R, Liyanage GY, Wijerathna PAKC, Manage PM. Characterization of compost and screening of antibiotic residues, antibiotic-resistant bacteria in commercially available compost in Sri Lanka. Proceedings of International Forestry and Environment Symposium; 2024 Jan 5-6, (Vol. 28); Nugegoda, Sri Lanka: University of Sri Jayewardenepura; 2024.
- Patel AR, Mokashe NU, Chaudhari DS, Jadhav AG, Patil UK. Production optimisation and characterisation of extracellular protease secreted by newly isolated *Bacillus subtilis* AU-2 strain obtained from *Tribolium castaneum* gut. Biocatalysis and Agricultural Biotechnology 2019;19:Article No. 101122.
- Rashwan MA, Alkoik FN, Saleh HAR, Fulleros RB, Ibrahim MN. Maturity and stability assessment of composted tomato residues and chicken manure using a rotary drum bioreactor. Journal of the Air and Waste Management Association 2021;71(5):529-39.
- Rich N, Bharti A, Kumar S. Effect of bulking agents and cow dung as inoculant on vegetable waste compost quality. Bioresource Technology 2018;252:83-90.
- Sahu PK, Singh S, Gupta AR, Gupta A, Singh UB, Manzar N, et al. Endophytic bacilli from medicinal-aromatic perennial Holy basil (*Ocimum tenuiflorum* L.) modulate plant growth promotion and induced systemic resistance against *Rhizoctonia solani* in rice (*Oryza sativa* L.). Biological Control 2020;150:Article No. 104353.
- Sarkar P, Chourasia R. Bioconversion of organic solid wastes into bio fortified compost using a microbial consortium. International Journal of Recycling of Organic Waste in Agriculture 2017;6:321-34.
- Shah R, Nair SS, Shah MD, Patil SA. Development of augmented microbial consortium for kitchen waste composting. Research Journal of Agricultural Sciences 2022;13(2):365-70.
- Sun L, Long M, Li J, Wu R, Ma L, Tang D, et al. Different effects of thermophilic microbiological inoculation with and without biochar on physicochemical characteristics and bacterial communities in pig manure composting. Frontiers in Microbiology 2021;12:Article No. 746718.
- Sun Q, Chen J, Wei Y, Zhao Y, Wei Z, Zhang H, et al. Effect of semi-continuous replacements of compost materials after inoculation on the performance of heat preservation of low-temperature composting. Bioresource Technology 2019; 279:50-6.
- Wan L, Wang X, Cong C, Li J, Xu Y, Li X, et al. Effect of inoculating microorganisms in chicken manure composting with maize straw. Bioresource Technology 2020;301:Article No. 122730.
- Wang L, Wang T, Xing Z, Zhang Q, Niu X, Yu Y, et al. Enhanced lignocellulose degradation and composts fertility of cattle manure and wheat straw composting by *Bacillus* inoculation. Journal of Environmental Chemical Engineering 2023;11(3):Article No. 109940.
- Wijerathna PAKC, Udayagee KPP, Idroos FS, Manage PM. Waste biomass valorization and its application in the environment. In: Pal DB, Tiwari AK, editors. Sustainable Valorization of Agriculture and Food Waste Biomass: Application in Bioenergy and Useful Chemicals. Singapore: Springer Nature; 2023. p. 1-28.
- Wijerathna PAKC, Udayagee KPP, Idroos FS, Manage PM. Novel bacterial consortium for the reduction of composting odor emission and enhancing compost maturation rate in municipal solid waste. Proceedings of 11th Ruhuna International Science and Technology Conference; 2024 Jan 24; Matara, Sri Lanka: University of Ruhuna; 2024.
- Zaccardelli M, Sorrentino R, Caputo M, Scotti R, De Falco E, Pane C. Stepwise-selected *Bacillus amyloliquefaciens* and *B. subtilis* strains from composted aromatic plant waste able to control soil-borne diseases. Agriculture 2020;10(2):Article No. 30.
- Zainudin MHM, Singam JT, Sazili AQ, Shirai Y, Hassan MA. Indigenous cellulolytic aerobic and facultative anaerobic bacterial communities enhanced the composting of rice straw and chicken manure with biochar addition. Scientific Reports 2022;12(1):Article No. 5930.
- Zhang Z, Shah AM, Mohamed H, Tsiklauri N, Song Y. Isolation and screening of microorganisms for the effective pretreatment of lignocellulosic agricultural wastes. BioMed Research International 2021;2021:Article No. 5514745.
- Zhimo VY, Biasi A, Kumar A, Feygenberg O, Salim S, Vero S, et al. Yeasts and bacterial consortia from kefir grains are effective biocontrol agents of postharvest diseases of fruits. Microorganisms 2020;8(3):Article No. 428.

INSTRUCTION FOR AUTHORS

Publication and Peer-reviewing processes of Environment and Natural Resources Journal

Environment and Natural Resources Journal is a peer reviewed and open access journal that is published in six issues per year. Manuscripts should be submitted online at <https://ph02.tci-thaijo.org/index.php/ennrj/about/submissions> by registering and logging into this website. Submitted manuscripts should not have been published previously, nor be under consideration for publication elsewhere (except conference proceedings papers). A guide for authors and relevant information for the submission of manuscripts are provided in this section and also online at: <https://ph02.tci-thaijo.org/index.php/ennrj/author>. All manuscripts are refereed through a **single-blind peer-review** process.

Submitted manuscripts are reviewed by outside experts or editorial board members of **Environment and Natural Resources Journal**. This journal uses double-blind review, which means that both the reviewer and author identities are concealed from the reviewers, and vice versa, throughout the review process. Steps in the process are as follows:



The Environment and Natural Resources Journal (EnNRJ) accepts 2 types of articles for consideration of publication as follows:

- *Original Research Article*: Manuscripts should not exceed 3,500 words (excluding references).
- *Review Article (by invitation)*: This type of article focuses on the in-depth critical review of a special aspect in the environment and also provides a synthesis and critical evaluation of the state of the knowledge of the subject. Manuscripts should not exceed 6,000 words (excluding references).

Submission of Manuscript

Cover letter: Key points to include:

- Statement that your paper has not been previously published and is not currently under consideration by another journal
- Brief description of the research you are reporting in your paper, why it is important, and why you think the readers of the journal would be interested in it
- Contact information for you and any co-authors
- Confirmation that you have no competing interests to disclose

Manuscript-full: Manuscript (A4) must be submitted in Microsoft Word Files (.doc or .docx). Please make any identifying information of name(s) of the author(s), affiliation(s) of the author(s). Each affiliation should be indicated with superscripted Arabic numerals immediately after an author's name and before the appropriate address. Specify the Department/School/Faculty, University, Province/State, and Country of each affiliation.

Manuscript-anonymized: Manuscript (A4) must be submitted in Microsoft Word Files (.doc or .docx). Please remove any identifying information, such as authors' names or affiliations, from your manuscript before submission and give all information about authors at title page section.

Reviewers suggestion (mandatory): Please provide the names of 3 potential reviewers with the information about their affiliations and email addresses. *The recommended reviewers should not have any conflict of interest with the authors. Each of the reviewers must come from a different affiliation and must not have the same nationality as the authors.* Please note that the editorial board retains the sole right to decide whether or not the recommended potential reviewers will be selected.

Preparation of Manuscript

Manuscript should be prepared strictly as per guidelines given below. The manuscript (A4 size page) must be submitted in Microsoft Word (.doc or .docx) with Times New Roman 12 point font and a line spacing of 1.5. *The manuscript that is not in the correct format will be returned and the corresponding author may have to resubmit.* The submitted manuscript must have the following parts:

Title should be concise and no longer than necessary. Capitalize first letters of all important words, in Times New Roman 12 point bold.

Author(s) name and affiliation must be given, especially the first and last names of all authors, in Times New Roman 11 point bold.

Affiliation of all author(s) must be given in Times New Roman 11 point italic.

Abstract should indicate the significant findings with data. A good abstract should have only one paragraph and be limited to 250 words. Do not include a table, figure or reference.

Keywords should adequately index the subject matter and up to six keywords are allowed.

Text body normally includes the following sections: 1. Introduction 2. Methodology 3. Results and Discussion 4. Conclusions 5. Acknowledgements 6. References

Reference style must be given in Vancouver style. Please follow the format of the sample references and citations as shown in this Guide below.

Unit: The use of abbreviation must be in accordance with the SI Unit.

Format and Style

Paper Margins must be 2.54 cm on the left and the right. The bottom and the top margin of each page must be 1.9 cm.

Introduction is critically important. It should include precisely the aims of the study. It should be as concise as possible with no sub headings. The significance of problem and the essential background should be given.

Methodology should be sufficiently detailed to enable the experiments to be reproduced. The techniques and methodology adopted should be supported with standard references.

Headings in Methodology section and Results and Discussion section, no more than three levels of headings should be used. Main headings should be typed (in bold letters) and secondary headings (in bold and italic letters). Third level headings should be typed in normal and no bold, for example;

2. Methodology

2.1 Sub-heading

2.1.1 Sub-sub-heading

Results and Discussion can be either combined or separated. This section is simply to present the key points of your findings in figures and tables, and explain additional findings in the text; no interpretation of findings is required. The results section is purely descriptive.

Tables Tables look best if all the cells are not bordered; place horizontal borders only under the legend, the column headings and the bottom.

Figures should be submitted in color; make sure that they are clear and understandable. Please adjust the font size to 9-10, no bold letters needed, and the border width of the graphs must be 0.75 pt. (*Do not directly cut and paste them from MS Excel.*) Regardless of the application used, when your electronic artwork is finalized, please 'save as' or convert the images to TIFF (or JPG) and separately send them to EnNRJ. The images require a resolution of at least 300 dpi (dots per inch). If a label needed in a figure, its font must be "Times New Roman" and its size needs to be adjusted to fit the figure without borderlines.

All Figure(s) and Table(s) should be embedded in the text file.

Conclusions should include the summary of the key findings, and key take-home message. This should not be too long or repetitive, but is worth having so that your argument is not left unfinished. Importantly, don't start any new thoughts in your conclusion.

Acknowledgements should include the names of those who contributed substantially to the work described in the manuscript but do not fulfill the requirements for authorship. It should also include any sponsor or funding agency that supported the work.

References should be cited in the text by the surname of the author(s), and the year. This journal uses the author-date method of citation: the last name of the author and date of publication are inserted in the text in the appropriate place. If there are more than two authors, "et al." after the first author's name must be added. Examples: (Frits, 1976; Pandey and Shukla, 2003; Kungsuwas et al., 1996). If the author's name is part of the sentence, only the date is placed in parentheses: "Frits (1976) argued that . . ."

Please be ensured that every reference cited in the text is also present in the reference list (and vice versa).

In the list of references at the end of the manuscript, full and complete references must be given in the following style and punctuation, arranged alphabetically by first author's surname. Examples of references as listed in the References section are given below.

Book

Tyree MT, Zimmermann MH. Xylem Structure and the Ascent of Sap. Heidelberg, Germany: Springer; 2002.

Chapter in a book

Kungsuwan A, Ittipong B, Chandkrachang S. Preservative effect of chitosan on fish products. In: Steven WF, Rao MS, Chandkrachang S, editors. Chitin and Chitosan: Environmental and Friendly and Versatile Biomaterials. Bangkok: Asian Institute of Technology; 1996. p. 193-9.

Journal article

Muenmee S, Chiemchaisri W, Chiemchaisri C. Microbial consortium involving biological methane oxidation in relation to the biodegradation of waste plastics in a solid waste disposal open dump site. *International Biodeterioration and Biodegradation* 2015;102:172-81.

Published in conference proceedings

Wiwattanakantang P, To-im J. Tourist satisfaction on sustainable tourism development, amphawa floating market Samut songkhram, Thailand. *Proceedings of the 1st Environment and Natural Resources International Conference*; 2014 Nov 6-7; The Sukosol hotel, Bangkok: Thailand; 2014.

Ph.D./Master thesis

Shrestha MK. Relative Ungulate Abundance in a Fragmented Landscape: Implications for Tiger Conservation [dissertation]. Saint Paul, University of Minnesota; 2004.

Website

Orzel C. Wind and temperature: why doesn't windy equal hot? [Internet]. 2010 [cited 2016 Jun 20]. Available from: <http://scienceblogs.com/principles/2010/08/17/wind-and-temperature-why-doesn/>.

Report organization:

Intergovernmental Panel on Climate Change (IPCC). IPCC Guidelines for National Greenhouse Gas Inventories: Volume 1-5. Hayama, Japan: Institute for Global Environmental Strategies; 2006.

Remark

* Please be note that manuscripts should usually contain at least 15 references and some of them must be up-to-date research articles.

* Please strictly check all references cited in text, they should be added in the list of references. Our Journal does not publish papers with incomplete citations.

Changes to Authorship

This policy of journal concerns the addition, removal, or rearrangement of author names in the authorship of accepted manuscripts:

Before the accepted manuscript

For all submissions, that request of authorship change during review process should be made to the form below and sent to the Editorial Office of EnNRJ. Approval of the change during revision is at the discretion of the Editor-in-Chief. The form that the corresponding author must fill out includes: (a) the reason for the change in author list and (b) written confirmation from all authors who have been added, removed, or reordered need to confirm that they agree to the change by signing the form. Requests form submitted must be consented by corresponding author only.

After the accepted manuscript

The journal does not accept the change request in all of the addition, removal, or rearrangement of author names in the authorship. Only in exceptional circumstances will the Editor consider the addition, deletion or rearrangement of authors after the manuscript has been accepted.

Copyright transfer

The copyright to the published article is transferred to Environment and Natural Resources Journal (EnNRJ) which is organized by Faculty of Environment and Resource Studies, Mahidol University. The accepted article cannot be published until the Journal Editorial Officer has received the appropriate signed copyright transfer.

Online First Articles

The article will be published online after receipt of the corrected proofs. This is the official first publication citable with the Digital Object Identifier (DOI). After release of the printed version, the paper can also be cited by issue and page numbers. DOI may be used to cite and link to electronic documents. The DOI consists of a unique alpha-numeric character string which is assigned to a document by the publisher upon the initial electronic publication. The assigned DOI never changes.

Environment and Natural Resources Journal (EnNRJ) is licensed under a Attribution-NonCommercial 4.0 International (CC BY-NC 4.0)





Mahidol University
Wisdom of the Land



Faculty of Environment and Resource Studies, Mahidol University, Thailand
999 Phutthamonthon Sai 4 Rd, Salaya, Phutthamonthon District, Nakhon Pathom 73170
E-mail: ennrjournal@gmail.com